REPORT DOCUMENTATION PAGE

Form Approved OMB No. 0704-0188

1. REPORT DATE *(31-03-2006)*	2. REPORT TYPE Final Performance Report	3. DATES COVERED *(01-01-2003 to 31-12-2005)*

4. TITLE AND SUBTITLE
Studies of Biosilicification, the role of proteins, Carbohydrates and model compounds in structure control

5a. CONTRACT NUMBER

5b. GRANT NUMBER
F49620-03-1-0099

5c. PROGRAM ELEMENT NUMBER

6. AUTHOR(S)
Carole. C. Perry and members of research team

5d. PROJECT NUMBER

5e. TASK NUMBER

5f. WORK UNIT NUMBER

7. PERFORMING ORGANIZATION NAME(S) AND ADDRESS(ES)

Nottingham Trent University School of Biomedical and Natural Sciences, Clifton Lane, Nottingham NG11 8NS United Kingdom

8. PERFORMING ORGANIZATION REPORT NUMBER

Final report

9. SPONSORING / MONITORING AGENCY NAME(S) AND ADDRESS(ES)
Dr Hugh C. De Long, AFOSR
975 North Randolph Street,
Suite 325, Room 3112
Arlington VA 22203-1768

10. SPONSOR/MONITOR'S ACRONYM(S)

11. SPONSOR/MONITOR'S REPORT NUMBER(S)

12. DISTRIBUTION / AVAILABILITY STATEMENT

Approved fro Public Release: Distribution Unlimited — A AFRL-SR-AR-TR-06-0111

13. SUPPLEMENTARY NOTES

14. ABSTRACT

'Si' (in some form) has been shown to be associated with post-translationally modified protein and carbohydrate biopolymer components of the plant cell wall from *Equisetum arvense*. Bioextracts from the plant cell wall and bioinspired additives from amino acids, peptides, proteins and molecules containing reactive groups such as amines and hydroxyl groups have been found to modify the properties of silicas generated in their presence. The observed patterns of behaviour are functionality and structure dependent and centre upon non-covalent interactions between a range of silicon containing species and the solution phase additives. Electrostatic interactions, hydrogen bonding, the hydrophobic effect and the ordering of water all play a role in determining the structures adopted by silica produced in aqueous solution. Routes to porous and non-porous silicas and to silicas that show a range of gross morphologies including spheres, ribbons and structures that superficially mimic the material they have been formed in conjunction with have been developed. The level of understanding of chemical factors that affect silica formation has been extensively increased and new silica based materials generated. It is extremely likely that the set of 'rules' governing (bio)silicification understood from this project will be used predictively in the future by others.

15. SUBJECT TERMS
Biosilicification, silica, interfacial chemistry, biomimetics, protein-mineral interactions.

16. SECURITY CLASSIFICATION OF:			17. LIMITATION OF ABSTRACT	18. NUMBER OF PAGES	19a. NAME OF RESPONSIBLE PERSON
a. REPORT	b. ABSTRACT	c. THIS PAGE		340	19b. TELEPHONE NUMBER *(include area code)*

Award No. F49620-03-1-0099

Title: "Studies of Biosilicification; the role of proteins, carbohydrates and model compounds in structure control"

Principal Investigator: Professor Carole C. Perry

Address: School of Biomedical and Natural Sciences
Interdisciplinary Biomedical Science Research Centre
The Nottingham Trent University
Clifton Lane
NG11 8NS
UK

Abstract

We have shown that 'Si' (in some form) is associated with post-translationally modified protein and carbohydrate biopolymer components of the plant cell wall from *Equisetum arvense*. We have shown that bioextracts from the plant cell wall and bioinspired additives from amino acids, peptides, proteins and molecules containing reactive groups such as amines and hydroxyl groups modify the properties of silicas generated in their presence. The observed patterns of behaviour are functionality and structure dependent and centre upon non-covalent interactions between a range of silicon containing species and the solution phase additives. We have shown that electrostatic interactions, hydrogen bonding, the hydrophobic effect and the ordering of water all play a role in determining the structures adopted by silica produced in aqueous solution. We have developed routes to porous and non-porous silicas and to silicas that show a range of gross morphologies including spheres, ribbons and structures that superficially mimic the material they have been formed in conjunction with. We have increased the level of understanding of chemical factors that affect silica formation and generated new silica based materials. We believe that the set of 'rules' governing (bio)silicification understood from this project will be used predictively in the future by others.

Published Papers from this funding period:

1. C.C. Perry (2003) "Silicification: the processes by which organisms capture and mineralize silica" *Reviews in Mineralogy and Geochemistry* **54**: 291-327

2. D. Belton, G. Paine, S. Patwardhan, C.C. Perry (2004) "The role of amino acids and lysine oligomers in (bio)silicification" J. Mater. Chem. **14**, 2231-2241

3. D. Belton, S.V. Patwardhan, C.C. Perry (2005) "*Bioinspired Silicification: putrescine homologues control silica morphogenesis*" Chem Commun 3475-3477

4. M.M. Tomczak, D.D. Glawe, L.F. Drummy, C.G. Lawrence, M.O. Stone, C.C. Perry, D.J. Pochan, T.J. Deming, R.R. Naik (2005) "Polypeptide templated synthesis of hexagonal silica platelets" J.A.C.S. 127(36) 12577-12582

5. D. Belton, S.V. Patwardhan, C.C. Perry (2005) "Spermine, Spermidine and their analogues generate tailored silicas" J. Mater. Chem. 15, 4629-4638

6. W.E.G. Muller, S.I. Belikov, W. Tremel, C.C. Perry, W.W.C. Gieskes, A. Boreiko, H.C. Shroeder (2006) "Siliceous spicules in marine demosponges (example Suberites domuncula)" Micron, 37(2), 107-120.

7. V.A. Annenkov, S.V. Patwardhan, D. Belton, E.N. Danilovtseva and C.C. Perry (2006) "A New Stepwise synthesis of a family of propylamines derived from diatom silaffins and their activity in silicification" Chem. Commun. 1521-1523

Papers in Press:

1. S. Patwardhan, D. Belton, G. Tilburey and C.C. Perry (2006) "the Role of Non-bonded Interactions in Additive mediated Amorphous Silica Structure Control" Proceedings of ACS Anaheim meeting, in the press

2. H.A. Currie, S.V. Patwardhan, C.C. Perry, P. Roach and N.J. Shirtcliffe (2006) "Natural and Artificial Hybrid Biomaterials" in G. Kickelbick ed. Hybrid Materials-Synthesis, Characterisation and Applications, Wiley-VGH in the press

Papers currently in review:

1. C.P.F. Wong, B. Kitchel., J. Huang, S.V. Patwardhan, D. Belton, C.C. Perry and D.L. Kaplan (2006) "Novel Nanocomposites from Spider Silk-Silica Fusion (Chimeric) Proteins, PNAS

Drafts of manuscripts to be submitted are attached:

2. G. Tilburey, S.V. Patwardhan, D.L. Kaplan, C.C. Perry "Are Hydroxyl containing biomolecules important in (bio)silicicification?"

July 2006, Biomineralisation Gordon Conference, USA

Posters presented by the group at:
July 2005, MC7 (David Belton, Graham Tilburey)
July 2005, School Research day (David Belton (Talk), Graham Tilburey 3rd place poster prize)
September 2005, Euromat (Heather Currie)

Consultative and advisory functions
To Dow Corning Technical Advisory Board in September 2005

Transitions/Collaborations in place with other scientists funded in this programme are as follows:
Professor David Kaplan, a study on the effect of sericin on silica formation has been completed and a manuscript is currently being prepared (G. Tilburey, see attached manuscript). The protein is also being investigated for use as a potential structure organiser for another biomimetic programme to generate alumina composite materials modelled on nacre from clusters and particles of the oxide and hydroxide phase produced by carefully controlled hydrolysis (yet to be done). A joint proposal to NIH has been submitted.
Professor Ken Sandhage: (1) plant material has been sent to him for interconversion into other oxide materials whilst maintaining morphological features. Diatom materials that have been transformed into titania have just (August 2004) been sent to us for surface area and porosity measurements. We anticipate receiving converted plant materials from him in due course. (2) Stober spheres of different sizes have been sent to him for transformation studies to look at the effect of surface activity and particle size on ease of transformation, again it is envisaged that samples will be returned for surface area and porosity studies.

Personnel:

- Dr Masood Javed (September 2003-September 2004 (left to become assistant Professor at an US off shore medical school in Luton, UK) (worked on protein separation and characterisation).
- Dr Heather Currie (5th January 2004-present) (to work on silicon involvement with carbohydrates within silicified plant cell walls).
- David Belton (July 2005-december 2005) 0.6 position (to work on model studies).
- Graham Tilburey (24th September 2003- present (PhD student) (to work on model systems)

Undergraduate Project students:
1. Emma Futcher (summer, 10 week project, 2nd year student, Durham University)- Biochemical analysis of silica extracts.
2. Carole Gadois (French foreign exchange student, level 2, 10 week project Apr-Jun 2005)- Effects of additives on undersaturated silicic acid.
3. Alice Mason (summer 2005, Nottingham High School for Girls, Nuffield Science Bursary Project)- Coating gold nanoparticles with silica.

APPENDIX-I: PUBLISHED PAPERS AND POSTERS

10 Silicification: The Processes by Which Organisms Capture and Mineralize Silica

Carole C. Perry

Division of Chemistry, Interdisciplinary Biomedical Research Centre
The Nottingham Trent University
Clifton Lane, Nottingham, NG11 8NS, United Kingdom

INTRODUCTION

Silicification is widespread in the biological world and occurs in bacteria, single-celled protists, plants, invertebrates and vertebrates. Minerals formed in the biological environment often show unusual physical properties (e.g., strength, degree of hydration) and often have structures that exhibit order on many length scales. The minerals are formed from an environment that is undersaturated with respect to silicon and under conditions of around neutral pH and low temperature ca. 4–40°C. Formation of the mineral may occur intra- or extra-cellularly and specific biochemical locations for mineral deposition that include lipids, proteins and carbohydrates are known. The significance of the cellular machinery cannot be over emphasized and it is with advances in experimental techniques (cell biology and materials characterization) and advances in understanding (including the ability to design laboratory experiments to mimic the biological environment) that much progress has been made in the field in recent years. In most cases the formation of the mineral phase is linked to cellular processes and if we understand this process the knowledge so gained could be used to good effect in designing new materials for biomedical, optical and other applications. The study of living organisms could result in wealth generation/creation. It should be noted that although significant advances have been made in the last ten years, new questions have arisen and there are many areas requiring exploration.

This contribution will place emphasis on the systems for which most is known, namely sponges and diatoms, however, it should be borne in mind that many other organisms from single-celled species such as choanoflagellates (Mann et al. 1982) and radiolaria through to higher plants and molluscs such as the limpet (Mann et al. 1986) make use of silica and form species specific structures that show structural organization on several length scales. Examples of some of the silicified structures observed for organisms that will be little discussed in this chapter are given in Figure 1. Table 1 provides definitions for the general terminology used in this contribution. At the end of the chapter, the bibliography lists some excellent reviews which can be used to provide more information on the topics discussed as well as providing an excellent source of further literature.

STRUCTURAL CHEMISTRY OF SILICA

Silica and silicates are extensively used in industry and medicine. The materials find use in paints, foods, medicines, adhesives, detergents, chromatography materials, catalysts and photonic materials (reviewed by Iler 1979). Silica may be produced at high temperature, via aqueous processing or by largely non-aqueous routes such as the low-temperature sol-gel process (reviewed in Brinker and Scherrer 1990; Hench and West 1990). Whatever the eventual use of the silica, it is its structure that determines its

1529-6466/00/0054-0010$05.00

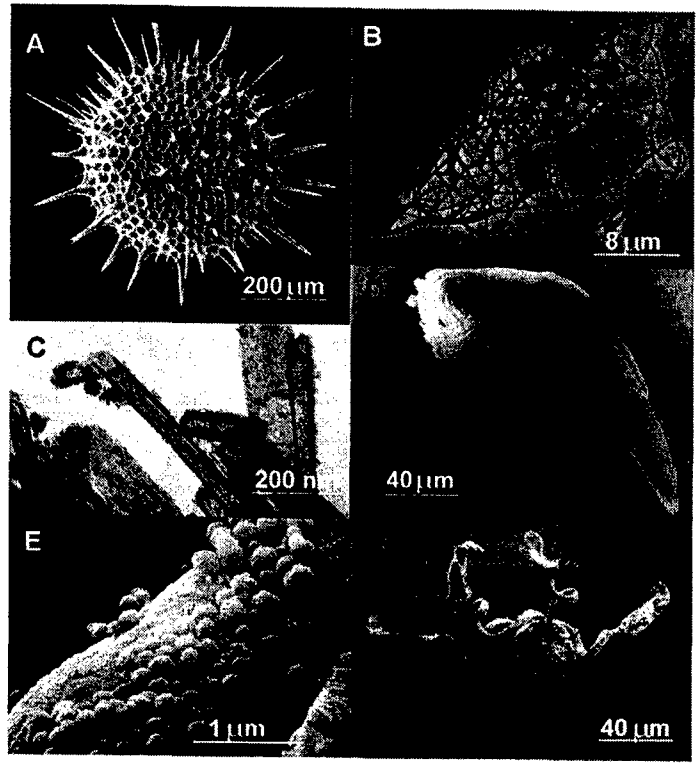

Figure 1. Electron microscope images of biosilicas from **(A)** Radiolarian, **(B)** choanoflagellate (courtesy of Professor Steve Mann, Bristol University), **(C)** silica tubes that surround goethite (iron containing) crystals in limpet teeth, **(D)** limpet tooth with iron containing mineral removed, **(E)** silica coated particles on the surface of the spore elators of *Equisetum arvense*, **(F)** spore and elators from *Equisetum arvense*.

properties. By structure we mean order and organization on length scales from angstroms to the size of the final object, morphology, surface area, porosity and surface functionality. The essential building block is the SiO_4 tetrahedron although other structural units such as the SiO_6 octahedron are also used. These units can be put together in a wide range of patterns to yield both porous and non-porous crystalline materials including silica based zeolite materials. As well as crystalline silica and silicates there exist an extremely diverse range of amorphous materials such as disordered precipitates, gels, glasses and shaped objects (spheres, screws, hollow tubes, etc; Stöber et al. 1968; Yang et al.1997; Miyaki et al. 1999) produced using a wide range of synthesis conditions.

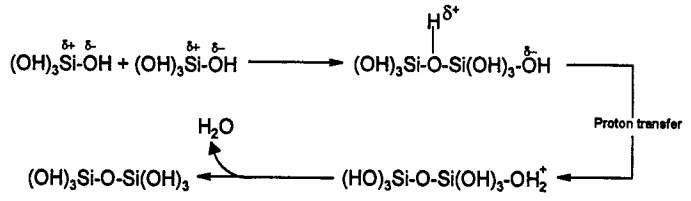

Figure 4. Mechanism of the condensation of two silicic acid molecules under conditions where neither contain $Si\text{–}O^-$ groups.

would, therefore, increase the pH of the reaction system in the absence of a buffer of some sort. At ca. neutral pH where silica is formed in biological organisms (or down to ca. pH 5 as proposed for silicification in diatoms; Vrieling et al. 1999) the proportion of ionized silicic acid molecules is very small (ca. 0.002% at pH 5 and ca. 0.18% at pH 7).

As the particles get progressively bigger, pK_a values for the removal of an hydrogen atom from a silanol group decrease such that at ca. pH 7, all particles with nanometer dimensions will carry a negative charge (even at ca. pH 5, ~2% of all silanol groups will be ionized). Thus charge will be present on the fundamental particles used to build up the silica structures observed in diatoms, sponges, etc. which will require some means of neutralizing the negative charge on the surface of each particle in order for a flocculated and/or aggregated material to form.

As a rule, silicic acid molecules condense in such a way as to produce a sufficient number of siloxane (Si–O–Si) bonds with oligomers cyclizing during the early stages of the process to give rings containing predominantly 3–6 silicon atoms linked by siloxane bonds, for examples see Figure 5. Almost all silicas except those formed under conditions of extreme acidity contain high proportions of cyclic species.

Once the cyclic species dominate, monomers and dimers and other small oligomers react preferentially with these (Tarutani 1989), as the oligomers have a higher density of ionized silanol groups. A process known as Ostwald ripening also occurs where smaller, more soluble particles, dissolve and release silicic acid that re-deposits onto the larger particles. At ca. neutral pH as the particles bear a negative charge on the surface they grow as isolated sol particles, Figure 6, until the levels of soluble silica reach the solubility of amorphous silica. If salts are present or under acidic conditions (e.g., within the diatom silica deposition vesicle), however, the surface negative charge that causes repulsion between individual particles is reduced or eliminated and the particles aggregate to form dense three-dimensional networks, Figure 6.

There are many studies of the kinetics of silica formation and the orders of reaction reported range from first to fifth (see references in Iler 1979; Perry and Keeling-Tucker 2000). Despite the differences in reported orders of reaction for silica deposition, it is universally acknowledged that orthosilicic acid concentration, temperature, pH and the presence of additional chemical species all affect the rate of oligomerization. The first two factors always cause a concomitant increase in the rate. The effect of pH is that, in general, silica prepared under acidic conditions is built up from extended networks and silica formed under basic conditions is built up from highly branched networks with pH

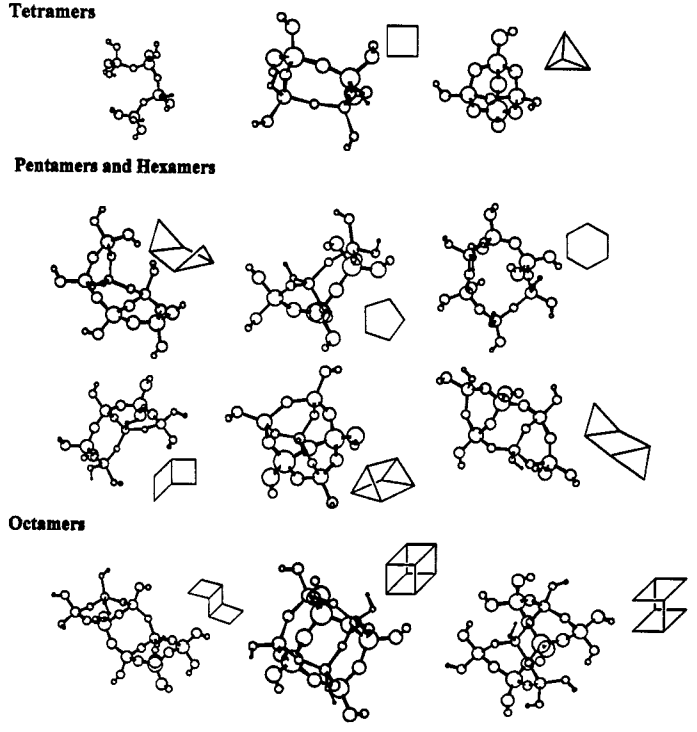

Figure 5. Examples of structures of silicates showing energy minimized structures (MM2 followed by application of the AM1 program) and idealized shape. The energy minimization was performed with all silanols protonated although the extent of deprotonation will vary according to the pH of the system. Included are five- and six-membered rings that are thought to exist in the approximately neutral solutions relevant to biological silica precipitation.

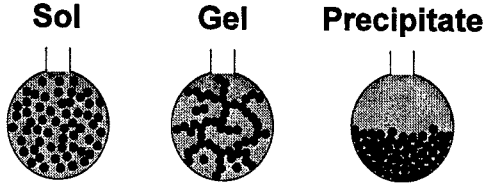

Figure 6. Schematic of a sol, gel and precipitate containing the same number of particles.

depicted in Figure 2 and it is difficult to obtain detailed structural information on the nature of these particles and how they are arranged within the silicified structures. Detailed structural studies of siliceous biominerals are, however, an extremely important starting point in studies of biosilicification. The structure of a particular mineral provides, in its make-up, information that may point to the path/mechanism by which it was formed. If we could correctly "read" the information that structures provide we may proceed to a much deeper understanding of the biosilicification process for the full range of organisms.

A wide range of techniques is now available to help us understand the structure of these complex amorphous materials. Examples of these techniques and the information they provide are described below.

Techniques for the study of biosilica structure

Small-angle and wide-angle X-ray diffraction techniques that can detect order at the nm level (i.e., to look for small crystalline regions within a structure) have been applied to both diatoms (Vrieling et al. 2000) and the primitive plant *Equisetum arvense* (Holzuter et al. 2003) and have found no evidence for crystallinity although small differences in instrument response to the technique have been observed by the authors for analysis along the length and across the fibers of the siliceous sponge from the Hexactinellida family, N.B. no crystallinity was detected. Other biosilicified materials should also be examined by this technique. Recent studies of model silica-protein composites and diatoms by ultrasmall angles (USAXS) have shown that structures on different length scales (including pore structures) could be identified by this technique (Vrieling et al. 2002).

Electron microscopy has been extensively used to look at the sizes of fundamental particles and their interconnection one to another. Figure 7 provides structural information on particle size and orientation for small regions of silica that were removed from plant hairs where a range of particle sizes and arrangements were observed. The technique can be used to follow structural changes with time and gel-like and particulate structures can be observed within the same organism at different development times,

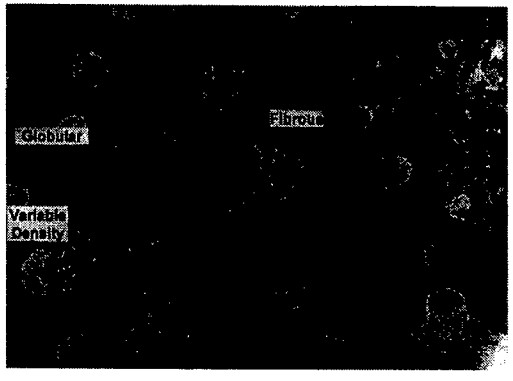

Figure 7. Transmission electron microscope image of silica from hairs on the lemma of *Phalaris canariensis* L. Examples of fibrillar, globular and other structural arrangements all obtained from a single cell hair sample.

Figure 8 (Perry and Fraser 1991) More information on the changes in structure with time will be found in the section on diatom silica structures later in the chapter. The technique can also give information on the degree of hydration by comparison of sample stability under the electron beam. Biosilicas, in comparison to silicas produced in the laboratory are much more stable under the electron beam. An extension of these studies would be to use CRYO transmission electron microscopy to look at the fundamental particles present in silicifying organisms. The technique has the advantage that contrast is enhanced and small chains, and rings of particles that are ca. 2 nm in diameter can be visualized. An example is shown in Figure 9 that was obtained from a model experiment to follow silica formation (Harrison and Loton 1995).

Electron microscopy has also widely been used to "look at" microscopic structures, see the many figures distributed throughout the chapter. The technique, in combination with energy dispersive X-ray analysis can be used to locate the mineral within the organism and to look for any co-localized species including metal ions. Maps of element localization can be produced and Figure 10 shows an example of maps produced for nettle hairs, a silicifying organism that also mineralizes calcium). The combination of

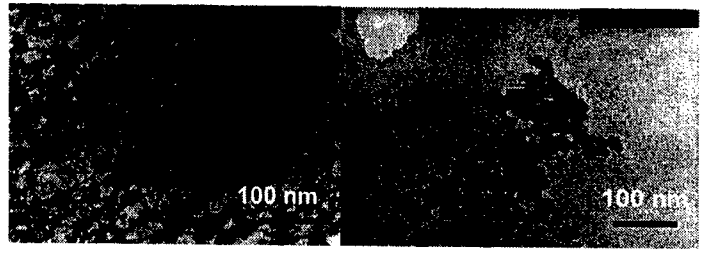

Figure 8. Transmission electron microscope images of gel-like and globular silica from the primitive plant *Equisetum arvense* at different stages of development.

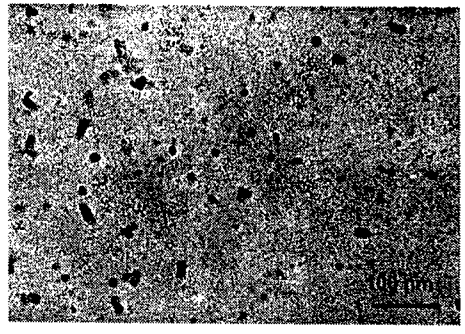

Figure 9. Cryo transmission electron microscope image of small (~2 nm diameter) silica particles arranged in chains and rings.

of such functional groups to the external environment. For example, reaction of silanol groups in a plant silica sample with trimethylchlorosilane (Mann et al. 1983)) provided evidence that many of the silanol groups in the intact plant hairs were probably protected against dissolution by reaction with the plant cell wall biopolymers as they were unavailable to react with the reagent. Use of NMR experiments designed to look at the relaxation behavior of selected species can provide circumstantial evidence for the extent of interaction between the siliceous phase and any organic phase (Perry 1989). Of the siliceous materials investigated to date (sponge, diatom, plant and limpet teeth), the strongest interactions between inorganic and organic phases is proposed to exist for diatoms.

Solution ^{29}Si NMR spectroscopy has, until now, found little use in the study of biosilicification owing to poor sensitivity and low natural abundance of the nucleus. Recent experiments using enriched silicon sources have started to probe the internal reaction environment of a silicifying diatom *Navicula pelliculosa* (Kinrade et al. 2002). Figure 13. shows the presence of silicic acid detected within the diatom. During some of

Figure 13. Reprinted with permission of the Royal Society of Chemistry from Kinrade et al. 2002. (a) Silicon-29 ^{1}H-decoupled NMR spectrum (149 MHz) of a synchronized culture of *Navicula pelliculosa* following 6 h feeding on ^{29}Si-enriched (75 atom%) silicon at 298 K. The spectrum was acquired over 9.3 h at 278.2 K using $\pi/2$ (16 μs) pulses with a cycling period of 11 s. The dominant feature centered at −110 ppm arises from Si-containing components in the NMR probe. The sample itself yielded a sharp orthosilicic acid peak at −71.0 ppm and a weak signal at −131.5 ppm with a half-height peak width of 25 Hz. (See vertical expansion). (b) The last of four successive 3.3 h silicon-29 ^{1}H-decoupled NMR spectra (99.4 MHz) acquired of another synchronized *Navicula pelliculosa* culture, following 6 h exposure to ^{29}Si (99.8 atom%) at 298 K in a medium also enriched (99.6 atom%) in ^{15}N. It was acquired at 273.5 K using $\pi/2$ (14 μs) pulses with a cycling period of 12 s. The strong orthosilicate peak at −71.0 ppm appeared in every spectrum. However, the peak at −131.5 ppm occurred only in the fourth spectrum and was considerably narrower than in Figure 13a, the half-height line-width being only 6 Hz. The signal accounted for ca. 5-10% of the detected Si. (c) Silicon-29 ^{1}H-decoupled NMR spectrum (99.4 MHz) at 273.5 K of the nutrient medium in Figure 13b immediately following the addition of 16 ppm ^{29}Si. No peak is apparent in the vicinity of −131.5 ppm. (See vertical expansion.)

the spectral accumulations an additional signal for silicon in five or six fold coordination was observed. Further experimentation using both solution and solid state NMR spectroscopy of silicon alone and in conjunction with other NMR active nuclei (^{1}H, ^{13}C, $^{14/15}$N) may prove beneficial in our search for the mechanisms by which silicas with controlled structure, form and chemistry are produced in the biological environment.

All of the above-mentioned techniques have many applications in the study of biomineral structures and provide us with clues as to the mechanisms by which such well controlled amorphous gel and particulate structures are formed. We must remember that the chemistry involved in the formation of such well-ordered amorphous materials is regulated by the organisms concerned. We will now consider the two classes of mineralizing organisms that live in water (freshwater and marine) and for which there is a significant amount of knowledge concerning both the mineral phase and the process of mineral formation.

SILICA FORMATION IN SPONGES

Introduction to sponges including structural chemistry

Sponges (the Porifera) are multi-cellular (differentiated) sedentary filter-feeder organisms that occur in both fresh water and marine environments. In the marine environment they can be found in both shallow waters and deep sea environments up to 300 meters where the environment for precipitation will/could be very different as concentrations of dissolved species, temperature, pressure and light levels differ from those found in shallow waters. They possess a well constructed and complex network of water connecting channels and choanocyte chambers, which are lined with the flagellated choanocyte cells (Brusca and Brusca 1990). Sponges can process their own volume of water in ~5 seconds (reviewed in Vogel 1977) thus supplying their cells with oxygen and food and allowing for the elimination of toxic gases. The network of water containing channels will be the route by which silicon, probably as orthosilicic acid will enter the organism.

There are three classes of sponges, two of which produce silicified spicules as their body support (the Hexactinellida and the Demospongiae) and one of which (the Calcarea) that produces calcium carbonate spicules. Spicules are secreted in specialized cells known as sclerocytes. Silicified spicules in the Demospongiae are deposited within a membrane bounded compartment around an axial organic filament but no organic axial filament is found in spicules from Calcarea. The locus of formation is different for these two classes of sponges with the siliceous spicules being deposited intracellularly and the calcium carbonate spicules being produced extracellularly around a number of sclerocyte cells (reviewed in Simpson 1984). The concentration of calcium in seawater is ca. 10 mM and the concentration of silicon is of the order of 2.5% of this value so it is perhaps surprising that silicon is used in the production of a mineral framework! One reason may be the high concentration of polyphosphate found in/with silicified sponges (probably produced by symbiotic bacteria that are not found in calcareous sponges) that is absent in calcareous sponges and would be counterproductive to the production of a carbonate containing calcium mineral (Muller et al. 2003). It is worth noting that work of Muller and others on model "primmorph" systems where silicon provided in the form of sodium hexafluorosilicate at a concentration of 60 micromolar promoted spicule formation but silicon provided as tetraethoxysilane at the same concentration did not promote spicule formation. However, no detailed information on how the silicon containing solutions were prepared has been provided in any of the publications describing this effect (Krasko et al. 2000).

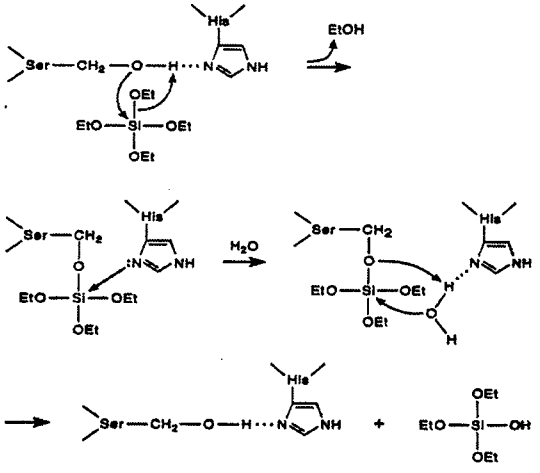

Figure 15. Mechanism of action of silicatein showing the key role of the amino acids present at the active site that are required for activity of the enzyme. Published with permission from Zhou et al. 1999.

Collagen, spiculogenesis and the effect of silicon concentration

Collagen is also required for the formation of the functional skeleton in sponges, particularly the Demospongiae where the spicules are glued together with a collagenous "cement" made of microfibrils (Garrone 1969). The Hexactinellida are different in that their spicules are largely held together with further deposits of silica. Collagens are extracellular matrix proteins that have a triple helical structure that readily form fibrils. Collagens typically contain a $(Gly–X–Y)_n$ (where X and Y are other amino acids) repeating sequence. Examples in the sponge world are n = 24 for *Suberites domuncula* (Schroder et al. 2000) and *E. Muelleri* with n = 79 (Exposito and Garrone 1990).

The formation of siliceous spicules requires the synthesis of both silica and collagen and has been found to only take place if silicon and iron (in available form) are present in the surrounding medium (Muller et al. 2003). The optimum concentration of silicon is between 5 and 100 micromolar, although this is species dependent (Jewell 1935) and detailed studies by Maldonado et al (1999) have shown that not only is silicon essential for spicule formation but that it also modifies the rich diversity of spicule types produced by a particular organism. As an example, Figure 16 shows examples for *Crambe crambe* (Schmidt) grown under different silicon concentrations. In explanation, for most natural populations of C Crambe only one spicule type is observed, namely small needles called styles (Maldonado et al. 1999), however, specimens in some localities also produce larger styles, C-shaped spicules (called isochelae) and centrally-branched aster-like desmas. An explanation for this variability has been obtained by laboratory studies using different concentrations of silicic acid in the growth medium (natural concentrations, ~0.03–4.5 micromolar), and elevated concentrations (~30 and 100 micromolar). The sponges reared in the control or "natural silicon concentration" cultures produced simple styles only but

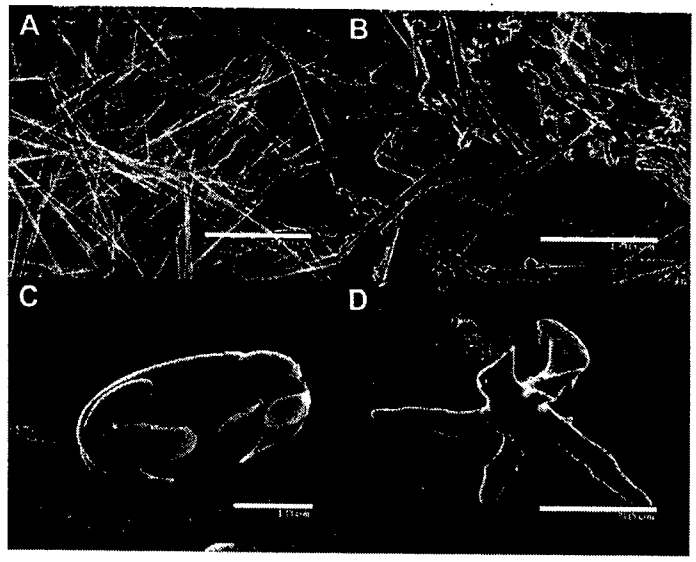

Figure 16. Examples of spicules formed under different concentrations of silicic acid. (A) Control (3 micromolar), only one needle-like spicule type called a style. (B) (30 micromolar) Three spicule types: small styles, Large styles and small C-shaped spicules called isochelae. (C) Larger version of an isochelae showing teeth. (D) Aster-like desma with a developed centrum from samples grown in 100 micromolar silicic acid. Scale bars for (A) and (B) are 100 microns, for (C) 10 microns, and for (D) 50 microns. Modified from Maldonado et al. 1999 and published with permission of Nature Publishing Group.

sponges grown in higher concentrations of silicic acid produced an abundance of at least three different spicule types although some of the spicules appeared deformed for the sponges grown at the highest concentration of silicic acid, perhaps suggesting problems with silicon transport under these conditions. The authors postulated that the changing composition of sea water, in respect of silicon concentration, caused, in part by the rise of the importance of diatoms in geological time around the Cretaceous-Tertiary boundary (Lowenstam and Weiner 1989) may have been a factor in the loss of many varieties of siliceous sponges from shallow waters where silicon concentrations were dramatically reduced. It is also of note that the sponge *Suberites domuncula* grows best at a silicon concentration of 60 micromolar (Simpson et al. 1985). Silicon concentration is also found to affect expression of a gene encoding collagen (the structural protein) and a morphogen, myotrophin (Krasko et al. 2000). Figure 17 shows the relative expression of both collagen and silicatein in the model primmorph system.

The formation of the sponge skeleton is mediated by an Fe^{2+} dependent enzyme (Holvoet and Van de Vyver 1985) and an iron chelator, 2,2'-bipyridine, when added to the sponge medium can inhibit skeletogenesis (as above). Model experiments on *Suberites domuncula* have shown that iron concentrations of 10 micromolar and above stimulate the formation of spicules and stimulate DNA and protein, including ferritin,

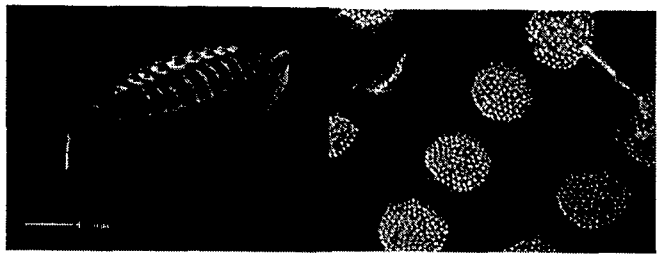

Figure 19. Field emission scanning electron microscope image of the diatom *Surirella sp.* to show the two valves, the raphes and girdle bands. Transmission electron microscope image of the diatom *Navicula pelliculosa* showing examples of the areolae. With the kind permission of Professor Rick Wetherbee.

mucilage is extruded to assist in movement, Figure 19. The silica from which these structures are built up is protected from the external environment by an organic matrix. Although the silica is defined as being "amorphous" at the angstrom level, microfibrillar and hexagonal columnar arrangements have been observed during the development of certain diatoms (Li and Volcani 1985). At maturity certain structures are built up from ~5 nm particles (Perry 1989) and small aggregates around 40 nm (Crawford et al. 2001), Figure 20. Structural studies that have used selective dissolution with sodium hydroxide at high pH have shown that the silica used to build up the diatom frustules varies within the frustule and also between species. The silica in diatoms has been proposed to exhibit proton buffering activity in the oceans, thus enabling the efficient conversion of inorganic bicarbonate to carbon dioxide (Milligan and Morel 2002).

The diatom reproductive cycle, Figure 21 results in the formation of two daughter cells, each retaining half of the original frustule with a new valve being formed within the original cell structure prior to separation of the daughter cells and completion of the girdle bands. At this point it is important to note that the first stage in the process of

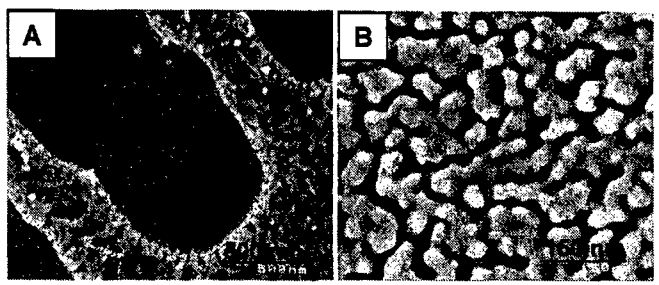

Figure 20. Scanning electron microscope image of ca. 40 nm particles visible within the diatom *Pinnularia sp.* cell wall after treatment with mild alkali. With the kind permission of Professor Rick Wetherbee.

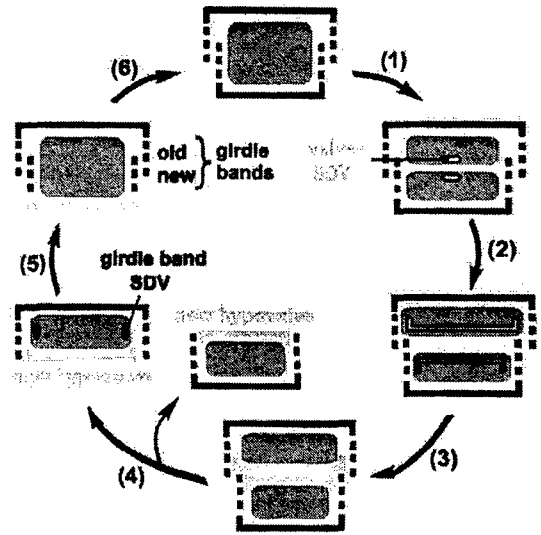

Figure 21. The diatom reproductive cycle. Modified from Kröger and Wetherbee (2000) and used with permission of the publishers. Diatom cells are represented schematically in cross section. The frustule is composed of two halves, the epitheca and the hypotheca. Each theca consists of a valve together with several girdle bands. The extent of silicification and the number of girdle bands are species specific. Stage (1) Division of the cytoplasm and the formation of a silica deposition vesicle within each daughter protoplast. (2) Growth of the silica deposition vesicles and concomitant formation of the new valves. (3) Exocytosis of the newly formed valve. (4) Separation of the daughter cells and the formation of silica deposition vesicles for the girdle bands.(5) Consecutive formation and secretion of the girdle bands. (6) DNA replication. Note, in the early stages of development the silicalemma is represented as thick black lines but at maturity it is no longer visible nor separable from the silica skeleton.

reproduction involves the cytoplasm of the enlarged original or mother cell dividing to provide two localities for the formation of one of each of the required epitheca or hypotheca. Each of the separated cytoplasmic regions "knows" which half of the frustule it is supposed to make! The new valves are formed within silica deposition vesicles of unknown origin that are bounded by a membrane called the silicalemma, the exact nature of which is unknown. It is pertinent to note that any entry of silicic acid and other biochemical components to the developing valve has to take place through the main body of the cytoplasm and for the silicic acid, through the existing valves as the two developing valve structures of the daughter cells are opposed to one another within the mother cell.

The first stage in silicification: transport of the raw ingredients into the cell!

Demonstrations that diatoms could take up silicon from the environment were presented in the mid 50's (Lewin 1955, 1957). In the late 90's evidence that silicic acid is the form in which silicon is generally sequestered were published (Del Amo and Brzezinski 1999) although it was noted that specific diatoms could also take up the

from the siliceous valve (hypotheca or epitheca) formed within the shaped vesicle. However, some information on the chemical environment present in the SDV is known as a result of the use of a fluorescent, cationic, lipophilic dye rhodamine 123 that can accumulate within the SDV that indicates precipitation under acidic conditions around pH 5 (Vrieling et al. 1999). The molecules, other than silica within the SDV are unknown.

Armed with the knowledge that the formation of species specific biominerals other than silica requires the services of biopolymers including proteins and carbohydrates a search has been carried out to find similar regulatory molecules for silicifying organisms including diatoms. For the production of silicified structures, the "control" molecules need to regulate nucleation (location and time of deposition in relation to the organism/cell cycle), growth and cessation of growth. Early observations came from the study of silicifying diatoms where a marked increase in protein concentration in the cell wall was found during silica deposition with carbohydrate incorporation only occurring after silicification (Coombs and Volcani 1968). Nakajima and Volcani also identified the presence of three unusual amino acids, namely 3,4-dihydroxyproline, ε-N-trimethyl-δ-hydroxylysine and its phosphorylated derivative from the cell walls of different diatoms including *Cylindrotheca fusiformis* (Nakajima and Volcani 1969, 1970). They were not able to proceed further with their investigations as they could not isolate the proteins containing these species. Other experiments designed to chemically inhibit protein synthesis during valve development produced morphological abnormalities, suggesting the requirement for *de novo* protein synthesis in biosilicification (Blank and Sullivan 1983). Although the SDV cannot be isolated, researchers have found ways to explore the identity of biopolymers associated with the silica phase. Protein containing extracts have been isolated from various freshwater and marine diatoms and their amino acid composition determined (Hecky et al. 1973; Swift and Wheeler 1992). Treatment of "cleaned" diatoms with buffered HF to dissolve the silica phase released material enriched in serine/threonine (ca. 25 mol%), glycine (ca. 25 mol%) and acidic residues (ca. 20 mol%) (Swift and Wheeler 1992). (It is perhaps notable that none of these researchers identified the unusual amino acids found by Nakajima and Volcani in their extracts). The model proposed by Hecky et al. (1973) envisaged that the serine/threonine-enriched protein would form the inner surface of the silicalemma and, as such, would present a layer of hydroxyls, facing into the SDV, onto which orthosilicic acid molecules could condense. This initial layer of geometrically constrained orthosilicic acid molecules would promote condensation with other orthosilicic acid molecules. Carbohydrates were also found in extracts from the diatoms and this was variously assigned a range of roles including action as a physical buffer between the organism and the aquatic environment, providing resistance to chemical and bacterial degradation and functioning as an ion exchange medium (Hecky et al. 1973).

More recently extremely sophisticated structural studies have been performed on a range of isolates from the diatom cell wall of *Cylindrotheca fusiformis* and three classes of proteins involved with the diatom cell wall identified. Of these groups of molecules, the frustulins with molecular weights ~75–200 kDa are mainly involved in forming a protective coat around the diatom and will not be discussed further (Kroger et al. 1994; Kroger and Sumper 2000). The second family of proteins are known as HEPs (hydrogen fluoride extractable proteins) or pleuralins (Kroger et al. 1997). The apparent molecular weights of these molecules are 150–200 kDa and they are highly acidic molecules with a structure comprising a signal peptide, a proline-rich (> 65%) region, a C-terminal domain and repeats of proline (> 22%)-serine (> 11%)-cysteine (> 11%) aspartate (> 9%) rich domains. The molecules have been sequenced and antibodies raised against the PSCD-domains so that experiments to investigate the cellular localization of these molecules could be performed. Immunoelectronmicrosopy studies showed that for the specific

pleuralin, HEP200 investigated, it is localized only where the epitheca overlaps the hypotheca. It is important to note that the molecule could not be localized during the developmental stages leading to silicification of the girdle bands suggesting that the role of this family of molecules is not with silicification but that it may be involved in establishing a reversible connection between the epitheca and hypotheca, Figure 23. During cell reproduction, this connection must be broken for the new hypotheca and epitheca to form but when these new valves have been formed the connection must again be closed so that the mechanical stability of the daughter cell can be maintained.

The third group of proteins, the low molecular weight (ca. 4–17 kDa (although these molecular weights will have been revised recently when a milder extraction agent was used (Kroger et al. 2002) silaffins (1A, 1B and 2) can also be released from the diatom cell wall using hydrogen fluoride and the sil–1–gene has been sequenced (Kroger et al. 1999, 2001). Structural information obtained for the sil–1 encoded polypeptide displays a modular primary structure that comprises an N-terminus signal peptide, an acidic region having high negative charge and a series of repeat units with a high content of post-translationally modified lysine and serine. Although the sil–1 polypeptide contains several different functional domains, only the repeat units containing high levels of post-translationally modified lysine and serine are found in the polypeptides isolated from diatoms, Figure 24. The structure of these low molecular weight species varies according to the extraction method used (Kroger et al. 2002). The use of a milder extractant, ammonium fluoride, previously used by others (Swift and Wheeler 1992; Harrison 1996) has yielded the most comprehensive information on this family of molecules (Kroger et al. 2002) with both lysine and serine showing post-translational modifications. A range of detailed structural methods including high resolution NMR (proton and multinuclear) and mass spectrometric techniques were required to provide unequivocal evidence for the proposed structures (Kroger et al. 1999, 2001). The chemical modifications of lysine involve the ε-amino group and give rise to ε-N-dimethyllysine or δ-hydroxy-ε-N,N,N-trimethyllysine residues or a modification that has a methyl group on the ε-amino group together with an oligomeric structure consisting of N-methylpropylamine units where between 5 and 10 methylpropylamine groups are attached to the lysine residue (Kroger et al. 1999, 2001). The ε-N-trimethyl-δ-hydroxylysine residue or its phosphorylated derivative as identified by

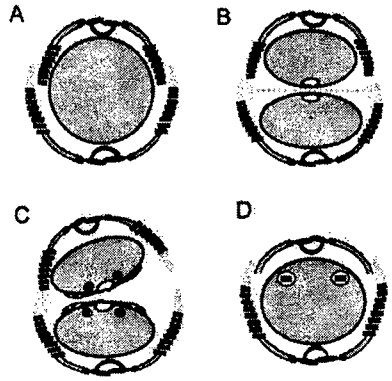

Figure 23. A model scheme showing the overlap of girdle bands and their separation during cell wall development. Published with permission from Kröger and Wetherbee 2000. (**A**) intact diatom, (**B**) cleavage of daughter cells, (**C**) separation of daughter cells, and (**D**) beginning of interphase. Pleuralins are involved in the opening and closing of the two theca during reproduction and the development of daughter cells.

approaches used to monitor the effect of biosilica extracts on silicification include kinetic studies of the early stages of oligomerization, measurement of the mass of centrifugable material obtained after a certain reaction time, the ability of the biopolymer extracts to bind silica and structural studies of rhe silica produced. Very early studies utilizing isolates from diatoms (Swift and Wheeler 1992) did not find any effect on the rate of polymerization of supersaturated solutions of orthosilicic acid at neutral pH contrary to the findings of more recent experiments.

Studies on the effect of silicatein α extracted from sponge spicules on polysiloxane synthesis at neutral pH have shown a ca. 10-fold increase in the amount of harvestable silica compared to experiments run in the presence of the denatured silicatein or proteins such as bovine serum albumin and trypsin (Cha et al. 1999). These studies did not report on whether the protein was occluded within the silica. A catalytic role for the silicatein in the polycondensation of the siloxanes was proposed in a manner analogous to the action of serine- and cysteine-based proteases. The suggested mechanism was that of a general acid/base catalyst with a specific requirement for both serine and histidine amino acids at the active site (Zhou et al. 1999). A scaffolding or structure-directing activity was also reported, as the polymerized silica was able to form a layer following the contours of the underlying protein filament (as extracted from the sponge), behavior that was not observed for the reaction performed in the presence of cellulose or silk fibroin fibers (Cha et al. 1999).

Experiments performed using low molecular weight silaffins (Kroger et al. 1999) in the presence of phosphate buffers have shown that these molecules accelerate the silica condensation process and aid in flocculation, the biopolymer extract being occluded in the silica formed. Silaffins were able to cause a metastable solution of silicic acid to spontaneously aggregate, with small ~50 nm diameter spherical particles being produced in the presence of mixtures of silaffins (1A, 1B and 2) with particles ~700 nm in diameter being produced in the presence of a solution containing a purified silaffin 1A. The silaffins, in the presence of a phosphate buffer, were found to be effective at promoting silicification at sub-neutral pH values down to pH 4. N.B. a pH value of around 5 has been measured for the lumen of the silica deposition vesicle (Vrieling et al. 1999). The provision of highly positively charged side chains has been thought to be very important in enabling the silaffins to promote condensation and aggregation under mildly acidic conditions. Most recently, phosphorylated silaffins, isolated when milder extraction methods were used to remove the siliceous phase have been examined for their silica forming ability (Kroger et al. 2002). NatSil–1A is able to precipitate silica from a monosilicic acid solution in the absence of additional phosphate (change of buffer systems) and the activity of silaffin–1A can be totally restored if an excess of phosphate is added to the system. As before, 400–700 nm diameter silica spheres were formed in a short reaction time. The authors conclude that the numerous phosphate groups in natSil–1–A serve as an intrinsic source of anions required for silica formation by diatoms. Further, they provided evidence that the zwitterionic structure of natSil–1–A (polyamine moieties and phosphate groups) form ionic strength dependent aggregates via electrostatic interactions. They hypothesize that silaffin self-assembly provides a template for silicic acid polycondensation and have shown through a detailed microscopic study the formation of silica spheres from an initial "plastic" silica–natSil–1–A phase. They believe that this "plasticity" may be important in the molding of diatom silica for all structural components other than those that require patterning on the nanoscale to produce nanoscale pores, for example. Other *in vitro* experiments have been conducted separately on the polyamines extracted from *Nitzschia angularis* (the species examined to date for which the largest number of polyamines have been found). These have also been investigated for their ability to promote silica formation (Kroger et al. 2000). A range of spherical silica particles were formed, the size and

distribution of sizes depending on the pH of the reaction mixture and the molecular weight of the polyamine fraction used. For experiments conducted at a fixed pH (pH 5) smaller sized particles were found when lower molecular weight polyamines (600–700 Da) were used. If pH is increased from ca. 5 to 8 then particle sizes fall from ca. 700 nm to 50 nm, all other experimental conditions remaining constant, Figure 25. It will be interesting to see what effect the combination of natSil–1–A and polyamines will have on silica formation, on its rate of precipitation and the form of the silica deposited.

How to go from molecular level chemical control to macroscopic control?

In all biomineralized organisms, chemical control at the molecular control is manifest in structural regulation at the visible level. It is still a mystery how three-dimensional structures are produced from information contained in chemical form (Pickett-Heaps et al. 1990). In all the studies described above, no mention has been made of the processes by which specific features in the diatom (or for that matter the sponge) are formed. An excellent review on this subject, amongst others by Hildebrand and Wetherbee (2003) is a good starting point for this subject. The entire cell components seem to be involved in formation of the silicified frustule with its many innate structural features including raphe, areolae, girdle bands etc. The process of silicification,, in conjunction with all the other stages of cell division are tightly coordinated. In order to study the relationships between cell organelles and silica deposition electron microscopy has proved invaluable as it is a technique that is able to visualize all components within the cell, albeit only in a static mode and in two dimensions. Microtubules, microfilaments and mitochondria have all been shown to occupy specific locations prior to and during silicification (Hildebrand and Wetherbee 2003 and references therein). The pattern of deposition in valves is generally from the outside in (Cox 1999) but there are examples for both centric and pennate diatoms where the deposition pattern is the opposite way round (Cox 1999; Schmid and Volcani 1983; Crawford and Schmid 1986). Pore patterns are also under cellular control and mathematical models based on the maintenance of optimal packing have been used to explain observed pore patterns (Longuet-Higgins 2001). Observation of diatom structures in detail suggests that a substantial amount of molding is involved in their formation. Evidence for this comes from the study of frustules where some surfaces appear smooth and some rough. The smooth surfaces are proposed to arise from silica being shaped directly by the silicalemma, or the outer membrane structure of the silica deposition vesicle. The shape of the silica deposition vesicle is not only governed by the chemical composition and structure of those molecules proposed to be involved in silica deposition. Microtubules, derived from actin and microfilaments are also involved (Chiappino and Volcani 1977; van der Meene and Pickett-Heaps 2002). Their role is in the determination of size and in manipulation of the shape of the silica deposition vesicle, however, much remains to be discovered concerning the relationship between the "chemistry" involved in silica precipitation and its subsequent manipulation within the silica deposition vesicle to produce objects that have both form and function. A model has been proposed by Sumper (2002) to explain the nanopatterning of silica in diatoms via phase separation. The polyamines isolated from a range of diatoms (Kroger et al. 2000) are methylated and exhibit amphiphilic properties. The model postulates the existence of repeated phase separation processes within the silica deposition vesicle which produce emulsions of microdroplets and, subsequently, nanodroplets or micelles consisting of a polyamine-containing organic phase. It is proposed that the contact sites between polyamine droplets and the aqueous phase that contains the hydrophilic silicic acid promotes silicic acid polymerization, the resulting silica occupying the spaces between the droplets. Modification of the size and packing of the droplets will then lead to different patterns of silica being observed.

Where to from here?

Silica formation in the natural environment requires the uptake, transport, condensation, growth, precipitation and molding of species involving silicic acid. Significant progress has been made in respect of transport and in respect of the role(s) played by biomacromolecules in the controlled formation of silica structures. However, much is not understood and there are many unresolved controversies concerning uptake, transport and the specific role of silica associated biomolecules such that there is plenty of scope for scientists wishing to enter the field and to make a contribution to the understanding of the processes required to make and mold an amorphous mineral that is able to withstand pressure (sponges are found at depths of ~300 m), dissolution (for all organisms found in water) and predation (water- and land-based species) by a range of animals. The information obtained in this search will, however, assist us in our understanding of the essentiality of silicon to life processes and in the generation of new materials with specific form and function for industrial application in the twenty-first century. A new approach to this area has been the use of a combinatorial phage peptide display library to select for peptides that bind silica (Naik et al. 2002). The information so gained from these studies may help us in our search for biomolecules necessary for the production of organized silicified structures in a wide range of biological organisms.

ACKNOWLEDGMENTS

The author would like to thank ESRC, AFRC, BBSRC, Ineos Chemicals, The EU and AFOSR for their interest and funding of research programs in biological and biomimetic silica chemistry. Members of my research group (David Belton, Neil Shirtcliffe, and Jian Xu) are thanked for help with preparation of figures.

BIBLIOGRAPHY

Bauerlein E (2003) Biomineralization of unicellular organisms: an unusual membrane biochemistry for the production of inorganic nano- and microstructures. Angewandte Chemie 42(6):614–641 (a review of biomineralization—iron oxide, calcium carbonate and silica—pertaining to single cell organisms)

Hildebrand M, Wetherbee R (2003) Components and control of silicification in diatoms. *In:* Silicon Biomineralization: Biology-Biochemistry-Molecular Biology-Biotechnology, Progress in Molecular and Subcellular Biology. Vol 28. Müller WEG (ed) Springer, New York, p 11–57 (a review on the "state of the art" in all aspects of diatom biomineralization research)

Jones JB, Segnit ER (1971) Nature of opal. I. Nomenclature and constituent phases. J Geol Soc Aust 18:57–68

Kroger N, Sumper M (2000) The biochemistry of silica formation. *In:* Biomineralization from biology to biotechnology and medical application. Bauerlein E (ed) Wiley-VCH, Weinheim, Germany, p 151–170 (a review on the role of the organic matrix in diatom silicification

Perry CC (2001) Silica in Encyclopedia of Life Sciences http:/www.els.net London, Nature Publishing Group, London (précis on silica in biological organisms)

Perry CC, Keeling-Tucker T (2000) Biosilicification: the role of the organic matrix in structure control. J Biol Inorg Chem 5:537–550 (a review on the specifics of silica chemistry, the organic matrix in sponges, diatoms and plants, *in vitro* reactions and molecular modeling)

Simpson TL, Volcani BE (eds) (1981) Silicon and Siliceous Structures in Biological systems, Springer-Verlag, New York (a book containing many wonderful images of silicified organisms) specific chapters of relevance are chapter 2 on silicon in the cellular metabolism of diatoms by Sullivan and Volcani, Chapter 6 on the siliceous components of the diatom cell wall and their morphological variation by Crawford, Chapter 7 on cell wall formation in diatoms, morphogenesis and biochemistry, Chapter 16 on the form and distribution of silica in sponges by Hartmann and Chapter 17 on ultrastructure and deposition of silica in sponges by Garrone, Simpson and Pottu-Boumendil. The book, although dated contains much relevant information to the study of silicification in diatoms and sponges as well as providing information on silicification in other organisms.

REFERENCES

Bhattacharyya P, Volcani BE (1980) Sodium-dependent silicate transport in the apochlorotic marine diatom *Nitzschia alba*. Proc Natl Acad Sci USA 77:6386–6390

Blank GS, Sullivan CW (1983) Diatom mineralization of silicic acid. VI. The effects of microtubule inhibitors on silicic acid metabolism in *Navicula saprophila*. J Phycol 19:39-44

Brinker CJ, Scherrer GW (1990) Sol-Gel Science—The Physics and Chemistry of Sol-Gel Processing, Academic Press, London

Brusca RC, Brusca GJ (1990) Invertebrates. Sinauer Associates Publishers, Sunderland, UK

Cha JN, Shimizu K, Zhou Y, Christiansen SC, Chmelka BF, Stucky GD, Morse DE (1999) Silicatein filaments and subunits from a marine sponge direct the polymerization of silica and silicones in vitro. Proc Natl Acad Sci USA 96:361–365

Chiappino ML, Volcani BE (1977) Studies on the biochemistry and fine structure of silica shell formation in diatoms. VIII. Sequential cell wall development in the pennate *Navicula pelliculosa*. Protoplasma 93:205–221

Chisholm SW, Azam F, Eppley RW (1978) Silicic acid incorporation in marine diatoms on light:dark cycles: use as an assay for phased cell division Limnol Oceanogr 23:518–529

Conway HL, Harrison PJ (1977) Marine diatoms grown in chemostats under silicate or ammonium limitation. IV. Transient response of *Chaeteroceros debilis*, *Skeletonema costatum* and *Thalossiosira gravida* to a single addition of the limiting nutrient. Mar Biol 43:33–43

Coombs J, Volcani BE (1968) Studies on the biochemistry and fine structure of silica-shell formation in diatoms. Chemical changes in the wall of *Navicula pelliculosa* during its formation. Planta 82:280–292

Cox EJ (1999) Variation in patterns of valve morphogenesis between representatives of six biraphid diatom genera. J Phycol 35:1297–1312

Crawford RM, Schmid AM (1986) Ultrastructure of silica deposition in diatoms. *In:* Biomineralization in lower plants and animals. Vol 30. Leadbetter BS, Riding R (eds) System Soc. Oxford Univ Press, Oxford, p 291–314

Crawford SA, Higgins MJ, Mulvaney P, Wetherbee R (2001) Nanostructure of the diatom frustule as revealed by atomic force and scanning electron microscopy. J Phycol 37:543–554

Del Amo Y, Brzezinski MA (1999) The chemical form of dissolved Si taken up by marine diatoms. J Phycol 35:1162–1170

Engelhardt G, Hoebbel D, Tarmale M, Samoson A, Lippmaa E (1982) Si-29 NMR investigations of the anion structure of crystalline tetramethylammonium-aluminosilicate and aluminosilicate solutions. Z Anorg Allg Chem 484:22–32

Exposito JY, Garrone R (1990) Characterisation of a fibrillar collagen gene in sponges reveals the early evolutionary appearance of two collagen families. Proc Natl Acad Sci USA 87:6669–6673

Frondel C (1962) The System of Mineralogy of DANA, 7th Edition. Vol 3. Wiley, New York

Garrone R (1969) Collagene, spongine et squelette mineral chez l'eponge *Haliclona rosea*. J Microscop 8:581–598

Goff SA, Ricke D, Lan TH, Presting G, Wang R, Dunn M, Glazebrook J, Sessions A, Oeller P, Varma A et al. (2002) A draft sequence of the rice genome (*Oryza sativa L. ssp. Japonica*) Science 296:92–100

Harrison CC (1996) Evidence for intramineral macromolecules containing protein from plant silicas. J Phytochem 41:37–42

Harrison CC, Loton N (1995) Novel routes to designer silicas-studies of the decomposition of $(M^+)_2[Si(C_6H_4O_2)_3]\cdot xH_2O$, the importance of M^+ identity on the kinetics of oligomerization and the structural characteristics of the silicas produced. J Chem Soc Faraday Trans 91:4287–4297

Hecky RE, Mopper K, Kilham P, Degens ET (1973) The amino acid and sugar composition of diatom cell walls. Marine Biology 19:323–331

Hench LL, West JK (1990) The sol-gel process. Chem Rev 90:33–72

Hildebrand M (2000) Silicic acid transport and its control during cell wall silicification in diatoms. *In:* Biomineralization: from biology to biotechnology and medical application. Baeuerlein E (ed) Wiley-VCH, Weinheim p 171-188

Hildebrand M, Volcani BE, Gassmann W, Schroeder JI (1997) A gene family of silicon transporters. Nature 385:688–689

Hildebrand, M, Dahlin K, Volcani BE (1998) Characterization of a silicon transporter gene family in *Cylindrotheca fusiformis*: sequences, expression analysis, and identification of homologs in other diatoms. Molec General Genetics 260:480–486

Hildebrand M, Wetherbee R (2003) Components and control of silicification in diatoms. *In:* Silicon Biomineralization: Biology-Biochemistry-Molecular Biology-Biotechnology. Progress in Molecular and Subcellular Biology Vol. 28. Müller WEG (eds) Springer, New York, p 11–57

Schmidt M, Botz, R, Rickert D, Bohrmann G, Hall SR, Mann S (2001) Oxygen isotopes of marine diatoms and relations to opal-A maturation. Geochim Cosmochim Acta 65:201–211
Schroder HC, Krasko A, Batel R, Skorokhod A, Pahler S, Kruse M, Muller IM, Muller WEG (2000) Stimulation of protein (collagen) synthesis in sponge cells by a cardiac myotrophin-related molecule from Suberites domuncula. FASEB J 14:2022–2031
Shimizu K, Cha J, Stucky GD, Morse DE (1998) Silicatein α: Cathepsin L-like protein in sponge biosilica. Proc Natl Acad Sci USA 95:6234–6238
Shimizu K, del Amo Y, Brzezinski MA, Stucky GD, Morse DE (2001) A novel fluorescent silica tracer for biological silicification studies. Chem Biol 8:1051–1060
Simpson TL (1984) The cell biology of sponges. Springer, Berlin Heidelberg New York
Simpson TL, Gil M, Connes R, Diaz JP, Paris J (1985) Effects of germanium (Ge) on the silica spicules of the marine sponge *Suberites domuncula*: transformation of the spicule type J Morphol 183:117–128
Simpson TL, Refelo LM, Kaby M (1979) Effects of germanium on the morphology of silica deposition in a freshwater sponge. J Morphol 159:343–354
Simpson TL, Volcani BE (eds) (1981) Silicon and Siliceous Structures in Biological Systems. Springer, New York
Stöber W, Fink A, Bohn, (1968) Controlled growth of monodisperse silica spheres in the micron size range. Colloid Interface Sci 26:62–69
Sullivan CW (1977) Diatom mineralization of silicic acid (II) Regulation of silicic acid transport rates during the cell cycle of *Navicula pelliculosa*. J Phycol 13:86–91
Sumper M (2002) A phase separation model for the nanopatterning of diatom biosilica. Science 295:2430–2433
Swift DM, Wheeler AP (1992) Evidence of an organic matrix from diatom biosilica. J Phycol 28:202–209
Tarutani T (1989) Polymerization of silicic acid: a review. Anal Sci 5:245–252
Van der Meene AML, Pickett-Heaps JD (2002) Valve morphogenesis in the centric diatom *Proboscia alalta* Sundstrom J Phycol 38:351–363
Vogel S (1977) Current-induced flow through living sponges in nature. Proc Natl Acad Sci USA 74:2069-2071
Vrieling EG, Gieskes WWC, Beelen TPM (1999) Silica deposition in diatoms: control by the pH inside the silica deposition vesicle. J Phycol 35:548–559
Vrieling EG, Beelen TPM, van Santen RA, Gieskes WWC (2000) Nano-scale uniformity of pore architecture in diatomaceous silica: a combined small and wide angle X-ray scattering study. J Phycol 36:146–159
Vrieling EG, Beelen TPM, van Santen RA, Gieskes WWC (2002) Mesophases of (bio)polymer-silica particles inspire a model for silica biomineralization in diatoms. Angew Chem Int Ed 41:1543–1546
Watt F, Grime GW, Brook AJ, Gadd GM, Perry CC, Pearce RB, Turnau K, Watkinson SC (1991) Nuclear microscopy of biological specimens. Nucl Instrum Meth Phys Res B54:123–143
Werner D (1966) Silicic acid in the metabolism of *Cyclotella cryptica*. Arch Mikrobiol 55:278–308
Wetherbee R, Crawford S, Mulvaney P (2000) The nanostructure and development of diatom biosilica. *In:* Biomineralization; from Biological to Biotechnology and Medical Applications. Baeuerlein E (ed), Wiley VCH, Weinheim, Germany, p 189–206
Yang H, Coombs N, Ozin GA (1997) Morphogenesis of shape and surface patterns in mesoporous silica. Nature 386:692–695
Yu J, Hu S, Wang J, Wong GK, Li S, Liu B, Deng Y, Dai L, Ahou Y, Zhang X et al. (2002) A draft sequence of the rice genome (*Oryza sativa L. ssp. indica*). Science 296:79–92
Zaslavskaia LA, Lippmeier JC, Kroth PG, Grossman AR, Apt KE (2001) Transformation of the diatom *Phaeodactylum tricornutum* with a variety of selectable markers and reporter genes. J Phycol 36:379–386
Zhou Y, Shimizu K, Cha JN, Stucky GD, Morse DE (1999) Efficient catalysis of polysiloxane synthesis by Silicatein α requires specific hydroxy and imidazole functionalities. Angew Chem Int Ed 38:780–782

ARTICLE

Journal of Materials Chemistry
www.rsc.org/materials

Towards an understanding of (bio)silicification: the role of amino acids and lysine oligomers in silicification

David Belton, Gary Paine, Siddharth V. Patwardhan and Carole C. Perry*

Division of Chemistry, Interdisciplinary Biomedical Research Centre, School of Science, The Nottingham Trent University, Clifton Lane, Nottingham, UK NG11 8NS. E-mail: Carole.Perry@ntu.ac.uk

Received 9th February 2004, Accepted 10th May 2004
First published as an Advance Article on the web 8th June 2004

In order to understand the role that proteins play in the generation of well regulated biosilica structures we need to understand the contribution of the components, singly and in combination. To this end we have performed a systematic study of the effect of amino acids and small peptide oligomers on silica formation from aqueous solution. Silicas produced from a potassium silicon catecholate salt at *ca.* pH 7 in the presence of the amino acids (Gly, Arg, Asn, Gln, Glx, Ser, Thr, Tyr, Pro, Ala, Lys) at a 2 Si : 1 amino acid molar ratio have shown that these amino acids affect the kinetics of small oligomer formation, the growth of aggregate structures and the morphology and surface properties of the silicas produced. The effects seen during the early stages of oligomer formation carry through to the properties of the particles and aggregates produced after extended periods of reaction. The behaviour of the amino acids relates to the pI and hydrophobicity of the individual amino acids. The presence of the nitrogen containing amino acids generates larger particles and the presence of amino acids containing hydroxyl and hydrophobic groups generates silicas with smaller particles than are produced for silicas produced in the absence of amino acids. An extensive study of the effect of the number of lysine and glycine units per peptide was also performed (for lysine, 1–5 and *ca.* 150 and for glycine, 1,4,5). Increasing the number of glycine units per additive molecule had little effect on the kinetics, aggregation, sample morphology, surface area and porosity of the silicas produced. A distinct relationship between the number of lysine units per additive molecule and an increased rate of oligomer formation, aggregate growth and a reduction in silica surface area and broadening of pore sizes was observed. A distinct change over in behaviour, particularly in regard to the porosity characteristics of the silica produced was noted for between $(lys)_3$ and $(lys)_4$ as well as this being the smallest size of peptide that was incorporated into the siliceous material formed. Aggregation was observed to accelerate exponentially over the full range of lysine oligomers used. Consecutive sequences of the same amino acid residues were shown to produce effects much larger than the sum of the effects of the individual residues, and at extremes mediate macroscopic morphological changes. The consequences of these findings for biosilicification are discussed. It is clear that all amino acid functional groups in proteins that are accessible to silica during the stages of formation from orthosilicic acid through to the final material have a role to play in determining the physical nature and structure of the material that forms.

Introduction

Scientists have been interested in biomineralisation for many years not only as a result of the sophistication that is achieved in the form of the crystalline and amorphous biomineral structures but also because composition and growth are so clearly regulated both spatially and temporally with minerals being produced under benign reaction conditions.[1] Furthermore, biominerals are extremely fine examples of organic–inorganic hybrid materials where the properties of the two phases when present together are more than the sum of their parts with peculiar strengths, resistance to degredation *etc.* being achieved.[2] These materials and new materials produced as a consequence of understanding the chemistry and biology used to form them could have tremendous technological implication in the development of materials and biomaterials with superior properties to those currently available.[3,4] Formation of ornate biosilica structures is of particular interest due to the peculiar physical and chemical nature of biosilica.[5–7] The silicas so formed show control of particles sizes, aggregation patterns and surface chemistry,[8–10] properties that are difficult to control during conventional syntheses. In addition, as the market for silicon-based materials is vast,[11] it is important to investigate the mechanisms underpinning the formation of biosilicas as an understanding of the processes may help us to develop novel silicon-based materials for potential application in areas as diverse as photonics, catalysis and biotechnology including drug delivery.[8] Biosilicas are formed in the presence of protein containing molecules with such molecules being isolated from the biogenic silica of higher plants,[12,13] sponges[14] and diatoms.[15–17] The proteinaceous materials have been proposed to regulate biosilicification *in vivo* in their respective systems.

In order to understand the role(s) of various biomolecules in biosilicification, various *in vivo* and *in vitro* studies have been undertaken. In particular, bioextracts from *Equisetum telmateia* and *Equisetum arvense* plants have been studied.[13,18] Upon amino acid analysis of the protein extracts, it was revealed that they contain relatively high amounts of proline and acidic residues (glutamic acid and aspartic acid) although it should be noted that the analysis procedure was not able to distinguish if the acids or their amide counterparts were originally present in the extracted proteins. When studied for their interaction with silicic acid, the bioextracts were found to direct the formation of silica in model studies performed *in vitro*.[8,13,18] These bioextracts when present at 1% by weight of the precipitatable silica (approximating to the living system), affected the kinetics of oligomer formation, reduced the primary particle size of silica from 4 nm to less than 2 nm and led to some crystalline silica being produced from aqueous solution at room temperature and pressure. Particular protein

DOI: 10.1039/b401882f

kinetics (the formation of trimers from monomers and dimers), reversible first order kinetics (the addition or removal of orthosilicic acid to/from trimers or larger oligomers) or Ostwald ripening was the dominant reaction (with little measurable change in the concentration of silicic acid being detected) were obtained. For the period where apparent third order kinetics were followed, a plot of $1/[Si(OH)_4]^2$ *vs.* time gave a straight line with the rate constant being obtained from the gradient of the plot. For the period where reversible first order kinetics were followed a plot of $\ln(A - A_t)$ *vs.* time gave a straight line of slope $(k_+ + k_-)$ where A is the concentration at any time and A_t the concentration of orthosilicic acid at equilibrium (here taken as the value measured after 24 hours reaction). The separate rate constants for the forward and reverse reaction were obtained using the equilibrium constant K, which is the ratio of the forward and reverse rate constants and is also the ratio of the oligomerised silica and the equilibrium concentration of orthosilicic acid present in solution.[28]

Photon correlation spectroscopy

Samples were also prepared for dynamic light scattering analysis. Samples were taken from the orthosilicic acid condensation experiments immediately on pH adjustment (amino acid study), or mixing (lysine oligomer study), and filtered through a 200 nm membrane into a 1 cm polymethylmethacrylate cell. Aggregation of silica particles was then monitored over a 40 hour period using a Coulter N4 plus photon correlation spectrometer with a He–Ne (632.8 nm) laser supply. All measurements were carried out at an angle of 90° and at 293 K. Measurements obtained were averages of the data collected over intervals of 2 to 60 minutes, the time selected depending on the rate of particle growth. Values of particle size are presented for comparative purposes and should not be taken as absolute values and are here referred to as 'apparent' particle size.

Scanning electron microscopy

For SEM studies, lyophilised samples were dispersed onto double-sided sticky tape and mounted on aluminium stubs with the edges of the sticky tape being painted with quick drying silver paint to prevent charging of the sample. All loose aggregates were removed by tapping the stub before the silica samples were gold coated with an argon plasma at 1.2 kV and 4 mbar pressure for 2 minutes using an Edwards S150B sputter coater. Images were acquired using a JEOL JSM-840A scanning electron microscope with an accelerating voltage of 20 kV. Average particle sizes were calculated by measuring all distinct particles within 1 μm^2 areas and averaging. If this proved impossible particle sizes were measured over larger areas of the obtained images.

Surface area analysis

Surface area measurements were obtained from 12–30 mg quantities of precipitated silica obtained after 168 hours reaction. Single point measurements and full BET isotherms were obtained using a fully automated Micromeritics Tristar 3000 (Ineos Silicas, Warrington). Samples were degassed at 403 K for a minimum of 16 hours before analysis at liquid nitrogen temperatures. The specific surface area was obtained *via* the BET method[30] where nitrogen is assumed to have a cross-sectional area of 0.16 nm^2. Pore size distributions were calculated by the application of BJH theory[31] to the desorption branch of the isotherms as all samples showed similar adsorption/desorption behaviour.

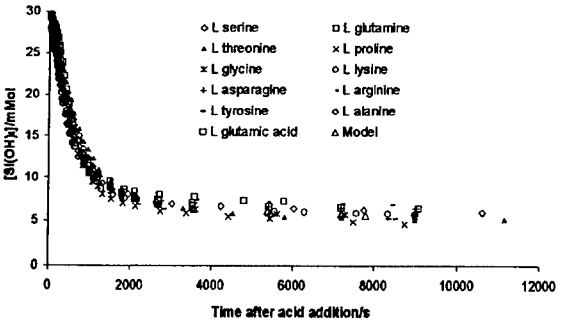

Fig. 1 Changes in orthosilicic acid concentration with time following initiation of the reaction by pH reduction to 7.0 for a 30 mmol dm^{-3} solution of $K_2[Si(Cat)_3]\cdot 2H_2O$ in the presence of 15 mmol dm^{-3} of selected amino acids.

Thermal gravimetric analysis

The organic material associated with the sedimentable silica was detected by thermal gravimetric analysis. Analysis was performed under nitrogen using a Stanton Redcroft TG 760 furnace, balance controller and UTP temperature controller with a heating rate of 10 K min^{-1} with data being sampled every 30 seconds. Entrained organic content was calculated by comparison of weight loss between 400 and 800 K relative to the silica produced from the catecholate complex alone.

Results

Solution chemistry

The residual undissociated complex for reactions performed in the presence of a 1 amino acid : 2 silicic acid molar ratio after 24 hours reaction varied from 0.2–0.6 mmol dm^{-3}, corresponding to an initial orthosilicic acid concentration for the condensation experiments of 29.4 to 29.8 mol dm^{-3} (98–99%). The pH of all solutions was in the range 6.8 ± 0.2. Silicic acid concentrations were monitored from 30 seconds after initiation of the reaction (by lowering of pH or mixing) until 24 hours of reaction had elapsed, Fig. 1 shows plots of silicic acid concentration with time in the presence of amino acids. The data for the blank model sample is shown for comparison. Table 1 lists the third order and apparent first order rate constants for the reactions performed in the presence of the amino acids. None of the experiments showed a dominant dimerisation phase where no loss in silicic acid with time was observed.

The region of 3rd order dominance occurred during the first 3 minutes of condensation for reaction with all the amino acids studied. Increased rates of condensation were observed for arginine, asparagine, lysine and glutamine and slower rates of condensation, compared to the blank system for reactions

Table 1 3rd and 1st order rate constants for orthosilicic acid condensation in the presence of selected amino acids

Amino acid	3rd k/ 10^{-6} mM^{-2} dm^6 s^{-1}	1st order condensation rate constant k_+/s^{-1}	1st order dissolution rate constant k_-/s^{-1}
Ser	0.97	0.001362	0.000238
Gln	1.56	0.001425	0.000275
Thr	0.48	0.001062	0.000138
Pro	1.18	0.001237	0.000163
Gly	0.84	0.001452	0.000248
Lys	1.62	0.001451	0.000249
Asn	1.60	0.001446	0.000254
Arg	2.04	0.001163	0.000237
Tyr	1.30	0.001318	0.000183
Ala	0.89	0.001225	0.000175
Glu	0.605	0.00129	0.00021
Blank	1.30	0.001201	0.000199

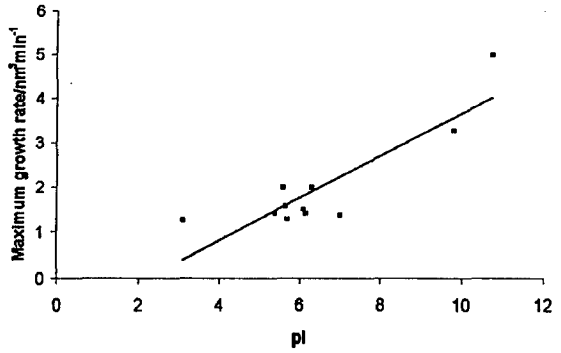

Fig. 5 Maximum growth rate of the structures as measured by photon correlation spectroscopy in relation to the isoelectric points of the side chain functional groups of selected amino acids. The line shows the trend only.

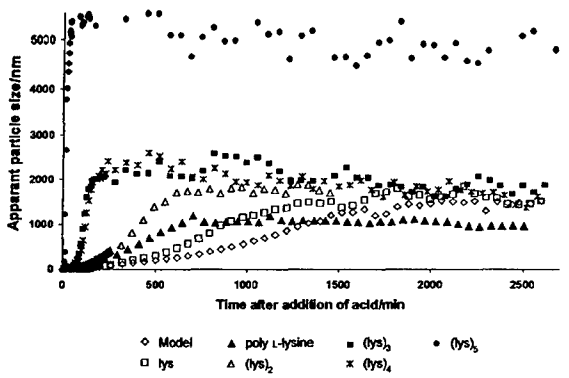

Fig. 6 Photo correlation spectra obtained from 30 mmol l^{-1} solutions of $K_2[Si(Cat)_3]\cdot 2H_2O$ in the presence of $(lys)_n$ where the total concentration of the lysine functional groups is 15 mmol l^{-1} over a period of 40 hours reaction.

For all systems a growth boundary was observed where there was an increased scatter in the data which was also marked by a decrease or cessation in the aggregation growth. The shortest times for this boundary were observed for L-arginine and L-lysine (1000 and 1300 min respectively), for all others the time was between 1500 and 1600 min. The rates and boundary times were found to be largely in line with the pI of the amino acids and was shown to be most significant where the amino acid side chains were expected to be charged at the pH of the experiments, Fig. 5.

For precipitation experiments performed in the presence of L-lysine homopeptides, aggregation rates were dramatically increased with lysine units from 3.3 nm^3 min^{-1} to 103 × 10^6 nm^3 min^{-1} for the range mono to penta L-lysine, Fig. 6, 7. Apparent maximum particle size increased from mono to penta L-lysine from 1800 nm to 5900 nm, Fig. 7. The boundary times decreased with increased L-lysine number from 1640–40 minutes and were followed by a period of contraction observed for di

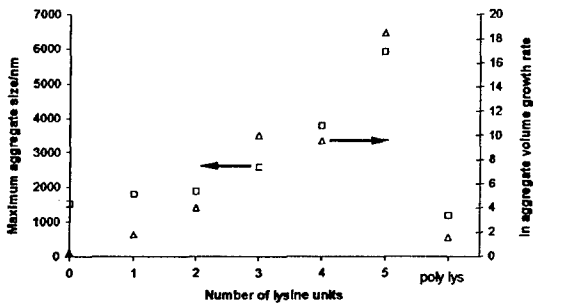

Fig. 7 Maximum growth rate and maximum apparent particle size for silica aggregating in the presence of lysine oligomers.

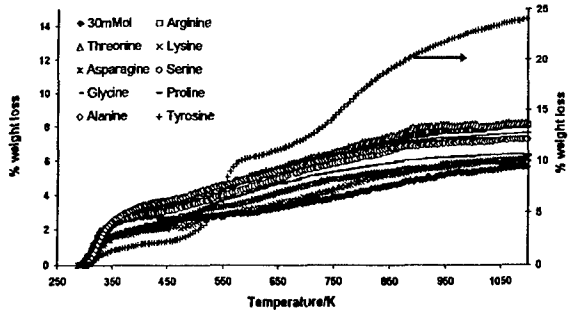

Fig. 8 Thermogravimetric analysis of silicas condensed in the presence of selected amino acids.

L-lysine to penta L-lysine but not for reactions carried out in the presence of the monomer or for the control reaction. Glycine oligomers showed little change in the aggregation rate (1.5–2.6 nm^3 min^{-1}), boundary times were all ~1500 min and no subsequent contraction was observed (data not presented).

Residual organic material in sedimented silica

Residual organic material entrained within the sedimentable silica (not removed on washing with distilled water) was determined as the weight lost during thermogravimetric analysis over the temperature range 400–800 K after subtraction of the underlying loss of weight through silanol condensation over the same range (*i.e.* for the blank system), Fig. 8 and 9. This temperature range corresponded to the thermal decomposition of organic compounds and resulted in the loss of CO_2, H_2O, NH_3 and some short chain volatile rearrangement products. In the experiments carried out under nitrogen, darkening of samples was observed, which may indicate the possibility of the presence of residual organic matter.

For silicas condensed in the presence of amino acids, only materials prepared in the presence of L-tyrosine showed a significant weight loss over the temperature region highlighted. This was thought to be due to its low water solubility rather than its incorporation into the silica matrix.

The L-lysine homopeptides showed increasing incorporation with increasing chain length with 9% penta L-lysine retained and 18% poly L-lysine retention, Fig. 10. Glycine oligomers by comparison showed little organic componant in the silica produced—the maximum found was ~0.5% in pentaglycine (data not presented).

Gas adsorption analysis

Silica samples produced in the presence of amino acids gave type IV isotherms with H2 hysteresis typical of micro/mesoporous materials. Surface area analysis by the BET method gave values between 538 and 730 m^2 g^{-1}. A correlation between surface area and side chain hydrophobicity was

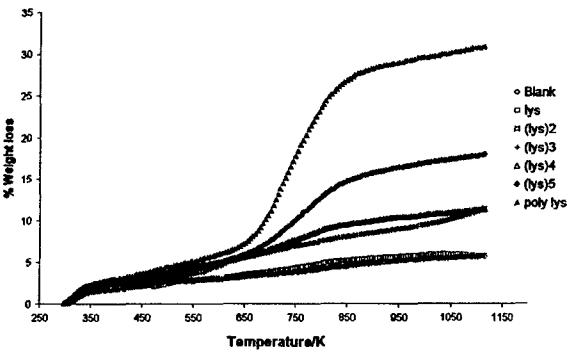

Fig. 9 Thermogravimetric analysis of silicas produced in the presence of $(lys)_n$.

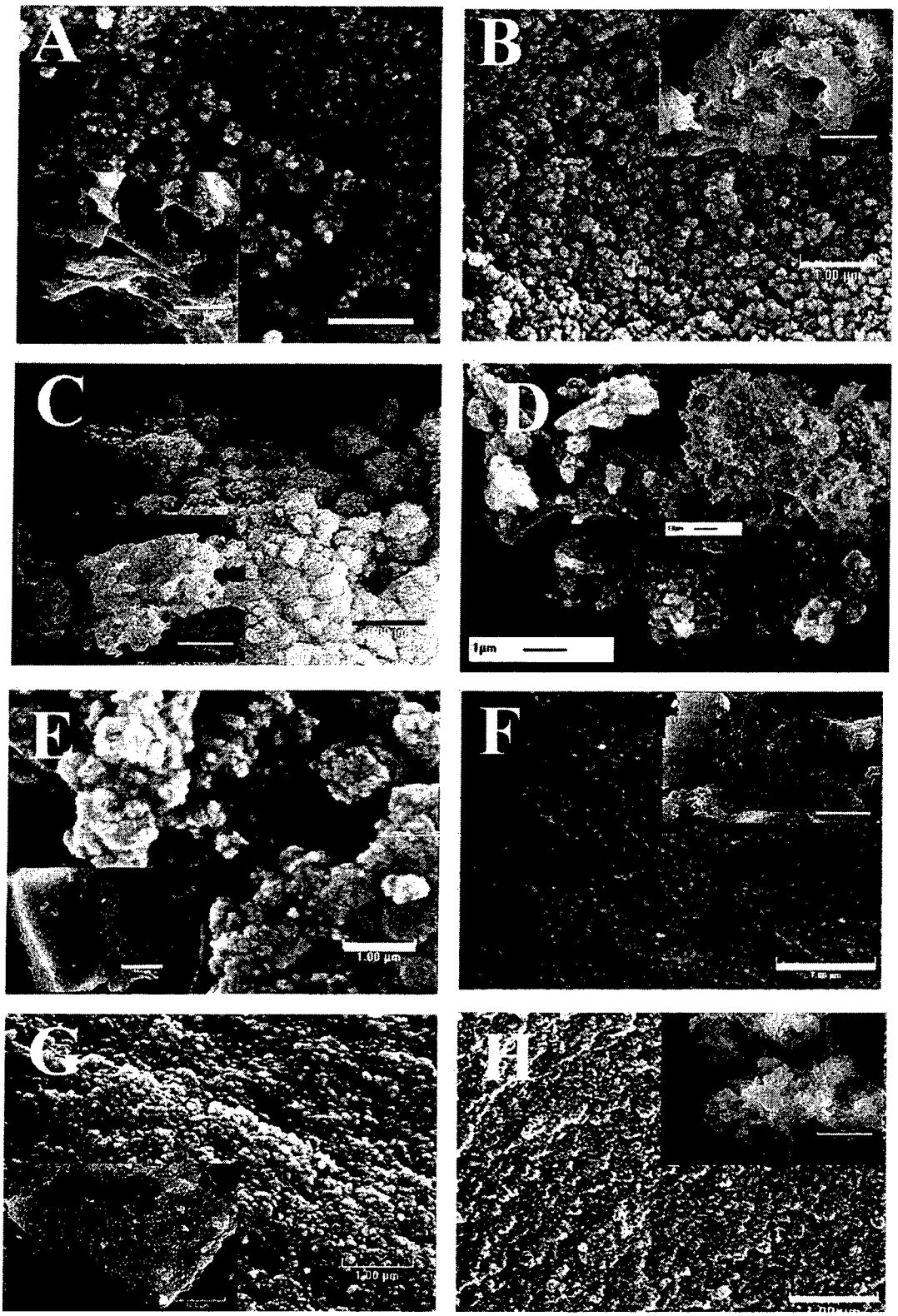

Fig. 15 Scanning electron micrographs of silicas produced in the presence of selected amino acids. A. arginine, B. asparagine, C. glutamic acid, D. glycine, E. glutamine, F. alanine, G. lysine, H. blank. Scale bars represent 1 μm (inserts 10 μm).

in silica formation, it is clear that all the nitrogen-containing amino acids investigated have an effect on the aggregation of silica particles. In order to investigate this phenomenon in detail and to explore the mechanism of the interaction, we further studied the effect of one specific amino acid (lysine) and its oligomers on silicification. Silica formation was carried out in the presence of di-, tri-, tetra-, penta- and poly-lysine samples. The representative SEM data of silica synthesized in the presence of lysine oligomers are presented in Fig. 17. The formation of distinct silica particles/aggregates was observed in the presence of lysine oligomers. The average particle sizes of silica particles formed using di-lysine, tri-lysine, tetra-lysine, penta-lysine and poly-lysine where the concentration of side chain functionalities was kept constant were respectively 108, 139, 85, 109, 122 and 467 nm. Comparatively larger particles were formed when poly-lysine was used as an additive. It

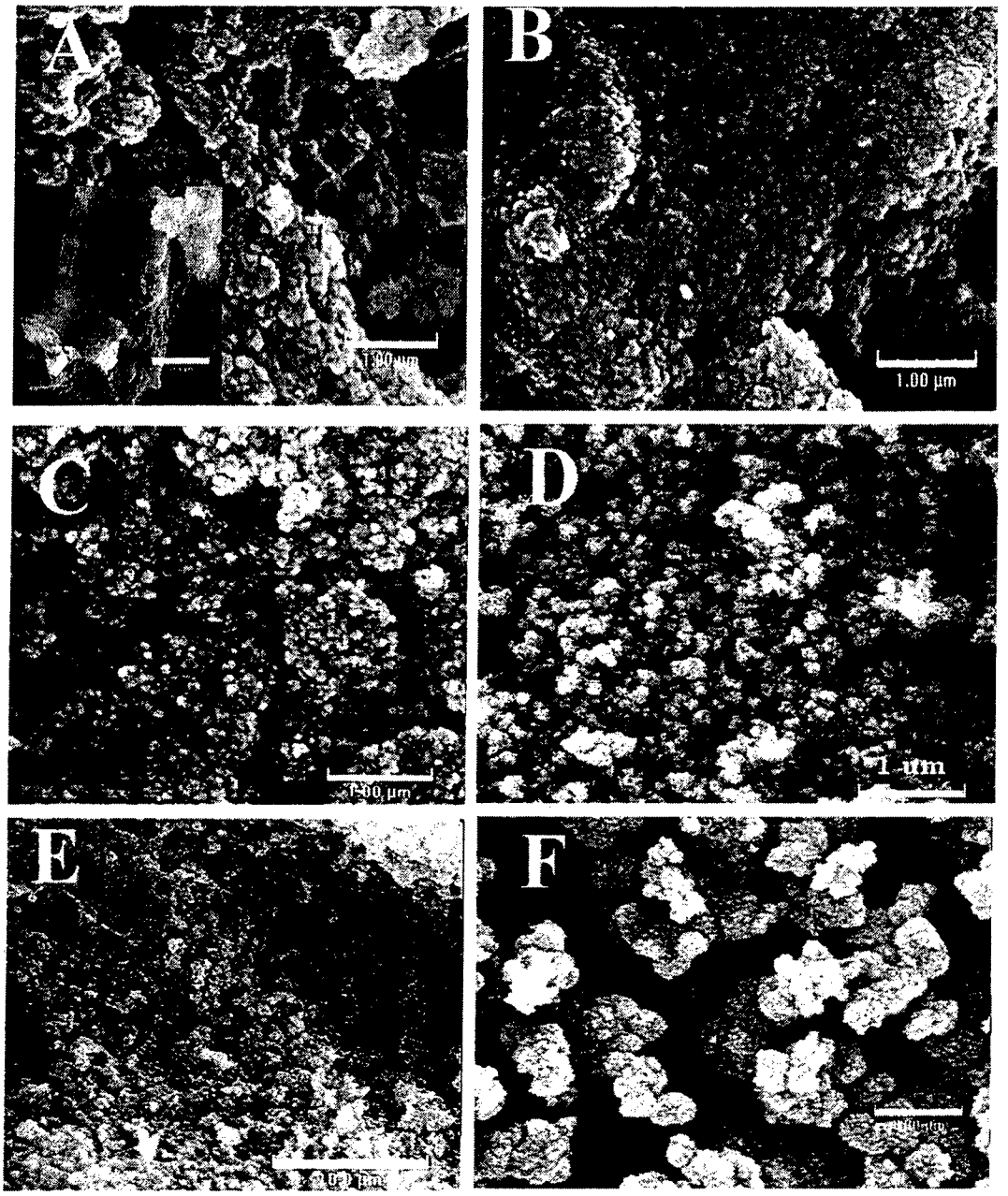

Fig. 17 Scanning electron micrographs of silicas produced in the presence of $(lys)_n$. A. $(lys)_2$, B. $(lys)_3$, C. $(lys)_4$, D. $(lys)_5$, E.and F. poly-lysine. Scale bars represent 1 µm for A–D, F and 10 µm for insert in A, E.

the presence of lysine and arginine homopeptides was reported.[22] These solutions were allowed to condense for 10 minutes prior to introduction of the peptides so would be expected to contain a significant population of silica oligomers. In this study amino acids and lysine homopeptides were added to a rapidly dissociating complex providing supersaturated monomeric silicic acid. The condensation rates in the early stages were found to be enhanced only moderately by comparison (approximate doubling of the 3rd order rate constant observed with $(lys)_5$). Co-addition of poly lysine and acid to the complex resulted in no observed immediate loss of molybdate active species, any precipitate formed was attributed to the formation of a cation exchanged poly lysine silicon catecholate complex with lower solubility than the potassium analogue. The indication was therefore that immediate silica precipitation previously reported was due to oligomer aggregation.[22]

Aggregation rates of the condensing silica observed by photon correlation spectroscopy showed increases for L-arginine and L-lysine. Although below neutral pH silica particles become less charged and tend to aggregate there is nonetheless a noticeable effect suggesting that residual surface charges are neutralised by the presence of the basic amino acid side chains. This effect was much more prominent for the aggregation of silica in the presence of the L-lysine homopeptides and suggests that these can cause bridging between particles similar to that described previously (refs. 22, 29 p. 386, 33*a*). The importance of the basic side chain on these homopeptides was demonstrated by the failure of L-glycine homopeptides to produce any effect. The increased apparent particle size observed with increased peptide chain length suggests that this bridging effect is strong enough to produce extended structures in solution but that they are too weak to survive the isolation process demonstrated by the absence of similar large scale structural changes observed by SEM.

The 'boundaries' observed in the PCS data are thought to occur at the stage where a continuous network of silica aggregates forms throughout the sample. The size fluctuations observed beyond this point are, we believe, due to structural inhomogeneities within this network. The subsequent general decrease in aggregate size in the systems involving lysine homopeptides could be a consequence of the bridging effect resulting in continued inter-particle silanol

have a role to play in determining the physical nature and structure of the material that forms. We believe that in biosilicification, amino acids may have a similar role to play *in vivo*. The combination of their effects in (bio)silicification and their intra- and inter-molecular 'arrangements' *in vivo* may be key features to controlling biosilicification.

Conclusions

The purpose of this study was to understand the role of biomolecules in biosilicification *via* individual and oligomeric amino acid effects on *in vitro* silicification. The main findings are presented in Table 3.

Individual amino acids variously reduced or accelerated the early kinetics of condensation and aggregation and produced silicas with surface areas which varied according to the isoelectric point of the amino acid. Introduction of $(lys)_n$ produced a slightly increased enhancement of the early kinetics but dramatically increased aggregation rates as silica condensation progressed, suggesting that aggregation may be a major influence on biosilica formation. Surface areas of the silicas were affected by the amino acids according to their hydrophobicities and a degree of control over both suface area, average pore size and size dispersity were exerted by the addition of lysine homopeptides of varying lengths. Effects on the morphologies of the silicas was observed even with individual amino acids, and with nitrogen containing amino acids producing granular materials.

Acknowledgements

The authors would like to thank Ineos Chemicals, the American Air Force and the European Union for funding of this project.

References

1 H. A. Lowenstam and S. Weiner, *On biomineralization*, Oxford University Press, New York, 1989.
2 P. Calvert and S. Mann, *J. Mater. Sci.*, 1988, **23**, 3801.
3 C. C. Perry, D. Belton and K. Shafran, in *Silicon Biomineralization*, ed. W. E. G. Müller, Springer Verlag, New York, 2003.
4 J. C. Weaver and D. E. Morse, in *Silicon Biomineralization*, ed. W. E. G. Müller, Springer Verlag, New York, 2003.
5 *Silicon and Siliceous Structures in Biological Systems*, ed. T. L. Simpson and B. E. Volcani, Springer-Verlag, New York, 1981.
6 F. E. Round, R. M. Crawford and D. G. Mann, in *The Diatoms: Biology & Morphology of the Genera*, Cambridge University Press, New York, 2003.
7 F. E. Round, R. M. Crawford and D. G. Mann, in *The Diatoms: Biology & Morphology of the Genera*, Cambridge University Press, New York, 1990.
8 C. C. Perry and T. Keeling-Tucker, *J. Biol. Inorg. Chem.*, 2000, **5**, 537.
9 C. C. Perry, J. Moss and R. J. P. Williams, *Proc. R. Soc. London*, 1990, **B241**, 47.
10 C. C. Perry, *Rev. Mineral. Geochem.*, 2003, **54**, 291.
11 T. Kendall, *Industrial Minerals*, March 2000, pp. 49.
12 C. C. Harrison (now Perry), *Phytochemistry*, 1996, **41**, 37.
13 C. C. Perry and T. Keeling-Tucker, *Colloid Polym. Sci.*, 2003, **281**, 652.
14 K. Shimizu, J. Cha, G. D. Stucky and D. E. Morse, *Proc. Natl. Acad. Sci. USA*, 1998, **95**, 6234.
15 R. E. Hecky, K. Mopper, P. Kilham and E. T. Degens, *Marine Biol.*, 1973, **19**, 323.
16 D. M. Swift and A. P. Wheeler, *J. Phycol.*, 1992, **28**, 202.
17 N. Kroger, S. Lorenz, E. Brunner and M. Sumper, *Science*, 2002, **298**, 584.
18 C. C. Perry and T. Keeling-Tucker, *Chem. Commun.*, 1998, 2587.
19 N. Poulsen, M. Sumper and N. Kroger, *Proc. Natl. Acad. Sci. USA*, 2003, **100**, 12075.
20 J. N. Cha, K. Shimizu, Y. Zhou, S. C. Christiansen, B. F. Chmelka, G. D. Stucky and D. E. Morse, *Proc. Natl. Acad. Sci. USA*, 1999, **96**, 361.
21 L. Sudheendra and A. R. Raju, *Mater. Res. Bull.*, 2002, **37**, 151.
22 T. Coradin, O. Durupthy and J. Livage, *Langmuir*, 2002, **18**, 2331.
23 T. Coradin, C. Roux and J. Livage, *J. Mater. Chem.*, 2002, **12**, 1242.
24 S. V. Patwardhan and S. J. Clarson, *Silicon Chem.*, 2002, **1**(3), 207.
25 J. N. Cha, G. D. Stucky, D. E. Morse and T. J. Deming, *Nature*, 2000, **403**, 289.
26 T. Coradin and J. Livage, *Colloids Surf. B*, 2001, **21**, 329.
27 T. Mizutani, H. Nagose, N. Fujiwara and H. Ogoshi, *Bull. Chem. Soc. Jpn.*, 1998, **71**, 2017.
28 C. C. Harrison (now Perry) and N. Loton, *J. Chem. Soc., Faraday Trans.*, 1995, **91**, 4287.
29 R. K. Iler, *The Chemistry of Silica*, John Wiley & Sons, New York, 1979.
30 S. Brunauer, P. H. Emmett and E. Teller, *J. Am. Chem. Soc.*, 1938, **60**, 309.
31 E. P. Barrett, L. G. Joyner and P. P. Halenda, *J. Am. Chem. Soc.*, 1951, **73**, 373.
32 J. Kyte. and R. Doolite, *J. Mol. Biol.*, 1982, **157**, 105.
33 (*a*) S. V. Patwardhan, N. Mukherjee, M. Steinitz-Kannan and S. J. Clarson, *Chem. Commun.*, 2003, 1122; (*b*) S. V. Patwardhan and S. J. Clarson, *J. Inorg. Organomet. Polym.*, 2002, **12**, 109.
34 S. V. Patwardhan, C. Raab, N. Hüsing and S. J. Clarson, *Silicon Chem.*, in press; S. V. Patwardhan and S. J. Clarson, unpublished data.
35 M. Sumper, S. Lorenz and E. Brunner, *Angew. Chem., Int. Ed.*, 2003, **42**, 5192.
36 L. L. Brott, D. J. Pikas, R. R. Naik, S. M. Kirkpatrick, D. W. Tomlin, P. W. Whitlock, S. J. Clarson and M. O. Stone, *Nature*, 2001, **413**, 291.
37 S. V. Patwardhan, N. Mukherjee, M. F. Durstock, L. Y. Chiang and S. J. Clarson, *J. Inorg. Organomet. Polym.*, 2002, **12**, 49.
38 H. R. Luckarift, J. C. Spain, R. R. Naik and M. O. Stone, *Nature Biotechnol.*, 2004, **22**, 211.
39 M. Sumper, *Science*, 2002, **295**, 2430.
40 R. Gordon and R. W. Drum, *Int. Rev. Cytol.*, 1994, **150**, 243.

Putrescine homologues control silica morphogenesis by electrostatic interactions and the hydrophobic effect†

David Belton, Siddharth V. Patwardhan and Carole C. Perry*

Received (in Cambridge, UK) 29th March 2005, Accepted 11th May 2005
First published as an Advance Article on the web 9th June 2005
DOI: 10.1039/b504310g

A systematic model study on the role(s) of putrescine homologues on silicification is presented and it is proposed that electrostatic forces between additive and silicic acid, and the hydrophobic behaviour of the additives are both important in silicification.

In nature, several classes of biosilicifying organisms process soluble silicon to generate hierarchically organised ornate biogenic silica structures under mild conditions of pH and temperature and exert precise control in shaping biosilica.[1] In contrast, current synthetic procedures typically employ relatively harsh conditions for the preparation of silicas and exhibit relatively poor morphological control.[2] In order to gain insights into biosilicification, several studies have been carried out on biosilicifying organisms wherein organic biomolecules have been isolated and identified (reviewed in ref. 3). These bioextracts control *in vitro* silicification *via* catalysis, aggregation and/or scaffolding.[4]

In this model study on bioinspired silica, we have chosen to investigate the roles of simple amines—putrescine homologues—on silicification [1,2-diaminoethane (DA2), 1,4-diaminobutane or putrescine (DA4), 1,6-diaminohexane (DA6), 1,8-diaminooctane (DA8) and 1,10-diaminodecane (DA10)]. Although several biomimetic analogues possessing amine functionalities, including aminoalkanes, have been investigated for their roles in silica synthesis *in vitro*,[4,5] the current study is the first extensive report on the use of low molecular weight alkyldiamines in bioinspired silicification. We also provide an insight into the processes occurring during the transformation of monomers to oligomers to useful material. The silica precursor used was a water soluble silicon complex—dipotassium silicon triscatecholate†—which rapidly liberates orthosilicic acid at neutral pH unlike alkoxysilane precursors that produce a mixture of pre-condensed polysilicic acid and we are therefore able to monitor the condensation of "true" monosilicic acid.[6] Throughout this study, the silicon to amine molar ratio was kept constant at one.

During silicic acid polymerisation, orthosilicic acid initially polymerises to yield dimers and trimers that will eventually lead to the formation of stable nuclei. A colorimetric molybdic acid assay was used to monitor the kinetics of silica polymerisation. The rates of trimerisation (a third order reaction with respect to monomer concentration; rate constant k_3) and further oligomerisation (a first order reversible reaction; rate constants k_+, k_-) were monitored by this silicomolybdate blue assay.[6,7] The rate constants for the formation of trimers from monomer and dimer were found to increase by *ca.* two fold for the DA2 system and *ca.* 2.5 times for the longer chain diamines when compared with the blank (with no trend observed over these samples); Fig. 1a. Increases in the third order rate constants were found to be statistically significant, exceeding two standard deviations calculated using four 'blank'data-sets. The next stage of the reactions involves the reversible addition of orthosilicic acid to already formed oligomers and showed less variation for the silicas prepared in the presence of diamines (Fig. 1a). Previous work on silicic acid condensation in the presence of Group 1 cations has shown a rate dependency related to the size of the hydration sphere of the cations.[7] Here the cationic species and concentration were constant and only the hydrophobic portion of the additive varied as the chain length of the diamine increased. The increase in trimerisation rate can be explained by the formation of a clathrate cage-like water structure around the nonpolar surfaces of the alkyldiamines. The cage-like structure may tie up some of the free water molecules (*i.e.* those not associated with ion hydration shells)[8] resulting in higher reactant (silicic acid) concentrations in the bulk aqueous environment and also a possible reduction in the hydration shells around the anionic silica species. Under these conditions, reactions involving anions, such as the condensation of a silicate anion with a neutral silicate species, would be expected to show an increase in rate as observed for condensation reactions performed

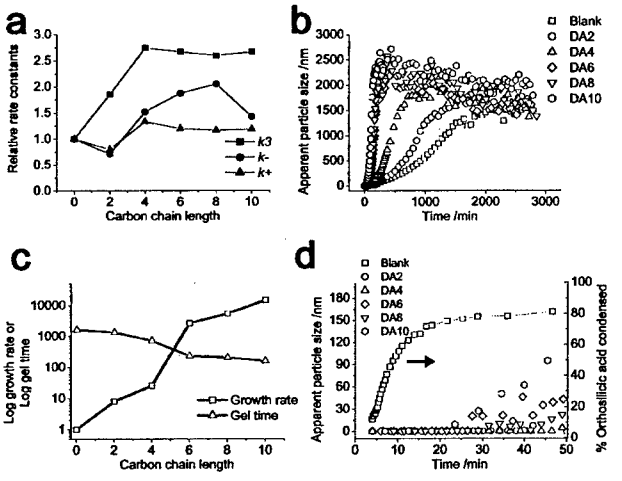

Fig. 1 (a) Effect of diamine chain length on trimerisation and oligomerisation reactions. (b) Particle growth with time, and (c) relative growth rate and gel time as a function of diamine chain length. (d) Comparison of particle aggregation with the free silicic acid as functions of time.

† Electronic supplementary information (ESI) available: Experimental methods and additional data from SEM, TEM, gas adsorption, TGA and FTIR analyses. See http://www.rsc.org/suppdata/cc/b5/b504310g/

*Carole.Perry@ntu.ac.uk

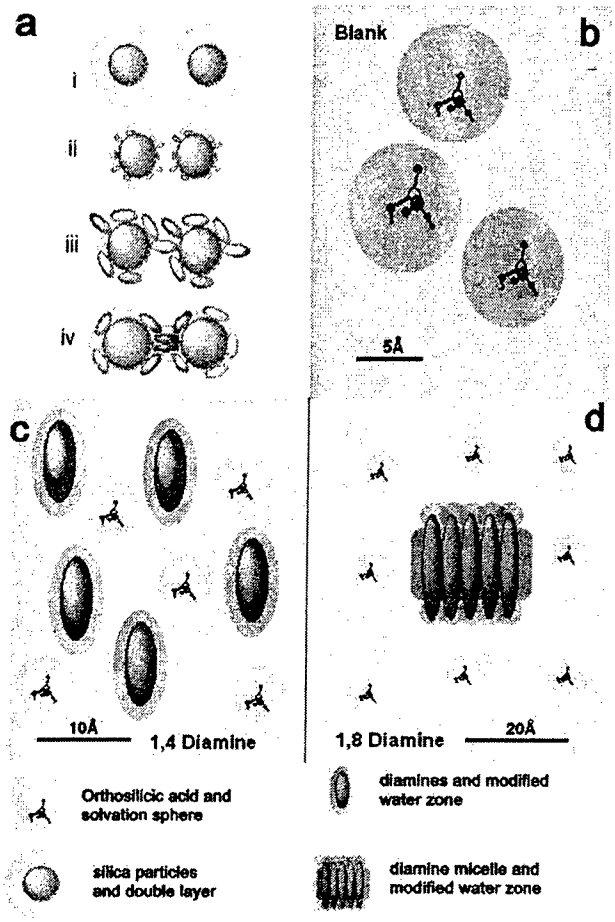

Fig. 4 Schematic representation of the effect of n-alkyldiamines on the condensation of silicic acid and subsequent silica particle aggregation modes. (a) Aggregation modes: i. in the absence of diamines, ii. charge neutralisation and reduction in the thickness of the double layer in the presence of shorter diamines, iii. particle bridging by longer chain diamines and iv. coacervation due to increased micellisation with increasing carbon chain length and hence hydrophobic character. (b)–(d) Kinetic control of diamines: (b) Blank, showing solvation barrier to condensation, (c) Addition of diamines with hydrophobic domains reduces the solvation barrier and hence increases the condensation rate. (d) Subsequently, the formation of micelles by longer chain diamines limits this effect by minimising the hydrophobic water surface. Colour shades are used to indicate the different 'ordering' of water (the darkest shade represents the most organised water).

TEM were slightly bigger (5–7 nm) when compared with the blank sample (4 nm) but with no specific trend (Figure S3). Confirmation that the structures observed were siliceous was made by EDS and FTIR analyses (Figure S3 and Figure S4). Selected area electron diffraction carried out on selected samples showed no evidence of ordering on the atomic or molecular scale, confirming the amorphous nature of the silica produced (data not shown).

The current *in vitro* bioinspired silicification study confirms the importance of amines in silica synthesis as has been proposed for biosilicas produced by diatoms in nature.[11] The alkyldiamines chosen for study were found to catalyse silica formation and promote silica aggregation, the latter contributing greatly to the structure and physical properties of the silicas generated. The electrostatic forces between the amine end-groups of the diamines and the silica oligomers are important in regulating silicification. This study has, however, shown that the hydrophobic behaviour exhibited by diamines on silica formation is in direct relation to the carbon chain length. The hydrophobic effect is a fundamental factor regulating *in vivo* processes, such as protein folding and protein–substrate interactions.[10,12] The stability and hence the function of proteins, for example, is altered by the presence of solute due to the rearrangement of water molecules. This effect is particularly enhanced when the solutes added are hydrophobic in nature. In the study described here, the addition of diamines to the reaction medium alters the water structure around silicic acid by the hydrophobic effect, thus changing the stability of silicic acid, modifying condensation and aging, and generating siliceous materials that differ greatly in their physical properties. Fig. 4 shows schematically the proposed effects of the n-alkyldiamines on the condensation of silicic acid and subsequent particle aggregation modes together with the effects of the diamines on the 'ordering' of water in the vicinity of the reactive species. It is thus thought that the results presented herein on controlled silica formation using alkyldiamines may help understand the role(s) such organic molecules (functionalities) may play in (bio)silicification. Current research is directed towards understanding the effects of amines found widely *in vivo* on silica formation *in vitro* and will be reported in due course.

The authors would like to thank Ineos Chemicals, the American Air Force and the European Union for funding of this project

David Belton, Siddharth V. Patwardhan and Carole C. Perry*
Interdisciplinary Biomedical Research Centre, School of Biomedical and Natural Sciences, Nottingham Trent University, Clifton Lane, Nottingham, UK NG11 8NS. E-mail: Carole.Perry@ntu.ac.uk; Fax: (+44) 115-8483384

Notes and references

1 *Silicon and Siliceous Structures in Biological Systems*, ed. T. L. Simpson and B. E. Volcani, Springer-Verlag, New York, 1981.
2 (*a*) R. K. Iler, *The Chemistry of Silica*, John Wiley & Sons, New York, 1979; (*b*) C. J. Brinker and G. W. Scherer, *Sol-Gel Science*, Academic Press, Boston, 1990.
3 C. C. Perry, *Rev. Mineral. Geochem.*, 2003, **54**, 291.
4 S. V. Patwardhan, S. J. Clarson and C. C. Perry, *Chem. Commun.*, 2005, **9**, 1113.
5 (*a*) T. Mizutani, H. Nagase, N. Fujiwara and H. Ogoshi, *Bull. Chem. Soc. Jpn.*, 1998, **71**, 2017; (*b*) T. Coradin and J. Livage, *Colloids Surf., B*, 2001, **21**, 329; (*c*) F. Noll, M. Sumper and N. Hampp, *Nano Lett.*, 2002, **2**, 91; (*d*) K. M. Roth, Y. Zhou, W. Yang and D. E. Morse, *J. Am. Chem. Soc.*, 2005, **127**, 325.
6 D. Belton, G. Paine, S. V. Patwardhan and C. C. Perry, *J. Mater. Chem.*, 2004, **14**, 2231.
7 C. C. Harrison and N. Loton, *J. Chem Soc., Faraday Trans.*, 1995, **91**, 4287.
8 F. Franks, *Water*, Royal Society of Chemistry, London, 1983.
9 S. D. Kinrade and D. L. Pole, *Inorg. Chem.*, 1992, **31**, 4558.
10 E. Fisicaro, C. Compari and A. Braibanti, *Phys. Chem. Chem. Phys.*, 2004, **6**, 4156.
11 N. Kroger, R. Deutzmann, C. Bergsdorf and M. Sumper, *Proc. Natl. Acad. Sci. USA*, 2000, **97**, 14133.
12 D. K. Eggers and J. S. Valentine, *J. Mol. Biol.*, 2001, **314**, 911.

Supplementary Material (ESI) for Chemical Communications

Supplemental Information

Putrescine Homologues Control Silica Morphogenesis by Electrostatic Interactions and the Hydrophobic Effect

David Belton, Siddharth V. Patwardhan and Carole C. Perry*

Interdisciplinary Biomedical Research Centre, School of Biomedical and Natural Sciences, The Nottingham Trent University, Clifton Lane, Nottingham, NG11 8NS, UK.
**E-mail: Carole.Perry@ntu.ac.uk*

Nova3200e surface area and pore size analyser. Samples were first degassed overnight at 150°C under vacuum. Surface areas were then determined *via* the BET method[S5] where nitrogen is assumed to have a cross-sectional area of 0.16 nm^2, over the range of relative pressures 0.05 – 0.3 at which the monolayer is assumed to assemble. Pore radii were determined by the BJH method[S6] using the desorption branch of the isotherm. This method assumes cylindrical pores. Isotherms obtained were typical of type IV with hysteresis loops characteristic of cylindrical pores with possibly some partial closure at the open ends. The entrapped organic material in silica was determined by thermogravimetric analysis under nitrogen as the weight loss between temperatures 500-800 K not attributable to silanol condensation.

S1. D. Belton, G. Paine, S. V. Patwardhan, C. C. Perry, *J. Mater. Chem.*, 2004, **14**, 2231.
S2. C. C. Harrison, N. Loton, *J. Chem Soc. Faraday Trans.*, 1995, **91**, 4287.
S3. N. Kroger, S. Lorenz, E. Brunner, M. Sumper, *Science*, 2002, **298**, 584.
S4. M. R. Knecht, D. W. Wright, *Langmuir*, 2004, **20**, 4728.
S5. S. Brunauer, P. H. Emmett, E. Teller, *J. Am. Chem. Soc.*, 1938, **60**, 309.
S6. E. P. Barrett, L. G. Joyner, P. P. Halenda, *J. Am. Chem. Soc.*, 1951, **73**, 373.

(c) Surface area analysis of diamine-mediated silica at varying time. ($t_{gel\ ½}$ and 7 days sample data is replotted from Figure 2a for comparison)

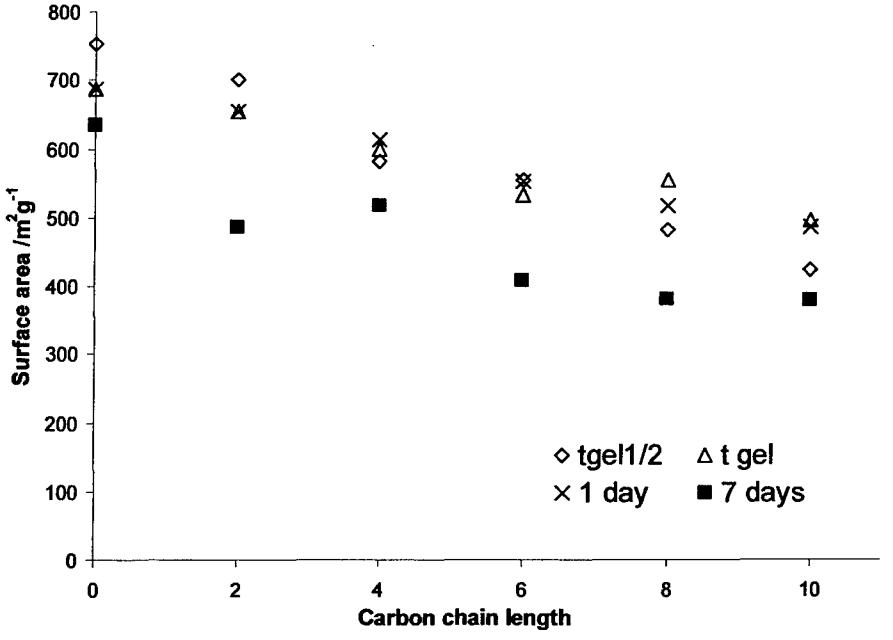

(d) Pore size analysis of diamine-mediated silica as a function of time.

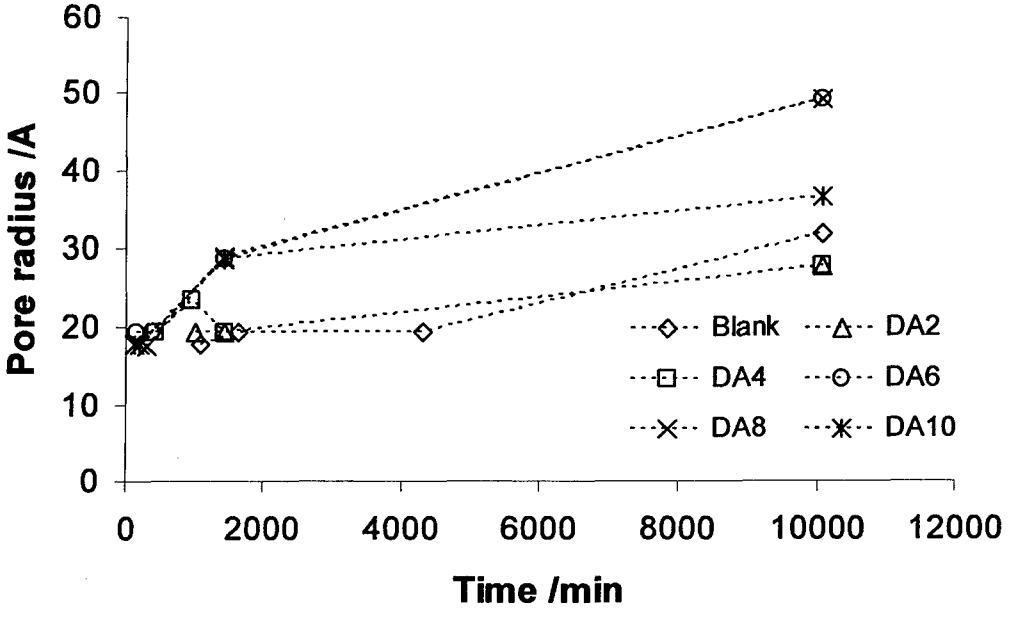

Supplementary Material (ESI) for Chemical Communications

Figure S2. Thermogravimetric analysis of silica samples.

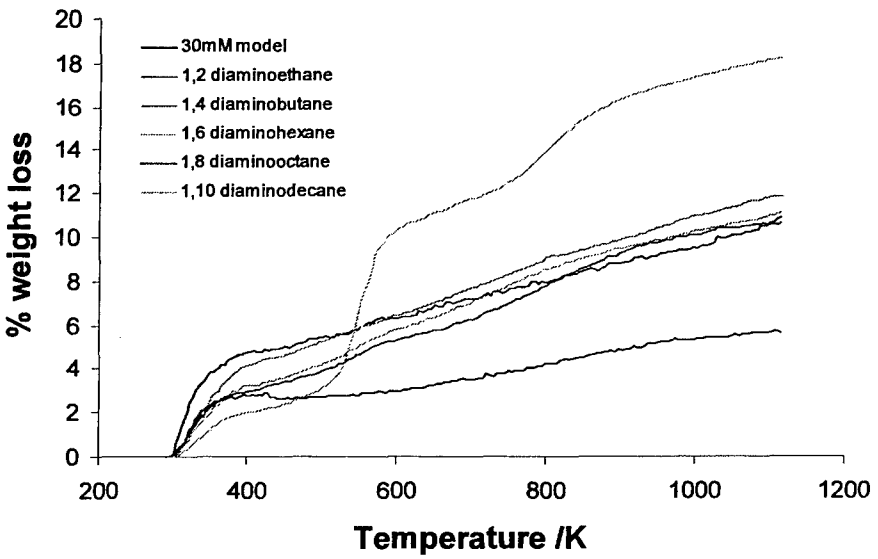

Supplementary Material (ESI) for Chemical Communications

Figure S4. Representative FTIR data obtained from silica with and without diamines.

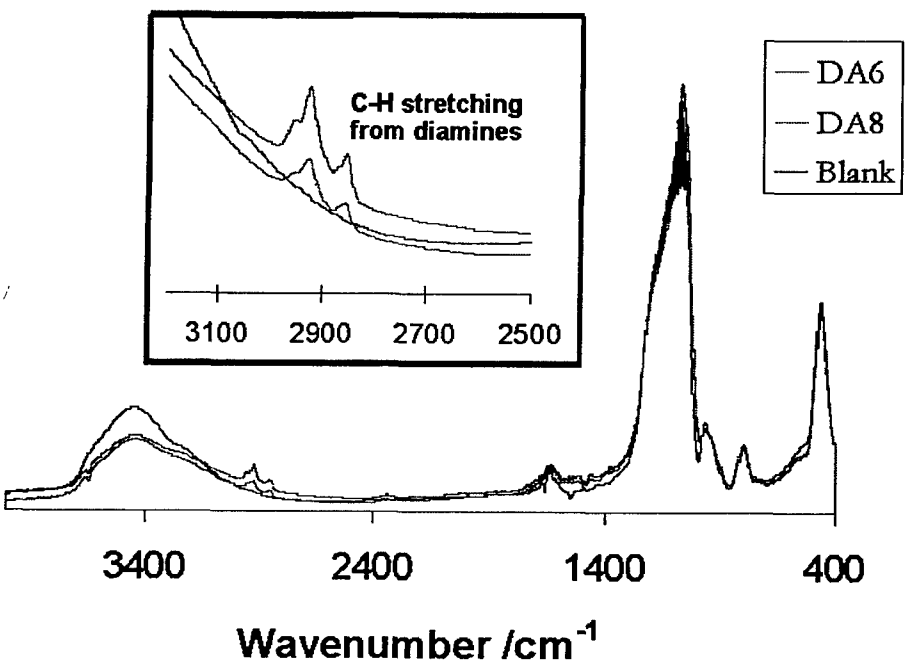

Supplementary Material (ESI) for Chemical Communications

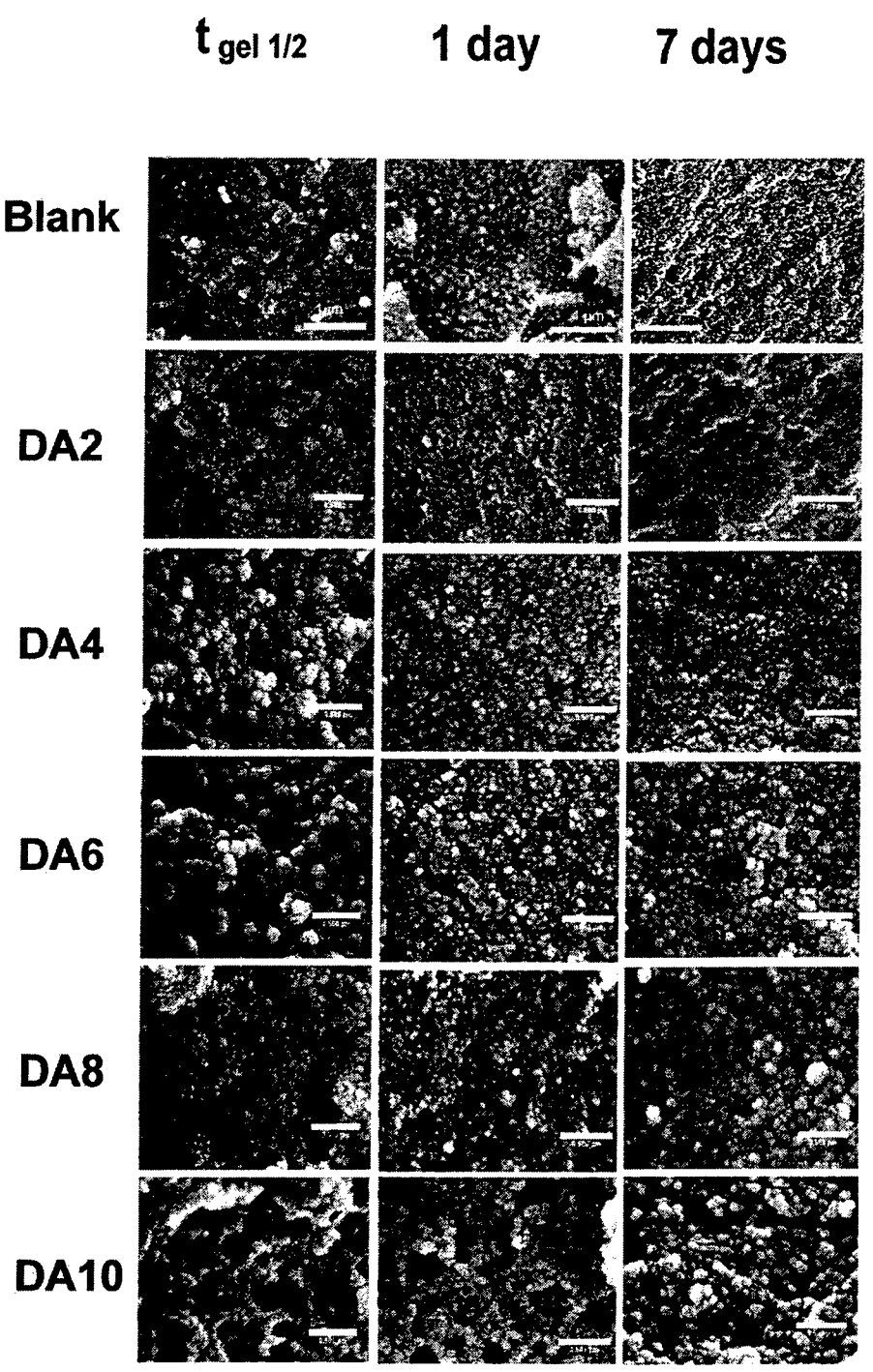

Figure 1B

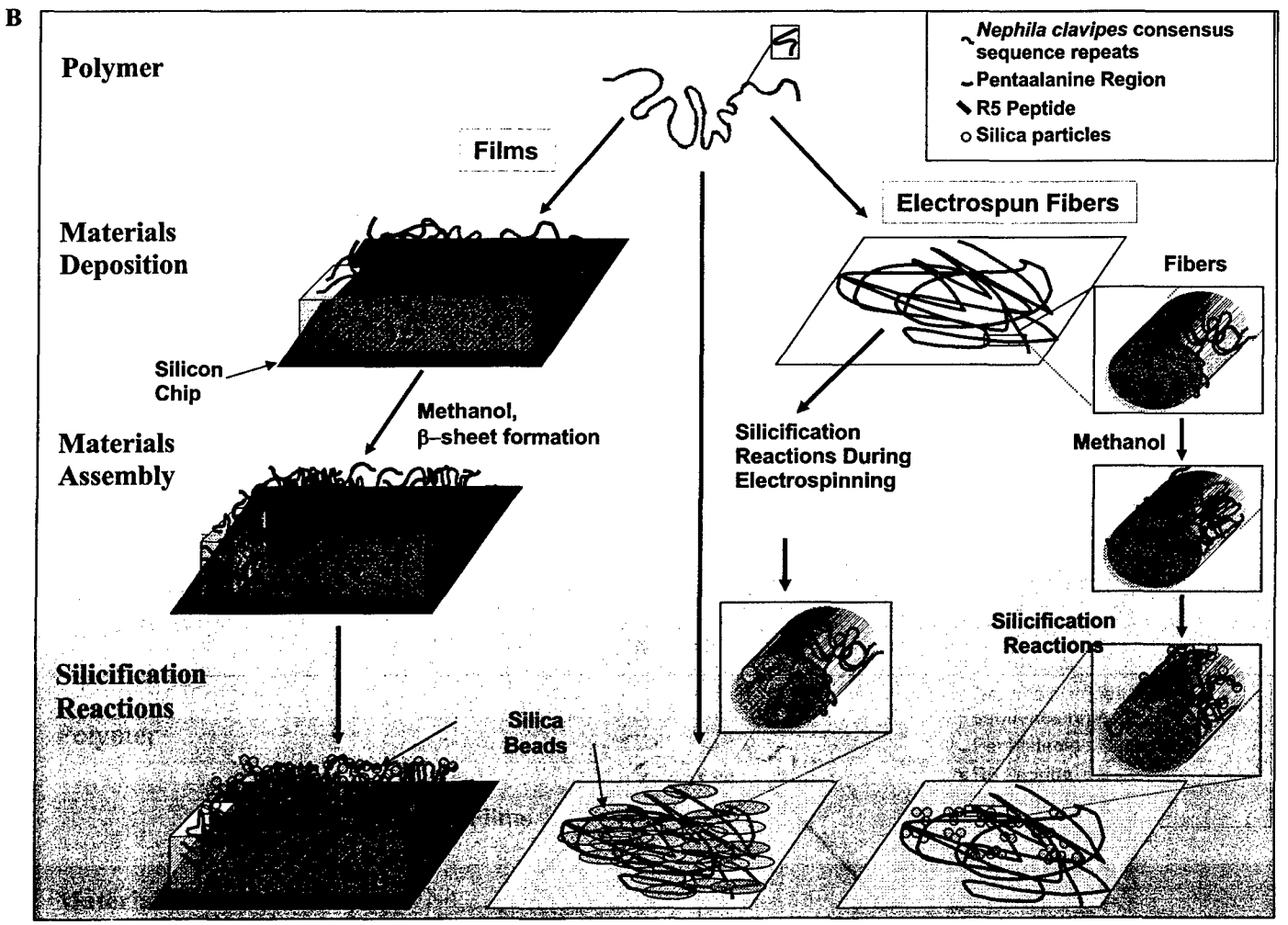
B
Polymer
Films
Electrospun Fibers
Nephila clavipes consensus sequence repeats
Pentaalanine Region
R5 Peptide
Silica particles
Materials Deposition
Silicon Chip
Methanol, β–sheet formation
Materials Assembly
Fibers
Methanol
Silicification Reactions During Electrospinning
Silicification Reactions
Silicification Reactions
Silica Beads

A. CRGD15mer+R5

*MASMTGGQQM GRGS**CRGD**TS* GRGGLGGQGA GAAAAAGGAG QGGYGGLGSQ GTSGRGGLGG 60
QGAGAAAAAG GAGQGGYGGL GSQGTSGRGG LGGQGAGAAA AAGGAGQGGY GGLGSQGTSG 120
RGGLGGQGAG AAAAAGGAGQ GGYGGLGSQG TSGRGGLGGQ GAGAAAAAGG AGQGGYGGLG 180
SQGTSGRGGL GGQGAGAAAA AGGAGQGGYG GLGSQGTSGR GGLGGQGAGA AAAAGGAGQG 240
GYGGLGSQGT SGRGGLGGQG AGAAAAAGGA GQGGYGGLGS QGTSGRGGLG GQGAGAAAAA 300
GGAGQGGYGG LGSQGTSGRG GLGGQGAGAA AAAGGAGQGG YGGLGSQGTS GRGGLGGQGA 360
GAAAAAGGAG QGGYGGLGSQ GTSGRGGLGG QGAGAAAAAG GAGQGGYGGL GSQGTSGRGG 420
LGGQGAGAAA AAGGAGQGGY GGLGSQGTSG RGGLGGQGAG AAAAAGGAGQ GGYGGLGSQG 480
TSGRGGLGGQ GAGAAAAAGG AGQGGYGGLG SQGTS**RGDC**G SEFSSKKSGS YSGSKGSKRR 540
ILCGR**HHHHH H** 551

B. 15mer+R5

*M**HHHHHH**SSG LVPRGSGMKE TAAAKFERQH MDSPDLGTDD DDKAMAS*GRG GLGGQGAGAA 60
AAAGGAGQGG YGGLGSQGTS GRGGLGGQGA GAAAAAGGAG QGGYGGLGSQ GTSGRGGLGG 120
QGAGAAAAAG GAGQGGYGGL GSQGTSGRGG LGGQGAGAAA AAGGAGQGGY GGLGSQGTSG 180
RGGLGGQGAG AAAAAGGAGQ GGYGGLGSQG TSGRGGLGGQ GAGAAAAAGG AGQGGYGGLG 240
SQGTSGRGGL GGQGAGAAAA AGGAGQGGYG GLGSQGTSGR GGLGGQGAGA AAAAGGAGQG 300
GYGGLGSQGT SGRGGLGGQG AGAAAAAGGA GQGGYGGLGS QGTSGRGGLG GQGAGAAAAA 360
GGAGQGGYGG LGSQGTSGRG GLGGQGAGAA AAAGGAGQGG YGGLGSQGTS GRGGLGGQGA 420
GAAAAAGGAG QGGYGGLGSQ GTSGRGGLGG QGAGAAAAAG GAGQGGYGGL GSQGTSGRGG 480
LGGQGAGAAA AAGGAGQGGY GGLGSQGTSG RGGLGGQGAG AAAAAGGAGQ GGYGGLGSQG 540
TSSSKKSGSY SGSKGSKRRI L 561

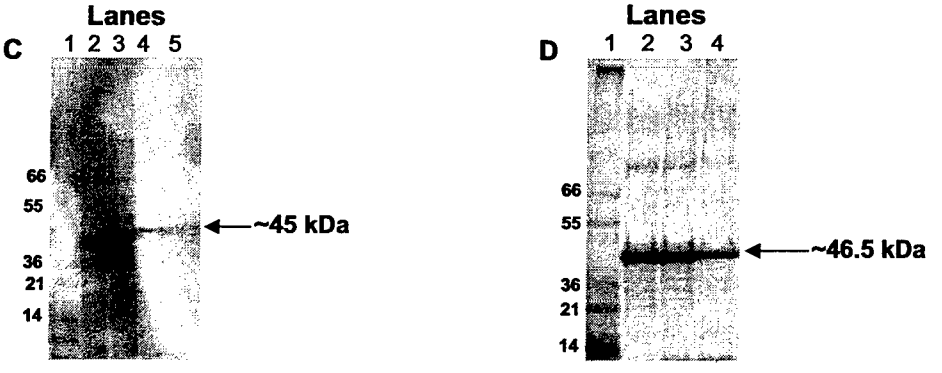

Figure 2

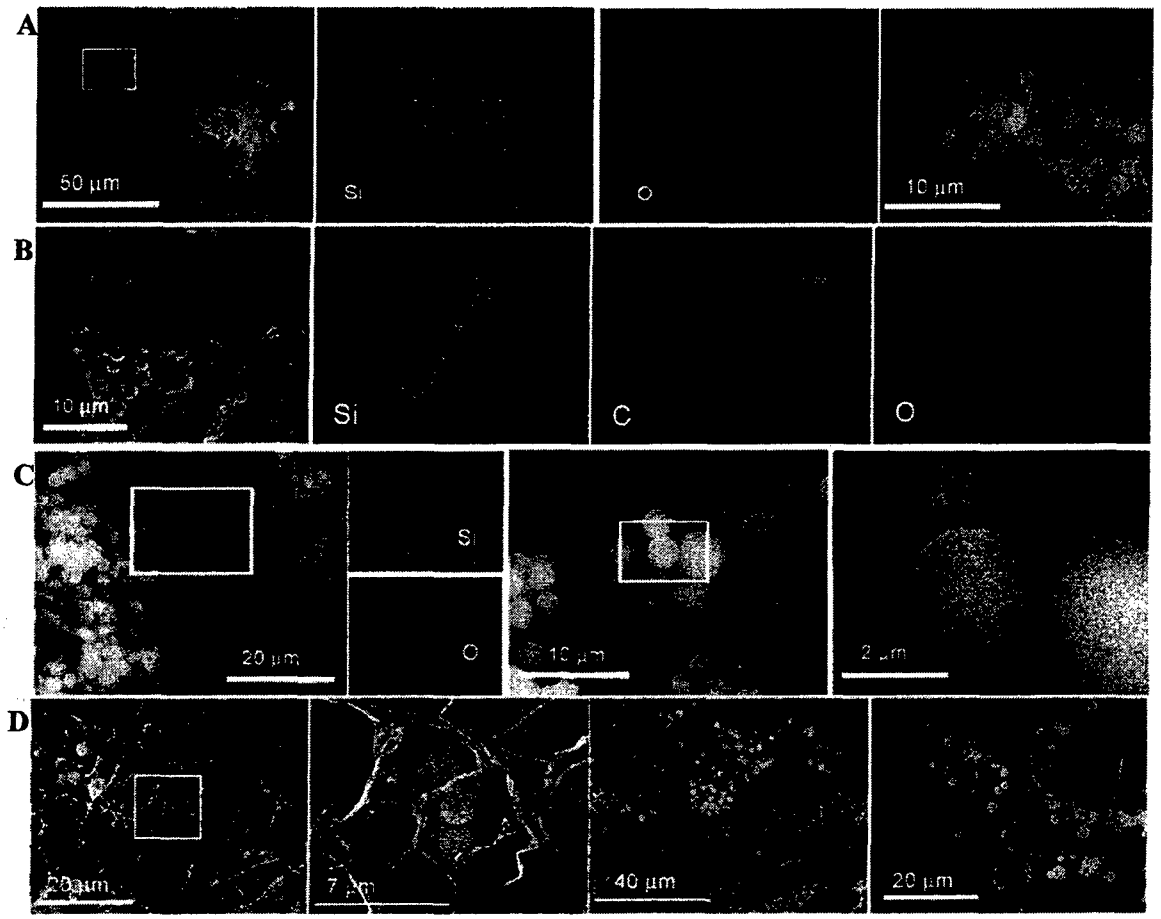
A
50 µm
Si
O
10 µm
B
10 µm
Si
C
O
C
Si
20 µm
O
10 µm
2 µm
D
20 µm
7 µm
40 µm
20 µm

Figure 4

Figure 6

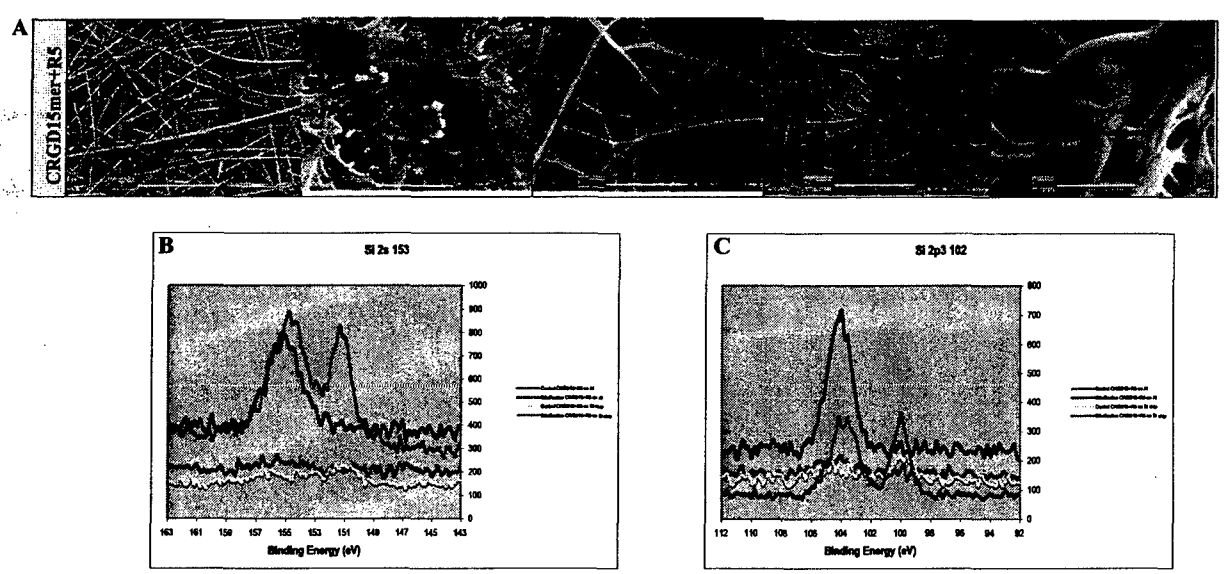
A
CRGD15mer+R5
B
Si 2s 153
1000
900
800
700
600
500
400
300
200
100
0
163 161 159 157 155 153 151 149 147 145 143
Binding Energy (eV)
C
Si 2p3 102
800
700
600
500
400
300
200
100
0
112 110 108 106 104 102 100 98 96 94 92
Binding Energy (eV)

Are hydroxyl containing biomolecules important in (bio)silicification? *A model study*

Graham Tilburey[1], Siddharth V. Patwardhan[1], Tufts One[2], Tufts Two[2], David Kaplan[2*], Professor Carole C. Perry[1*]

[1] Department of Chemistry, School of Biomedical and Natural Sciences, Nottingham Trent University, Nottingham, NG11 8NS, UK.

[2] Departments of Biomedical Engineering, Chemistry or Chemical & Biological Engineering & Bioengineering & Biotechnology Center Tufts University, Medford, Massachusetts 02155, USA.

** Correspondence should be addressed to Carole C. Perry (Carole.Perry@ntu.ac.uk) and David L. Kaplan (david.kaplan@tufts.edu).*

formation of crystalline silica during silica formation under ambient conditions *in vitro*.[5, 6] Analysis of amino acids composition of the proteinaceous component suggested the presence of beta-sheet forming residues which were thought to interact in the early stages of silicification by providing a molecular template.

Morse and coworkers reported that the silicatein α protein extracted from a sponge (*Tethya aurantia*) silica spicules catalyses the hydrolysis of the alkoxide group present in the tetraethoxysilane (TEOS, a silica precursor), which aids silica formation. Silicatein α was shown to share high structural homology with Cathepsin L, a human hydrolytic enzyme.[7] It was proposed that the catalytic effect exhibited by silicatein α was due to the activity of the serine-26 and histidine-165 side chains that occupy positions corresponding to the catalytic sites in cathepsin L.[8, 9] It was suggested that hydrogen bonding between the serine-26 hydroxyl group and imidazole nitrogen of the histidine-165 residue aids nucleophilic attack on the silicon centre generating a C-O-Si covalent bonded intermediate, addition of water completes the hydrolysis of tetraethylorthosilicate.[8, 9] Silicatein α was found to contain distinct hydroxyl-containing amino acid domains, (not present in Cathepsin L) which were hypothesised to act as templates for silica formation.

Kroger *et al.* isolated three protein families called frustulins, pleuralins, and silaffins and species specific long chain polyamines (LCPA) from purified diatom cell walls.[10] Publications so far have indicated that frustulins are a family of calcium binding glycoproteins which do not seem to be involved with the silica forming process but are associated with the cell wall.[11] Pleuralins are tightly associated with the frustule and specifically with the terminal gridle bands of the theca.[12] Silaffins and LCPA have been shown to facilitate silicification *in vitro*. Interestingly the silaffin proteins

where no Si-O-C bonds were observed and at that time lead to the conclusion that interactions between the organic matrix and the mineral phase may be non-covalent.[19]

It is commonly believed that hydroxyl-rich biomolecules interact with (poly)silicic acids and regulate biosilicification. There is evidence to suggest that the interaction between silicon species and molecules containing hydroxyl functionality could be either covalent or non-bonded. However, it is quite clear from the literature reviewed above that the roles of hydroxyl functionalised biomolecules and their biomimetic analogues in silica formation are not fully understood. Here we investigate the role of two proteins rich in hydroxyl containing amino acids, native sericin extracted from *Bombyx mori* and a sericin precursor in the formation of silica *in vitro*. Furthermore, we investigate the role of hydroxyl containing "small" model molecules in silica formation to study the interactions between silicon species and hydroxyl functionalised species, if any.

Experimental

Materials

Dipotassium tris (1,2-benzene-diolato-*O, O,*) silicate (97% Aldrich) was used as the precursor of orthosilicic acid. Ammonium molybdate tetrahydrate (ACROS 99%) and concentrated hydrochloric acid (37% Fisher Scientific) were used to make the molybdic acid solution. Solutions containing oxalic acid (99% Fisher Scientific), sodium sulphite (BHL), 4-methylaminophenolsulphate (ACROS 99%) and sulfuric acid (98% Fisher Scientific) were used to reduce the yellow silicomolybdic acid complex to a blue silicomolybdous acid complex. The alkanediols used in the model studies; 1,2 Ethanediol 99% was purchased from BDH , 1,3 Propanediol 98% was purchased from ACROS, 1,4 Butanediol 99%, 1,5 Pentanediol 96%, 1,6 Hexanediol 99% and 1,7 Heptanediol 95% were purchased

alkanediols were typically added into the model reaction at 15mM (Si:OH 1:1 i.e. 100%), 30mM (Si:OH 1:2 i.e. 200%), 60mM (Si:OH 1:4 i.e. 400%) and 150mM (Si:OH 1:10 i.e. 1000%). It should be noted that the precursor for orthosilicic acid, (dipotassium tris (1,2-benzene-diolato-*O, O,*) silicate) generates three molar equivalents of catechol which is itself a diol (Si:OH ratio 1:6). The effect of catechol on the condensation of orthosilicic acid has been normalised throughout all the experiments by comparison of data against a blank condensing system where no additional hydroxyl containing molecules has been added.

Kinetic studies were carried out using a colorimetric method where 10 µl aliquots of the condensing system were placed into a molybdic acid solution at *ca.* pH 1, which is know to quench the reaction. The molybdic acid solution complexes with orthosilicic acid including that generated from the rapid dissociation of dimeric silicon containing species. The solution was then reduced to give a blue coloured silicomolybdous acid complex, which was measured at 810 nm using a Unicam UV2 UV-VIS spectrometer and the corresponding orthosilicic acid concentration calculated using a linear calibration curve.[20]

The particle formation, growth and aggregation behaviour of the condensing system was measured using PCS. In each case, samples were transferred into a 1 cm polymethylmethacrylate cell and allowed to condense over a 24 hour period while particle formation, growth and aggregation was monitored by Coulter N4 Plus Photon Correlation Spectroscopy (PCS) with He-Ne 632.8 nm laser. Silica was isolated from the condensing system after 24 and 168 hours reaction by centrifugation, washing three times with deionised water and lyophilised for further analysis.

presence of sericin proteins showed that the sericin proteins exhibited no significant catalytic effect on the formation of trimers (k_{3rd}) at any of the concentrations studied (**Figure 1a**). In addition, no statistically significant effects were observed on the oligomerisation process (k_+ and k_-), **Figure 1a**. There was no evidence for the stabilisation of orthosilicic acid at equilibrium for any of the concentrations of sericin proteins studied (reflected from the values of k_- in **Figure 1a**).

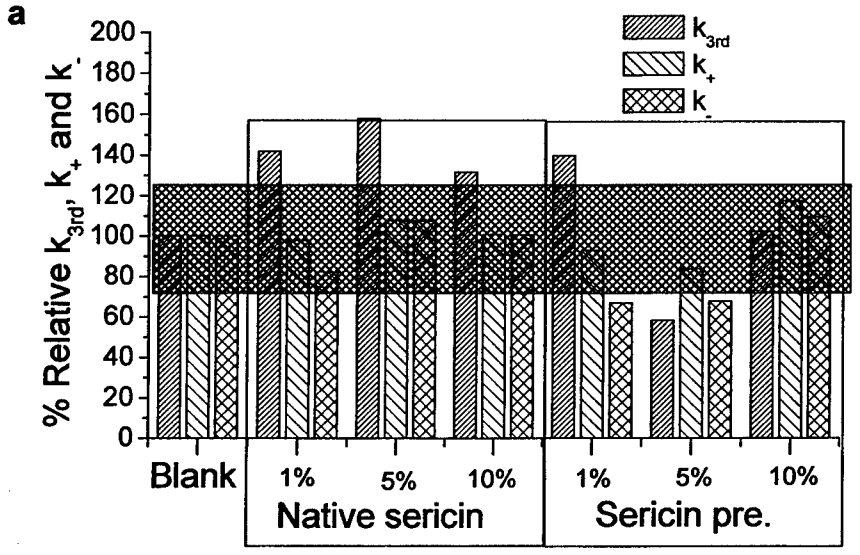

were found to aggregate in solution as evidenced from PCS data shown in **Figure 1b** for selected examples. For the blank silica sample, particle formation is apparent after *ca.* one hour of reaction. For the samples with protein added to the reaction medium, the initial protein aggregates were found to dissociate once silica particles started to form (i.e. after 1h reaction time), **Figure 1b**. Thereafter the rate of particle growth and aggregation was found to be similar to the blank system. It should be noted that no precipitation was observed even after 20 hours of reaction. The dissociation of the sericin protein aggregates over 1-3 hour period of reaction suggests only weak intramolecular interactions between protein molecules and silicate species, and therefore it seems unlikely that sericin is acting as a template for silica formation. After seven days of reaction time, silica samples were precipitated, washed with water and lyophilised for nitrogen adsorption analysis. The data obtained from nitrogen adsorption on silica samples prepared in the presence of sericin proteins is presented in **Figure 1c**. The presence of sericin proteins even at 10% did not have any statistically significant effects on surface area and porosity of silicas generated when compared with the blank system.

The results obtained from sericin-silica polymerisation experiments are in striking contrast with the effects of other biomolecules studied in the past, e.g. R5, silaffins, cationic recombinant proteins, polylysines, polyarginine, polyhistidine, lysozyme, etc.[24, 25] Although, these biomolecules and sericin proteins are capable of hydrogen bonding, the main difference is that the former are highly cationically charged under experimental conditions (i.e. pH 7). This enables silicon species and protonated amino groups to interact electrostatically, often promoting aggregation and sometimes catalysing condensation reactions. Hydroxyl functionalised size chains and do not interact electrostatically with silica molecules. Instead, hydrogen bonding can occur between the lone pair on

stages of silica polymerisation studied. **Figure 2a** shows the kinetic results obtained for the alkanediols at a silicon to hydroxyl ratio of one.

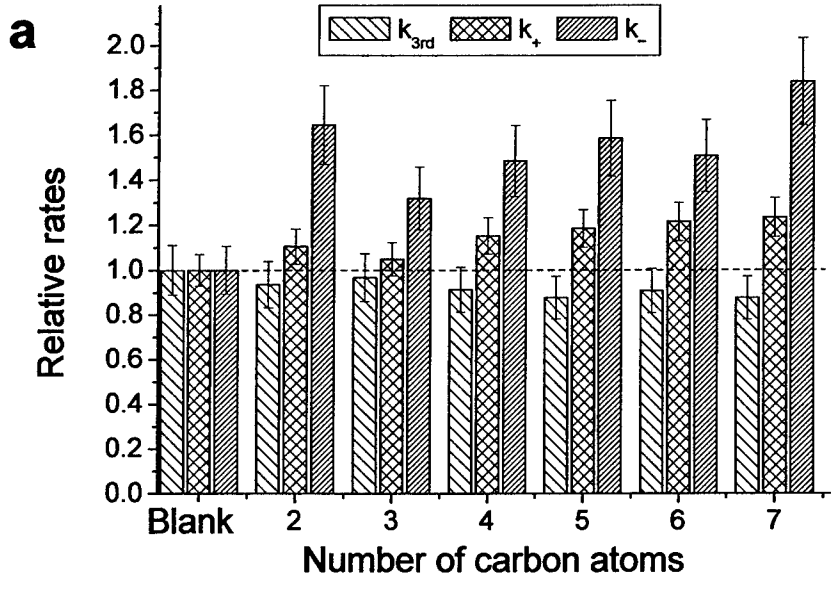

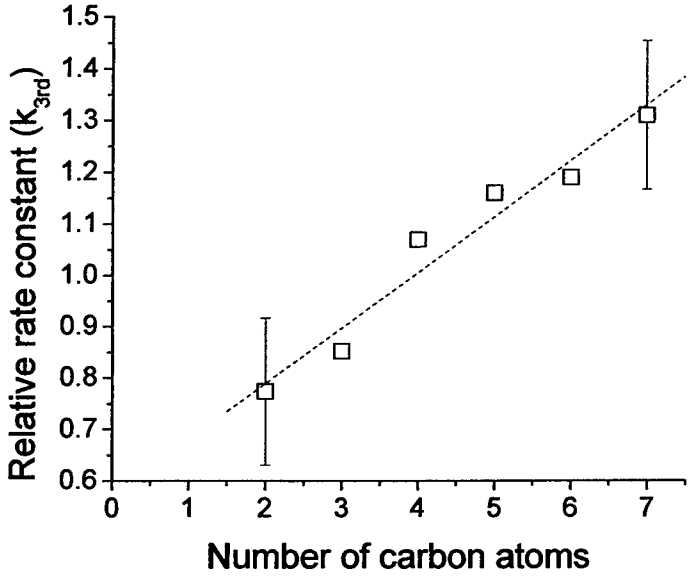

in solution. 1,2 ethanediol is miscible in water and hence the hydrophobic effect is not observed. Instead 1,2 ethanediol is incorporated into the bulk water structure. Increasing the hydrophobicity of the alkanediol at this concentration may create micelles which could be favourable due to reduced solubility of longer carbon chain alkanediols. We investigated the possible formation of micelles in alkanediols at Si:OH 1:4 using PCS. Figure **3a** shows the formation of structure assumed to be micelles in alkanediols of increasing carbon chain length. It can be seen that 1,2 ethanediol and 1,3 propanediol do not form any structures in water (determined by the low counts rate). With increasing carbon chain length in 1,4 and 1,5 the alkanediol molecules become more hydrophobic creating unstable domains of molecules (not thought to be micelles due to instability) and micellar structures for 1,6 hexanediol and 1,7 heptanediol. Similarly, we investigated the formation of micelles in the model system in the absence of silicon, which contains KCl and catechol **Figure 3a.** The results show no statistical change in the structures formed in the presence of the alkanediols of carbon chain length 2-5 similar to that observed in water (no salts). But formation micelles in 1,6 hexanediol and 1,7 heptanediol.

The formation of micelles could effectively make orthosilicic acid more reactive due to the hydrophobic effect,[26] seen as an increase in the rate of formation of trimers. Further increase in alkanediol concentartion are expected to show no further increases as once the critical micelle concentration is reached further increases will have little effect. Where the alkanediol remains miscible with water(1, 2 ethanediol and 1,3 propanediol), hydrogen bonds can form with orthosilicic acid reactive as seen from a reduction in k_{3rd} (**Figure 2b**). This was also confirmed in the case of 1,2 ethanediol where it was found that an increase in diol concentration (Si:OH ratio from 1:4 to 1:10) showed further reduction in relative k_{3rd} rate constant 0.77 to 0.64. Particle growth monitored using PCS in the presence of alkanediols at different Si : OH ratios revealed no significant effect, however in the alkanediols where micelles are formed (1,6 hexanediol and 1,7 heptanediol), an initial aggregate size is observed similar to the structure observed in the micelle study (**Figure 3b**). These aggregates were found to dissociate from 100 to 375 minutes as silica particles form and thereafter the aggregation rate was found to be similar to the blank. Interestingly a similar behaviour was observed for sericin (**Figure 1b**), providing further evidence that hydrogen bonding alone is not strong enough to act as a template for silica formation.

The materials produced from the use of alkanediols were characterised by SEM, TGA and gas adsorption. SEM micrographs shown in **Figure 4** show a small increase in granularity with increasing carbon chain length. The particle size roughly increased with increasing carbon chain length. Particle sizes for a given alkanediol decreased from 24h isolated silica to 7 day isolated silica due to Ostwald ripening (data not shown). Thermal gravimetric analysis showed that the alkanediols were not retained within the silica even at Si:OH ratio of 1:10. Gas adsorption measurement showed

Conclusion

The role of both hydroxyl functionalised biomolecules and alkanediols on silica formation have been systematically investigated *in vitro*. The results indicate that in aqueous systems the effect of hydroxyl-containing additives is negligible and dependent on the molar ratio of silicon: hydroxyl groups. The evidence presented above leads us to believe that Si-O-C bonds are unlikely to form but further work, including NMR analysis, is required to support this hypothesis. If covalent bonds between silicon and hydroxyl functionalised additives were formed, one would expect to observe significant changes in the rate of condensation of orthosilicic acid as well as changes in the morphology and structure of the silica produced together with entrapment of the additives in the silica formed. However, the data presented herein suggests that there is negligible effect of hydroxyl-containing additives on silica formation, which is contrary to what has commonly been thought.

Supp. Info: Kinetic data from 1:2, 1:4 and 1:10 Si:OH ratio.

Acknowledgements

AFOSR, EU, SJC

References

1. T. L. Simpson and B. E. Volcani, eds., *Silicon and Siliceous Structures in Biological Systems*, Springer-Verlag, New York, 1981.
2. R. E. Hecky, K. Mopper, P. Kilham and E. T. Degens, *Mar. Biol.*, 1973, **19**, 323-331.
3. K. D. Lobel, J. K. West and L. L. Hench, *Mar. Biol.*, 1996, **126**, 353-360; K. D. Lobel, J. K. West and L. L. Hench, *J. Mater. Sci. Lett.*, 1996, **15**, 648-650.
4. C. C. Harrison, *Phytochemistry*, 1996, **41**, 37-42.
5. C. C. Perry and T. Keeling-Tucker, *Colloid Polym. Sci.*, 2003, **281**, 652-664; C. C. Perry and T. Keeling-Tucker, *J. Biol. Inorg. Chem*, 2000, **5**, 537-550.
6. C. C. Perry and T. Keeling-Tucker, *Chem. Commun.*, 1998, 2587-2588.
7. K. Shimizu, J. Cha, G. D. Stucky and D. E. Morse, *Proc. Natl. Acad. Sci. USA*, 1998, **95**, 6234-6238.
8. J. N. Cha, K. Shimizu, Y. Zhou, S. C. Christiansen, B. F. Chmelka, G. D. Stucky and D. E. Morse, *Proc. Natl. Acad. Sci. USA*, 1999, **96**, 361-365.
9. Y. Zhou, K. Shimizu, J. N. Cha, G. D. Stucky and D. E. Morse, *Angew. Chem. Int. Ed.*, 1999, **38**, 780-782.
10. M. Sumper and E. Brunner, *Advanced Functional Materials*, 2006, **16**, 17-26; M. Sumper and N. Kroger, *J. Mater. Chem.*, 2004, **14**, 2059 - 2065.
11. W. H. van de Poll, E. G. Vrieling and W. W. C. Gieskes, *Journal Of Phycology*, 1999, **35**, 1044-1053.
12. N. Kroger, G. Lehmann, R. Rachel and M. Sumper, *Eur. J. Biochem.*, 1997, **250**, 99-105.

Supplemental information

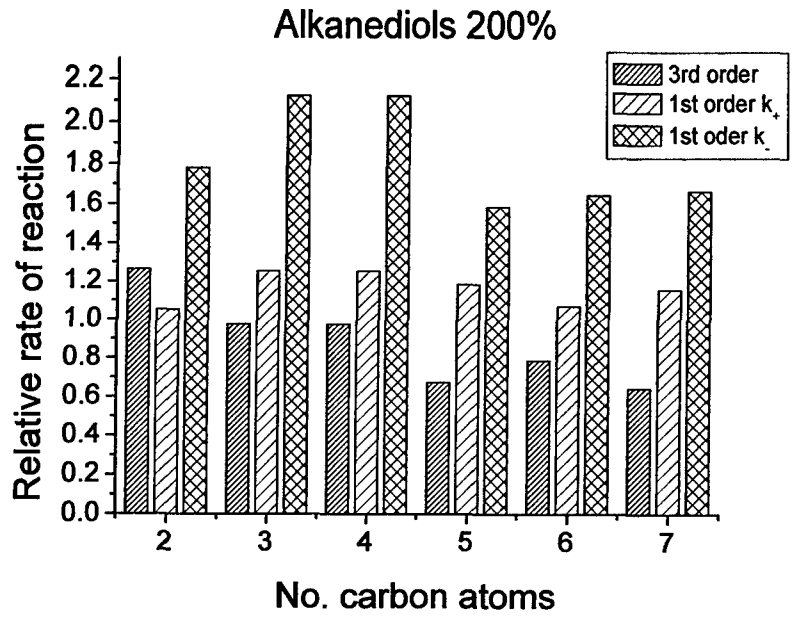

Alkanediols at 200%, showing slight increases in reverse 1st order.

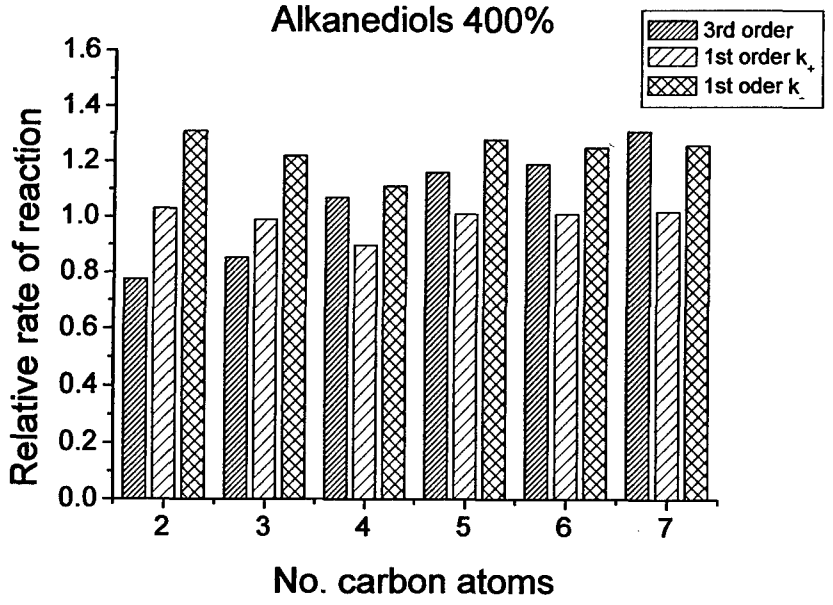

Complete alkanediol data at 400%.

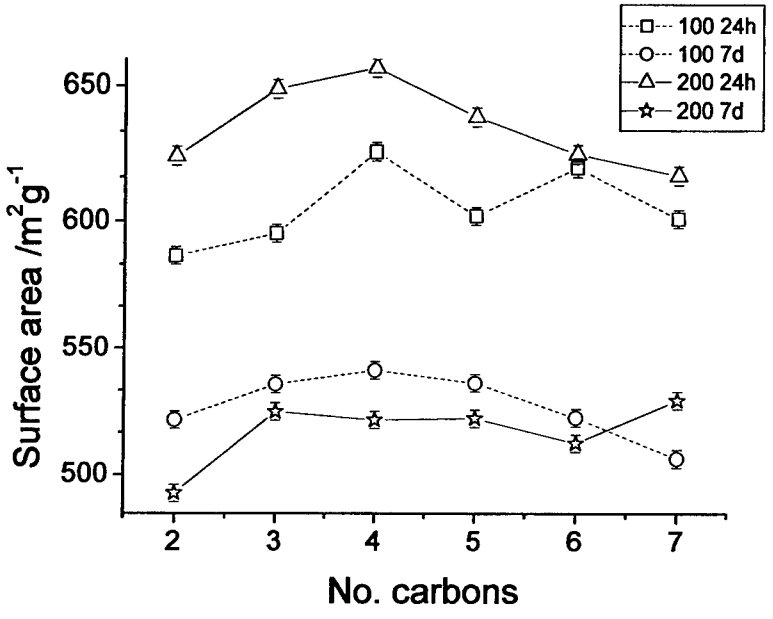

Surface area data.

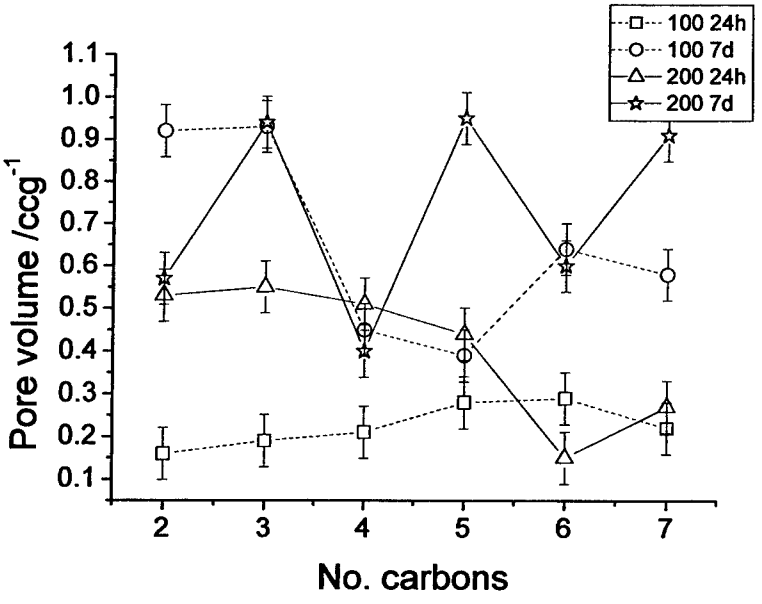

Pore volume data.

Resolution of complex monosaccharide mixtures from plant cell wall isolates by high pH anion exchange chromatography.

To be submitted to J. Chromatography A. H.A. Currie and C.C. Perry

Introduction

The plant cell wall is a highly complex three dimensional network of interwoven polysaccharide chains embedded in a gel matrix of galacturonic acid rich polysaccharides connected by calcium bridges. This network also contains many structural proteins and glycoproteins combined with and partially cross linked by phenolic substances (Chrispeels 1999; Fry 1988). As a result of this intricate structure, the identification and quantification of the individual components can be both problematic and time consuming.

The use of high pH anion exchange chromatography coupled with pulsed amperometric detection (HPAEC-PAD) has been used for a number of years for the detection and quantification of both mono and oligosaccharides. The use of this technique is advantageous due to the high levels of detection possible (down to picomolar levels). Also, it allows the determination of intact monosaccharides without pre or post column derivatisation, decreasing the time of analysis and eliminating a decrease in recovery due to incomplete derivatisation (Hardy *et al* 1988; Lee 1990; Garna *et al* 2004). The separated mono or oligosaccharides are therefore recoverable for further examination, vital when sample size is restricted. The use of this technique for the analysis of plant monosaccharide composition has been examined by a number of researchers with varied success largely due to the complexity of the material.

Several groups (Martens and Frankenberger 1991 and Samuelson *et al* 1999) have proposed separate methods for the separation of neutral and charged

this increased to incorporate 125mM sodium acetate in 200mM sodium hydroxide to elute galacturonic acid. D-glucosamine and glucuronic acid were not investigated. A post column injection of 300mM sodium hydroxide was used to aid detection. The separation of the individual monosaccharides was not shown and therefore it is not possible to comment on the accuracy of this method.

This paper describes the optimisation of the separation of ten monosaccharides from plants by comparing two column types CarboPac PA10 and the newest column the PA20. The advantages and disadvantages of each column are discussed with the optimum methods for each column described.

Potential (V)	Integration
+0.1	
+0.1	Begin
+0.1	End
-0.2	
-0.2	
+0.6	
-0.1	
-0.1	

ıadruple waveform utilised for the detection of carbohyd

.te	**Elution profile**
ıin	Isocratic 4.5mM NaOH
ıin	Isocratic 3mM NaOH
ıin	Isocratic 1.5mM NaOH
ıin	Isocratic 1.5mM with a gradient increasing to 4 between 45-60mins.
ıin	As D with increasing NaOH gradient to 150mM 80mins.
ıin	As D with increasing CH_3COONa gradient fro 45mM between 65-100mins.

ɔn profiles examined using the CarboPac PA10 to separa
es of the plant cell wall.

.te	**Elution profile**
ıin	Isocratic 1.5mM NaOH with a gradient increas 25mM between 20-40mins
ıin	Isocratic 4.5mM NaOH with a gradient increas 25mM between 20-40mins
ıin	Isocratic 6mM NaOH with a gradient increasin 25mM between 20-40mins
ıin	Isocratic 9mM NaOH with a gradient increasin 25mM between 20-40mins

n profiles examined using the CarboPac PA20 to separat
es of the plant cell wall

internal standard which is significantly broadened in comparison to the other traces. This was found to be a result of deterioration of the column with use. The column was regenerated with the use of strong acid before being re-equilibrated but this result was not permanent and the deterioration of resolution was an ongoing problem with this particular column. A further reduction in the concentration of sodium hydroxide used, as shown in Figure 1C did greatly improve the separation to baseline of most of the monosaccharides, however galactose is apparent only as a shoulder on the glucosamine peak but this is clearly an improvement on the first method where the two peaks were indistinguishable. It was found that a combination of method C with method A giving an increase from the isocratic 1.5mM up to 4.5mM between 45 and 60 minutes (Figure 1D) along with a decrease in flow rate, resulted in a clear differentiation between the individual neutral monosaccharides of the plant cell wall.

Separation of charged uronic acids from the plant cell wall using the PA10 column.

In addition to the neutral sugars, galacturonic and glucuronic acids are also present in the plant cell wall. The charge of these two monosaccharides results in a greater affinity to the column and therefore an increase in eluent strength is required to liberate them from the column. Method E, which utilised a rapid increase in sodium hydroxide solution to 150mM, was first tested for its ability to release these charged sugars, Figure 1E. However, the increased level of sodium hydroxide was insufficient to liberate the sugars from the column. This indicated that the use of a "pusher" would be required and a solution of sodium acetate was employed for this purpose with an increasing gradient from 3-45mM over the course of 35 minutes after the neutral monosaccharides had been released. This method resulted in the clear release of the uronic acids from the column in the order D-galacturonic acid followed by D-

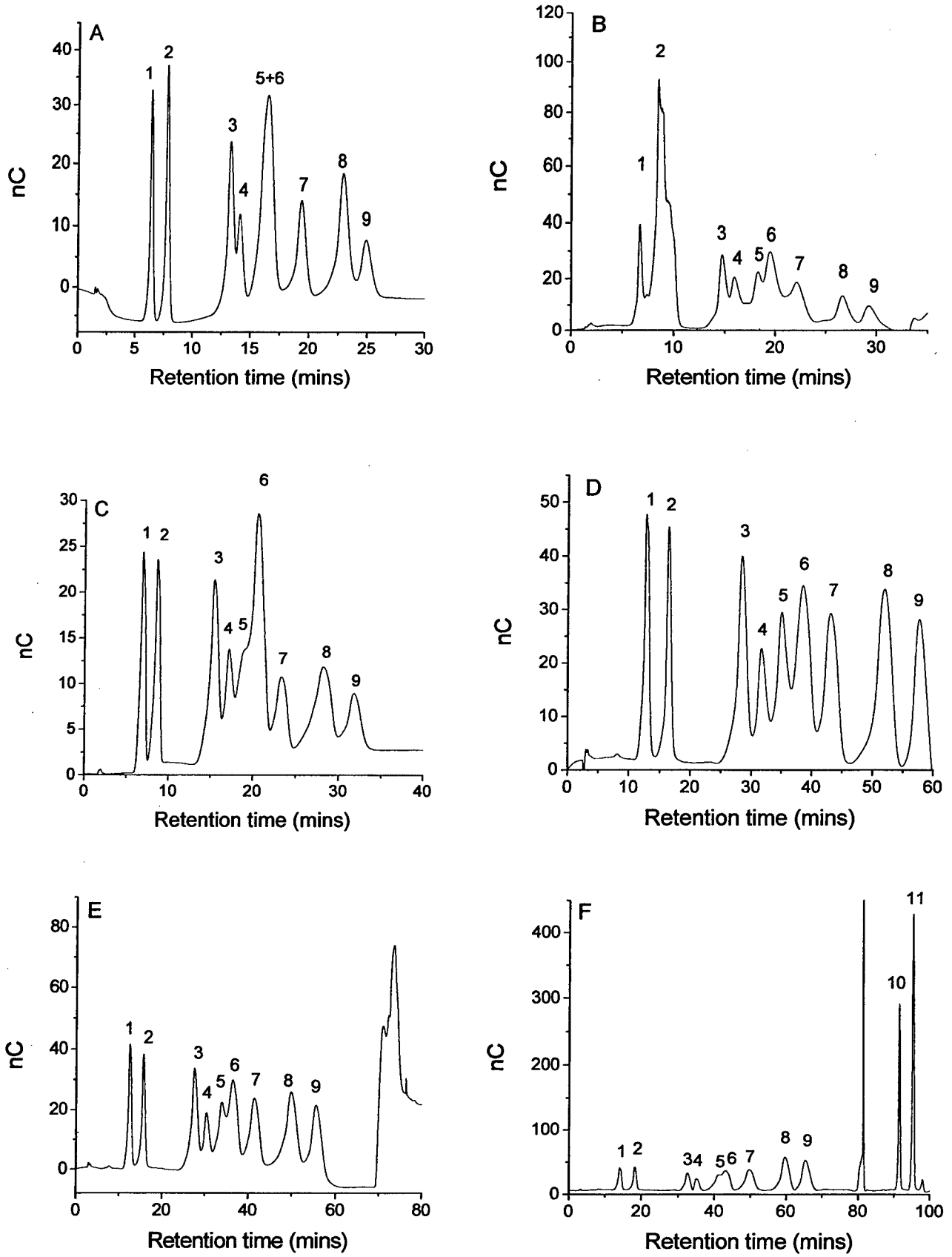

Figure 1. Optimisation of the separation of monosaccharides on the CarboPac PA10. Methods A-D were developed for the separation of the neutral monosaccharides and E-F demonstrate the separation of the charged uronic acids. The monosaccharides are indicated as follows 1) fucose 2) 2 deoxy D-galactose 3) arabinose 4) rhamnose 5) galactose 6) glucosamine 7) glucose 8) xylose 9) mannose 10) galacturonic acid 11) glucuronic acid.

Separation of monosaccharides from the plant cell wall using the PA20 column.

The use of the CarboPac PA 20 column was also examined with separations obtained shown in Figure 2. The initial elution conditions tested again utilised the low level isocratic sodium hydroxide concentration 1.5mM to separate the neutral monosaccharides (Figure 2A). From this trace it is possible to observe a clear baseline to baseline separation for most of the monosaccharides with the exception of D-galactose and D-glucosamine which co elute and with galactose present as a shoulder on the glucosamine peak. The charged uronic acids are clearly resolved by the increasing sodium acetate gradient indicating that no changes in sodium acetate concentrations were required for their separation. The repeatability of this method was again examined and is shown in table 5. The use of a 1.5mM sodium hydroxide isocratic solution is the lowest level suitable for monosaccharide analysis with a pH of 11.9, PAD detection with gold electrodes is most suited to pH≥12 (Dionex technical note 20). As this low concentration method was not wholly suitable for the separation of galactose and glucosamine it was necessary to investigate higher sodium hydroxide gradients.

An increase in sodium hydroxide concentration to 4.5mM did start to show a slight separation of galactose and glucosamine at a retention time of 10 minutes, but now the increase in charge due to the higher sodium hydroxide concentration lead to glucosamine starting to elute slightly earlier than galactose with a small degree of peak splitting (Figure 2B). However, this alteration of sodium hydroxide concentration also resulted in the co-elution of L-arabinose and L-rhamnose. The time between the D-xylose and D-mannose peaks is also significantly reduced. Further increase of the sodium hydroxide concentration to 6mM (Figure 2C) again demonstrated the co-elution of L-arabinose and L-rhamnose and there is a reduction

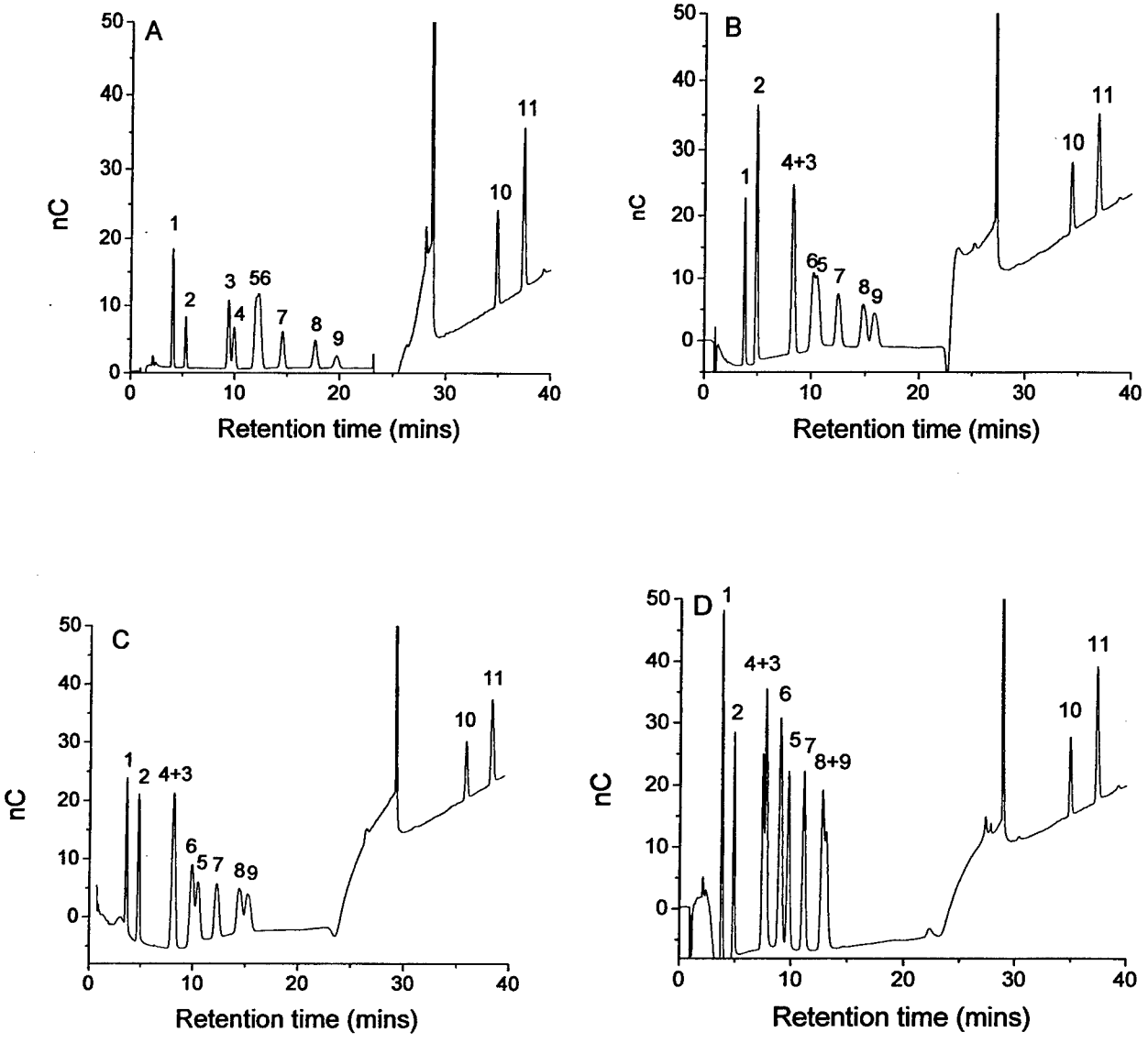

Figure 2. Optimisation of the separation of monosaccharides on the PA20 column. The monosaccharides are indicated as follows 1) fucose 2) 2 deoxy D-galactose 3) arabinose 4) rhamnose 5) galactose 6) glucosamine 7) glucose 8) xylose 9) mannose 10) galacturonic acid 11) glucuronic acid.

Discussion

The separation of the complex mixture of monosaccharides found in the plant cell wall presents researchers with a challenging chromatographic problem. The separation of monosaccharides by use of high pH anion chromatography with pulsed amperometric detection (HPAEC-PAD) is a valuable technique for the separation, identification and quantification of monosaccharides. Small quantities, down to picomole level can be observed using this technique and derivatisation of the monosaccharides is not required as in mass spectrometry and gas chromatography allowing their recovery after separation (Hardy et al 1988). HPAEC-PAD allows for the differentiation of monosaccharides which are chemically very similar and their quantification by relation to the PAD response. Separation is achieved through the exploitation of the weakly acidic nature of monosaccharide hydroxyl groups at high pH (>12). The monosaccharides can then be resolved as oxyanions utilising the slight variations in the p*K*a values of the monosaccharides (Lee 1990).

The PA10 column was capable of achieving of a full separation of the monosaccharides examined but did have several disadvantages. The run was prohibitively long with the final time being 130 minutes after cleaning and regeneration due to the low flow rate required. Also as observed in Figure 1F there was a vast difference in the scale required to examine the neutral monosaccharides and the uronic acids making quick comparison of different samples very time consuming. The durability of the column was also brought into question as the quality of the early eluting peaks deteriorated with increased usage. This can be observed by the broadening of the internal standard peak and its poor resolution from fucose shown in figure 1B.

References

1. Fry, S.C. 1988. *Plant cell wall: Chemical and metabolic analysis*, Longman Scientific and Technical, Essex, UK.
2. Chrispeels, M.J., In R. Cummings, J. Esko, H. Freeze, G. Hart, J. Marth (Editors) Essentials of Glycosbiology Cold Spring Harbour Laboratory Press New York, 1999, p. 305.
3. Hardy, M.R., Townsend, R.R., Lee, Y.C. 1988 *Anal. Biochem.* **170** 54
4. Lee, Y.C. 1990 *Anal Biochem* **189** 151
5. Garna, H., Mabon, N., Wathelet, B., Paquot, M. 2004 *J. Agric. Food Chem.* **52** 4652
6. Martens, D.A. and Frankenberger, W.T. 1991 *J of Chromatogr.* **546** 297
7. Samuelson, A.B., Cohen, E.H., Paulsen, B.S., Brüll, L.P., Thomas-Oates, J.E. 1999 *Carb. Res.* **315** 312
8. De Ruiter, G.A., Schols, H.A., Voragen, A.G.J., Rambouts, F.M. 1992 *Anal. Biochem.* **207** 176
9. Salvador, L.D., Suganuma, T., Kitahara, K., Tanoue, H., Ichiki, M. 2000 *J. Agric. Food Chem.* **48** 3448
10. Rocklin, R.D., Clarke, A.P., Weitzhandler, M. 1998 *Anal. Chem.* **70** 1496
11. Dionex technical note 20.
12. Gardner, S.L., Burrell, M.M., Fry, S.C., 2002. *Phytochem.* **60** 241
13. Cataldi, T.R.I., Margiotta, G., Iasi, L., Di Chio, B., Xiloannis, C., Bufo, S.A. 2000. *Anal. Chem.* **72** 3902
14. Zablakis, E., Huang, J., Müller, B., Darvill, A.G., Albersheim, P. 1995 *Plant Physiol.* **107** 1129.

Condensation of silicic acid in the presence of amine modified dextran (DEAE-dextran).

The presence of tertiary and quaternary amines in diatom biosilica has been shown by Sumper et al[1], but their activity in the biosilicification process and whether they act in isolation or as a component of the larger silaffin peptides is not clear. These amine species are polycationic electrolytes under most biologically neutral conditions and as such, these species are known to be able to stabilise or destabilise lyophobic sols in aqueous media[2,3]. A number of studies of silica condensation in the presence of polyelectrolytes have been carried out[4,5] resulting mainly in the formation of aggregated spheres (although Sumper et al produced a stabilised sol using a polyallylamine/TMOS system as a precursor to the formation of diatom like silica structure[6]). In all of these previous studies however the backbone of the polyelectrolyte was hydrocarbon which would tend to induce aggregate/micelle formation in aqueous medium through the hydrophobic effect and effectively form high localised amine concentrations on to which silica particles can aggregate or into which monosilicic acid can condense. In silaffins the amine side chain species are separated by non cationic amino acids which have a much greater hydrophilicity than the hydrocarbon backbone of the synthetic polyelectrolytes resulting in a more disperse separation of amine functionality. The use of silaffins in silicification studies however is limited through their prohibitive cost so a cheaper naturally based hydrophilic polyelectrolyte was sourced.

A commercially available amine modified dextran, DEAE-dextran, which contains tertiary and quaternary amines was selected as a biologically inspired polyelectrolyte for the study of the effects of a hydrophilic polycation on the condensation of silica.

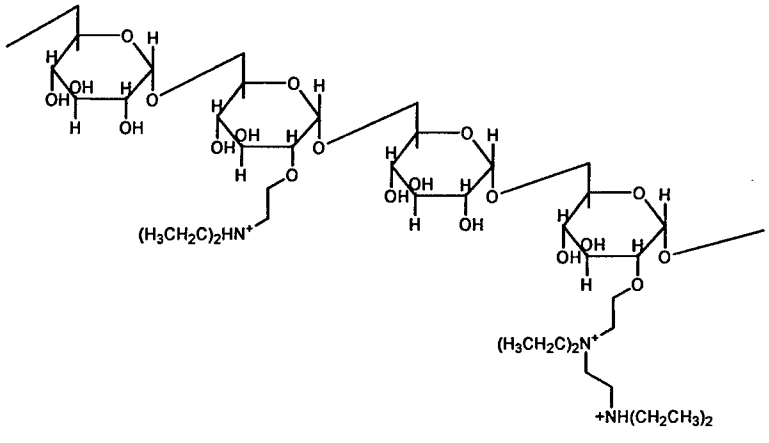

Addition of hydroxide ions sequentially deprotonated the amine groups and the inflection points indicated the complete removal of protons from each of the amine group types. The data showed that the single isolated tertiary amine group was fully deprotonated at pH 9.5, the tandem tertiary amine at pH 6.3 and that the quaternary amine remained protonated at pH 11. The aqueous solution behaviour of the modified dextran was then explored by photon correlation spectroscopy over this range of pH values:

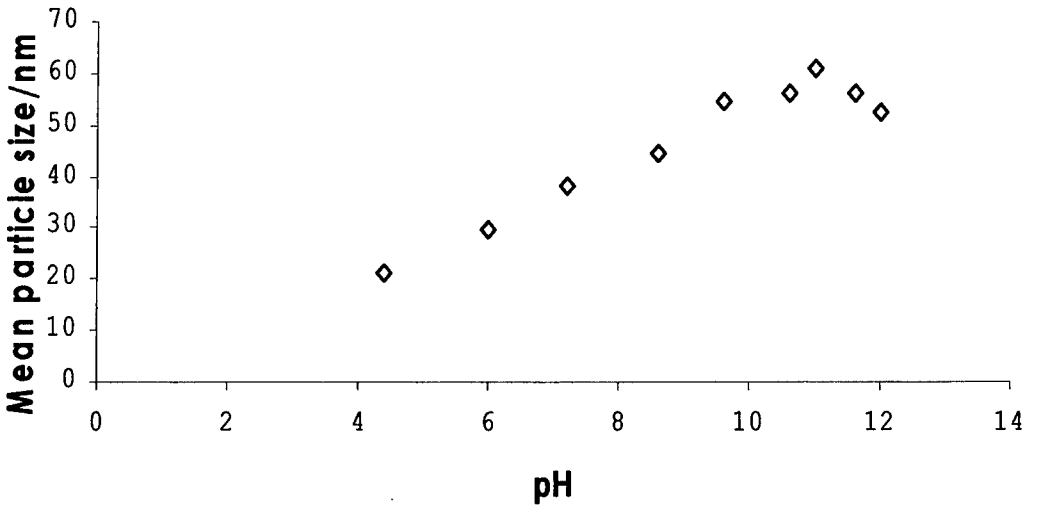

Figure 3. Observed particle size (PCS) dependence on pH.

The amine concentration was maintained at 30mMdm^{-3} and the pH adjusted by the addition of 0.1M KOH. The apparent polymer solution diameter was observed to increase at increasing pH i.e. with decreasing charge. This is a typical polyelectrolyte phenomenon as the molecules tend to aggregate as surface charge is reduced. Above pH 11 the hydroxyl groups on the dextran glucose units are expected to begin to deprotonate to give anionic surface charge and the molecules begin to disaggregate as indicated by the observed reduction in particle size. However some of these effects may be due to the change in ionic strength of the solution. In order to assess the significance of ionic strength on the solution characteristics of the polymer measurements were conducted where the ionic strength was manipulated by the addition of potassium chloride. The concentration of the polymer was again held at 30 mMdm^{-3} with respect to the amine concentration and the ionic strength adjusted from 0 to 1.0 molkg^{-1} with no pH adjustment (i.e. the DEAE-dextran should be fully charged).

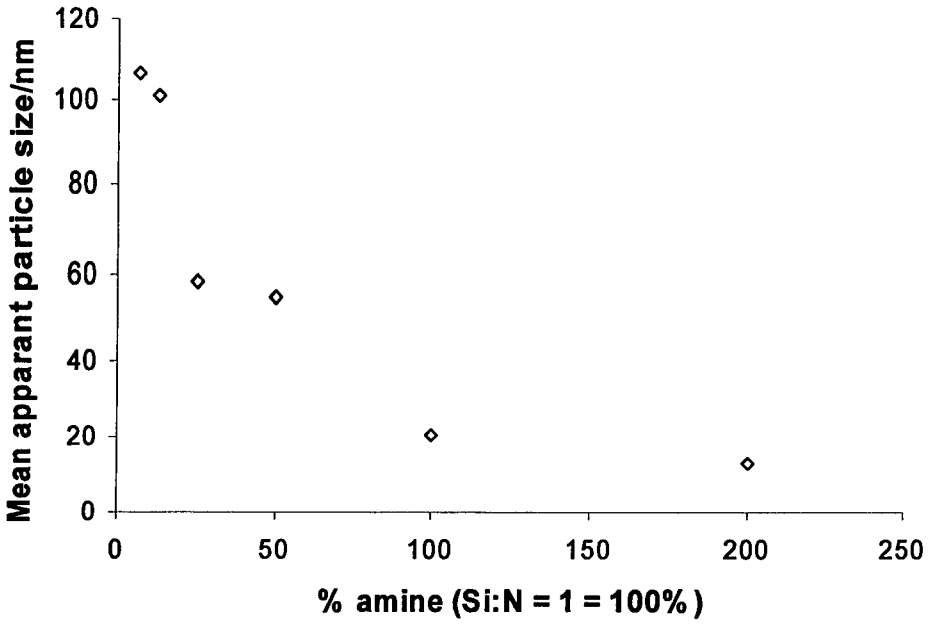

Figure 5 Observed particle size dependence with DEAE-dextran concentration.

Model silica condensation in the presence of DEAE-dextran.

30mMdm^{-3} monosilicic acid solutions were prepared in the presence of equimolar amine concentrations supplied by DEAE at pH's over a range of 5.6 to 7.2. The rate of disappearance of monosilicic acid was monitored by the molybdenum blue method and the early stage 3rd order rate constants determined for a range of pH values and

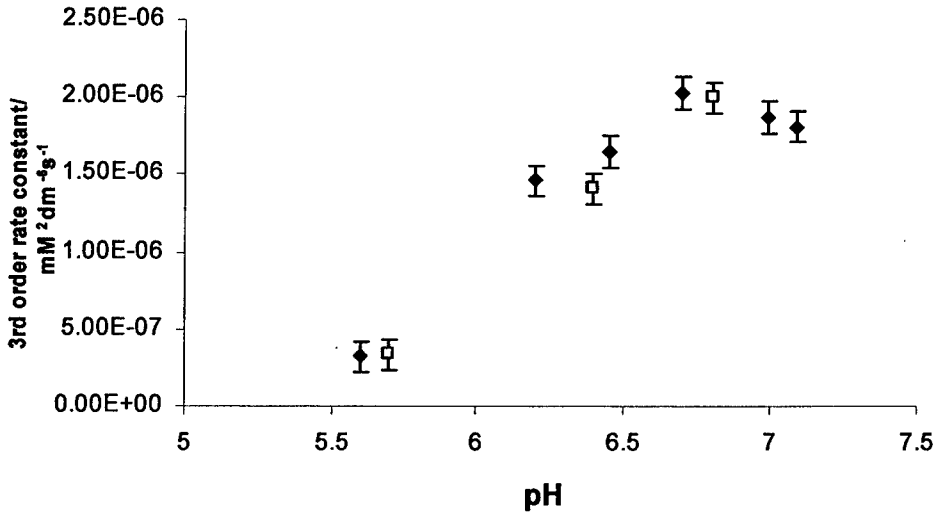

Figure 6. 3rd order rate constants obtained for 30mMdm^{-3} condensing monosilicic acid solutions in the presence (filled diamonds) and absence (open squares) of DEAE-dextran.

corresponding kinetic data showed that normal rates of condensation were observed and that the monosilicic acid fully condensed to non molybdenum active species as observed for the model blank. The presence of stable small oligomeric silicate species in the condensed solutions could not be confirmed by ^{29}SiNMR spectroscopy suggesting that the solution species were amorphous in nature and therefore the probability was that the monosilicic acid had condensed to primary particles which had then been stabilised as a sol by the polyelectrolytic DEAE-dextran.

Samples which had been allowed to condense and mature for 4 days were freeze dried and then re-dissolved to the same concentration in deionised water. Particle analysis was then conducted by multi angle photon correlation spectroscopy and the results before and after freeze drying compared.

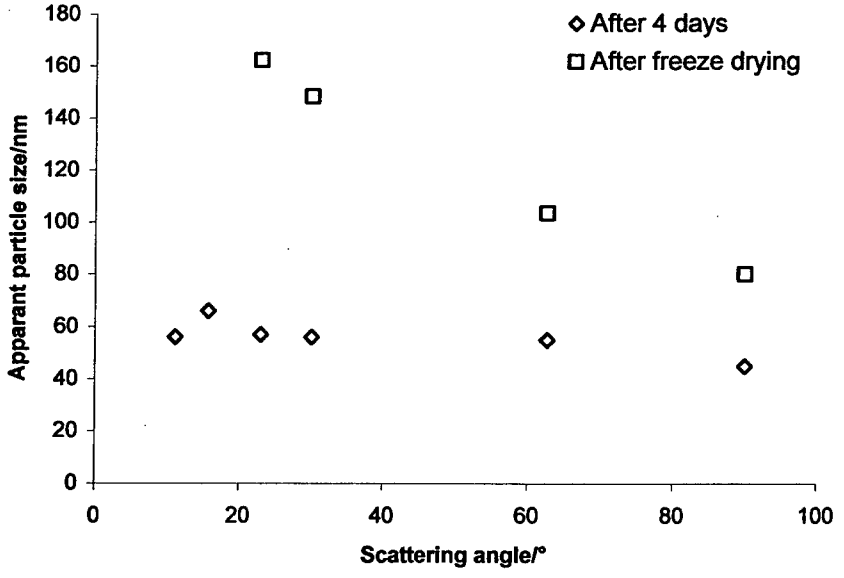

Figure 8. Multi angle photon correlation spectroscopy of DEAE-dextran stabilised silica sol before and after freeze drying.

The results obtained (figure 8) showed that although the reconstituted DEAE-dextran/silica solution was still unchanged in appearance to the naked eye compared to that before freeze drying there had been some associations during the process which resulted in a more disperse or anisotropic set of solution species. However no attempt to dis-aggregate the material had been made during re-dissolution so the irreversibility of the changes brought about by removal of the aqueous phase were not assessed.

In the case of SEM the material was deposited on a sticky carbon patch and coated with gold using an argon plasma. The samples for TEM were re-dispersed in ethanol and formvar coated copper grids dipped in and dried.

The morphological structure observed (figure 9) is thought to be due to phase separation during the freeze drying process followed by melting and evaporative oxidation of the DEAE-dextran during the heat treatment and the intact structure indicates that the stabilised silica particles have relatively active surfaces to generate this rigidity between the primary particles observed by TEM.

Other morphological features observed (figure 10) showed long fibrillar motifs, sheets with pores and also granular motifs.

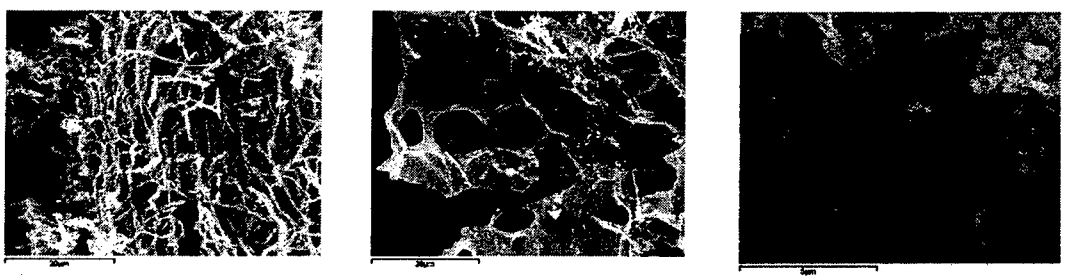

Figure 10. Scanning electron micrographs of other morphological features found scale bars a) and b) 20µm c) 5µm

As an extension to this work increasing levels of silica were condensed in the presence of the modified dextran to ascertain what level of silica can be stabilised and what the influence of silica concentration on morphology was. The level of the monosilicic acid precursor was increased by 2, 4 and 8 fold and the condensation process was allowed to proceed for 7 days. After this time the samples all appeared transparent to the naked eye. The siliceous material was isolated by dialysis, freeze drying and heat treatment as before and then observed by electron microscopy.

It was found that the modified dextran could stabilise a condensing concentration of monosilicic acid equivilant to 4 times its amine concentration. At higher concentrations the silica was observed to form a loosely held gel more usual with this model condensing system in the absence of additives.

and would explain their absence at lower monosilicic acid concentrations where the net composite charge would be higher.

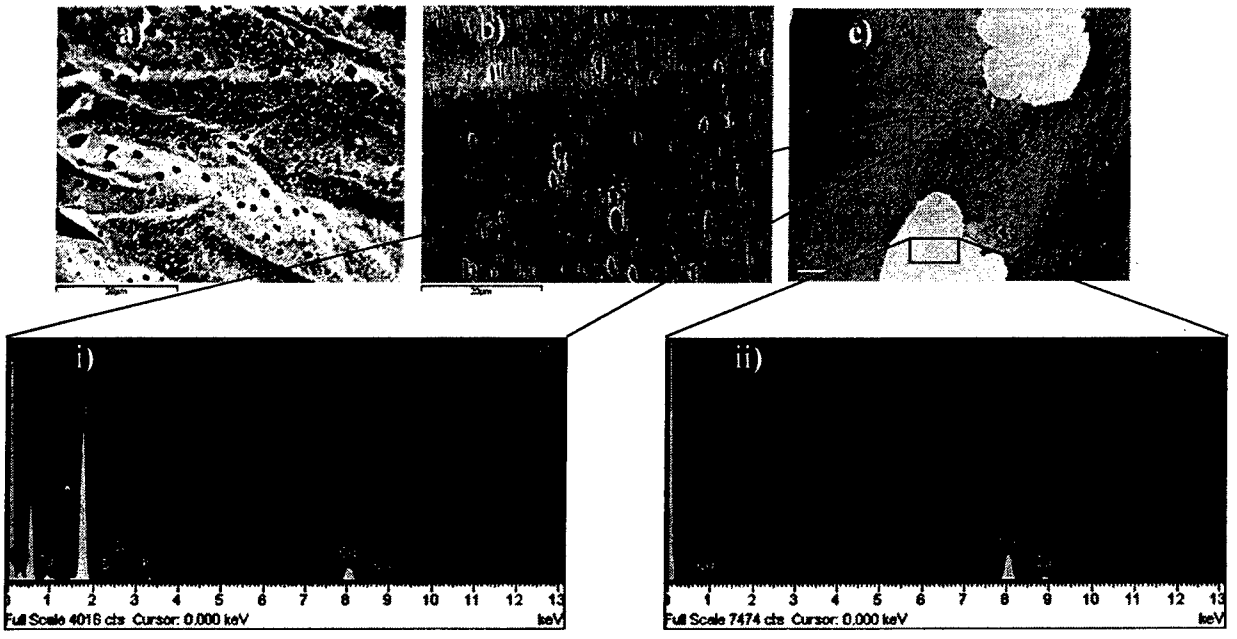

Figure 12. Electron micrographs. a) SEM of heat treated material from dialysis of 400% experiment b) SEM of non re-hydrated dialysis membrane (both scale bars 20μm) c) TEM of heat treated material from dialysis of 400% experiment (scale bar 500nm). Inserts show SAED spectra of membranous area (i) and holes (ii).

Summary.

Deae-dextran was shown by photon correlation spectroscopy to exhibit typical polyelectrolte properties. Its inclusion into a model silica condensing system showed it to have little or no effect on the condensation mechanism but was able to stabilise or destabilise the emerging sol depending on concentration ratios. Morphologies of the silica isolated from the sols suggested phase separation effects and these morphologies were influenced by silica to amine ratio.

References.

1). S. Wenzl, R. Deutzmann, R. Hett, E. Hochmuth and M. Sumper, *Angew. Chem. Int. Ed.*, 2004, **43**, 5933-5936.

2). G. M. Lindquist, R.A. Stratton, J. Coll. Int. Sci., 1976, **55** (1), 45,

The effect of bioinspired additives on the dissolution of silica in an undersaturated system (Graham Tilburey)

In the development of new silica based materials much focus has been placed on biological organisms and biosilicification, where remarkable nano-patterned materials are produced in a genetically controlled manner. Biosilicas are inorganic-organic hybrid materials. The organic phase has been isolated from several biological systems; higher plants, sponges and diatoms. Glycoproteins have been extracted from *Equisetum telmateia*,[1] silicatein, a central protein filament has been extracted from sponge spicules (*Tethya aurantia*).[2] Several classes of biomolecules have been isolated from silicified diatom cell walls including silaffins[3] and long chain polyamines.[4] The four classes of biomolecules have been investigated for their effect on silica formation *in vitro*, where crystalline silica, silica rods and silica spheres of specific diameters were produced, respectively. The silica precursor used to study silica formation *in vitro* in the presence of biomolecules from diatoms was tetramethoxysilane (TMOS), for silicatein from sponges, tetraethoxysilane (TEOS) and glycoproteins from *Equisetum arvense*, dipotassium tris(1,2 benzene-diolate-*O,O*)silicate. This makes comparison of the activity of the biomolecules difficult, especially when in some experimental systems the silica precursor, (TMOS and TEOS) is not a single species and therefore the species available to interact with the biomolecules is largely unknown.

Bioinspired additives have been investigated since the identification of key chemical features for silica formation. Amino acids,[5-8] small amine containing molecules (less than 1 kDa)[5, 6, 9-13] and polyelectrolytes have all been investigated. Structural control has been observed where spheres of a desired diameter can be formed usually using TMOS as the precursor. Common amine functionality exists between the additives that have exhibited a significant effect on the formation of silica. The role of additives in silica formation has been comprehensively reviewed recently, where the effects of additives on silica formation are elegantly characterised into three categories; additives can (1): catalyse condensation reactions, (2): influence aggregation and/or (3): act as scaffolds for silica formation.[14] Belton *et al.* have proposed that the hydrophobic effect, a mechanism involving the rearrangement of bulk water around reactive species is key to explaining subtle differences in the rate of condensation and aggregation for silica condensation reactions performed in the presence of diaminoalkanes and the electrostatic effect is key to explaining highly significant effects on the rate of aggregation of silica particles.[10] Kroger and Sumper have proposed a mechanism for the condensation of silicic acid molecules in the presence of propyleneamines, which centres around hydrogen bonds being formed between an unprotonated amine group and silicic acid.[15] Belton *et al.* proposed a mechanism for silica formation involving electrostatic interactions between a hydroxyl group situated at a silica particle surface and an unprotonated amine group, thereby catalysing condensation through a Sn2 mechanism.[12] The silica precursors used in *in vitro* studies vary greatly from an ethylenegylcol modified silane (tetra(2-hydroxyethyl)orthosilicate), alkoxysilanes (TEOS) and (TMOS)), sodium silicate and dipotassium tris(1,2 benzene-diolate-*O,O*)silicate, each having their advantages and disadvantages in use. To our mind, the main advantage of using dipotassium tris(1,2 benzene-diolate-*O,O*)silicate as primarily used throughout this study, is that a pure solution of orthosilicic acid is liberated upon dissociation of the complex. We believe this is crucial to gain a complete understanding of the interactions between

Initial experiments to compare the effect of bioinspired additives were all conducted on silicic acid containing solutions that were diluted after 60 minutes of reaction. The additives studied were; Poly(allylamine hydrochloride) (PAH, mw 15000), Poly-L-lysine (PLL, mw 22100) , Polythylenimine (PEI, mw 25000), 1,10 diaminoalkane 97% (1,10 DA), Diethylenetriamine 99% (DETA), triethylenetetraamine 97% (TETA), Tetraethylenepentaamine 98% (TEPA) Pentaethylenehexamine (PEHA), Dipropylenetriamine (N3) and tetrapropylenepenataamine (N5). The additives were purchased from Sigma-Aldrich, except N3 and N5 which were synthesised and characterised in house.[13] The ratio of Si:N was set at 1:6. The experimental procedure involved an initial dilution of the 30mM solution to 2mM followed by an immediate dilution to 1mM with a solution containing the chosen additive at the required concentration. The molybdenum blue method was used to monitor the dissolution of the silica species in solution as previously described.

A study of pre-condensed silica solutions following dilution to 1mM silica in the presence of PEHA.

The effect of PEHA at a ratio of 1Si:6N on pre-condensed silica systems was also studied. Condensation times were 3, 5, 7, 15, 60 and 160 minutes prior to dilution. The concentration of silicic acid was monitored immediately after dilution and thereafter using the molybdenum blue method previously described.

As the precipitation of silica could not be monitored by photon correlation spectroscopy, due to a poor detector response, an alternative qualitative approach was undertaken, whereby the total amount of silica remaining in solution was measured. Upon mixing of the additive solution and precondensed silica solution, 2ml portions of the resulting solution were pipetted into 2.5ml eppendorf tubes and left to stand. At predetermined reaction times, samples were centrifuged for 2 minutes at 15000 r.p.m. in a Sanyo micro centaur and 0.5ml of the supernatant pipetted into 1ml of 2M NaOH and the samples heated for 1 hour in a water bath at 80°C, allowed to cool before 200µl of the NaOH digested silica solution was taken and added to 16.5ml of the molybdic acid solution so that the total amount of silicic acid present in the supernatant could be measured.

Results and Discussion.

<u>Undersaturated Solution Studies</u>

The additives chosen are all known for their ability to accelerate silica formation from aqueous solution[10, 12, 13, 16, 17] and were inserted into a 1mM solution of silicic acid. Silicic acid concentrations were measured for ca. 24 hours using the molybdenum blue method. Over a 24 hour period the concentration of silicic acid remained constant irrespective of the additive added and the ratio of Si:N used, Figure 1.

- The molybdenum blue method cannot differentiate between monomeric and dimeric species; therefore any initial condensation observed by this method must arise from the formation of trimers. The choice of a pre-reaction time of three minutes was chosen to represent a period of maximum concentration of these species.
- The formation of small oligomers dominates after 3 minutes and ends around 10 minutes, when the arbitrary distinction between oligomers and particles is usually made. The time point 7 minutes was selected as a mid point during this process and was used to investigate the stability of oligomers in a 1mM silica system.
- Particles are first observed by PCS after 60 minutes and this determined the selection of the 60 minute condensing time.
- The 5 and 15 minute condensing times were selected to investigate other species that might exist between these known milestones.
- The time point 160 minutes was selected to investigate the stability of larger particles.

Figure 2a shows dissolution curves for the different pre-condensation times commensurate with the different species present in the samples. Analysis of the initial rates of dissolution of the samples after different periods of pre-condensation, Figure 2b shows that the initial rate of dissolution of silica species varies with the initial reactant species in a non-systematic manner. The initial rate of dissolution is representative of the stability and population of species present in solution. The data suggest that the stability of the silica species reaches a minimum after 5-7 minutes where the initial rate of dissolution is fastest. Interestingly, Figure 2b shows an initial decrease in particle stability, suggesting trimers are more stable than oligomers and larger oligomers are less stable than smaller ones. As the condensation time is increased still further, an increase in stability is observed as the silica species increase in size (PCS data not shown). The dissolution curve for 3 minutes appears to show a different profile when compared to the profile of 7-15 minutes. This suggests that the population of small oliogmers at 3 minutes is small, if present at all and the dissolution rate approximates more closely to a single species in solution than at any of the other condensation times studied.

the chosen bioinspired additives on pre-condensed silica systems that had been allowed to react for 60 minutes before diluting to 1mM. The choice of time was predicated by our studies that have shown that presence of the bioinspired additives dramatically increases the rates of silica condensation/ aggregation as assessed by PCS. At the chosen reaction time, the reaction system contains both particles and molybdate detectable silicic acid with the measured particle size being ca. <1nm (measured by PCS) and the free silicic acid concentration being *ca.* 6mM.

Figure 3(a) shows the dissolution of silica species in the presence of ethyleneamines of increasing chain length.

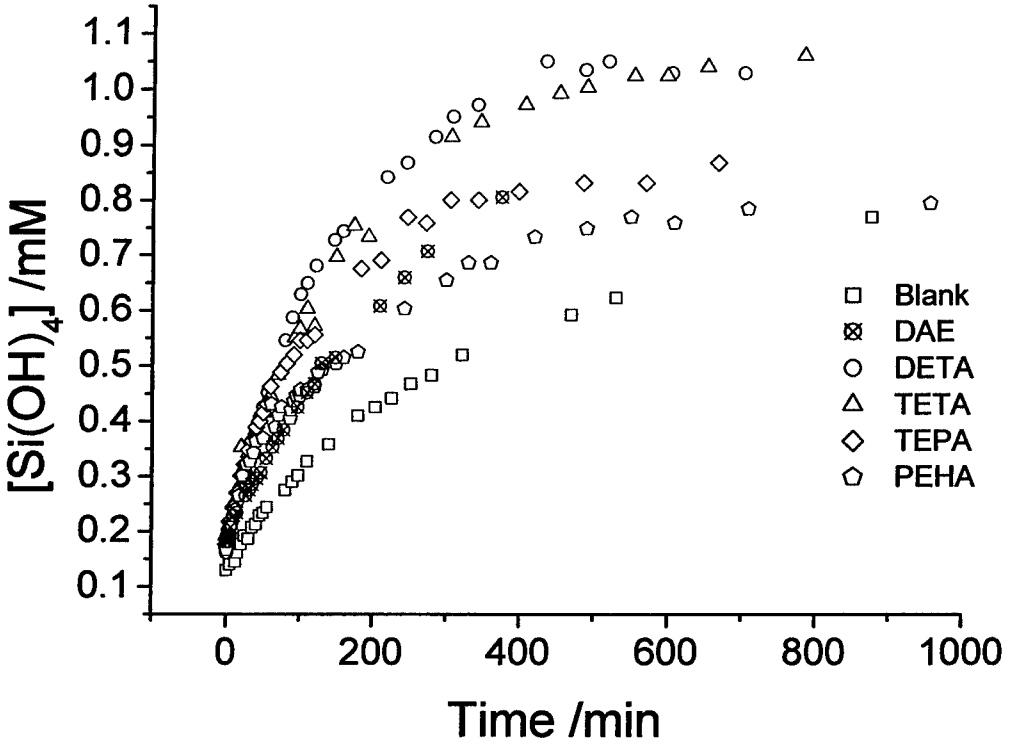

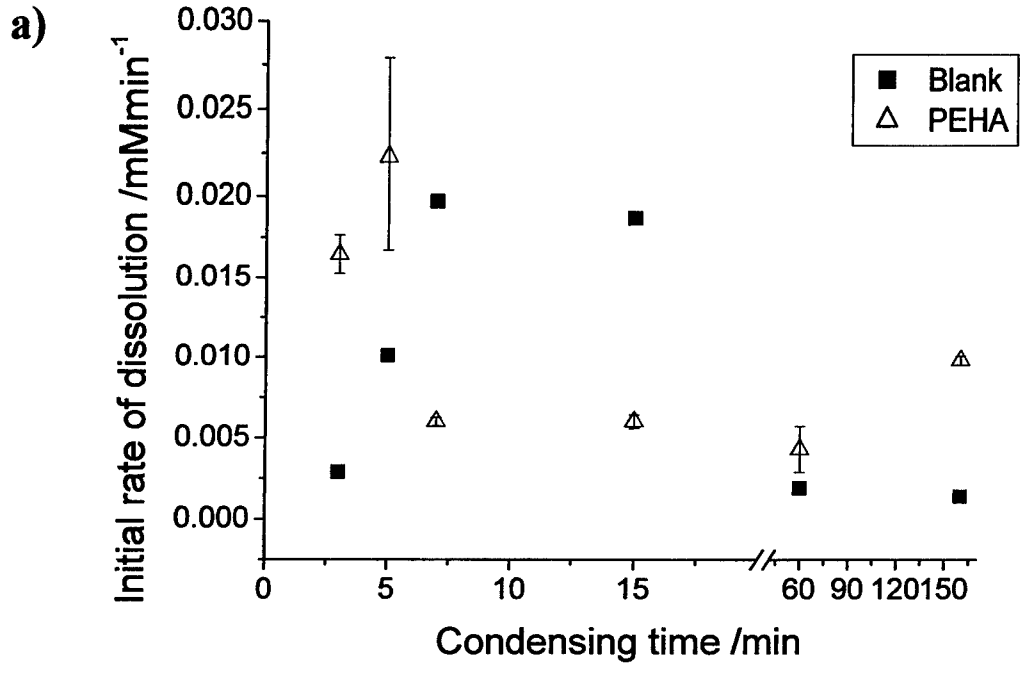

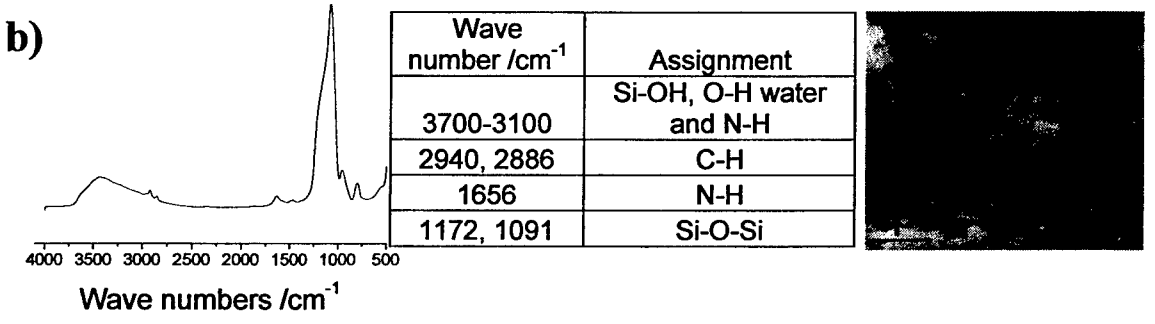

Wave number /cm^{-1}	Assignment
3700-3100	Si-OH, O-H water and N-H
2940, 2886	C-H
1656	N-H
1172, 1091	Si-O-Si

Figure 4. (a) – The relative rate of dissolution of pre-condensed silica systems in the presence and absence of PEHA, (b) Left; FTIR spectra, middle; assignment of main bands, right SEM of the precipitate isolated after 60 minutes in the presence of PEHA (pre-condensing time 60 minutes followed by dilution to 1mM in the presence of PEHA with a precipitate being recovered after a period of 60 minutes further reaction).

Figure 4 shows that prior to a stable particle being formed (Dave Belton PhD thesis) the presence of PEHA in the sample solution destabilises the silica species, as evidenced by an increase in the initial rate of dissolution. When the pre-condensation time was increased to 7 minutes and more, precipitation was observed. We hypothesise that at this and later pre-condensation times the first sufficiently negatively charged silica species are present in solution. The introduction of a cationically charged species to the solution enables electrostatic interactions to occur between PEHA and the charged silica species, leading to the formation of larger entities that precipitate out. The ability of PEHA to bridge between particles thus promoting aggregation and precipitation is also seen as a reduction in the initial rate of dissolution, Figure 4. This effect was observed to be most prominent for samples with a fairly short pre-condensation time, as after 15 minutes of pre-condensation, the presence of PEHA appeared to destabilise the silica species in solution as evidenced by an increase in the initial rate of dissolution. The reason behind this observation is

References:

1. C. C. Perry and T. Keeling-Tucker, *J. Biol. Inorg. Chem*, 2000, **5**, 537-550.
2. J. N. Cha, K. Shimizu, Y. Zhou, S. C. Christiansen, B. F. Chmelka, G. D. Stucky and D. E. Morse, *Proc. Natl. Acad. Sci. USA*, 1999, **96**, 361-365.
3. N. Kroger, S. Lorenz, E. Brunner and M. Sumper, *Science*, 2002, **298**, 584-586.
4. M. Sumper and N. Kroger, *J. Mater. Chem.*, 2004, **14**, 2059 - 2065.
5. T. Mizutani, H. Nagase, N. Fujiwara and H. Ogoshi, *Bull. Chem. Soc. Jpn.*, 1998, **71**, 2017-2022.
6. L. Sudheendra and A. R. Raju, *Mater. Res. Bull.*, 2002, **37**, 151.
7. T. Coradin and J. Livage, *Colloids Surf. B*, 2001, **21**, 329-336.
8. D. Belton, G. Paine, S. V. Patwardhan and C. C. Perry, *J. Mater. Chem.*, 2004, **14**, 2231-2241.
9. L. L. Brott, D. J. Pikas, R. R. Naik, S. M. Kirkpatrick, D. W. Tomlin, P. W. Whitlock, S. J. Clarson and M. O. Stone, *Nature*, 2001, **413**, 291.
10. D. Belton, S. V. Patwardhan and C. C. Perry, *Chem. Commun.*, 2005, 3475-3477.
11. K. M. Roth, Y. Zhou, W. Yang and D. E. Morse, *J. Am. Chem. Soc.*, 2005, **127**, 325-330.
12. D. Belton, S. V. Patwardhan and C. C. Perry, *J. Mater. Chem.*, 2005, **15**, 4629-4638.
13. V. V. Annenkov, S. V. Patwardhan, D. Belton, E. N. Danilovtseva and C. C. Perry, *Chem. Commun.*, 2006, **published online**, DOI:10.1039/B515967A.
14. S. V. Patwardhan, S. J. Clarson and C. C. Perry, *Chem. Commun.*, 2005, **9**, 1113-1121.
15. N. Kroger and M. Sumper, in *Biomineralization: from biology to biotechnology and medical application*, ed. E. Baeuerlein, Wiley-VCH, Editon edn., 2000.
16. S. V. Patwardhan, N. Mukherjee and S. J. Clarson, *Silicon Chem.*, 2002, **1**, 47.
17. S. V. Patwardhan, N. Mukherjee, M. Steinitz-Kannan and S. J. Clarson, *Chem. Commun.*, 2003, **10**, 1122-1123.

Biochemical Studies of Plant Cell Walls from Equisetum arvense: Towards an understanding of 'Si' (in some form) interactions with the plant cell wall.
H.A. Currie

Methods

Treatment of Plant materials

Equisetum arvense was collected and freeze dried within 24 hours of collection before milling into a fine powder.

- Cell wall extraction from *Equisetum arvense*

The plant cell wall was extracted using ice cold ethanol to extract low molecular weight sugars, amino acids, organic acids and many inorganic salts associated with the surface of the plant.
The milled dried plant tissue (20g) was added to 70% ice cold ethanol (200ml) and vortexed and cooled to 0°C at least five times. The mixture was then stirred at 0°C for 5 hours before filtration under vacuum. The insoluble residue was then washed with further aliquots (totalling 1l) of 70% ethanol. The insoluble material could then be dried for storage or used for further extraction.

- Extraction of Pectic polysaccharides

The extraction of some pectic polysaccharides was carried out using the aqueous chelating agent CDTA.

Alcohol insoluble residue was stirred in a 50mM solution of CDTA pH 7.0 at room temperature for 16 hours. The insoluble material was removed by centrifugation and extracted again by this method. The supernatant was retained and dialysed using 3,500MW cut off membrane for the removal of the CDTA. After dialysis, (to a conductivity ≤ 1 µS) the CDTA soluble extract was freeze dried prior to further examination. This process was then repeated with the insoluble material to generate a second extract.

- Extraction of less soluble pectins and hemicelluloses

The extraction of the hemicelluloses and less soluble pectins is accomplished with the use of alkali after treatment with a chelating agent. However, due to the possibility of alkaline degradation of polysaccharides this extraction is carried out in the presence of the strong reducing agent Sodium borohydride which can partially suppress the degradation.

The CDTA insoluble material was extracted further with a mixture of 50mM sodium carbonate and 20mM sodium borohydride. This suspension was stirred for 16 hours at 4°C.and the soluble extract removed by centrifugation and the supernatant collected and dialysed using 3,500MW cut off membrane to a conductivity ≤ 1µS. A second extraction with alkali and sodium borohydride was achieved by repetition of this process with the insoluble material. Once dialysed, the extracts were freeze dried before further examination.

- Colorimetric assays for carbohydrate determination
  - Anthrone Assay for hexose content

carried out by the method detailed in Fry (1988). To 10mg of extract, 1ml of 0.1M sodium hydroxide was added, sealed and incubated in the dark for 1 hour at 25°C. After incubation 0.1ml of 2M trifluoroacetic acid was added followed by 1ml of ethyl acetate (butan-1-ol could also be used) the vessel was sealed and vigorously mixed before centrifugation for 10 minutes at 2,500g. The organic phase was removed and retained. To the lower aqueous phase a further 1ml of ethyl acetate was added and the centrifugation repeated. The organic phase was again removed and combined with the previous organic layer before the addition of 1ml of 0.01M trifluoroacetic acid. The ethyl acetate was then removed under vacuum and the released phenolics re-dissolved in acetone before separation by thin layer chromatography.

The hydrolysed phenolics were spotted onto silica gel thin layer chromatography plates along with the phenolic standards cinnamic acid, coumaric acid, ferulic acid and sinapic acid. The samples and standards were then run in the dark with a mobile phase consisting of a 9:1 ratio of toluene: acetic acid. The Rf values obtained from the samples were calculated and compared to the Rf values of standard phenolic species to determine the identity of the phenolics from the standards.

- The Fractionation of the CDTA extracts

Separation of the pectin extracts released from the cell wall by treatment with CDTA was carried out using the method of Redgewell and Selvendran (1986)
A suspension of the CDTA extract was suspended in 50ml of distilled water at 4°C overnight then stirred for 2 hours at room temperature in 0.1M phosphate buffer pH 6.5.
The suspension was then pumped at a rate of 0.8ml/minute onto a column of the ion exchange resin DEAE-Trisacryl equilibrated with 0.05M phosphate buffer. The column was then eluted with

- 200ml of 0.05M phosphate buffer (pH6.5),
- 200ml of 0.05M phosphate buffer (pH6.5) containing 0.125M Sodium chloride,
- 200ml of 0.05M phosphate buffer (pH6.5) containing 0.25M Sodium chloride,
- 200ml of 0.05M phosphate buffer (pH6.5) containing 0.5M Sodium chloride,
- 200ml of 0.05M phosphate buffer (pH6.5) containing 1M Sodium chloride.

While eluting, 10ml fractions were taken for analysis for the protein content and the carbohydrate content (described later).
Once all eluents had passed through the column, the resin was cleaned by washing with 200ml of 0.05M phosphate buffer with 2M sodium chloride.

- The fractionation of the hemicellulose extracts

Separation of the hemicellulose extracts was carried out using the method of Konno *et al* (2002) utilising the ion exchange resin DEAE Sepharose CL-6B. The extract was stirred in 20mM phosphate buffer (pH 6.5) and this buffer was also used to equilibrate the column. Once the sample was loaded onto the column, it was then eluted with

- 200ml of 0.02M phosphate buffer (pH6.5),
- 200ml of 0.02M phosphate buffer (pH6.5) containing 0.125M Sodium chloride,
- 200ml of 0.02M phosphate buffer (pH6.5) containing 0.25M Sodium chloride,
- 200ml of 0.02M phosphate buffer (pH6.5) containing 0.5M Sodium chloride,
- 200ml of 0.02M phosphate buffer (pH6.5) containing 1M Sodium chloride

Again while eluting 10ml fractions were taken for analysis for both protein and carbohydrate content.

The gel was poured into the assembled gel mould to 1 ½ comb depths from the top edge of the plate sandwich then overlaid with water saturated butanol to exclude air and ensure a flat surface. Polymerisation was allowed to occur at room temperature for approximately 45 minutes. The butanol was removed and the surface of the gel washed with electrode buffer. The stacking gel was then prepared for pouring on top of the resolving gel.

Stacking gel was prepared with
1ml 40% acrylamide stock
2.5ml 0.5M Tris buffer pH 6.8
100µl 10% (w/v) Sodium Dodecyl Sulphate
6.4ml distilled water

For Polymerisation
20µl N,N,N',N'-Tetramethylethylenediamine (TEMED)
50µl Ammonium persulphate (APS) 10% (w/v)

The comb was positioned in the gel mould apparatus at a 45° degree angle and the stacking gel mix was carefully added to the top of the resolving gel. The comb was lowered into the stacking gel to form individual wells, taking care to avoid the introduction of any bubbles. The gels were fixed into the electrode tank and the inner and outer gel reservoirs filled with electrode buffer.

Tris-Glycine electrode buffer was prepared with
3.1g Tris base
14.4g glycine
1g Sodium dodecyl sulphate
pH to 8.3 made up to 1l.

The prepared samples were applied to the wells and the tank was connected to the power pack and run at a constant current of 100 volts for approximately 1 hour until the tracking dye was approximately 0.5cm from the bottom of the gel.

Once the run was complete the gel could be stained using coomassie blue or silver staining.

- Coomassie brilliant blue G staining

Staining of gels with Coomassie brilliant blue G was carried out by submerging and gently agitating the gel in a staining solution consisting of 25% (v/v) ethanol, 10% (v/v) acetic acid and 0.25% (w/v) Coomassie brilliant blue G. The gels were stained for a minimum of 1 hour, but could be held in this state for longer provided there was no evaporation of the staining solution which could lead to the gel drying.
Proteins present on the gel on the gel are stained dark blue but were not observed due to background staining of the whole gel. De-staining of the gel was achieved by submerging and gently agitating the gel in a de staining solution of 25% (v/v) ethanol and 10% (v/v) acetic acid.

Results

- Cell Wall extracts

Plant cell wall extracts were prepared as per the methods section with the first extracts from CDTA being referred to as C1 and the second CDTA extracts as C2. The Sodium carbonate/sodium borohydride extracts are referred to as N1 and N2 respectively.
Repeats of extracts are preceded by A,B,C etc.

These extracts were analysed for carbohydrate content initially by colorimetric assay.

- Anthrone assay for the detection of hexose sugars

A standard concentration calibration was used to determine the quantity of six carbon hexose and deoxyhexose sugars. The quantities of the hexose sugars per mg of sample are shown in Figure 1. The results of this assay quantify the levels of hexose sugars which include D-glucose, D-galactose, D-mannose and also the deoxy hexoses, L-rhamnose and L-fucose. However, the limitation of this detection method is that the individual sugars levels cannot be quantified. This will be examined using high pH anion chromatography and the initial work has already been carried out (see accompanying paper "Resolution of the complex monosaccharide mixtures from plant cell wall isolates by high pH anion exchange chromatography").

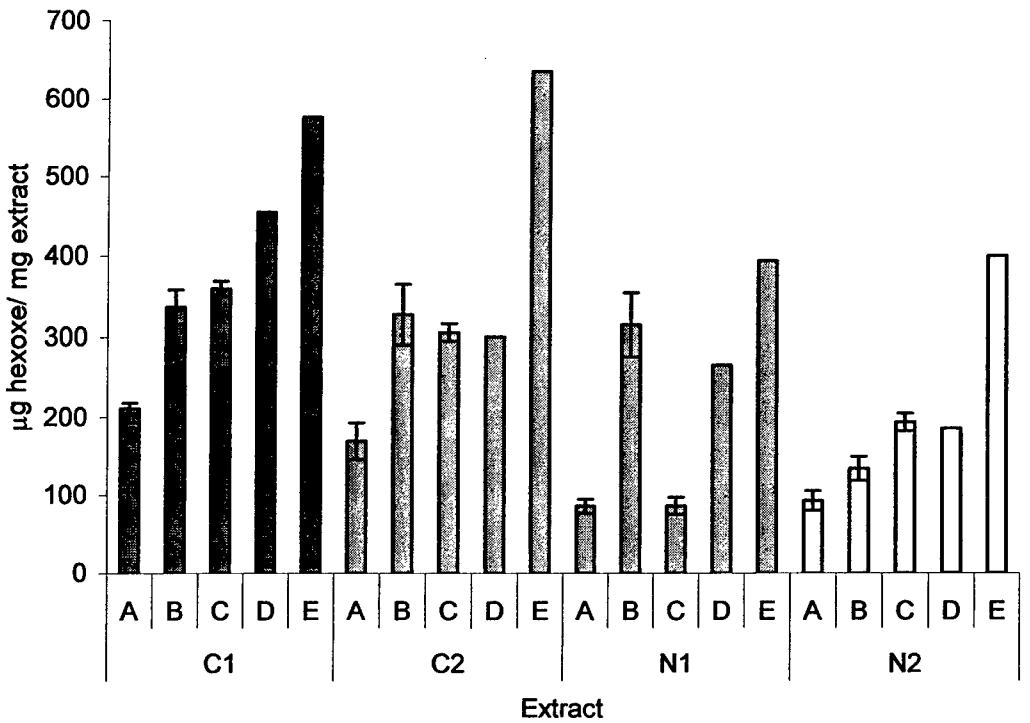

Figure 1. The results of colorimetric assays for the determination of hexose sugars. Results given as a mean value as all assays carried out in duplicate or triplicate standard deviation given where triplicate results were obtained.

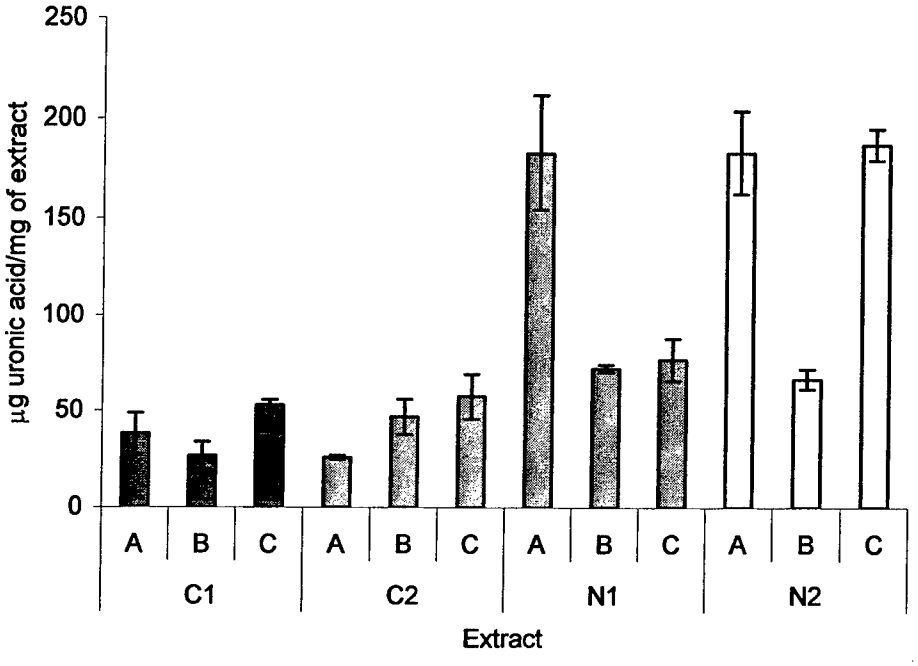

Figure 3. Results of the m-hydroxybiphenyl assay for uronic acid content. Mean values of repeats are plotted and standard deviation given for triplicate samples.

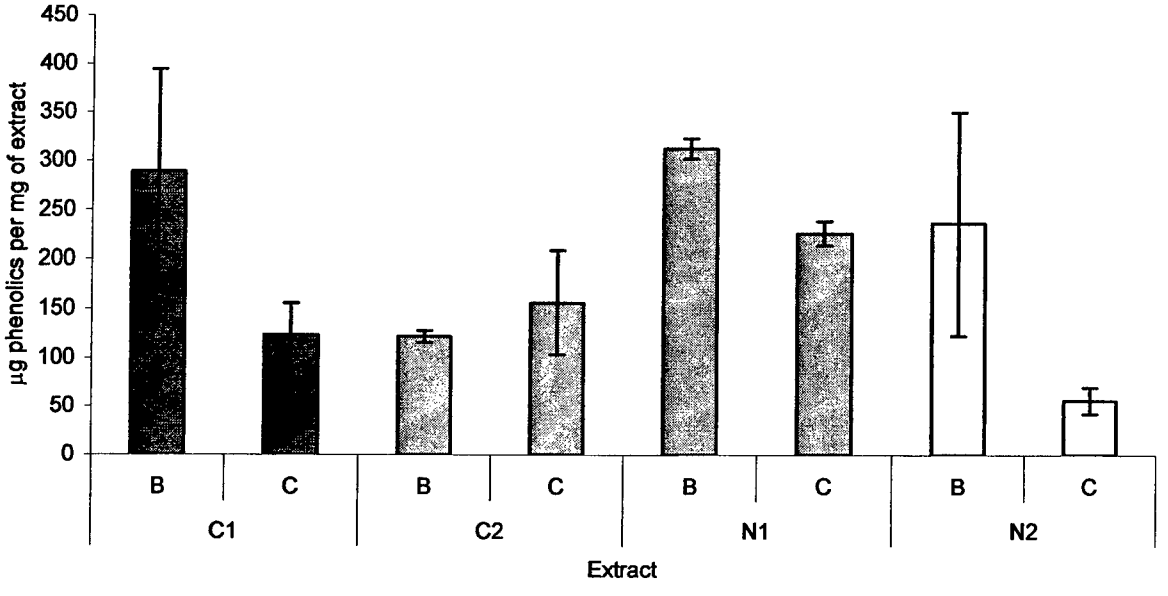

Figure 4. The determination of phenolic content using Folin and Ciocalteu's reagent.

Extract	Percentage protein	Polymerised Silica
AC1	8.72%	0.85μg/mg

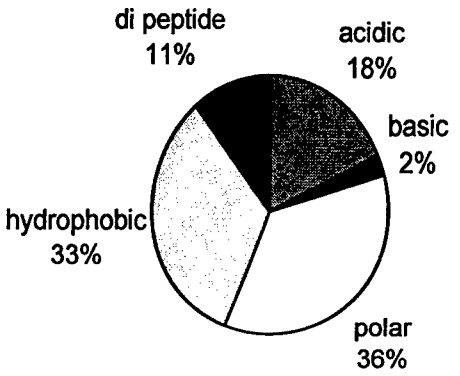

Figure 6. The amino acid composition of the first CDTA extract from separation A.

The CDTA soluble extracts were separated on the basis of charge and size by anion exchange chromatography on DEAE Trisacryl resin with phosphate buffer and an increasing sodium chloride concentration. Fractions of 10mls each were collected and tested for protein and the fractionation of this AC1 extract is shown in Figure 7. From this figure it is possible to observe 2 clear protein containing groups between fractions 0-20 (a) and 70-85 (b). These groups were pooled and dialysed before freeze drying.

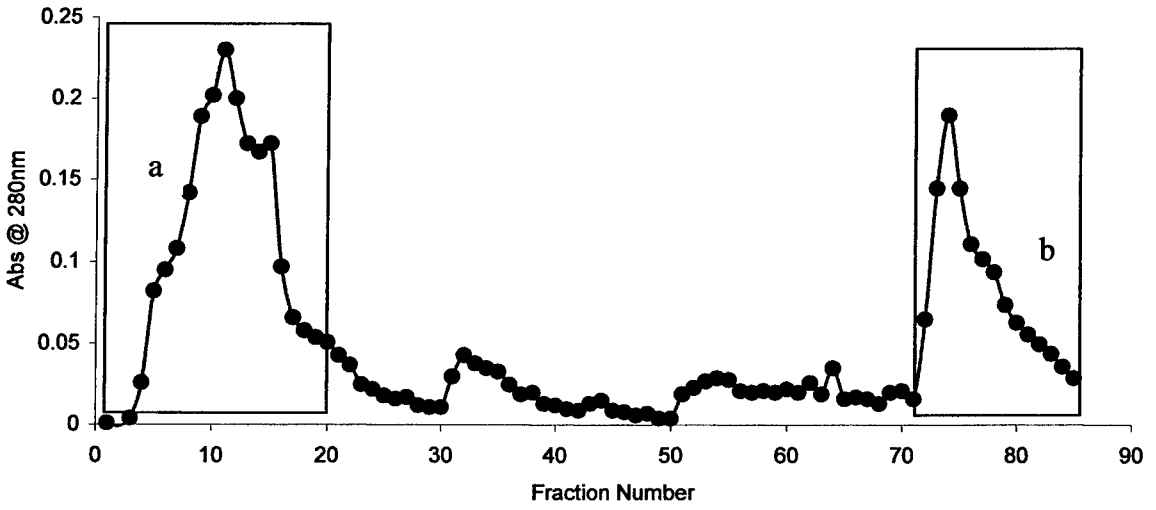

Figure 7. The protein content of fractions after anion exchange of sample AC1 and the peaks analysed.

Determination of an approximate molecular weight by running samples AC1a and AC1b on SDS-PAGE was not possible as no bands were resolved, most likely due to a protein content too low to be detected by coomassie or silver staining. Analysis of the protein content of each peak was carried out and the results are shown in Figure 8.

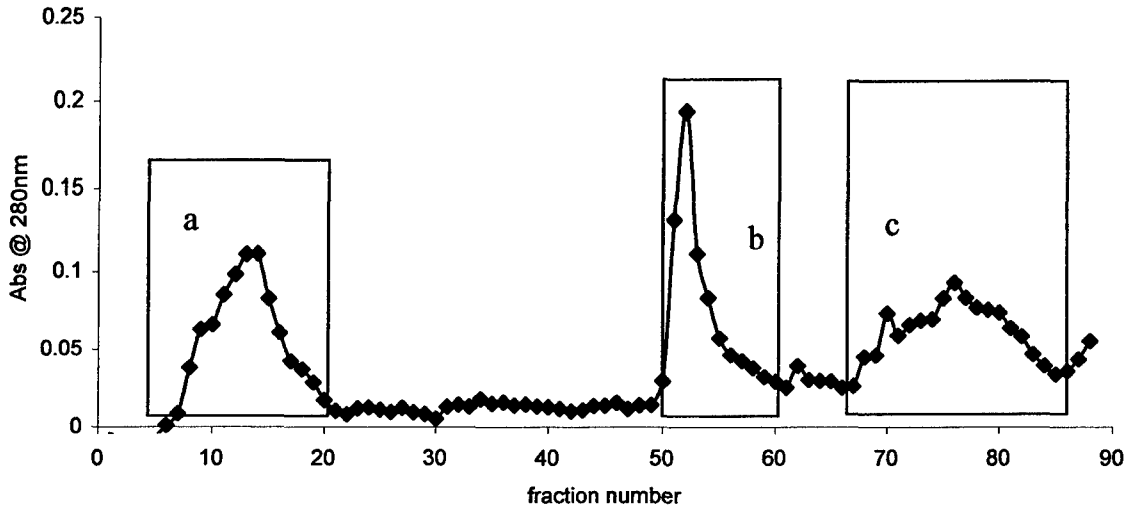

Figure 10. The protein content of fractions after anion exchange of extract AC2 no material was recovered after dialysis of the broad peak c.

The first and second protein extracts were analysed for amino acid composition and the results are shown Figure 11. From here it can be observed that fraction b has a more acidic charge while fraction a is slightly more basic. However, the greatest difference in composition is the very low amount of dipeptides found in fraction b. The dipeptides analysed by this technique are glycine-proline and proline-hydroxyproline. The presence of both these dipeptides can be indicative of an alpha helical structure which occurs from the repeating triplet glycine-proline-hydroxyproline. This could suggest a difference in secondary structure between the two proteins isolated.

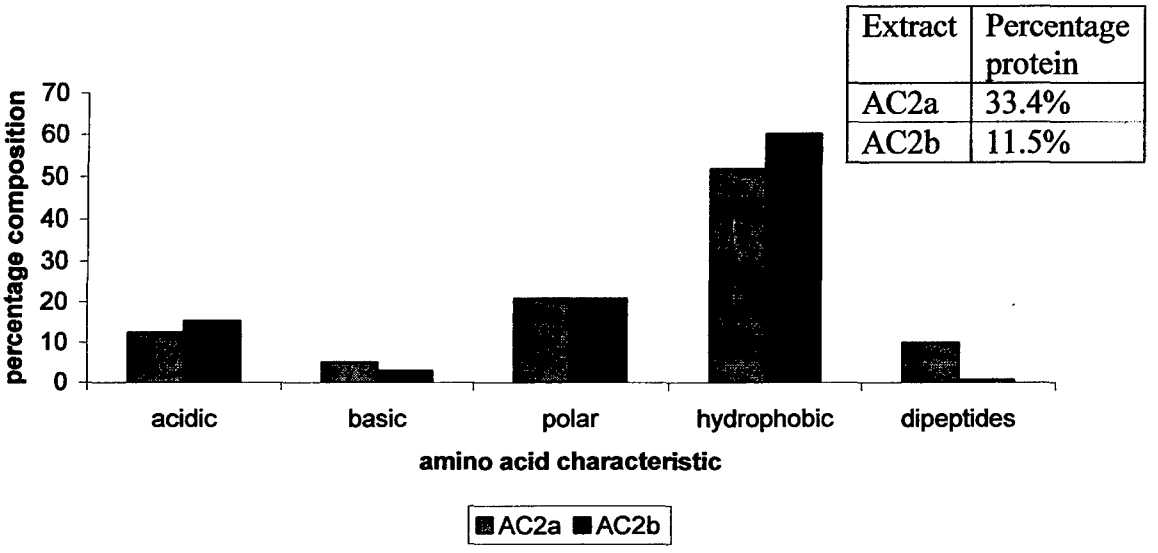

Extract	Percentage protein
AC2a	33.4%
AC2b	11.5%

Figure 11. A comparison of the characteristics of the amino acids found by gas chromatography in the fractions after separation by anion exchange chromatography.

The structures of the plant cell wall which remained after extraction with CDTA were isolated by the use of a sodium carbonate/ sodium borohydride solution; the material obtained was then separated by anion exchange chromatography on Sepharose CL-6B. The

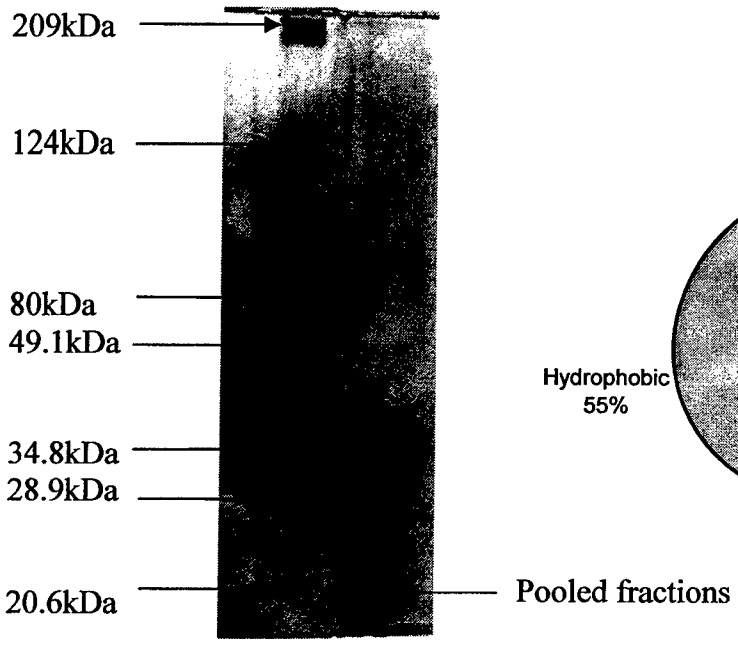

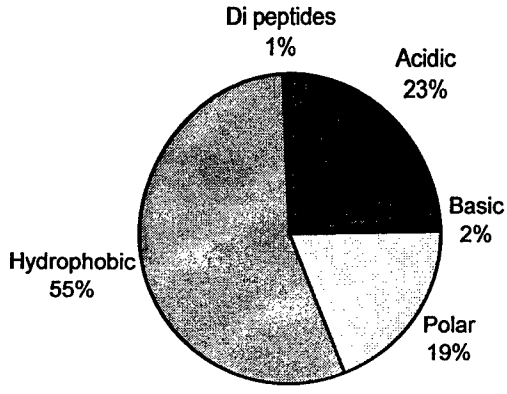

Extract	Percentage Protein	Polymerised Silica
AN1a	8.9%	10.7µg/mg

Figure 13. The analysis of the fraction AN1a after anion exchange chromatography by SDS-PAGE and gas chromatography for amino acid composition.

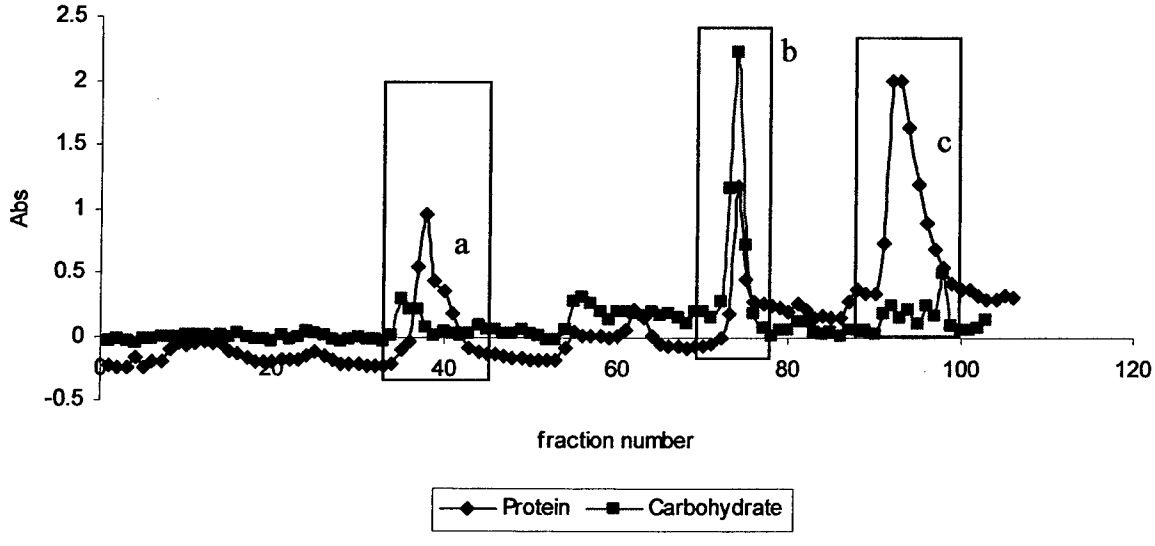

Figure 14. Protein and carbohydrate analysis of extract AN2.

the sample size. From this figure it is possible to observe that the fraction containing the greatest amount of silica is retained longest on the column but does not show any correlation either amount of protein or with protein of increasing or decreasing charge.

Extract	Percentage protein	Silica
BC1a	4.6%	3.5μg/mg
BC1b	19%	ND
BC1c	24%	1.9μg/mg
BC1d	14%	11.6μg/mg

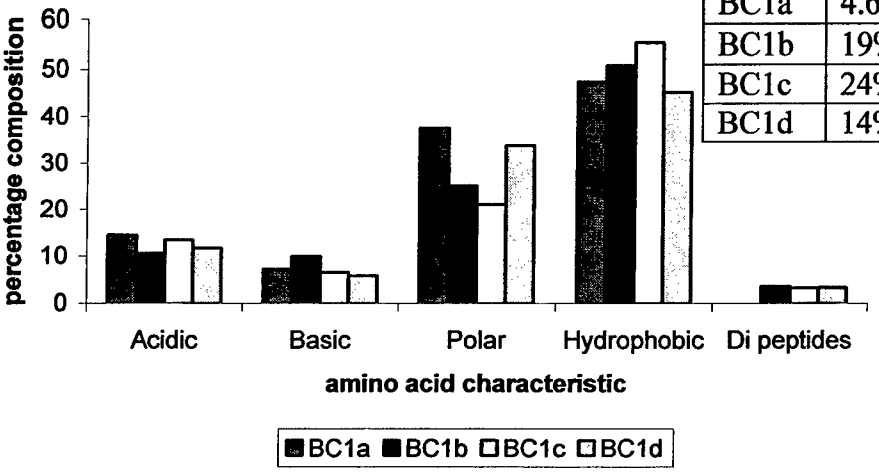

Figure 17. The amino acid and silica composition of extract BC1 after anion exchange chromatography. (ND=Not Determined due to sample limitations).

The extract BC2 was also fractionated by anion exchange chromatography and the protein and carbohydrate measured by spectroscopy and assay respectively. The results of this separation are shown in Figure 18 and this again shows obvious peaks between fractions 3-14 (A), 25-40 (B), 46-55 (C) and 65-80 (D). This is similar to the previous second CDTA extract, AC2, with the exception of the second peak (fractions 25-40) which was absent from separation A. This may be a result of the improved protein detection at the wavelength 214nm over the previous detection used at 280nm which detects the aromatic amino acids. The individual peaks were pooled and dialysed before investigation of the amino acid composition by gas chromatography. The quantity of polymerised silica was also examined by ICP analysis and all these results are shown in Figure 18.

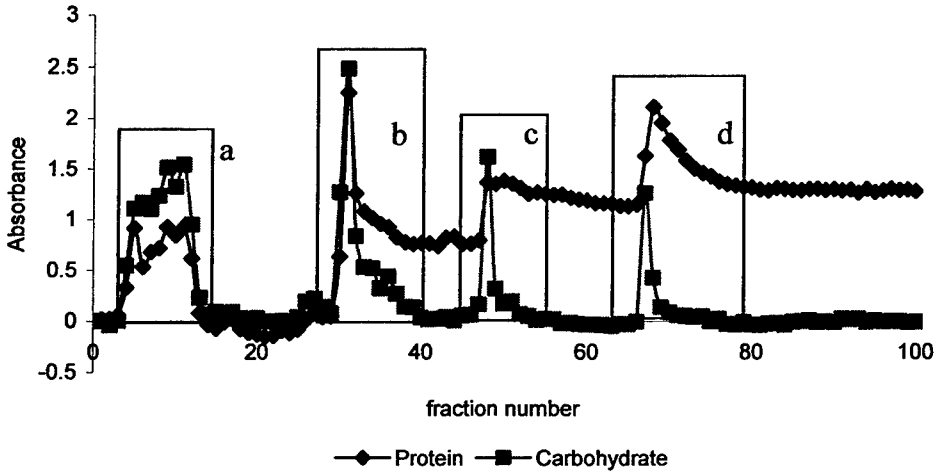

Figure 18. Protein and carbohydrate analysis of the second extract by CDTA, separation B.

again predominantly hydrophobic. Silica measurements for these fractions are still to be examined.

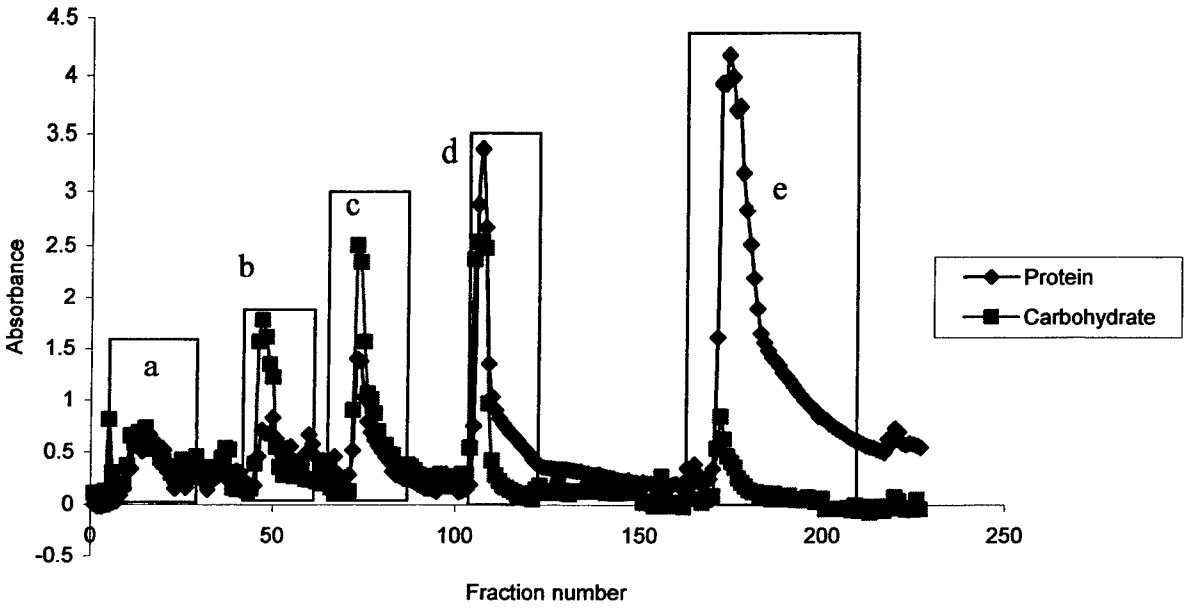

Figure 21. Protein and carbohydrate analysis after anion exchange chromatography of extract BN1.

Extract	Protein content
BN1a	29.5%
BN1b	28.8%
BN1c	9.8%
BN1d	4.1%
BN1e	23.1%

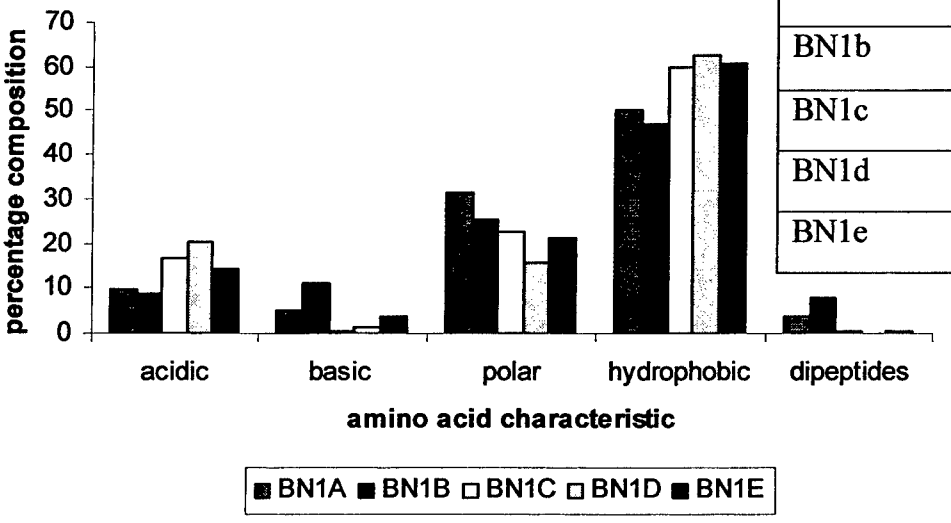

Figure 22. Analysis of the different protein components after anion exchange chromatography of the sodium carbonate/sodium borohydride extract.

The fractionation of the BN1 extract was again carried out by anion exchange chromatography on DEAE Sepharose CL-6B and the individual fractions were analysed for carbohydrate by assay and protein by UV spectroscopy at 214nm. The results of this separation are shown in Figure 23 from which it is possible to observe the peaks which were further examined, fraction 20-25 (A), 40-52(B), 53-57(C), 58-67(D), 68-79(E), 83-104(F),

A third separation, C has also been fractionated with the first and second CDTA extracts were fractionated by anion exchange chromatography using DEAE Trisacryl resin. Each collected fraction was then analysed by assay for carbohydrate and UV spectroscopy for protein and the results of this are shown in Figure 25.

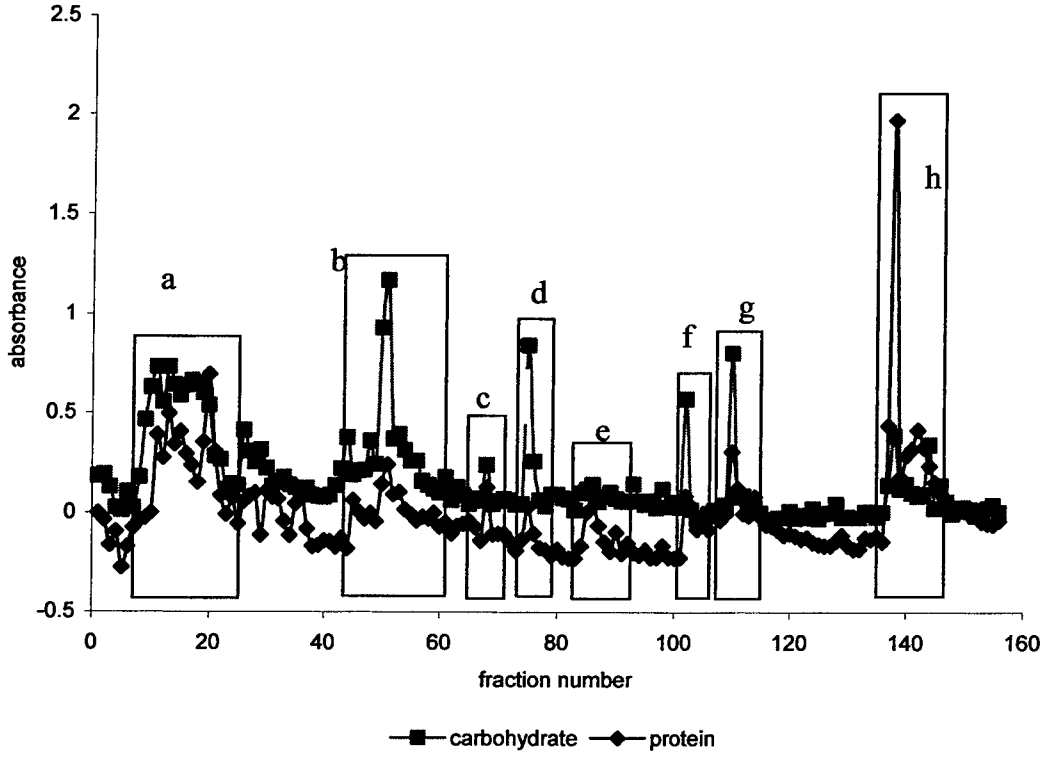

Figure 25. Protein and carbohydrate analysis of extract CC1 after anion exchange chromatography.

The peaks were poled as follows into fractions 7-23(A), 41-60(B), 67-69(C), 73-78(D), 83-91(E), 101-104(F), 109-115(G), 136-150(H). The first four fractions have been analysed by gas chromatography for amino acid composition and protein content and the results are shown in Figure 26.

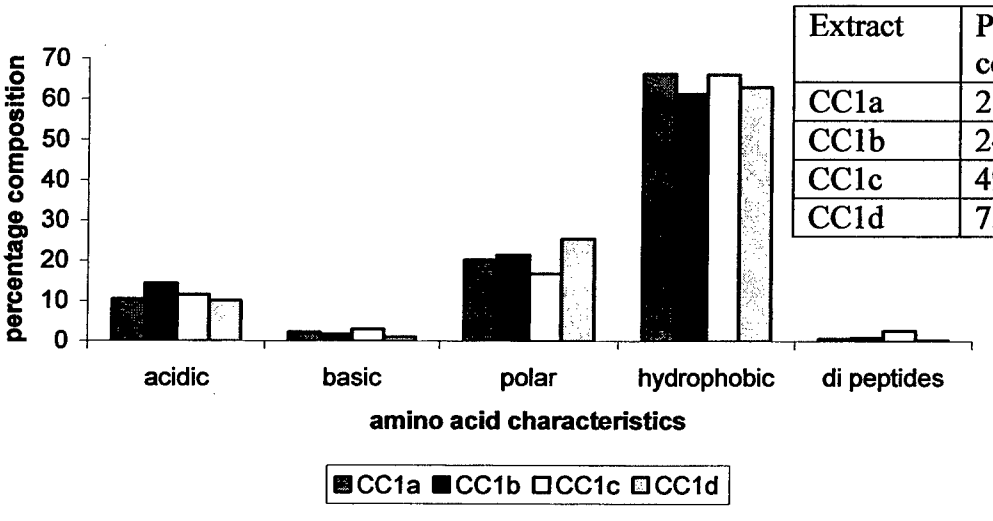

Extract	Protein content
CC1a	21.5%
CC1b	24.1%
CC1c	49.4%
CC1d	7.5%

the structural aspects of the carbohydrate moieties including additional linkage information

- The amino acid composition of the proteins present has been analysed. However, this has not provided important information on the primary amino acid sequence. The extracts would be analysed using proteomics to collect this information. It is also hoped that I will be able to obtain new skills in molecular biology techniques to obtain the genetic sequence coding for these proteins.

- Obtaining the genetic information of the proteins would enable the use of bioinformatics to correlate the proteins studied with their tertiary/quaternary structure and the functions of other similar identified proteins.

Model studies of biosilicification showing controlled structure and form

Graham Tilburey

2005

Transfer Report

Nottingham Trent University

1. Introduction

Silicon is the second most abundant element in the earth's crust. Silicon is not found in its elemental form, but in combination with oxygen to form silica, and other elements to form silicates it accounts for an estimated 90% of the earth's minerals[1]. Silica ($SiO_2.nH_2O$) and silicates are extremely important industrial materials with an extensive array of applications including paints, foods, adhesives, detergents, separation media, catalyst and medicines[2]. The global market for silica has been estimated to be worth around two billion dollars per year[3], thus emphasizing the importance of this compound in everyday life. The eventual use of the silica is determined by its structural properties such as morphology, surface area and porosity. Silica is essentially an inorganic polymer comprising of SiO_4 tetrahedra. The Si-O-Si bond lengths and angles can vary which enables a wide variety of patterns to form. This yields porous and non-porous crystalline materials. Amorphous materials also exist where no long range order is observed. Synthetic precipitated silica is usually prepared at high temperature, via aqueous processing or by low temperature, non-aqueous sol-gel routes which has been reviewed[4,5] however these method usually do not exhibit the desired level of structural control for present day needs.

1.1 Silicic acid polymerisation in aqueous solution

Monosilicic acid is the simplest soluble form of silica, it is essentially four hydroxyl groups tetrahedrally co-ordinated to a central silicon atom; $Si(OH)_4$ (N.B. this has never been isolated). Silicic acid is weakly acidic with a pK_a of 9.8 and is almost universally found[2], in sea water it is present at an average concentration of 70μM[6]. In water, at 25°C, it is stable for long periods of time at levels below 100ppm (~1mM). However, once the concentration exceeds the solubility of the amorphous solid phase, at 100-200ppm, it undergoes autopolycondensation reactions[2,7]. This process can be divided into three distinct stages:

- Polymerisation of monomers to form stable nuclei of a critical size (typically 1-2 nm).
- Growth of nuclei to form particles.
- Aggregation of particles to from particles, branched networks or structural motifs.

Silicic acid condenses to form silica typically by two mechanisms (Equations 1 and 2) which occur simultaneously in a supersaturated solution of silicic acid. The first mechanism involves the condensation of two silicic acid molecules with the release of water;

$$Si(OH)_4 + Si(OH)_4 \rightleftharpoons (HO)_3Si{-}O{-}Si(OH)_3 + H_2O \qquad \text{Equation 1}$$

In this process no charged species are generated from the condensation and hence no net pH change of the solution is observed. The second mechanism involves an ionised and an unionised silicic acid molecule in a bimolecular collision[8,9](Equation 2).

$$Si(OH)_4 + Si(OH)_3O^- \rightleftharpoons (HO)_3Si{-}O{-}Si(OH)_3 + OH^- \qquad \text{Equation 2}$$

The negatively charged oxygen atom attacks the electropositive silicon centre (nucleophilic attack and hence is the favoured reaction of the two mechanisms) generating an unstable five coordinate species, which decomposes to yield a hydroxyl ion, thereby increasing the pH of the reaction system. As oligomers grow in size the pKa of the silanol group decreases, this generating more ionised species for reaction via this mechanism.

Silicic acid condenses first to a dimers, further reactions produce trimers and then cyclic oligomers containing between 3 and 6 silicon atoms linked with a siloxane bonds. Once the cyclic species dominate, monosilicic acid reacts preferentially with these species, as the oligomers will have a higher density of ionised silanol groups[10]. Ostwald ripening also occurs; where smaller more soluble particles dissolve and release silicic acid that re-deposits onto the larger particles. Figure 1 taken from Iler[2] describes silicification under different conditions and the structure of the silica produced under these conditions.

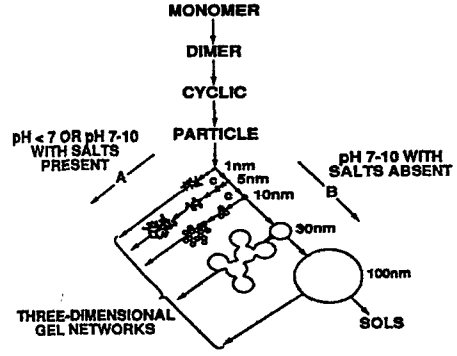

Figure 1 – The structural characteristic of silica formed under various reaction conditions. Image taken from ref. 10.

Present day methods for producing silica usually involve high temperatures in aqueous processing or by low temperature non-aqueous method such as sol gel processing[4,5]. In contrast the silica generated by nature is technologically more advanced and is generated under comparatively mild conditions. The desire for greater structural control during silica formation is necessary to enable the design and production of materials that exhibit advanced properties. In order to gain the necessary information to enable this technological advance, research in the field has been directed towards biological organism, (such as diatoms, sponges and higher plants) where nano-structured materials are generated with remarkable control in mild physiological conditions.

1.2 Diatoms – The isolation of organic molecules and their role in (bio)silicification.

Diatoms are the most extensively studied organism with regard to biosilicification. Kroger *et al* have isolated and characterised a number the organic constituents associated with diatom biosilica. Three families of cell wall proteins have been isolated and characterised from the diatom *Cylindrotheca fusiformis*; frustrulins[11], pleuralins[12,13] and

cathepsin L. Figure 2 shows the proposed mechanism for the catalysis of TEOS at neutral pH in the presence of silicatein α[24].

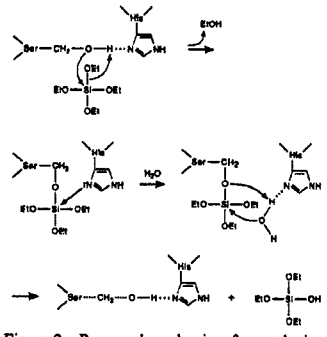

Figure 2 – Proposed mechanism for catalysis of TEOS to silica.

Site directed mutagenesis of the silicatein α was carried out, where mutants of the protein were produced. Each of the catalytic sites (serine[26] and histidine[165]) was substituted in the protein with an alanine residue (methyl side group). It was shown that by replacing either the serine or histidine residues, the "catalytic" activity of the protein was reduced by an order of magnitude. Furthermore it was shown that the "catalytic" activity of silicatein α could be significantly reduced by thermal denaturation. This destroys the three dimensional structure of the protein[25].

Although aesthetically pleasing this mechanism has quite obvious problems associated with it when being proposed as a mechanism for biosilicification. TEOS is not available as a natural precursor for silica and as such this somewhat invalidates the mechanism with respect to biosilicification. This however, does not mean this mechanism is not occurring *in vitro*. Secondly this mechanism would only be active while the proteinacious filament does not have silica deposited on itself. Upon the deposition of silica onto the filament the interaction between protein and TEOS can no longer occur. We think that there are other biomolecules (that have not been isolated thus far) as well as silicatein that are actively assisting biosilicification in sponges even when silicatein molecules are covered with silica.

1.4 Plants – Extraction of organic molecules that influence silicification

Biopolymer extracts have also been made from higher plants namely form hairs found on the lemma of the grass, *Phalaris canariensis*[26], *Equisetum telmateia*[27,9], and *Equisetum arvense*. Protein containing biomolecules associated with the siliceous phase of *Phalaris canariensis* and *Equisetum telmateia* were first discovered by Harrison[28] (formally Perry). The biomolecules were isolated after a first acid treatment of 4:1 mixture of concentrated Nitric:sulphuric acid which was heated for 24 hr at 60-70°C (NS) and a second more extensive acid treatment of a mixture of 1:1 concentrated Nitic:perchloric acid at 60°C for 30 minutes six times (NSNP), followed by the dissolution of the silica using a 1-3% NH_4F buffered solution of HF[28].

These studies were continued by inserting biomolecules from *Equisetum telmateia* after the first acid treatment into a model silicifying system utilising $K_2[Si(C_6H_4O_2)_3].xH_2O$ as a source of soluble silica. At circumneutral pH the compound dissociates and produces silicic acid which immediately undergoes polycondensation reactions due to the supersaturation of the solution. The polycondensation reactions were monitored with respect to time using the colorimetric silicomolybdate blue method. The addition of the biomolecules extracted from *Equisetum telmateia* at 1% w/w to the condensing system increased the rate of formation of trimers by 22% in comparison to the blank condensing system. The rate of dissolution of silicic acid from oligomers was reduced by 33%. Electron microscopy revealed the presence of lath-like structures that are composed of 1-2nm primary particles after 1 hour and after 48h the material exhibited order over 600nm. When analysed using electron diffraction *d*-spacings observed were comparable to quartz[29].

Three chemically different biomolecular extracts were made from *Equisetum telmateia*. The first two extract were produced as previously described using strong acids, NS and NSNP and the third was produced after gel electrophoresis revealed the presence of low molecular weight glycoproteins which were removed using 5 kDa tangential flow. The first extract and most readily released is enriched with Serine/threonine (25 mol%), glycine (20 mol%) and acidic residues (25 mol%), the second has reduced amounts of glycine and hydroxyl containing residues, with glycine largely being replaced by proline and a two-fold increase in lysine. Tangential flow purification of NSNP produced an extracted that had greater acidic functionality, a reduction in hydroxyl functionality and an increase in proline functionality. The biomolecules were inserted into the model silicifying system as described above and increased the rate of trimerisation. The largest increase was seen using the TFNS extract, which also affected the rate of formation of oligomers, (trimers or bigger). A slight decrease in rate was observed in the presence of NS and NSNP. The biomolecular extracts also reduced the size of the fundamental particles size exhibited, morphology and crystallinity of the silica structures produced[27].

1.5 The role of additives in silicification

The role of additives in silicifying systems has been shown to affect each aspect of silicification from the formation of small oligomers, through to the morphology of the silica. Iler presented the role of organic additives in silicification before 1979[2]. More recently a significant number of investigations employed a biomimetic approach, where organic molecules used were designed from the bioextracts isolated from biological biosilicifying organisms. Complex organic polymers to simple inorganic and organic molecules have been shown to control the morphology, with a number of morphologies being observed[30,31].

Polyamines were targeted primarily because of the post translational modifications observed in silaffins. Upon the addition of the polyamines isolated from diatoms to a pre-hydrolysed solution of TMOS the polyamines induced rapid precipitation of silica sphere with characteristic diameters[32]. One of the first groups to study amine containing molecules was Mizutani *et al* where it was found that polyamines in particular poly(allylamine) hydrochloride, poly(L-lysine hydrobromide) and poly(L-arginine hydrochloride) showed increased activity. It was postulated that the amines were acting as catalysts by stabilising the $Si\text{-}O^-$ created during condensation, and were incorporated

Precursor	(Bio) Macromolecule(s)	Buffer [a]	Temp (°C)	Time (min)	Structures	Size
Ethylene glycol modified silane (EGMS)	PAH[40]	Phosphate	20	< 5	Spheres	300-500 nm; 1-3 μm
	PLL[40]	Phosphate	20	< 5	Spheres Hexagons	200-400 nm Edges: 400-1000 nm Thickness: 40-60 nm
Tetramethoxy silane [b] Polyamine stabilised sol 40nm	Silaffin[Error! Bookmark not defined.]	Various	20	5	Fused spheres,	50-700 nm Pores
	Polyamines[41]	Sodium Phosphate	25	Few seconds	Roughly hexagonal framework.	
	Synthetic R5	Phosphate[42]	20	3-5	Spheres	200-400 nm
		Phosphate-citrate[43,50,54]	20	5	Spheres	200-400 nm
	PAH[42, 44-53]	Phosphate	20	5-20	Spheres	500-3000 nm
	PLL[42, 45-47, 49, 54, 55]	Phosphate	20	5	Fibres Spheres Disks	d = 100 nm 200-400 nm 250-350 nm
	Dendrimer[56]	Phosphate	20	Not stated	Spheres	75-325nm
Tetraethoxysilane [c]	Silicatein filaments[22]	Tris-HCl	20	12 hr	Network [d]	NA
	Cys-lys block copolypeptides [e]	Tris-HCl	Not reported	24 hr	Spheres	100 μm
					Columns	l = 10 μm; d ~ 500 nm
	Lys [f]	Tris-HCl	30	500 hr	Gel	--
	Ser [f]	Tris-HCl	30	500 hr	Gel	--
	PLL	Tris-HCl	30	48-72 hr	Gel	--
	Cysteamine[57]	Tris-HCl		5.5hr	Spheres	40-100nm
Water Glass	Lys[58]	Tris-HCl	Not reported	180	Gel	--
	PLL [g]	Tris-HCl	Not reported	NA	Gel	--
	PLL[42]	Phosphate	20	5	Spheres	200 nm
	R5[42]	Phosphate	20	5	Spheres	200 nm
Sol[Error! Bookmark not defined.]	PLL	Tris-HCl	20	NA	Gel	--
	Poly-L-arginine	Tris-HCl	20	NA	Gel	--
Catechol Complex[g]	None [i]	H_2O + HCl	2-53	0-240	Aggregates	< 20 nm [h]
	Amino acids,	H_2O + HCl	25	Lys, Arg, 1000, 1300 all others	Aggregates	Glycine 84nm, Alanine 48nm.
			25	1500-1600		
	Lys_{1-5}, PLL	H_2O + HCl	25	T_{gel} = 1640-40 Lys_{1-5} PLL, immediate.	Particles	Lys_{1-5} 108, 139, 85, 109, 122, PLL, 467nm
	Diamines	H_2O + HCl	25			
Sodium monosilicate hydrate[33]	PAH	Borate buffer (pH 8.5)	20	~20	Gel	--
	PLL	Borate buffer (pH 8.5)	20	~20	Gel	--

[a] The buffers maintained the pH of the system around 7.0 unless specified.
[b] A comprehensive list of the various (bio)macromolecules used can be found in ref. 50.
[c] TEOS typically requires an alcohol to become miscible with an aqueous solution.
[d] The silicatein filaments were found to be covered by a layer of interconnected network silica particles (< 200 nm).
[e] A comprehensive list of various diblock copolypeptides can be found in ref. 22.
[f] A comprehensive list of other amino acids and peptides can be found in ref. 59.
[g] A comprehensive list of other amino acids and peptides can be found in ref. **Error! Bookmark not defined.**, 60.
[h] The precipitate was found to be aggregates of sizes 50-70 nm of these primary particles (1-20 nm).
[i] See ref. 34, 36 for several recent investigations using silicon catecholate complex precursor.

2. Materials and Method

2.1 Dipotassium tris(1,2-benzene-diolato-*O*,*O*)silicate as a model silicifying system.

Dipotassium tris(1,2-benzene-diolato-*O*,*O*)silicate was chosen as the silicifying precursor because it is viewed that the system generates a solution of silicic acid. There are several silicifying systems that have been used to study the effect of additives on silicification: sodium silicate, tetramethoxysilane (TMOS) and tetraethoxysilane (TEOS). The later two require hydrolysis to remove the methoxy or ethoxy groups which when used for *in vitro* studies undertaken by Kroger *et al* takes 15 minutes and thus any silicic acid generated during this initial period starts to condense and experiments have shown that only 20% of the original starting material is present as silicic acid (as detected by the molybdenum blue method) after this initial time period[34]. Furthermore each molecule of precursor may not undergo complete hydrolysis (the removal of all four alkoxy groups) which generates a vast array of species in solution as well as generating methanol and ethanol in their respective precursors. Sodium silicate is supplied as a highly basic trimer ($Na_2Si_3O_7$) which upon neutralisation starts to condense. Dipotassium tris(1,2-benzene-diolato-*O*,*O*)silicate dissociates upon the addition of acid to give a solution of silicic acid as determined by the molybdenum blue method. A 30mM solution of Dipotassium tris(1,2-benzene-diolato-*O*,*O*)silicate was used to study the effect of additives upon silicification. This system allows pH and temperature to be studied as well as being an aqueous based system; however the generation of catechol and KCl in the system are undesirable but unavoidable.

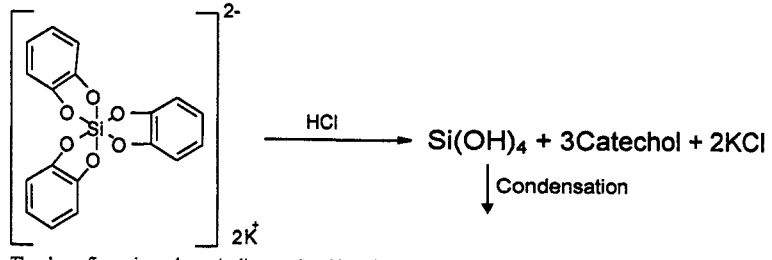

The above figure is a schematic diagram, bond length are not drawn to scale.

2.2 The silicomolybdate blue method for detection of silicic acid.

2.2.1 Molybdenum reagent

Ammonium molybdate tetrahydrate (20g) was dissolved in deionised water (500ml). Concentrated hydrochloric acid (60ml) was added and diluted to 1000ml with deionised water after cooling.

2.2.2 Reducing reagent

Oxalic acid (20g), 4,Methylaminophenolsulphate (6.67g) and sodium sulphite (4g) were dissolved in deionised water (500ml). Concentrated sulphuric acid (100ml) was added and the solution diluted to 1000ml with deionised water after cooling.

density of 1g cm^{-3}) and filtered under vacuum using a whatman No. 1 paper and dried at room temperature. The treatment with ethanol is used to remove waxes and chlorophyll from the plant.

2. Digestion of the organic material was achieved using a 200ml mixture of concentrated nitric and sulphuric acid (4:1). This was added to the plant material and heated to 70-80°C for 24 hours using a water bath. The digestion mixture was diluted with an equal amount of water and centrifuged at 3000 r.p.m. using a Sorvall RT7 plus centrifuge for 10 minutes. The supernatant was discarded.

3. The pellet was further acid treated by repeating step two for 12 hours instead of 24 hours.

4. Further acid treatment was used to remove any tightly bound organic material to the silica surface. 10ml of a 1:1 mixture of concentrated nitric and 20% perchloric acid was added to the pellet and digested at 60°C for 30 minutes. The sample was diluted and centrifuged as above and the procedure repeated a further 5 times.

5. The pellet was washed 3 times with 40ml of distilled water to remove any residual acid and freeze dried.

6. The silica was then digested using 1% HF buffered with ammonium fluoride until no silica remained. If more HF was required to digest the silica fully, the sample was centrifuged, the HF poured off and more added until no silica remained. The supernatant was then dialysed 3500da against distilled water at 4°C until the water had a conductivity of less than 1μS. The dialysate was then freeze dried and the remaining material frozen at -20°C until required.

2.7.2 Extraction of polyamines

1. Plant material was prepared in the same ways as in step 1 for the isolation of intra silica protein. This material was boiled with a 100mM EDTA, 2% SDS solution twice for a few minutes in an attempt to remove the intracellular components, however as fore mentioned this procedure was developed for diatoms, which are singled celled organisms and the complex structural characteristics of plants would suggest that this procedure would not achieve a similar material as found when digesting diatoms.

2. The samples were centrifuged at 6000 r.p.m. for 5 minutes and the supernatants discarded. The pellets were washed with 40ml of 95% acetone and then centrifuged as described previously. The acetone wash was discarded and the above procedure repeated three times with distilled water.

3. The remaining material was then dried in an oven at 40°C overnight (approximately 16 hours), followed by digestion with 1% HF buffered by 3% ammonium fluoride. The sample was dialysed against deionised water (as previously described) and freeze dried.

2.7.3 Extraction of glycoproteins

1.5g of ethanol treated plant material was suspended in 10ml of 1mM $CaCl_2$ with 15g of glass beads and vortexed on full power with a Scientific industries vortex genie 2 for five minutes. When using diatoms or cells this procedure produces lysed cells, however the structural difference between a plant and a single celled organism are great, thus similar material will not be generated. The material was then centrifuged at 6000 r.p.m. for 5 minutes. The pellet were resuspended in 10ml of 1mM $CaCl_2$ and centrifuged as described above. This procedure was repeated until the supernatant was clear (6-8 washings). Once again the material was resuspended in 10ml of $CaCl_2$ which was chilled using an ice bath and sonicated using a (**biochemistry probe sonicator**). The sample washed with $CaCl_2$ as previously described. When using diatoms pure cell walls are produced. The plant material was then shaken with 10ml of 100mM EDTA adjusted to pH 8 for 24 hours at 4°C. The sample was centrifuged at 6000 r.p.m. for 5 minutes, the supernatant was collected. The pellet was treated with 10ml of deionised water and centrifuged as previously described. The supernatant was collected and combined with the EDTA supernatant. The mixture was then dialysed as previously described.

2.8 Ion exclusion chromatography

Ion exchange chromatography was carried using a Hiload 16/60 Superdex 200 column, the bio-molecular extracts were loaded onto the column in distilled water. Increasing ionic strength of sodium chloride was then passed down the column to elute the biomolecules. The fractions were collected in 10ml portions and their UV absorbance measure at 405nm, the fractions which showed an increase in absobance were collected freeze dried, redisolved in a minimum amount of water and dialysed as previously described.

The extraction and separation procedures were included for completeness, however this work was carried out by Masood

2.9 Amino acid analysis

Amino acid analysis was carried out at MRC Immunochemistry Unit at Oxford university where an Applied Biosystems 420A amino acid analyser was used to analyse the amino acids present in the biomolecule extracts isolated from *Equisetum Arvense*.

2.10 Analysis of biomolecules using the model system

The biomolecules extracted from *Equisetum Arvense* were inserted into the model system at 1% by weight of precipitated silica. Approximately 10mg of silica is precipitated from 10ml of 30mM solution of Dipotassium tris(1,2-benzene-diolato-*O*,*O*)silicate at circumneutral pH after alternate washing and centrifugation with 3 portions of 40ml of deionised water. The silica formed in the presence of the biomolecular extracts was isolated by centrifugation after 7 days and washed with deionised water as previously described and freeze dried. The same experiment was repeated but instead of the kinetic being monitored the sample was analysed using dynamic light scattering.

2.11 Investigating Diamines in solution with out silica

PAP1	5.479	1.275	0.920
PAP2	1.454	1.067	0.670
CaP1 unbound	5.289	1.402	1.195
CaP1 0.5M	3.527	0.834	0.624
CaP1 0.75M	4.643	1.283	0.800
CaP1 2M	3.910	1.421	1.028
CaP2 0.25M	4.633	1.433	1.073
CaP2 0.75M	4.963	1.078	0.594
CaP2 1M	6.477	1.382	1.288
CaP2 2M	4.347	1.491	0.930
CaP4	5.890	1.212	0.876
CaP4A	5.176	1.532	1.595
CaP4A 0.25M	4.466	1.141	0.740
CaP4A 2M	3.952	1.358	0.880

Figure 2 – The kinetics of the isolated biomolecules

The amino acid composition for each of the extracts is presented in graphs 1-4 in appendix 1. It can clearly be seen than there is a clear relationship between CaP, CaP2 and Cap4A. The results show a high percentage of the protein isolated is glycine which is consistent throughout all the extracts isolated using the EDTA cell wall extraction procedure. Interestingly the differences in composition between CaP and CaP2 and CaP4A are probably due to the extraction of a significant amount of the other amino acids as seen in CAP. This seems to support an incomplete extraction as hypothesized previously in CaP2 and CaP4A. Glycine is present in high amounts in all the samples exhibiting a substantial increase in 3rd order kinetics (except in PAP1) it would seem a reasonable assumption that the percentage of glycine in the sample is directly related to the rate of formation of trimers (the 3rd order rate constant) see Figure 3.

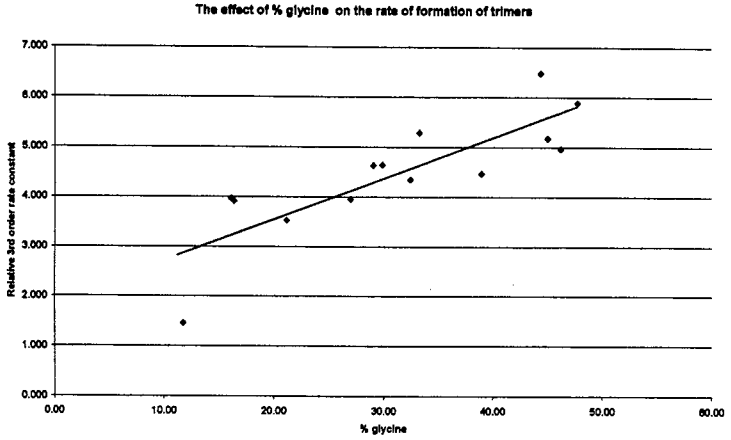

Figure 3 – A plot of % glycine in the sample against third order rate constant

It should be noted that all though there appears to be some correlation between the percentage of glycine in the sample and the 3rd order rate constant this can be misleading because the amount of protein in each sample varies greatly thus the actual amount of glycine in each sample would produce a completely different curve. The occurrence of glycine in such high quantities is not especially surprising. Glycine is the second most abundant protein and has no functionalized side chain[61]. It was shown by Belton *et al* not to affect the rate of condensation either as a homopeptide or as a single molecule however the role of glycine may not be directly related to the increase in 3rd order rate constant but as a spacing unit to create the specific morphology in the protein in order to effectively catalyse the formation of trimers from monomeric silicic. The trend observed in graph ? maybe due to an increasing number of active sites in the protein which would be proportional to the amount of glycine required to create the active sites. With sequence information this hypothesis could be confirmed and the proteins specifically cleaved to identify the active site involved in silicification

Dynamic light scattering of some randomly selected biomolecular extracts are presented appendix 1 in graph 5 it can be seen that none of the extracts so far greatly influence the rate of aggregation in direct contrast to the addition of additives to various model system which have been shown to drastically influence the rate of aggregation[30,31]. However it should be noted that none of the synthetic additives investigated so far by our group have substantially increased the third order kinetics as much as the extracts have.

Nitrogen gas adsorption measurements were only carried out on a limited number of samples because after chromatographic separation procedures had been undertaken the weight of the protein from each fraction was very small. A reduction in the volume of silicifying system was made thus affecting the amount of silica being isolated. This unfortunately meant that gas adsorption could only be carried out on a limited number of samples.

Sample	Area/m^2g^{-1}	Volume/ccg^{-1}	Radius/A
Blank	609.47	0.63	23.9
PAP1	617.7	1.17	32.02
PAP2	669.26	0.89	28.78
SiP1	594.66	0.64	21.24
CaP1 unbound	635.91	0.91	32.81

Figure 4 – Characteristics of silica isolated after 7 Days from biomolecular extracts

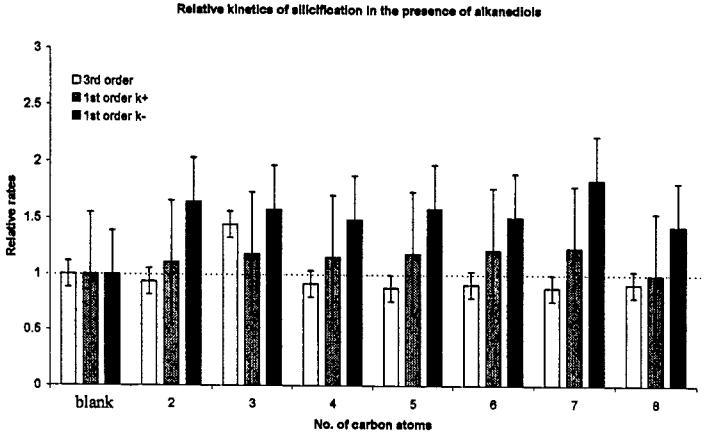

Figure 7 – Relative kinetics in the presence of alkanediols

It can be seen from figure 7 that the reverse 1st order kinetics are fatser but how significant this observation is well illustrated by the error bars. The increase in rate is due to the dissolution of silicic acid from oligomers. This seems to suggest that the alkanediols are stabilising the final concentration of silicic acid. To investigate this effect further the alkanediols were inserted into the model system at 200% or 30mM to see if further stabilisation would occur if the concentration of the alkanediol was increased. Further stabilisation of silicic acid was not evident from the kinetic results, which can be seen in appendix 2 graph 1. If stabilisation of silicic acid is occurring as indicated by the kinetic experiments, dynamic light scattering measurement would be expected to be slower than the blank model system (figure 8). The stabilisation of silicic acid in affect reduces the silicic acid concentration in the solution because some is bound to the alkanediol thus it is not free and available for condensation reactions. This results in a slower rate of aggregation. However this model does not explain why increasing the concentration of alkanediol does not affect either the kinetics or the aggregation rate further. What should be noted is that the alkanediol is not the only species in solution capable of hydrogen bonding with silicic acid. Water is present in excess which is also capable of bonding with silicic acid. This is expected to be why a more prominent effect is not seen when condensation occurs in the present of the alknaediols.

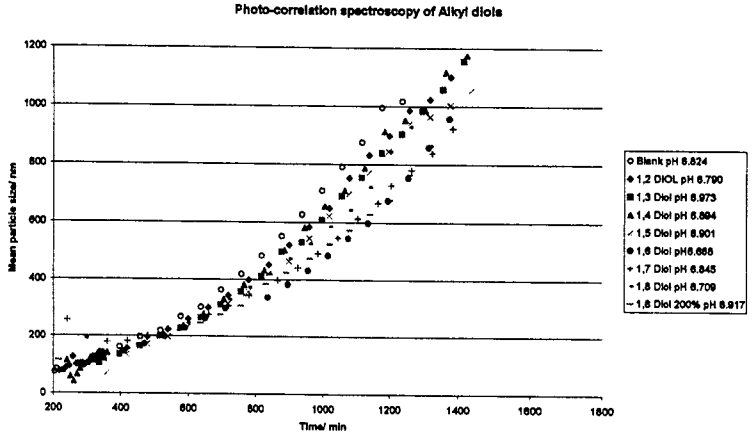

Figure 8 – Dynamic light scattering of alkanediols.

As previously explained hydroxyl containing additives produce silica which has smooth surface appearance and this is also exhibited when silica is formed in the presence of the alkanediols. The silicas produced from these systems were isolated at 24H and 7 days and gas adsorption measurements undertaken. Surface areas did were reduced in comparison to the 7 day blank and reduced with the increase from 100% to 200% alkanediol showing a further reduction as can be seen in table 1 appendix 2. It is not clear if this affect is due to the entrapment of the alkanediol in the silica. This could be established using TGA and will be investigated in due course. This is shown in appendix 2 figures 1-4, but it should be noted that appears to be no significant affect of the increase in carbon chain length on the structure of the silica produced.

Investigating Diamines in solution with out silica

The interactions between KCl, catechol and alkyldiamines were investigated using dynamic light scattering. A solution containing KCl and catechol showed no aggregates by dynamic light scattering (data not shown) as did a solution of 1,4 diaminobutane in water however upon the addition of 1,6 diaminohexane and larger molecules aggregates appear to be formed and in the case of 1,10 diaminodecane a structural growth is observe at neutral pH as can be seen from figure 9.

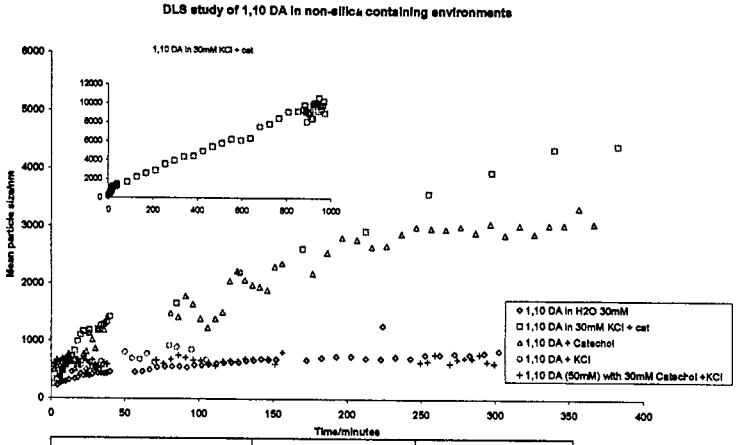

Sample	Rate of formation/nm^{3}s^{-1}	Final aggregate size/nm
1,10 + H_2O	0.0702	1206
1,10 + Catechol	0.3919	3015
1,10 + KCl	N/A	770
1,10 + KCl + Catechol	0.5546	9466
1,10 (50mM) + KCl + Catechol	N/A	653

Figure 12 - 1,10 Diaminodecane in the various aqueous based systems.

Similar experiments were carried out using 1,10 diaminodecane and the results can be seen in figure 12 with similar results. A slight increase in aggreagate size was observed upon the addition of KCl to the system. Which could indicate the formation of a complex involving the chloride ion and both protonated amine groups, this is graphically illustrated in Figure 13.

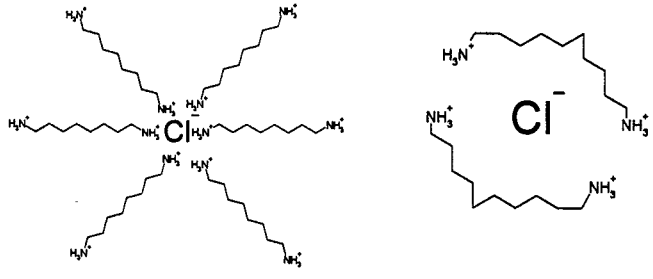

Figure 13 – Possible arrangement of 1,8 diaminooctane (left) and 1,10 diaminodecane (right).

This occurrence of the two different structures could be because the 1,8 diaminoocatane molecule is not long enough to wrap itself around the chloride ion. Thus 1,10

diaminodecane would only show small increase in size upon the addition of KCl where as 1,8 diaminooctane would show a larger increase in aggregate size as observed.

In the presence of catechol aggregate growth was observed, with a precipitate being formed but in the presence of KCl larger aggregates are observed suggesting KCl helps to stabilise the complex until the aggregates get so large that they can no longer stay in solution and precipitate. Increasing the concentration of diaminodecane from 30mM to 50mM causes no such aggregates to be observed.

4. Conclusions

The results presented above have show that biomolecules of different amino acid composition affect the rate of silicification and more particularly the rate of formation of trimers from silicic acid as determined by the molybdenum blue method. The composition of the extracts isolated also varies quite dramatically even when the same extraction procedure is used. This indicates that there is a need for more thorough extraction procedures to be developed in order to isolate the same material consistently, thus this will enable more in depth studies to be carried out on the extracts made from *Equisetum Arvense*. The extracts analysed so far have been shown to have high glycine content which when plotted against the third order rate constant there appeared to be some correlation between the rate of formation of trimers and the percentage glycine in the sample. Glycine does not contain any functionalised side chains, which indicates that this is unlikely to affect the rate of formation of trimers directly and has been shown not to in simple homopeptide molecules[34]. It was hypothesised that the amount of glycine could be proportional to the number of active sites in the extract suggesting that glycine might be used as spacing unit to separate functionalised amino acids which catalyse the formation of silica.

The effect of alkanediols on silicification was investigated in which it was found that the amount of silicic acid after 24 hours was higher than observed for the blank system indicating that the alkanediols stabilise silicic acid. The effect was found to be independent of the concentration of alkanediol and this was hypothesised to be because water is in such large excess that any affect exhibited by the alkanediol would be negligible. The silicas isolated were found to have a smooth surface morphology and exhibited lower surface areas when the amount of alkanediol was increased, which might indicate that the alkanediol is being entrapped into the silica structure, this could be confirmed by TGA.

The structure exhibited by diaminoalkanes in the absence of silica was investigated. Structures were observed in aqueous solutions of the 1,6-1,10 diaminoalkanes and upon the addition of KCl larger structures were observed which could indicate the formation of a complex between the protonated amine groups and chloride ions. Two possible configurations were proposed, the formation of a surfactant type micelle and a chelate type co-ordination of the diaminoalkane to the chloride ion, although no experimental evidence for this has been obtained.

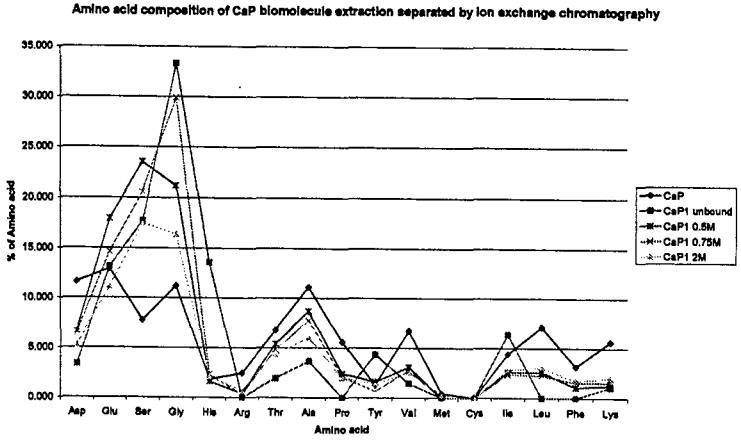

Graph 2 – Amino acid composition of CaP extracts separated by ion chromatography

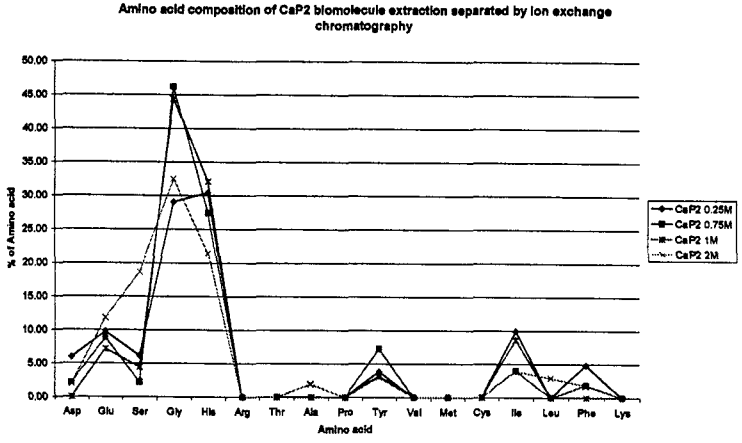

Graph 3 – Amino acid composition of extract CaP2 extracts separated by ion exchange chromatography

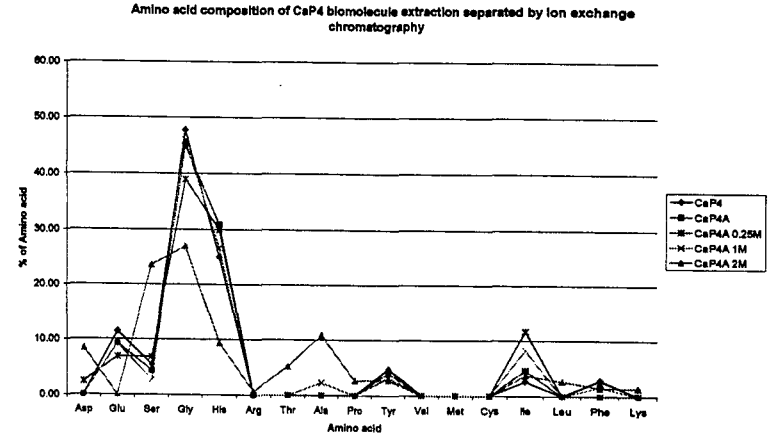

Graph 4 – Amino acid composition of extract CaP4A extracts separated by ion exchange chromatography

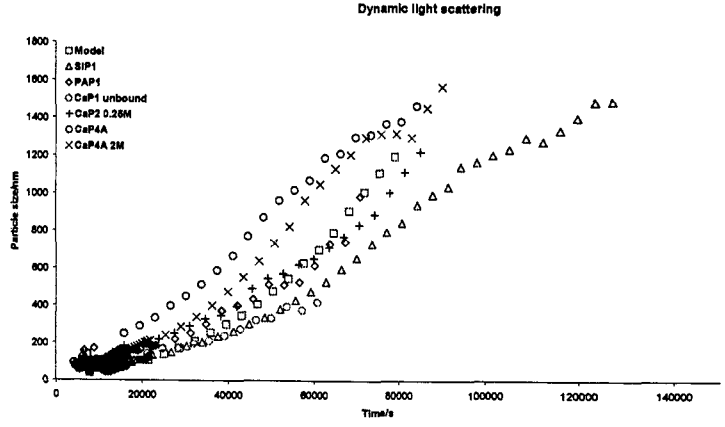

Graph 5 – Dynamic light scattering of selected biomolecular extracts.

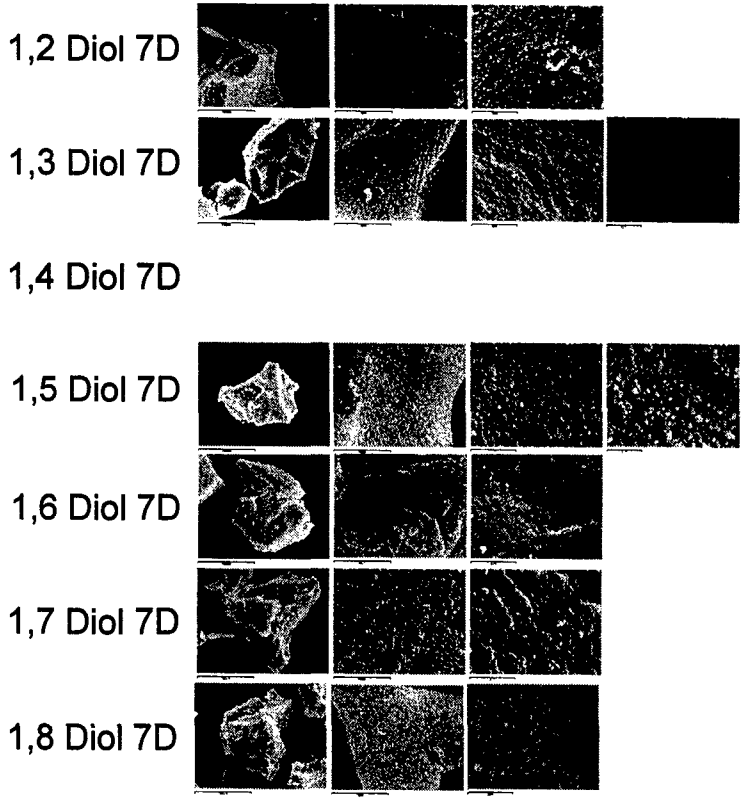

Figure ? – 7Day SEM images of 100% alkanediols

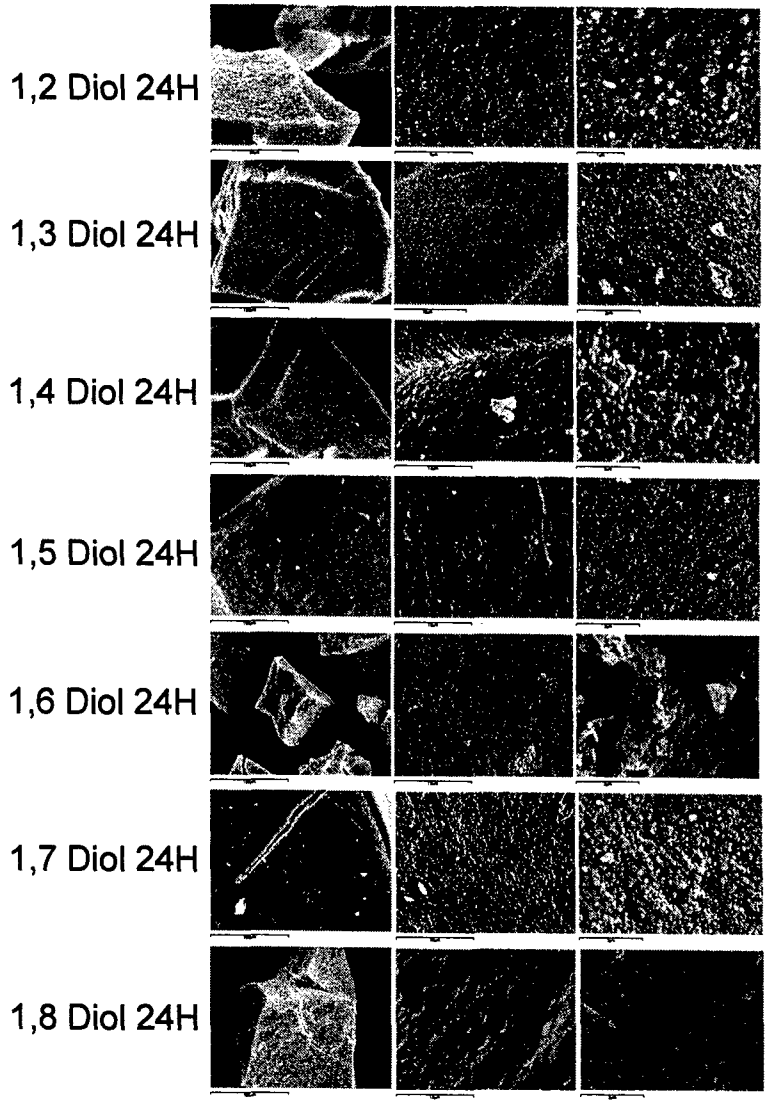

Figure ? – 24 hour SEM images of 200% alkanediols

[32] Kroger. N., Deutzmann. R., Bergsdorf. C. and Sumper. M. Species-specific polyamines in diatoms control silica morphology. PNAS (2000) **97** 26 14133-14138.
[33] Mizutani. T., Nagase. H., Fujiwara. N and Ogoshi. H. Silicic acid polymerization catalysed by amines and polyamines. Bull. Chem. Soc. Jpn. (1998) **71** 2017-2022.
[34] Belton. D., Paine. G., Patwardhan. S and Perry. C.C. Towards an Undertsnading of (Bio)silicification: The role of amino acids and lysine oligomers in silicification. (2004) J. Mater. Chem. **14** 2231-2241
[35] Manzel. H., Horstmann. S., Behrens. P., Barnreuther. P and Krueger. I. Chemical properties of polyamines with relevance to the biomeralisation of silica. Chem. Commun. (2003) 2994-2995.
[36] Unpublished data Belton *et al*
[37] R. E. Hecky, K. Mopper, P. Kilham, and E. T. Degens, Mar. Biol. **19**, 323 (1973).
[38] K. D. Lobel, J. K. West, and L. L. Hench, *Mar. Biol.* 126, 353 (1996).
[39] Q. Y. Sun, T. P. M. Beelen, R. A. van Santen, S. Hazelaar, E. G. Vrieling, and W. W. C.
[40] Patwardhan. S. V., Raab. C., Husing. N. and Clarson, Silicon chemistry **Could BE in press**
[41] Sumper. M. Biomimetic patterning of silica by long chain polyamines. Angew. Chem. Int. Ed. (2004) **43** 2251-2254.
[42] Patwardhan, S. V.; Ph.D. Dissertation, Silicification and biosilicification: The role of bimacromolecules in bioinpired silica synthesis. Department of Materials Science and Engineering, University of Cincinnati, 2003.
[43] Clarson, S. J.; Whitlock, P. W.; Patwardhan, S. V.; Brott, L. L.; Naik, R. R.; Stone, M. O. **TITLE** Science & Engineering **2002**, *86*, 81.
[44] Patwardhan, S. V.; Clarson, S. J. *Polym. Bull.* **2002**, *48*, 367.
[45] Patwardhan, S. V.; Clarson, S. J. *Silicon Chem.* **2002**, *1*, 207.
[46] Patwardhan, S. V.; Clarson, S. J. *J. Inorg. Organomet. Polym.* **2002**, *12*, 109.
[47] Patwardhan, S. V.; Clarson, S. J. *Mat. Sci. Eng. C.* **2003**, *23*, 495.
[48] Patwardhan, S. V.; Clarson, S. J. *Division of Polymeric Materials: Science & Engineering* **2003**, *88*, 40.
[49] Patwardhan, S. V.; Clarson, S. J. *Polymer Preprints* **2003**, *44*, 610.
[50] Patwardhan, S. V.; Clarson, S. J. In *Macromolecules Containing Metal and Metal-Like Elements*; Abd-El-Aziz, A. S.; C. E. Carraher, J.; C. U. Pittman, J.; Sheats, J. E.; Zeldin, M., Eds.; John Wiley & Sons, in press.
[51] Patwardhan, S. V.; Mukherjee, N.; Clarson, S. J. *J. Inorg. Organomet. Polym.* **2001**, *11*, 117
[52] Patwardhan, S. V.; Mukherjee, N.; Clarson, S. J. *Silicon Chemistry* **2002**, *1*, 47.
[53] Patwardhan., S. V.; Durstock, M. F.; Clarson, S. J. In *Synthesis and Properties of Silicones and Silicone-Modified Materials*; Clarson, S. J.; Fitzgerald, J. J.; Owen, M. J.; Smith, S. D.; vanDyke, M. E., Eds.; Oxford University Press, 2003; Vol. 838, pp 366.
[54] Patwardhan, S. V.; Mukherjee, N.; Clarson, S. J. *J. Inorg. Organomet. Polym.* **2001**, *11*, 193.
[55] Patwardhan, S. V.; Mukherjee, N.; Steinitz-Kannan, M.; Clarson, S. J. *Chem. Commun.* **2003**, *10*, 1122.
[56] Knecht. M.R., Sewell. S.K., Wright. D.W. Size control of dendrimer-templated silica. Langmuir (2005) **21** (5): 2058-2061
[57] Roth, K. M., Zhou. Y., Yang. W. and Morse.D. E. Bifunctional small molecules are biomimetic catalysts for silica synthesis at neutral pH. J. Am. Chem. Soc. (2005) **127** 325-330
[58] Coradin, T.; Durupthy, O.; Livage, J. *Langmuir* **2002**, *18*, 2331.
[59] Sudheendra, L.; Raju, A. R. *Mater. Res. Bull.* **2002**, *37*, 151
[60] Coradin, T.; Livage, J. *Colloids Surf. B* **2001**, *21*, 329.
[61] https://www.mcmp.purdue.edu/~mcmp304/AATutorial/gly-popup.shtml

APPENDIX-III: EXAMPLE ABSTRACTS OF PROJECT STUDENT REPORTS

Allan Monoy (Foreign exchange student, final year project, summer 2004)

The Use of Molybdic Acid Assay for Detection of SiO_2 and GeO_2

Abstract: Germanium and silicon are known to have some similar chemical properties, like electronegativity or electronic configuration. It is also known that germanium interferes in biosilicification. Knowing that it is possible now to synthesise silica using a bio-inspired route, a similar way of synthesis has been attempted. Dipotassium germanium triscatecholate has been used as precursor for germanic acid and the compatibility of it with the molybdenum blue assay procedure has been checked. NMR experiments and titration have been made in order to determine the dissociation of the precursor. Synthesised samples have been characterised by SEM (Scanning Electron Microscopy), EDS (Energy Dispersive Spectroscopy), XRD (X-Ray Diffraction) and TGA (Thermal Gravimetric Analysis)

At the same time, an attempt to develop a process for accurately quantifying the amount of precipitated silica has been tried. The main feature is to depolymerise silica by using a boiling solution of NaOH. The resulting silicic acid reacts with molybdic reagent leading to the formation of a yellow-coloured solution of which the absorbance can be measured by a UV-spectrometer.

Gerard Pujol (Foreign exchange student, final year project, Jan-Jun 2004)

FTIR determination of diamines in silica.

Abstract: A single method has been developed for determination of diamines in silica bulk using Fourier transform infrared (FTIR). The spectra of each diamine calibration were obtained at a nominal resolution of 4 cm^{-1} from 4000 to 400 cm^{-1} accumulating 32 scans. The diamines that have been used, were 1,8-diaminooctane, 1,6-diaminohexane, 1,10-diamiodecane and 1,10-diaminodecane HCl. The 1,8-; 1,6-diamin and 1,10-diaminodecane HCl have exhibited a good linear calibration, with a higher regression coefficient (R^2) and good statistical characteristics to be used to quantify, instead the 1,10-diaminodecane has exhibited a non-linear model and it has been impossible the quantification with this calibration analysis. Using this analysis, it is thus possible to measure diamine content in silica samples.

Juancho Ubiria Garcia-Anton (Foreign exchange student, final year project, 2004-5)

Analysis of diamines in silica by FTIR.

Abstract: The objective of work until now has been to confirm that if is possible to carry out diamines quantification in silica by FTIR and the study of interaction of silica with diamines. In order to do it I had to carry out the analysis of different samples of diamines that I had to prepare, this diamines were: 1,2; 1,4; 1,6; 1,8; 1,10 diamines, and I made half of the samples with silica and half without silica. Analysing this samples with FTIR and trying to do a calibration I should draw a conclusion about the interaction silica-diamines furthermore, obviously, to quantify diamines.

J|A|C|S
ARTICLES
Published on Web 00/00/0000

Polypeptide-Templated Synthesis of Hexagonal Silica Platelets

Melanie M. Tomczak,† Diana D. Glawe,‡ Lawrence F. Drummy,† Charles G. Lawrence,† Morley O. Stone,† Carole C. Perry,§ Darrin J. Pochan,|| Timothy J. Deming,⊥ and Rajesh R. Naik*,†

Contribution from the Materials and Manufacturing Directorate, Air Force Research Laboratory, Dayton, Ohio 45433, Department of Engineering Science, Trinity University, San Antonio, Texas 78212, Department of Chemistry and Physics, The Nottingham Trent University, Nottingham NG11 8NS, U.K., Department of Materials Science and Engineering, University of Delaware, Newark, Delaware 19716, and Department of Bioengineering, University of California at Los Angeles, Los Angeles, California 90095

Received April 15, 2005; E-mail: rajesh.naik@wpafb.af.mil

Abstract: Several studies have demonstrated the use of biomimetic approaches in the synthesis of a variety of inorganic materials. Poly-L-lysine (PLL) promotes the precipitation of silica from a silicic acid solution within minutes. The molecular weight of PLL was found to affect the morphology of the resulting silica precipitate. Larger-molecular weight PLL produced hexagonal silica platelets, whereas spherical silica particles were obtained using low-molecular weight PLL. Here we report on the polypeptide secondary-structure transition that occurs during the silicification reaction. The formation of the hexagonal silica platelets is attributed to the PLL helical chains that are formed in the presence of monosilicic acid and phosphate ions. Hexagonal PLL crystals can also serve as templates in directing the growth of the silica in a manner that generates a largely mesoporous silica phase that is oriented with respect to the protein crystal template.

Introduction

The synthesis of inorganic materials using biomimetic approaches has become an important area of research. Biomimetic synthesis is a potential route for the synthesis of inorganic materials under mild conditions, and numerous studies have already demonstrated the use of biotemplates in the synthesis of inorganic materials.[1−6] In the biological world, the organic matrix (proteins, carbohydrates) plays an important role in the synthesis and morphology of inorganic materials.[1,2,5,6]

Proteins play an important role in synthesis of intricate silica structures in marine organisms such as sponges and diatoms. The silicatein[1] and silaffin[2] proteins identified in marine sponges and diatoms, respectively, are involved in the formation of the elegant silica structures observed in these organisms. Furthermore, the addition of silicatein or silaffin to a silicic acid precursor solution in vitro results in the formation of silica under ambient conditions.[1,2] These studies have been extended to show that synthetic peptides and polyamines can also be used to mimic the biosilicification reactions that occur in living organisms.[7−11] Biomimetic approaches have some distinctive advantages over the traditional sol−gel methods for the synthesis of silica. Most importantly, the benign reaction conditions and the ability to manipulate the (bio)template are key attributes that differentiate biomimetic approaches from traditional chemical methods.[12−16] The ability of organisms to carry out the biosilicification process in "one pot" has also led to the development of biomimetic strategies for the encapsulation of biomolecules and nanoparticles.[17−19]

† Air Force Research Laboratory.
‡ Trinity University.
§ The Nottingham Trent University.
|| University of Delaware.
⊥ University of California at Los Angeles.

(1) Cha, J. N.; Katsuhiko, K.; Zhou, Y.; Christiansen, S. C.; Chmelka, B. F.; Stucky, G. D.; Morse, D. E. *Proc. Natl. Acad. Sci. U.S.A.* **1999**, *96*, 361−365.
(2) Kroeger, N.; Deutzmann, R.; Sumper, M. *Science* **1999**, *286*, 1129−1132.
(3) Naik, R. R.; Stringer, S. J.; Agarwal, G.; Jones, S. E.; Stone, M. O. *Nat. Mater.* **2002**, *1*, 169−172.
(4) Lee, S.-W.; Mao, C.; Flynn, C. E.; Belcher, A. M. *Science* **2002**, *296*, 892−895.
(5) Shankar, S. S.; Rai, A.; Ankamwar, B.; Singh, A.; Ahmad, A.; Sastry, M. *Nat. Mater.* **2004**, *4*, 482−488.
(6) Perry, C. C.; Keeling-Tucker, T. *J. Biol. Inorg. Chem.* **2000**, *5*, 537−550.
(7) Coradin, T.; Durupthy, O.; Livage, J. *Langmuir* **2002**, *18*, 2331−2336.
(8) Naik, R. R.; Brott, L. L.; Clarson, S. J.; Stone, M. O. *J. Nanosci. Nanotechnol.* **2002**, *2*, 95−100.
(9) Patwardhan, S. V.; Mukherjee, N.; Steinitz-Kannan, M.; Clarson, S. J. *Chem. Commun.* **2003**, 1122−1123.
(10) Knecht, M. R.; Wright, D. W. *Langmuir* **2005**, *25*, 2058−2061.
(11) Coradin, T.; Livage, J. *Colloids Surf. B* **2001**, *21*, 329−336.
(12) Cha, J. N.; Stucky, G. D.; Morse, D. E.; Deming, T. J. *Nature* **2000**, *403*, 289−292.
(13) Naik, R. R.; Whitlock, P. W.; Rodriguez, F.; Brott, L. L.; Glawe, D. D.; Clarson, S. J.; Stone, M. O. *Chem. Commun.* **2003**, 238−239.
(14) Rodriguez, F.; Glawe, D. D.; Naik R. R.; Hallinan, K. P.; Stone, M. O. *Biomacromolecules* **2004**, *5*, 261−265.
(15) Glawe, D. D.; Rodriguez, F.; Stone, M. O.; Naik, R. R. *Langmuir* **2005**, *21*, 717−720.
(16) Coffman, E. A.; Melechko, A. V.; Allison, D. P.; Simpson, M. L.; Doktycz, M. J. *Langmuir* **2004**, *20*, 8431−8436.
(17) Luckarift, H. R.; Spain, J. C.; Naik, R. R.; Stone, M. O. *Nat. Biotechnol.* **2004**, *22*, 211−213.
(18) Naik, R. R.; Tomczak, M. M.; Luckarift, H. R.; Spain, J. C.; Stone, M. O. *Chem. Commun.* **2004**, 1684−1685.
(19) Roth, K. M.; Zhou, Y.; Yang, W.; Morse, D. E. *J. Am. Chem. Soc.* **2005**, *127*, 325−330.

10.1021/ja0524503 CCC: $30.25 © xxxx American Chemical Society

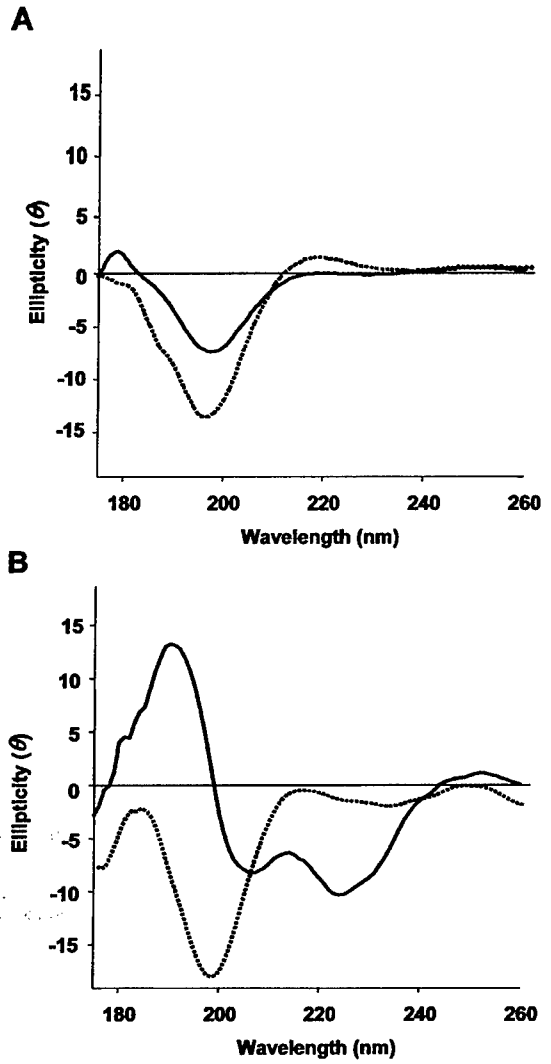

Figure 2. Circular dichroism spectra of (A) PLL_{20} and (B) PLL_{222} in sodium phosphate buffer pH 7.5 (dotted line) or pH 11.2 (solid line).

PLL previously described by Padden and co-workers[21,25] and more recently by the Pochan and Deming groups using PLL_{200} (chain length = 200).[26,27] The formation of hexagonal PLL crystals is suggested to occur due to the supramolecular assembly of α-helical chains of PLL that assemble in the presence of phosphate counterions. Supramolecular assembly failed to occur in solutions when PLL was either in the random coil or β-sheet conformation.[26]

The secondary structure of proteins is commonly determined using circular dichroism (CD) spectroscopy. PLL can adopt three different secondary conformations depending on pH and temperature.[28,29] PLL adopts a random coil conformation at pH 7.0, an α-helical conformation at pH 11, and a β-sheet structure after heating to 52 °C.[29] The CD spectra of the two PLL representative chain lengths used in this study at pH 7.5 and pH 11 are

(25) Padden, F. J.; Keith, H. D. *J. Appl. Phys.* **1965**, *36*, 2987–2995.
(26) Cui, H.; Thompson, J.; Nowak, A. P.; Deming, T. J.; Pochan, D. J. *Polym. Mater. Sci. Eng.* **2004**, *91*, 461.
(27) Cui, H.; Krikorian, V.; Thompson, J.; Nowak, A. P.; Deming, T. J.; Pochan, D. J. *Macromolecules* **2005**, *38*, DOI 10.1021/ma050776q.
(28) Satoh, M.; Hirose, T.; Komiyama, J. *Polymer* **1993**, *34*, 4762.
(29) Grigsby, J. J.; Blanch, H. W.; Prausnitz, J. M. *Biophys. Chem.* **2002**, *99*, 107–116.

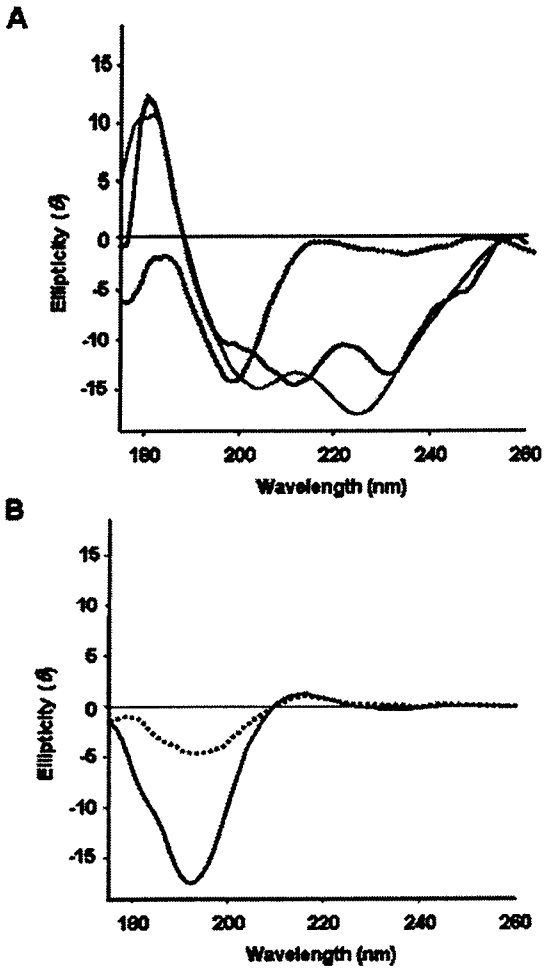

Figure 3. In situ circular dichroism spectra of PLL_{222} in the presence of silicic acid in sodium phosphate buffer pH 7.5 at $t = 0$ (dotted line), 0.5 min (solid line), and 1 min (blue line). (B) In situ CD spectra of PLL_{20} in the presence of silicic acid at $t = 0$ (dotted line) and $t = 1$ min (solid line).

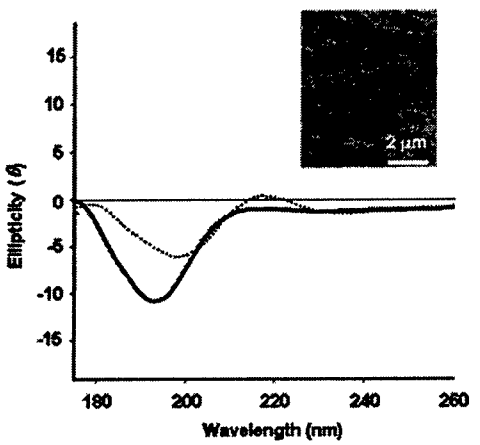

Figure 4. In situ circular dichroism spectra of PLL_{222} in the absence (dotted line) or in the presence (solid line) of silicic acid in 10 mM Tris buffer pH 7.5. (Inset) SEM micrograph of the silica precipitate obtained using PLL_{222} in Tris buffer.

shown in Figure 2. The shorter-chain PLL_{20} adopts a random coil conformation in both pH 7.5 and pH 11 (phosphate buffer solutions), as evidenced by the minima around 200 nm (Figure 2A). In comparison, the longer-chain PLL_{222} assumes a random

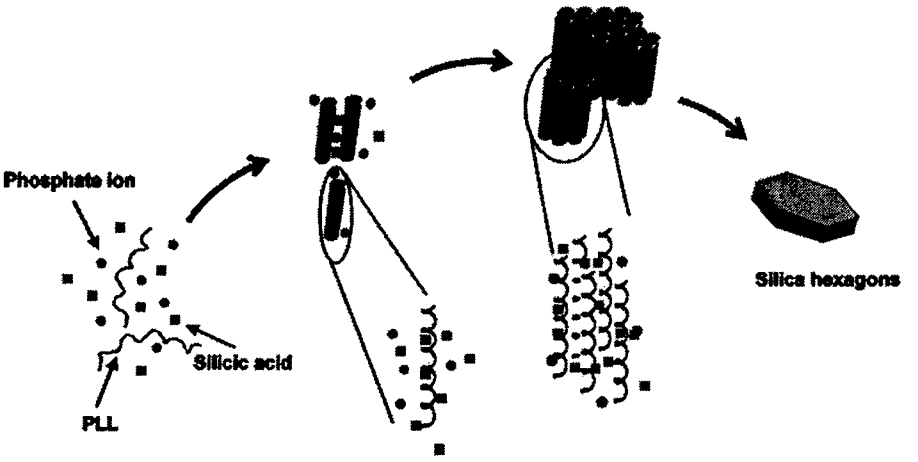

Figure 7. Proposed model for the formation of hexagonal silica platelets.

in the presence of counterions, which in turn exhibit silica-precipitating activity to produce silica spheres. In our case, long-chain PLL can be induced into a helical conformation in the presence of the silicate precursor and phosphate anions, which eventually results in the formation of hexagonal silica platelets.

Polypeptides and other silica-templating peptides have been previously shown to be entrapped within the silica matrix.[13,18,31] Thermogravimetric analysis (TGA) of the PLL_{222}-derived silica platelets shows that they contain ~20%/wt polypeptide. This suggests that PLL polypeptide chains are entrapped with silica matrix. Following this notion, we determined whether preformed hexagonal PLL crystals could serve as templates in the silicification reaction. PLL_{222} crystals were grown as previously described.[21,26,27] Figure 5A shows a SEM micrograph of the hexagonal crystals of PLL_{222}. Both lamellar and multilamellar hexagonal crystals of varying sizes could be observed in the SEM micrographs, similar to those in previously published reports.[21,26,27] We also observed that, in some cases, drying the crystals from aqueous suspension results in distortion and collapse of the crystals. In addition, the crystals also appeared to be sensitive to the electron beam. Prolonged exposure of the PLL_{222} crystal resulted in electron beam damage (Figure 5B).

The preformed PLL crystals were exposed to silicic acid to determine the silica-precipitating activity of the crystals. As shown in Figure 5, C-E, the PLL crystals become covered with silica during the silicification reaction, and EDX analysis confirmed the presence of a silica coating on the PLL crystal (Figure 5F). The silicified PLL crystals were also further analyzed by TEM. The TEM micrographs show that the hexagonal silica-coated PLL crystal appears to be mesoporous (Figure 6B). The *d* spacings of the silicified hexagonal platelets were calculated from the electron diffraction pattern to be 1.52, 0.87, and 0.76 nm corresponding to the (100), (110), and (200) planes, respectively, with a lattice parameter of $a = 1.76$ nm (Figure 6C). This diffraction pattern does not correspond to any of the silica polymorphs but rather reflects the *d* spacings of the underlying PLL crystal.[21,26,27] Similar behavior has also been observed for the templated formation of crystalline silica using plant bioextracts.[33,34] It should be noted that the crystallinity of the silica platelets could be attributed to that the fact that the silicification reaction is restricted to the surface of the preformed PLL crystal unlike that with the PLL polypeptide that results in amorphous hexagonal plates.[9,14]

The lattice parameter of the PLL crystals dried from solution in our study was measured to be around 0.92 nm (Supporting Information Figure S2), much smaller than the previously measured lattice parameters of hydrated or freeze-dried PLL crystals.[21,27] Most likely, the crystals in our study are defective due to dehydration of the crystal, during imaging, that resulted in the collapse of the PLL side chains. In contrast, the silicified PLL crystals maintain their integrity due to the presence of a silica coating, and possibly due to the infiltration of the silicic acid into the interstices that effectively result in the cross-linking of the neighboring PLL chains. PLL crystals have been shown to be porous and can allow for the infiltration of small molecules.[21,27] Therefore, the PLL crystals can swell and change their lattice spacing depending on hydration, presence of counterions, and infiltration of silicate precursors into the crystal lattice. The silica platelets retain the shape and features of the underlying protein template after calcination in air. The electron diffraction pattern of the calcined platelet shows the (100) planes only (Figure 6D), and the *a* parameter of the hexagonal unit cell was calculated to be 1.59 nm. Although this suggests that lattice does shrink slightly when the protein template is removed, the silica platelet does retain the shape and mesoporous features of the crystal template. Retention of the meso/nanoporous structure in the calcined platelet suggests that the silicate precursor was also able to infiltrate the PLL crystal lattice.

Together, our results suggest that long-chain PLL undergoes a rapid secondary-structure transition from a random coil to a helical structure in the presence of silicic acid and phosphate ions. The negatively charged silicate precursor, along with phosphate ions, allows for the secondary-structure phase transition of PLL to occur at neutral pH. The formation of the helical PLL chains during the silicification reaction results in the formation of hexagonal silica platelets. Preformed PLL hexagonal crystals can also serve as templates to direct the growth of a mesoporous silica phase that is oriented in respect of the protein crystal template.

(31) McKenna, B. J.; Birkedal, H.; Bartl, M. H.; Deming, T. J.; Stucky, G. D. *Angew. Chem., Int. Ed.* **2004**, *43*, 5652–5655.
(32) Brunner, E.; Lutz, K.; Sumper, M. *Phys. Chem. Chem. Phys.* **2004**, *6*, 854–857.
(33) Keeling-Tucker, T.; Perry, C. C. *Chem. Commun.* **1998**, 2587–2588.
(34) Perry, C. C.; Keeling-Tucker, T. *Colloid Polym. Sci.* **2003**, *281*, 652–664.

Spermine, spermidine and their analogues generate tailored silicas†

David J. Belton, Siddharth V. Patwardhan and Carole C. Perry*

Received 8th July 2005, Accepted 23rd August 2005
First published as an Advance Article on the web 22nd September 2005
DOI: 10.1039/b509683a

Biosilicifying organisms such as diatoms, sponges and higher plants deposit ornate "glassy" siliceous materials with well defined properties such as particle size and porosity at precisely controlled growth rates. Here we present the *in vitro* synthesis and characterisation of "glassy" silica with tailored properties by using naturally occurring amines—spermidine and spermine—and their analogues. These additives were found to regulate the growth rates, particle sizes, maturation, surface areas, porosities and morphologies of the siliceous materials prepared. In particular, the combination of unique catalytic effects and aggregation behaviours that are dependent on or related to chain length, intramolecular N–N spacing and C : N ratio of the additives was found to be responsible for controlling materials properties. Mechanisms regulating the generation of silicas showing a range of material characteristics are proposed.

Introduction

The silica industry worldwide is worth an estimated $2 billion annually[1] in products used in such diverse areas as rubber reinforcement, desiccants, flocculants, binding agents and catalysts. The simple chemical structure of silica or hydrated silica belies the complexity of their chemistries and it is this complexity which enables and determines the suitability of the material for the myriad of known applications. These functions ultimately depend on the surface chemistry, molecular structure, morphology and porosities of the silicas that are manufactured either from the vapour phase by pyrolysis and condensation of tetrachlorosilanes, or from aqueous media as for the production of silica gels/sols and precipitated silicas. All of these manufacturing methods require harsh conditions of temperature and pH and also involve the use and production of environmentally damaging precursors and waste streams, respectively.[1,2] By comparison, biologically controlled silica production occurs under benign conditions and results in materials of superior form and function starting from a source of soluble silica, monosilicic acid, $Si(OH)_4$, at concentrations of only a few tens of parts per million.[3] Needless to say the drive to greener manufacturing methods has resulted in considerable expenditure of research funding and time being invested into elucidating the mechanisms utilised by the organisms.

Research programmes have already identified biomolecular species intimately associated with biosilica including the silicatein proteins found as the axial filament of sponge spicules,[4] long chain poly(amine)s and the silaffin proteins found in the silica casing of diatoms[5] and glycoproteins found in the silica of higher plants.[6] The diatom silaffin proteins are relatively enriched with lysine residues that are modified by the attachment of long chain poly(propylamine)s to the side chain. Similar poly(propylamine)s terminated by a putrescine group are also found in isolation.[7] These poly(amine)s appear to be a homologous group, synthesised as a continuation of the putrescine, spermidine and spermine metabolic pathway—all common naturally occurring poly(amine)s.[8] Due to their prevalence in nature it is therefore possible that the utilisation of these poly(amine)s may be an adventitious one and that, at least *in vitro*, other poly(amine)s with different amine separations may cause similar effects to those observed for the molecules isolated from diatoms. The possibility of using similar molecules that are cheaper and readily available to produce superior silica products under more benign conditions is desirable.

A considerable body of work already exists on the chemical and biomimetic effects of amine species on the condensation of silicic acid systems and characterisation of the harvested silica,[9] but any mechanistic differences between the chemical and biological routes are still poorly understood. A range of amines and poly(amine)s have shown catalytic effects and generated unusual *in vitro* silica structures from a range of precursors.[9,10] Studies of the effects of amino acids and homologous peptides with a range of silica precursors (silicon–catecholate complex, sodium silicate and tetraethoxysilane) showed enhanced condensation, aggregation and harvestable silica yields.[11] Silica sphere and hexagonal silica production of varying sizes and dispersities has been shown to occur in poly(L-lysine)–tetramethoxysilane (TMOS) systems and mechanical factors (*e.g.* shear) leading to the production of platelets, and elongated fibre-like structures for these systems have also been reported.[12,13] In addition, studies using poly(allylamine) hydrochloride have shown similar sphere formation control[14] and transformation from sphere to honeycomb structures when the precursor was changed from TMOS to a poly(amine) stabilized silica sol.[15] Silica formation in the presence of poly(ethylenimine)-functionalised porphyrin rings and benzene rings, and linear poly(ethylenimine)s has generated complex structures such as filamentous aster, fibrillar sponge and leaf morphologies. Electron microscopy has shown that the silica fibres consist of a coating of silica particles

School of Biomedical and Natural Sciences, Nottingham Trent University, Clifton Lane, Nottingham, UK NG11 8NS. E-mail: Carole.Perry@ntu.ac.uk; Tel: +44 (0)115 8486695
† Electronic supplementary information (ESI) available: Fig. S1–5. See http://dx.doi.org/10.1039/b509683a

Table 1 Some molecular properties and models of the amines used in this study[a]

	N	Amine	l	l_1	l_2	l_3	l_4	l_5
	2	MEDA	3.78	3.78	—	—	—	—
	3	DETA	7.36	3.75	3.75	—	—	—
	3	SPDN	11.17	5	6.23	—	—	—
	4	TETA	11.1	3.75	3.76	3.78	—	—
	4	SPN	16.1	5	6.24	4.96	—	—
	5	TEPA	14.72	3.75	3.76	3.76	3.76	—
	6	PEHA	18.45	3.75	3.76	3.76	3.76	3.78

[a] N = number of amines per molecule, l = end-to-end distance of molecules. l_i = distance between ith and i + 1th amines.

of the amine signals against that of the chemical shift reference and comparing with a set of standards prepared using known amounts of poly(amine) measured under the same solution conditions against the same chemical shift reference.

For surface area and pore analysis, freeze dried samples were degassed at 120 °C for 15 h and nitrogen gas adsorption/desorption isotherms were measured using a Quantasorb NOVA 3200e surface area and pore size analyser. Surface areas were determined by the multipoint BET method and pore size distributions and pore volumes determined by the BJH method.[25,26]

For ^{1}H NMR spectroscopy, all samples were measured in 5 mm glass NMR tubes from aliquots taken directly from the experiments with no sample preparation. Spectra were accumulated from 32 scans with a pulse delay time of 1 s using a Jeol JNM-EX270 Fourier transform nuclear magnetic spectrometer. A tube insert containing sodium 2,2 dimethyl-2-silapentane-5-sulfonate (DSS) in D_2O provided the chemical shift reference and deuterium lock signal with the DSS dimethyl signal also being employed as a reference for quantification purposes.

Morphological studies were performed by scanning electron microscopy. Freeze dried samples were dusted on to sticky carbon pads on aluminium sample holders and gold coated with an argon plasma at 10^{-3} bar and 1.2 mA. Images were obtained using a Jeol JSM-840A scanning electron microscope at an accelerating voltage of 20 kV.

Results

The effects of naturally occurring poly(amine)s—spermidine and spermine—and a series of linear ethyleneamine homologues (EAs) of between 1 and 5 repeat ethyleneamine units on a model silica condensing system have been studied. The physical characteristics of the amines used in this study—intra-amine distances—are listed in Table 1.

Silica samples prepared in the presence of amines were collected after 7 d, dried and their morphology studied. SEM images obtained on silica condensed in the presence of the homologous ethyleneamines showed an increasingly granular structure with increased molecular length; uniform coalesced spheres of around 200–250 nm diameter being formed in the presence of PEHA (Fig. 1). Interestingly, it was found that the addition of spermidine to the condensing system results in large particles, similar to TEPA, while in the presence of spermine, the morphology of silica prepared is closer to TETA. Furthermore, for the silica samples synthesised from TMOS in the presence of EAs, distinct particles with particle sizes varying from *ca.* 240–500 nm, were observed (Fig. 2). It is noted that no precipitation was evident in the absence of any

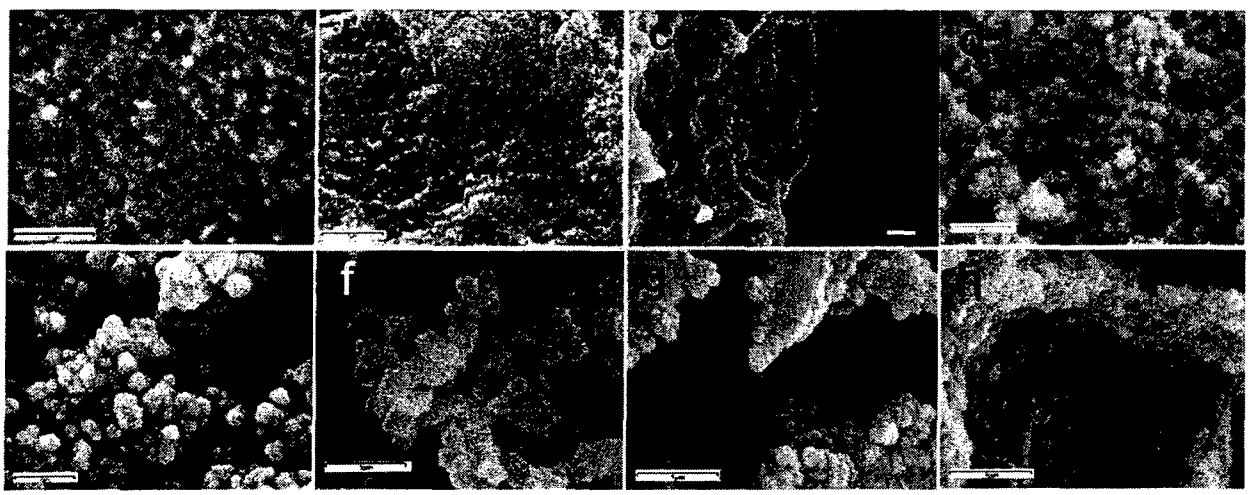

Fig. 1 Typical scanning electron microscopy images of silica samples isolated from EAs after 7 d when the silicon complex was used as the silica precursor; (a) blank, (b) MEDA, (c) DETA, (d) TETA, (e) TEPA, (f) PEHA, (g) SPDN, (h) SPN; bars = 1 μm.

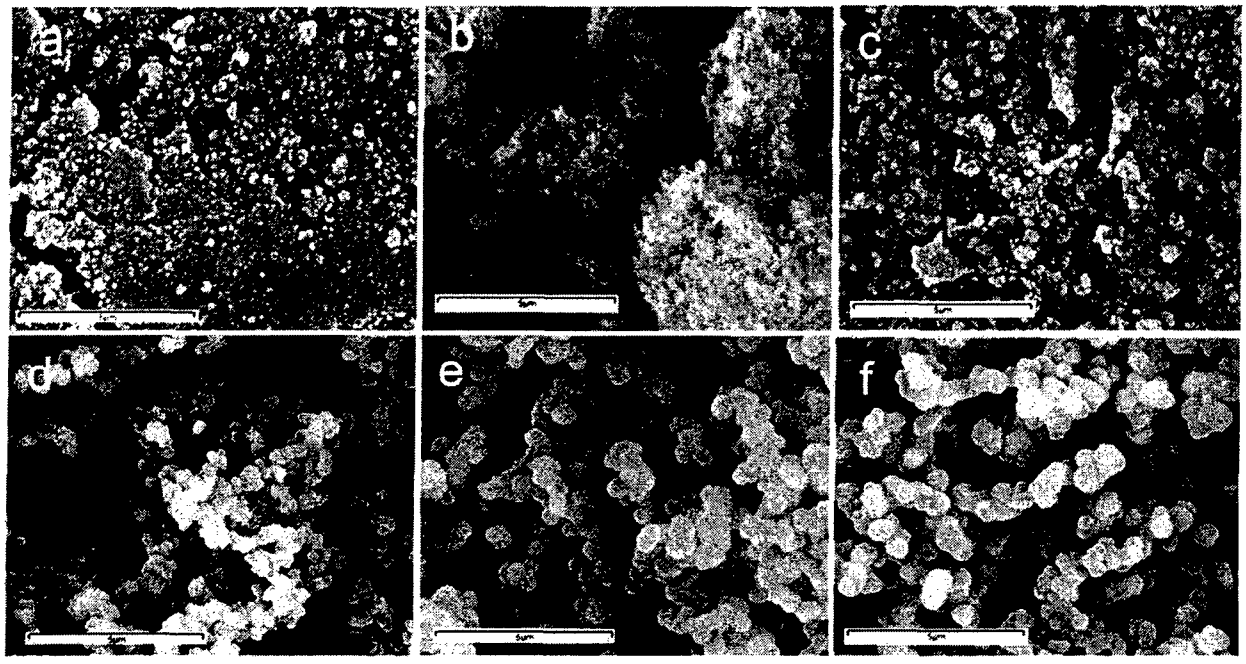

Fig. 4 Scanning electron microscopy images of silica samples isolated from PEHA at a range of PEHA concentrations when the silicon complex was used as the silica precursor. The PEHA concentrations were (a) 10%, (b) 25%, (c) 50%, (d) 100%, (e) 200%, (f) 800%; bars = 1 μm for 10% and 5 μm for other samples.

Furthermore, when the ratio of amines from PEHA to Si was varied from 0.1 to 8 (*i.e.* 10–800%) material isolated at fixed time points showed an increased aggregate uniformity and particle size as initial PEHA content was increased (Fig. 4). A switchover in silica morphologies was observed at around N : Si = 0.5, where the formation of particulate silica was evident. The particles appeared sharper suggesting that they were highly condensed.

Surface areas determined by multipoint BET analysis showed a reduction with increased additive size and maturation times (Fig. 5a). The reduction in surface area was particularly noticeable in the case of silica condensed in the presence of PEHA where surfaces were reduced to such an extent that measurements could not reliably be made. The natural poly(amine)s showed similar surface area trends when compared on the basis of chain length but were slightly more effective when compared on the basis of amine moiety per molecule. Pore volumes and radii determined by the BJH method[26] for silica condensed in the presence of the ethyleneamine homologues both showed a general increase with molecular length up to TEPA, but on increasing to PEHA practically no mesopores and only a much reduced micropore population was detected (refer to the electronic supplementary information, Fig. S1–2). Using the pore volume and radii data, estimates of pore numbers were made showing that the transition between porous and essentially nonporous materials was observed at ethyleneamine homologues in excess of four amines per molecule (Fig. 5b). The surface areas of the samples precipitated from TMOS experiments followed a similar trend, wherein DETA and PEHA showed surface areas of 360.51 and 17.43 $m^2\ g^{-1}$, respectively, and pore volumes as low as 0.02 $cm^3\ g^{-1}$ (data not shown).

The increased pore sizes with increasing chain length and decreasing surface area with maturation time can be regarded as typical behaviour for increasingly rapidly aggregating silica nanoparticles of uniform size. The rapid aggregation causing disperse pore size formation due to time constraints on particle reorientation and compaction and, importantly also on Ostwald ripening, probably resulted in the observed surface area reduction. The behaviour of the naturally occurring poly(amine)s throughout suggest that they influence the condensation and aggregation process largely as a consequence of their chain length and charge separation and as such do not behave in an unexpected manner *in vitro*.

Due to the unusual ability of PEHA to generate almost "glassy" silicas, further analysis was carried out by varying PEHA concentration. Increasing the PEHA concentration between 10–200% (3 and 60 mM) with respect to amine : silicon content resulted in a large decrease in the observed surface areas (Fig. 5c and, in the supplementary information, S3–4). Heat treatment of the silica to remove any entrained organic material resulted in a restoration of some of the surface area but this was almost entirely due to the appearance of micropores. Some porosity could be measured at $t_{1/2gel}$ (*ca.* 12 $m^2\ g^{-1}$) for these samples but at longer maturation times even this disappeared. Pore volume/radii measurements made, show that the material isolated at $t_{1/2gel}$ for PEHA contained a range of pores in the micro to meso domains but by 60 min, (which was also the time of onset of precipitation), all but the micropores had disappeared (supplementary Fig. S1–4).

The solution chemistry of the silicifying systems was studied in order to investigate the earlier stages of silica formation in the presence of ethyleneamines, spermidine and spermine. The effect of these additives on silica formation kinetics was

about 70 min. Aggregation was not observed for any of the additives until a minimum of 75% of the available orthosilicic acid had condensed to non-molybdenum blue active species with the exception of experiments where PEHA had been added in which case aggregation/growth was observed when as little as 30% condensation had occurred (Fig. 6a). Data for the natural poly(amine)s used, spermidine and spermine, fell broadly in line with the ethyleneamine homologues in terms of chain length and amine content per molecule with spermidine having a slightly pronounced effect in relation to its amine content and spermine a slightly reduced effect.

Additional experiments conducted where the level of PEHA was varied from 10–200% (*i.e.* 3–60 mM) with respect to amine group content showed an increased aggregation rate with increasing concentration and a decreasing gelation/precipitation time (Fig. 7). At levels exceeding 100% PEHA, only small changes in growth rates and gelation/precipitation time was observed, and at levels below 100% PEHA concentration, gelation and not precipitation occurred. Silica isolated from these experiments showed an increasing ease of re-suspension in water with increasing PEHA content even after extensive washing to remove any extraneous poly(amine), which may suggest a possibility of stabilisation of particulate silica in solutions in the presence of higher PEHA concentrations (see below).

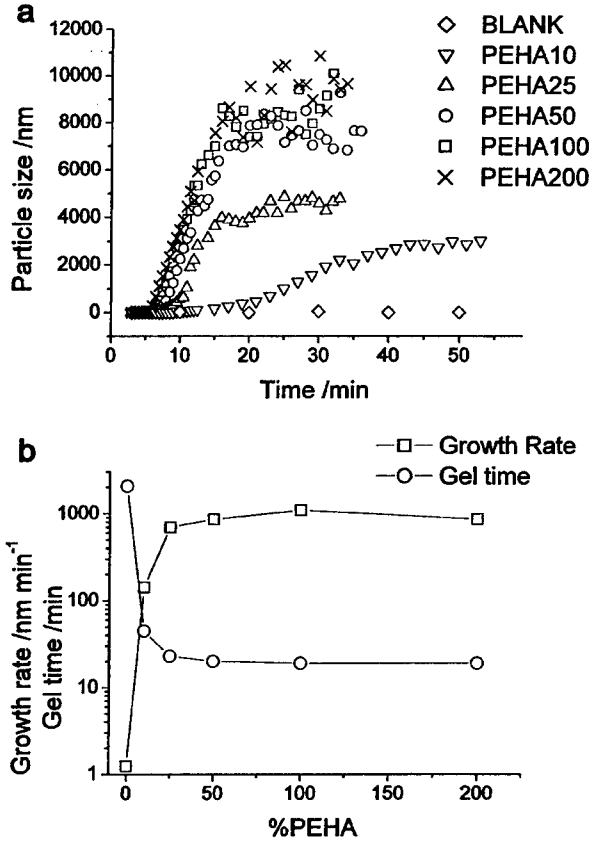

Fig. 7 Aggregation behaviour (a), and growth rates and gelation times (b) of silica in the presence of a range of PEHA concentrations.

Discussion

The effects on particle growth/aggregation were considered to be very pronounced in comparison with the limited effect of the additive on initial condensation. An obvious cause of increased aggregation is charge neutralisation of the anionically charged silica particles by the cationically charged amine species. Assuming a silica particle surface made up of mostly Q3 species and 50% silanol group dissociation, (a reasonable assumption at the pH of the experiments),[27] the minimum surface inter-anion distance can be estimated to be approximately 5.4 Å, *i.e.* every other silanol group. The shortest ethyleneamine homologue used in this study was MEDA with an inter-amine distance of 3.9 Å (see Table 1). Clearly this results in the molecule only being able to attach *via* one amine group as shown in Scheme 1b. All of the other ethyleneamine homologues used have inter-amine distances which allow them to attach along the surface of the particles (Scheme 1c).

It is known from previous studies that amines, such as those studied herein, are able to bind with inorganic polyanions.[28] If the poly(amine)s all orient along the particle surface then increased aggregation would be a consequence of the collapse of the electrical double layer and an increased rate with chain length would not be observed. However it is thought that, at the concentrations of amines used, surface saturation occurs allowing some of the molecules only to attach at limited number of points. The amine chains are thus forced to extend into, and if long enough, beyond the double layer boundary (Scheme 1d–e). The increase in aggregation rates observed with increasing poly(amine) length therefore suggests that at least some of the chains extend into the bulk solution and are therefore able to bridge between neighbouring particles. The step change in rate of aggregation and gel times observed from MEDA to TETA corresponds to an increased molecule length from 3.8 to 11.1 Å suggesting that for these particles the surface double layer is of this order. Work carried out previously by our group using diamines also showed a step change in aggregation rates between the addition of 1,4 diaminobutane and 1,6 diaminohexane corresponding to an inter-amine distance of 6.3–8.7 Å respectively suggesting a shared chain length mechanism, *i.e.* spanning of the electrical double layer, for the observed step change.[21] The naturally occurring poly(amine)s used in this study, spermidine and spermine were 11.2 and 16.1 Å in length, respectively, and accordingly showed the accelerated aggregation effects. Gels formed showed increasing opacity with poly(amine) chain length and the longest, PEHA, precipitated silica within minutes.

Almost universally for the silica condensing model used herein, particle growth is not observed by DLS until in excess of 75% of the available monosilicic acid has condensed to non-molybdenum reactive species *i.e.* after a large population of primary particles has formed. However, monosilicic acid levels at the time of onset of particle formation in the presence of PEHA were around 70% of the initial concentration, suggesting that a smaller number of primary particles were mopping up the available monosilicic acid to form the larger low surface area spheres as observed by SEM and gas adsorption. These silica spheres of 200–250 nm in diameter had aggregated sufficiently for isolation by centrifugation within 30 min of the

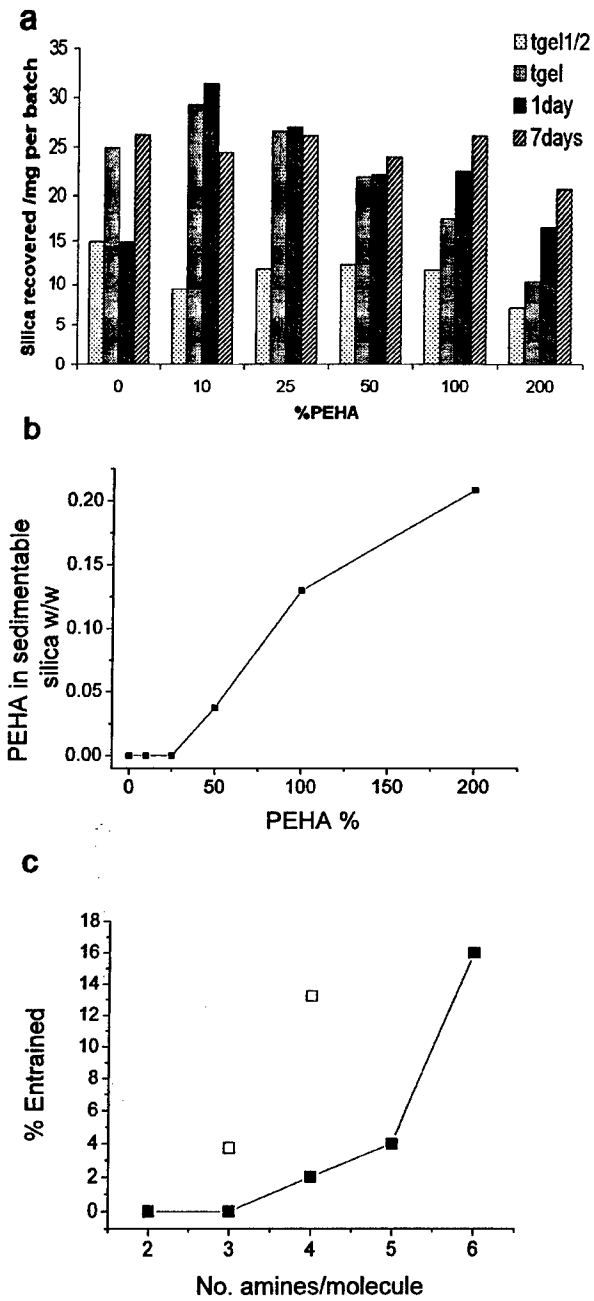

Fig. 8 (a) Sedimentable silica obtained from a range of PEHA concentrations, samples isolated at different time intervals; (b) PEHA occluded in sedimentable silica; (c) ethyleneamines entrained in silica samples. Hollow symbols in (c) represent spermidine and spermine data.

surface area measured by multipoint BET after heat treatment of the silica to 650 °C (Fig. 5). The nature of the microporosity found associated with the surface area increase suggest that its origin is layers of PEHA in the silica spheres rather than molecules trapped in the interstitial voids.

Conclusions

The effects of poly(amine)s of a range of chain lengths, architectures and basicities on the condensation of monosilicic acid and the formation and aggregation of silica particles have been investigated. Slight catalytic activity over condensation correlating with chain length was observed, but not thought to be significant, and the naturally occurring amines used showed no special additional effects. Particle growth and aggregation also showed chain length-dependent acceleration effects which were also observed with the naturally occurring amines. However, as the chain was extended to 6 repeat ethyleneamine units, a transition in behaviour (and possibly the condensation mechanism) was observed. That this transition was pH and amine concentration dependent was also shown, allowing the proposal of a mechanism to be made to explain the observations. The mechanism involves particle stabilisation by reversal in charge and increase in magnitude of the outer double layer. This is followed by uncharged amine groups facilitating the condensation of monosilicic acid on to the stabilised spheres *via* reversible proton exchange, the process driven by water being preferred over hydroxyl ions as the leaving group. Due to the observed pH sensitivity of the process, which is thought to arise from intramolecular amine spacing, it should be possible to tailor reactions using the careful choice of amine group basicity and charge separation to enable similar highly condensed silica spheres to be produced over a range of pHs. Also, it could be possible that similar mechanisms occur during the biosilicification process, however this is only speculative at this point in time. The undertaking of studies on a similar range of repeat unit propyleneamine homologues could help to clarify this matter and work is being undertaken in this direction. It should be noted that preliminary modelling studies[30] on propylamines and butylamines indicate interesting trends in protonation behaviour that are being utilised to direct our silica formation studies.

Acknowledgements

The authors would like to thank the American Air Force and the European Union for funding of this project.

References

1 T. Kendall, *Ind. Miner.*, 2000, 49.
2 R. K. Iler, *The Chemistry of Silica*, John Wiley & Sons, New York, 1979; C. J. Brinker and G. W. Scherer, *Sol–Gel Science: The Physics and Chemistry of Sol–Gel Processing*, Academic Press, Boston, 1990.
3 T. L. Simpson and B. E. Volcani, *Silicon and Siliceous Structures in Biological Systems*, Springer-Verlag, New York, 1981; W. E. G. Muller, *Silicon Biomineralization*, Springer, Berlin, 2003.
4 K. Shimizu, J. Cha, G. D. Stucky and D. E. Morse, *Proc. Natl. Acad. Sci. USA*, 1998, **95**, 6234.
5 M. Sumper and N. Kroger, *J. Mater. Chem.*, 2004, **14**, 2059.
6 C. C. Harrison, *Phytochemistry*, 1996, **41**, 37; C. C. Perry and T. Keeling-Tucker, *Colloid Polym. Sci.*, 2003, **281**, 652.
7 N. Kroger, R. Deutzmann, C. Bergsdorf and M. Sumper, *Proc. Natl. Acad. Sci. USA*, 2000, **97**, 14133.
8 S. S. Cohen, *A Guide to the Polyamines*, Oxford University Press, New York, 1998.
9 S. V. Patwardhan, S. J. Clarson and C. C. Perry, *Chem. Commun.*, 2005, **9**, 1113.
10 S. V. Patwardhan, C. Raab, N. Husing and S. J. Clarson, *Silicon Chem.*, 2003, **2**, 279.
11 D. Belton, G. Paine, S. V. Patwardhan and C. C. Perry, *J. Mater. Chem.*, 2004, **14**, 2231; T. Coradin and J. Livage, *Colloids Surf., B*, 2001, **21**, 329; T. Coradin, O. Durupthy and J. Livage, *Langmuir*,

Micron 37 (2006) 107–120

www.elsevier.com/locate/micron

Review

Siliceous spicules in marine demosponges (example *Suberites domuncula*)

Werner E.G. Müller [a,*], Sergey I. Belikov [b], Wolfgang Tremel [c], Carole C. Perry [d], Winfried W.C. Gieskes [e], Alexandra Boreiko [a], Heinz C. Schröder [a]

[a] *Institut für Physiologische Chemie, Abteilung Angewandte Molekularbiologie, Universität, Duesbergweg 6, D-55099 Mainz, Germany*
[b] *Limnological Institute of the Siberian Branch of Russian Academy of Sciences, Ulan-Batorskaya 3, RUS-664033 Irkutsk, Russian Federation*
[c] *Institut für Anorganische Chemie, Universität, Duesbergweg 10-14, D-55099 Mainz, Germany*
[d] *Department of Chemistry and Physics, Nottingham Trent University, Clifton Lane, Nottingham NG11 8NS, UK*
[e] *Department of Marine Biology, Biological Center, Center for Ecological and Evolutionary Studies, University of Groningen, P.O. Box 14, 9750 AA Haren, The Netherlands*

Received 2 August 2005; revised 4 September 2005; accepted 5 September 2005

Abstract

All metazoan animals comprise a body plan of different complexity. Since—especially based on molecular and cell biological data—it is well established that all metazoan phyla, including the Porifera (sponges), evolved from a common ancestor the search for common, basic principles of pattern formation (body plan) in all phyla began. Common to all metazoan body plans is the formation of at least one axis that runs from the apical to the basal region; examples for this type of organization are the Porifera and the Cnidaria (diploblastic animals). It seems conceivable that the basis for the formation of the Bauplan in sponges is the construction of their skeleton by spicules. In Demospongiae (we use the model species *Suberites domuncula*) and Hexactinellida, the spicules consist of silica. The formation of the spicules as the building blocks of the skeleton, starts with the expression of an enzyme which was termed silicatein. Spicule growth begins intracellularly around an axial filament composed of silicatein. When the first layer of silica is made, the spicules are extruded from the cells and completed extracellularly to reach their the final form and size. While the first steps of spicule formation within the cells are becoming increasingly clear, it remains to be studied how the extracellularly present silicatein strings are formed. The understanding of especially this morphogenetic process will allow an insight into the construction of the amazingly diverse skeleton of the siliceous sponges; animals which evolved between two periods of glaciations, the Sturtian glaciation (710–680 MYA) and the Varanger-Marinoan ice ages (605–585 MYA). Sponges are—as living fossils—witnesses of evolutionary trends which remained unique in the metazoan kingdom.

Keywords: Sponges; Porifera; Suberites domuncula; Spicules; Biosilica; Silica formation; Silicatein; Evolution

Contents

* Corresponding author. Tel.: +49 61 31 39 25910; fax: +49 61 31 39 25243.
E-mail address: wmueller@uni-mainz.de (W.E.G. Müller).
URL: http://www.biotecmarin.de/.

0968-4328/$ - see front matter © 2005 Elsevier Ltd. All rights reserved.
doi:10.1016/j.micron.2005.09.003

1. Introduction

Since Aristotle [384–322 BC] (cited in Camus, 1783) sponges have occupied a distinguished position among the animals because of their biomedical potential (see Arndt, 1937), their beauty and also their enigmatic evolutionary origin. Lord G. Campbell, (1876) a sub-lieutenant on board the 'Challenger' wrote that "sponges are...the most characteristic inhabitants of the great depths all over the world...some of which rival in beauty". Difficulties in their systematic positioning and their relationship to other multicellular organisms have resulted in their designation as 'Zoophytes' or 'Plant–animals', a taxon placed between plants and animals (Spix, 1811), until finally they were recognized as genuine metazoans, which evolved first from the animal ancestor, the urmetazoan (Müller, 2001). Based on intense molecular biological/cell biological studies it became overt that sponges are not 'simple blobs' but contain and express a variety of metazoan-like transcription factors and in turn form sophisticated tissue assemblies (commented by: Pilcher, 2005). The sponges have been grouped into siliceous sponges and calcareous sponges (Haeckel, 1872), and after the discovery/appreciation of the glass sponges (Schulze, 1887) divided into three classes: Demospongiae [mostly sponges with a skeleton, composed of siliceous spicules], Hexactinellida [always siliceous skeleton] and Calcarea [always calcareous skeleton] (see Hooper, 1997). Sponges were united to the phylum Porifera, based on the existence of characteristic and distinct pores on the surface of the animals (Grant, 1835; Lieberkühn, 1859).

Sponges were also termed 'living fossils' (Müller, 1998) since they represent the evolutionary oldest, still extant taxon which testifies the developmental level of animals living in the Neo-Proterozoic Eon (1000–520 million years ago [MYA]). This is important to note since two major 'snowball earth events' occurred during this period of time, the Sturtian glaciation (710–680 MYA) and the Varanger-Marinoan ice ages (605–585 MYA), which very likely resulted in the covering of the earth by a continuous ice layer and supposedly caused extinction of most organisms on earth at that time (Hoffman et al., 1998).

The primordial earth surface comprised initially insoluble silicates, carbonates, and also phosphates. During the cycle of silicate weathering and carbonate precipitation, prior or simultaneously with the glaciations, a dissolution of surface rocks composed of insoluble silicates [$CaSiO_3$] resulted in the formation of soluble calcium carbonate [$CaCO_3$] and soluble silica [SiO_2], under consumption of atmospheric CO_2 (Walker, 2003). These soluble minerals leached subsequently out to the oceans, rivers and lakes and there again led to a re-precipitation of the dissolved minerals to new compositions as part of the sedimentary rocks. Such processes are dependent upon temperature, pH and atmospheric carbon dioxide; passively, the minerals are transformed diagenetically to secondary structures. An example is given from the Proterozoic/Cambrian period (Fig. 1A), the Wilkawillina Limestone at Finders Ranges (Australia). There, through secondary re-precipitation of dissolved minerals, a passive diagenesis of Ca-carbonate into 50 μm large deposits occurred. The resulting spicule-like structures are seen in thin sections and are reminiscent of sterrasters found in sponges from the family of Geodiidae (siliceous sponges); microanalysis, however, revealed that these spicule-like structures do not at all contain silicon (Fig. 1A-c), but calcium (Fig. 1A-b).

In contrast to passive re-precipitation, biogenic deposition of minerals by metazoans is first seen in sponges. The oldest sponge fossils (Hexactinellida) have been described from Mongolia and were assessed to have lived coeval with the diverse Ediacara fauna of Namibia more than 540 MYA (Brasier et al., 1997). Hence, the Hexactinellida are the oldest group of sponges as documented there and later in fossil records of the Sansha section in Hunan (Early Cambrian; China; Steiner et al., 1993), where more or less completely preserved sponge fossils, e.g. *Solactiniella plumata* (Fig. 1B-a), have been found. This fossil is noteworthy since it shows, besides the unusual body preservation also very intact spicules; the approximately 40 mm large specimen comprises 0.5–5 mm long spicules with a diameter of 0.1 mm (Fig. 1B-b). Some of them are broken and present the open axial canals (Fig. 1B-c). The oil-shales of the Messel pit, near Darmstadt (Germany), are very rich in fossil freshwater sponges; among them is *Spongilla gutenbergiana* from the Middle Eocene (Lutetian), approximately 50 MYA (Fig. 1C) (Müller et al., 1982). Sometimes spicule assemblies are found (Fig. 1C-a), which are very reminiscent of complete animals; most spicules found in such nests are 160–230 μm long oxeas (Fig. 1C-b). Many

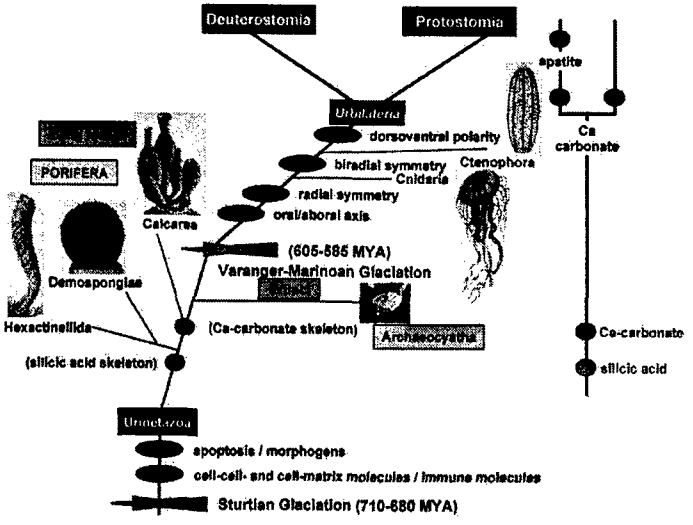

Fig. 3. Phylogenetic position of the Porifera between the Urmetazoa and the Urbilateria. The major evolutionary novelties which have to be attributed to the Urmetazoa are those molecules which mediate apoptosis and control morphogenesis, the immune molecules and primarily the cell adhesion molecules. The siliceous sponges with the two classes Hexactinellida and Demospongiae emerged first and finally the Calcarea, which possess a calcareous skeleton, appeared. These three classes of Porifera are living fossils that provide a reservoir for molecular biological studies. The Archaeocyatha, sponge related animals with a calcareous skeleton, became extinct. The Calcarea are very likely a sister group of the Cnidaria. From the latter phylum the Ctenophora evolved which comprise not only an oral/aboral polarity but also a biradial symmetry. Finally the Urbilateria emerged from which the Protostomia and the Deuterostomia originated. Very likely the Urmetazoa emerged between the two major 'snowball earth events', the Sturtian glaciation (710–680 MYA) and the Varanger-Marinoan ice ages (605–585 MYA). In the two poriferan classes Hexactinellida and Demospongiae the skeleton is composed of amorphous and hydrated silica, while the spicules of Calcarea are composed of Ca-carbonate. The latter biomineral is also prevalent in Protostomia and also in Deuterostomia. In vertebrates the bones are composed of Ca-phosphate [apatite].

in the formation and differentiation of the third germ layer, the mesoderm, in tripoblastic animals. Recently, two T-box genes have been isolated from the sponge *S. domuncula*; a *Brachyury* gene and a homologue of the *Tbx2-3-4-5* genes from chordates, which there are interestingly involved in the formation of the limbs. Functional studies demonstrated that the expression of the *Brachyury* gene is upregulated in differentiating sponge cells during formation of canal-like structures. Based on this observation we postulate that already in sponges a primordial axis formation is genetically fixed. This assumption was subsequently confirmed by the isolation and phylogenetic characterization of five members of the forkhead gene family from the sponge *S. domuncula*.

3.4. Transcription factors: homeodomain molecules

The developmental processes resulting in the formation of a body axis require a head center; e.g. in bilaterians, the Spemann's organizer. The genes which are involved in the establishment of the head organizer during embryogenesis have been grouped into three classes of homeobox genes, the Paired-class, the Antennapedia-class and the Lim-class genes. Also in this area a strong progress was made in sponges in the last few years. A paired-class (*Pax-2/5/8*)-gene had been isolated from the freshwater sponge *E. fluviatilis*, which encodes a complete although substantially degenerated homeodomain. In *S. domuncula* a cDNA encoding a LIM/homeobox protein has been isolated which comprises high sequence similarity to the related LIM homeodomain proteins in other animals.

3.5. Genes in S. domuncula indicative for Wnt signaling

The Wnt signaling pathway is a cell communication system which regulates cell-fate decisions, tissue polarity and morphogenesis. The Frizzled protein is the membrane receptor for the Wnt secreted glycoproteins. Through the canonical Wnt signaling pathway, the activated Frizzled binds to Dishevelled (Dsh), which leads to the stabilization and accumulation of ß-catenin in the nucleus, where it activates the TCF/LEF transcription factor. Very recently we isolated the gene encoding the Frizzled receptor from *S. domuncula*, suggesting that a Wnt-pathway involved in cell-fate determination and morphogenesis was already established in sponges.

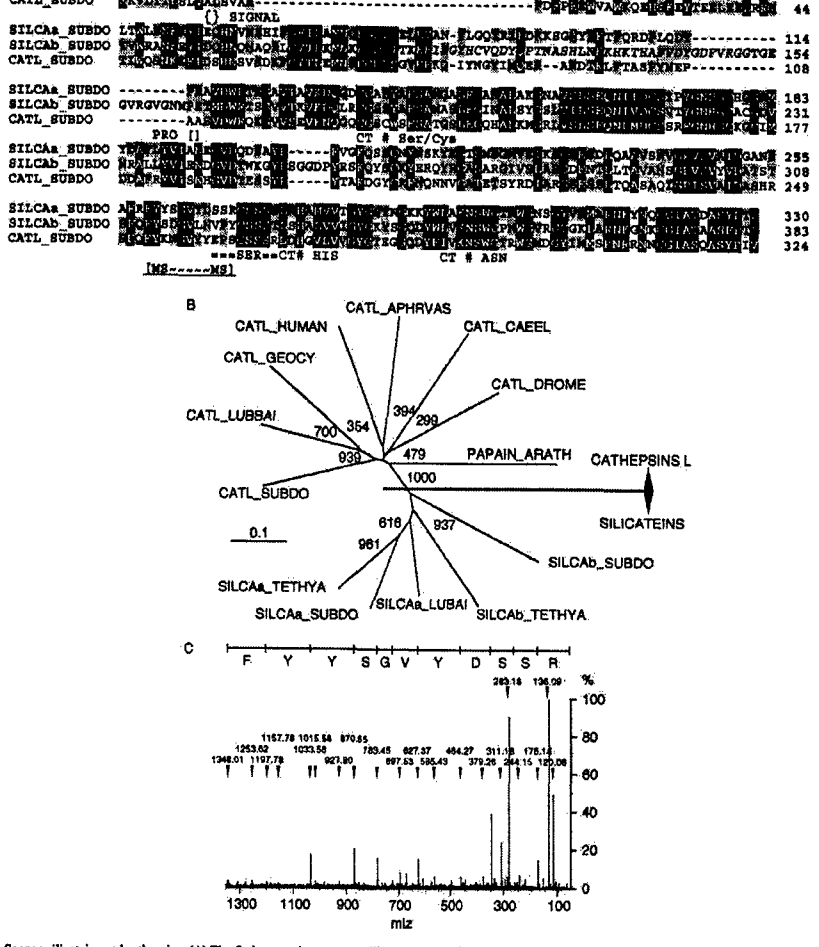

Fig. 4. Sponge silicateins and cathepsins. (A) The *S. domuncula* enzymes, silicatein-α (SILICAa_SUBDO; CAC03737.1) and the β-isoenzyme (SILICAb_SUBDO, AJ547635.1) as well as the cathepsin L sequence (CATL_SUBDO, AJ784224) were aligned. Residues conserved (similar or related with respect to their physico-chemical properties) in all sequences are shown in white on black and those in at least two sequences in black on gray. The characteristic sites in the sequences are marked: the catalytic triad (CT) amino acids, Ser (#) in silicateins and Cys in cathepsin, as well as His (#) and Asn (#), and the processing site for the conversion of the proenzyme to the mature enzyme ([] PRO). The serine cluster ([~Ser~]) and the cleavage site of the signal peptide are indicated ({ }). The region of the silicatein-α protein sequence, identified by ESI-MS, is marked (MS~~~MS). (B) The radial phylogenetic tree was constructed after the alignment of these sequences together with the silicateins-α from *Tethya aurantia* [*T. aurantium*] (SILICAa_TETYA, AAC23951) and *Lubomirskia baicalensis* (SILICAa_LUBAI, AJ872183), silicatein-β from *T. aurantia* (SILICAb_TETYA, AF098670), as well as with the cathepsin L sequences from the sponges *Geodia cydonium* (CATL_GEOCY, Y10527), *L. baicalensis* (CATL_LUBAI, AJ96849) and *Aphrocallistes vastus* (CATL_APHRVAS, AJ968951) as well as from higher Metazoa:

From these studies we conclude that silicatein is not only present in the axial filament of the spicules, but is also located on their surface.

7. Development of spicules in primmorphs

In *S. domuncula*, the formation of spicules is a rapid process and surely proceeds more frequently in embryos or in primmorphs, than in adult specimens. Since all studies on the formation of spicules had hitherto been performed with sections through tissue samples from adult animals the conclusion was published that the formation of the megascleres proceeds extracellularly in the bulky mesohyl of the animals (Uriz et al., 2000; Weaver and Morse, 2003). We applied the primmorph system and could establish unequivocally that the initial steps of spicule formation occur intracellularly in the sclerocytes (Müller et al., 2005).

Sclerocytes in primmorphs produce after an cultivation period of 5 days readily spicules, provided the medium contains silicic acid. As shown in Fig. 7A, the 15 μm large sclerocyte produces one spicules of a length of 6 μm; the lengths of the spicules in those cells vary between 0.7 and 8 μm with diameters of up to 0.9 μm. After the spicules reach a size of > 5 μm, the sclerocytes contract and expand to surround the entire spicule. At higher magnification it can be observed that the blunt end of one spicule, within a sclerocyte, is tightly associated with fibrils, which are very likely involved in the extrusion of the spicules out of the cells (Perović-Ottstadt et al., 2005). It is apparent that especially in the beginning spicule formation starts within vesicles of the cells (Fig. 7A).

The formation of—at least—the first silica layer around the axial filament starts within the sclerocyte. It was reported that the central canal of the spicules is filled only with the axial filament, which is composed of silicatein (Uriz et al., 2000). Also in the primmorph system (Müller et al., 2005) we could show that in the primordial stage the spicule growth starts around the axial filament. There clods with highly electron dense material become visible, which represent the first

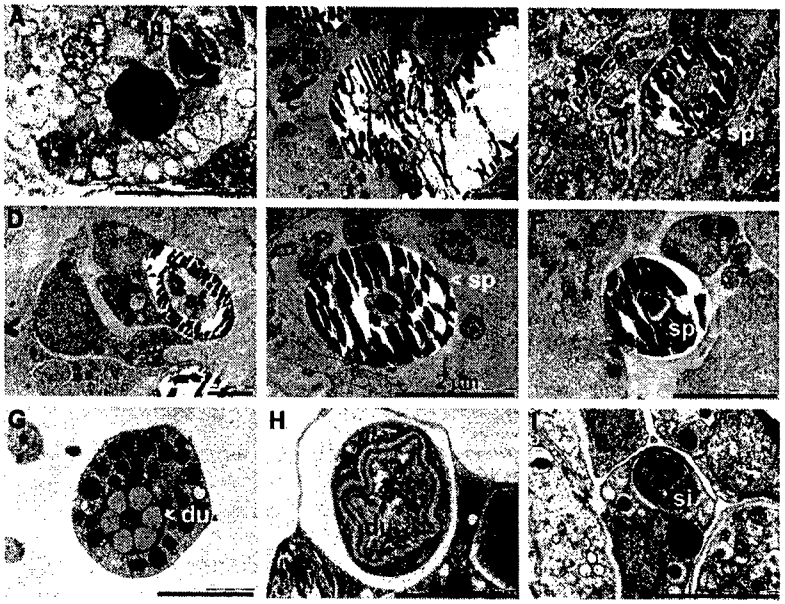

Fig. 7. Maturation stages of the axial filament; TEM analysis of the different phases of spicule formation in primmorphs. (A) In sclerocytes the spicule (sp) formation starts within vesicles of sclerocyte. (B) The axial canal of newly growing spicule comprises hollow fibrillar structures of three (shown here) to six tube-like ducts. (C) Subsequently, the axial filament shows membrane structures, which in a later stage (D) comprises besides those structures also a thin, electron dense axial filament. (E) The electron dense axial filament in the canal increases and displaces the membrane structures. (F) Finally, the axial canal changes from nearly circular to triangular and comprises the electron dense axial filament. (G) The cross section of one hollow fibrillar structure, in the initial phase of spicule formation in the sclerocyte, is shown. Six ducts (du) are seen. (H) All ducts fuse together. Both in the center and around the hollow fibrillar structures, very dense silica deposits (de) are see. (I) Finally, the hollow ducts disappear and larger silica (si) deposits are seen in the primordial spicule. Scale bars: 2 μm.

deposits of spicules. During progression of growth in the extracellular space, the diameter of the axial filament decreases from 1.5 to 0.8 μm while simultaneously the size of the spicule increases up to 450 μm and a diameter of 5 μm. In this phase the spicules are found extracellularly (Fig. 7B). In the next growth stage, two types of structures can be distinguished within the axial canal. First, the 1.6 μm thick axial canal is filled primarily with membrane structures (Fig. 7B) or a comparably thin axial filament is seen, besides the membrane structures (Fig. 7C–E). The 0.8–0.2 μm axial filament has the same electron density as in the initial stage of spicule formation. Among the cellular structures are many 10–15 nm round fibrils of not yet defined nature. The axial filament in the canal increases again in size and becomes more electron dense (Fig. 7E). In the final stage the axial canal changes from nearly circular to triangular (Fig. 7F). Interesting are the hollow fibrillar structures which are seen in sections through spicules in the transition phase (Fig. 7B) from those which comprise complete membrane structures in the axial canal (Fig. 7C) and spicules which show in the canal a more compact axial filament (Fig. 7F). In the transition phase (Fig. 7B), the hollow fibrillar structure fills almost the complete space in the canal.

These hollow fibrillar structures, newly described here, show six tube-like ducts, which are initially regularly arranged around a central filled canal of spicules inside the cells (Fig. 7G). The diameter of those hollow fibrillar structures measures approximately 1.3 μm. In the following stage the regular arrangement of this structure changes and the hollow ducts fuse which each other and also with the central filled canal (Fig. 7H). Now first silica depositions are seen within the structure and also outside of it. Finally the fused hollow ducts disappear and larger silica deposits are observed (Fig. 7I); in this phase the growing spicule is still located within the cells. At present we assume that the function of the hollow fibrillar structure is to provide the guidance for the formation of the silicatein axial filament and to allow also the deposition of the first silica clods. Until now, no solid evidence is available to indicate that in the axial filaments of the spicules entire cells occur.

8. Distribution of silicatein within primmorphs

To obtain results on the distribution of silicatein within the 3D-cell aggregates, the primmorphs, immunogold labeling studies with antibodies against silicatein were performed. Pre-immune serum gave only a low (if at all) labeling signal. More detailed information was given in a recent study (Müller et al., 2005). If, however, the immune serum was used, a dense accumulation of gold granules became visible in the sclerocytes (Fig. 8A). Fine structure analysis revealed that at

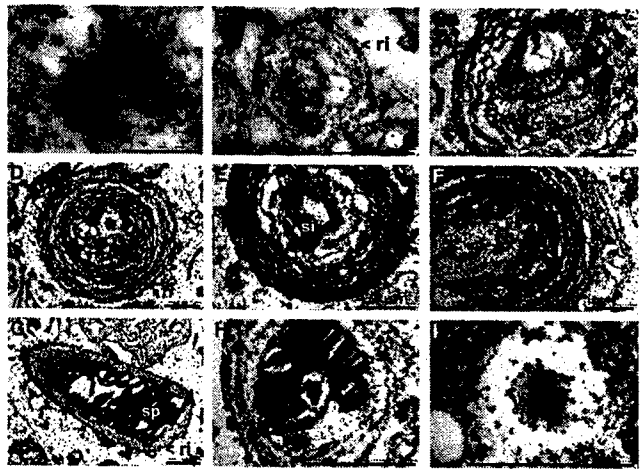

Fig. 8. Immunogold electron microscopy of cross sections through growing spicules in primmorphs; the immune complexes between the polyclonal anti-silicatein antibodies had been visualized with nanogold anti-rabbit IgG. (A) Sclerocytes with a strong accumulation of gold granules, reflecting the condensation of silicatein molecules. (B) At a higher magnification concentric rings (ri) are seen that surround a center with granules of a higher density. (C) In a later stage first electron dense linear clods (> <) become visible around which the rings are arranged. (D) The inner rings fuse and electron dense linear clods are formed. (E) The electron dense material (silica [Si]) accumulates in the center of the multi-lamellar silicatein-reacting material. (F) Higher magnification of (E). (G) The first layer of silica at a growing spicule (sp) is formed around which the concentric ring(s) (ri) remain present. (H) Finally, the silica layer grows and the number of rings increase. (I) The silicatein-antibodies react with the axial filament (af) and the deposits of the silica rings, leaving space for non-reacting material. Scale bars: 2 μm.

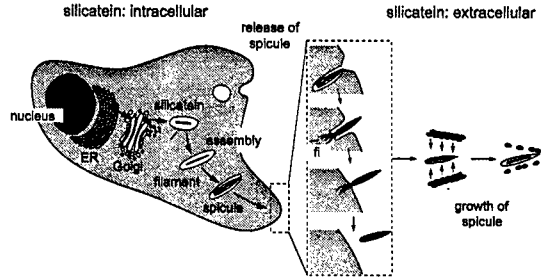

Fig. 11. Schematic outline of spicule formation in *S. domuncula*: intracellular phase. The initial steps of spicule synthesis occur intracellularly where the silicatein is processed to the mature form. During this processing the silicatein undergoes phosphorylation. Very likely with the help of other proteins the silicatein molecules assemble to a rod, the axial filaments. Around this filament the first deposition if silica proceeds. Small spicules are released/extruded from the cells perhaps facilitated by forces coming from associated filaments (fi). These structures have been identified in the axial canal of the spicules. In the extracellular space the spicules growth top their final size. Until now only the 34.7 kDa pro-silicatein has been identified in the extracellular space, suggesting that only small amounts of the enzyme undergoes maturation in this compartment.

Silica is the major constituent of sponge spicules in the classes Demospongiae and Hexactinellida. The spicules of these sponges are composed of hydrated, amorphous, noncrystalline silica. The initial secretion of spicules occurs in Demospongiae in specialized cells, the sclerocytes; there silica is deposited around an organic filament. The synthesis of spicules is a rapid process. Inhibition studies revealed that skeletogenesis of siliceous spicules is enzyme-mediated, more particularly, by an Fe^{++}-dependent enzyme.

The formation of siliceous spicules in sponges is certainly genetically controlled; this process initiates the morphogenesis phase. A series of genes, coding for structural proteins (silicatein and mannose-binding lectin) as well as for a regulatory protein (mago nashi), that are assumed to be involved in the control of spicule synthesis and Bauplan formation in demosponges have recently been identified (to be published). In addition, data demonstrated that at suitable concentrations, silicate induces genes, e.g. those encoding collagen, silicatein and myotrophin (Krasko et al., 2000). A major step forward to elucidate the formation of the siliceous spicules on molecular level was the finding that the 'axial organic filament' of siliceous spicules is in reality an enzyme, silicatein, which mediates the apposition of amorphous silica and hence the formation of spicules. The skeletal framework of the sponges is highly ordered. Both in demosponges and in hexactinellids, it can be seen that the growth of the sponges proceeds in a radiate accretive manner, meaning that growth zones which are highly ordered are delimited by growth lines.

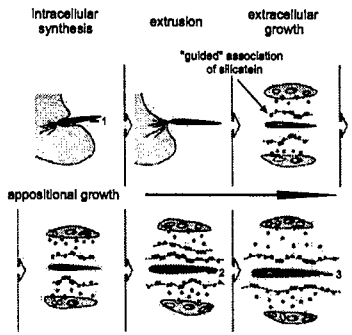

Fig. 12. Scheme of the process of the appositional growth of the spicules in the extracellular space (mesohyl). There, the silicatein molecules are arranged in strings which follow the shape and orientation of the spicules. It is assumed that the silicatein strings mediate laterally the formation of the different lamellar layers around the spicules (appositional growth). It is not yet known if the formation of the strings is based on silicatein–silicatein interactions alone, or if it is structured by a associated protein ('guided' association). In this scheme the appositional growth of the spicules by three layers are highlighted.

In conclusion, this survey provides an attempt towards an understanding of spicule formation. Future studies should provide experimental data to solve the question how biosilica, the product of the enzyme silicateins, is formed to give the spicules with their complex morphology. It can be assumed that soluble morphogens which might interact with their corresponding receptors, activate transcription factors that are involved in morphogenesis of the spicules.

Acknowledgements

We thank Dr M. Steiner (TU Berlin) for providing us with fossils and Ms E. Sehn (Zoological Institute; University of Mainz [Germany]) for the valuable technical assistance. Furthermore we are thankful to Ms U. Schloßmacher for valuable information and help to analyze spicule formation. This work was supported by grants from the European Commission (SILIBIOTEC), the Deutsche Forschungsgemeinschaft, the Bundesministerium für Bildung und Forschung Germany [project: Center of Excellence *BIOTEC*marin] and the International Human Frontier Science Program.

References

Adell, T., Grebenjuk, V.A., Wiens, M., Müller, W.E.G., 2003. Isolation and characterization of two T-box genes from sponges, the phylogenetically oldest metazoan taxon. Development, Genes & Evolution 213, 421–434.

Arndt, W., 1937. Schwämme. In: Pax, F., Arndt, W. (Eds.), Die Rohstoffe des Tierreiches. Georg Bomtraeger, Berlin, pp. 1578–2000.

Bowerbank, J.S., 1864. A Monograph of the British Spongiadae. Ray Society, London.

Brasier, M., Green, O., Shields, G., 1997. Ediacarian sponge spicule clusters from southwest Mongolia and the origins of the Cambrian fauna. Geology 25, 303–306.

Bütschli, O., 1901. Einige Beobachtungen über Kiesel- und Kalknadeln von Spongien. Zeitschrift wissenschaftliche Zoologie 64, 235–286.

Campbell, L.G., 1876. Log Letters from "The Challenger". MacMillan, London.

Camus, M., 1783. Histoire des Animaux d' Aristote. Desaint, Paris.

Cha, J.N., Shimizu, K., Zhou, Y., Christiansen, S.C., Chmelka, B.F., Stucky, G.D., Morse, D.E., 1999. Silicatein filaments and subunits from a marine sponge direct the polymerization of silica and silicones in vitro. Proceedings of the National Academy of Sciences USA 96, 361–365.

Cleverol, S., Burlet-Schiltz, O., Gairin, J.E., Monsarrat, B., 2003. Characterization of protein variants and post-translational modifications. ESI-MS analyses of intact proteins eluted from polyacrylamide gels. Molecular & Cellular Proteomics 2, 483–493.

DeLage, Y., 1892. Embryogénie des éponge. Archives De Zoologie Experimental (sér 2) 10, 345–498.

Donati, V., 1753. Auszug einer Natur-Geschichte des Adriatischen Meers. CP Franckens, Halle.

Grant, R.E., 1835. Porifera. In: Bailliere, H. (Ed.), Outlines of Comparative Anatomy. London, pp. 1–656.

Haeckel, E., 1872. Die Kalkschwämme. Georg Reimer, Berlin.

Hoffman, P.F., Kaufman, A.J., Halverson, G.P., Schrag, D.P., 1998. A neoproterozoic snowball earth. Science 281, 1342–1346.

Hooper, J.N.A., 1997. Sponge Guide. Queensland Museum.

Krasko, A., Batel, R., Schröder, H.C., Müller, I.M., Müller, W.E.G., 2000. Expression of silicatein and collagen genes in the marine sponge Suberites domuncula is controlled by silicate and myotrophin. European Journal of Biochemistry 267, 4878–4887.

Krasko, A., Schröder, H.C., Batel, R., Grebenjuk, V.A., Steffen, R., Müller, I.M., Müller, W.E.G., 2002. Iron induces proliferation and morphogenesis in primmorphs from the marine sponge Suberites domuncula. DNA & Cell Biology 21, 67–80.

Lieberkühn, N., 1856. Zur Entwicklungsgeschichte der Spongillen. Archiv für Anatomie und Physiologie, 399–414.

Lieberkühn, N., 1859. Neue Beiträge zur Anatomie der Spongien. Archiv für Anatomie und Physiologie, 515–529.

Müller, W.E.G., 2001. How was metazoan threshold crossed: the hypothetical Urmetazoa. Comparative Biochemistry Physiology [A] 129, 433–460.

Müller, W.E.G., 2005. Origin of Metazoa: sponges as living fossils. Naturwissenschaften 85, 11–25.

Müller, W.E.G., in press. Spatial and temporal expression patterns in animals. In: Meyers RA (ed.) Encyclopedia of Molecular Cell Biology and Molecular Medicine. Wiley VCH GmbH, Weinheim 13, 269–309.

Müller, W.E.G., Zahn, R.K., Maidhof, A., 1982. Spongilla gutenbergiana n.sp., ein Süßwasserschwamm aus dem Mittel-Eozän von Messel. Senckenbergiana lethaea 63, 465–472.

Müller, W.E.G., Wiens, M., Adell, T., Gamulin, V., Schröder, H.C., Müller, I.M., 2004. The Bauplan of the Urmetazoa: The basis of the genetic complexity of Metazoa using the siliceous sponges [Porifera] as living fossils. International Review of Cytology 235, 53–92.

Müller, W.E.G., Rothenberger, M., Boreiko, A., Tremel, W., Reiber, A., Schröder, H.C., 2005. Formation of siliceous spicules in the marine demosponge Suberites domuncula. Cell & Tissue Research 321, 285–297.

Perović-Ottstadt, S., Schröder, H.C., Batel, R., Giovine, M., Wiens, M., Krasko, A., Müller, I.M., Müller, W.E.G., 2005. Arginine kinase in the demosponge *Suberites domuncula*: regulation of its expression and catalytic activity by silicic acid. Journal of Experimental Biology 208, 637–646.

Pilcher, H., 2005. Back to our roots. Nature 435, 1022–1023.

Reitner, J., 1992. Coralline Spongien. Der Versuch einer phylogenetisch-taxonomischen Analyse. Berliner Geowissenschaftliche Abhandlungen (E) 1, 1–352.

Schäcke, H., Müller, I.M., Müller, W.E.G., 1994. Tyrosine kinase from the marine sponge *Geodia cydonium*: the oldest member belonging to the receptor tyrosine kinase class II family.. In: Müller, W.E.G. (Ed.), Use of Aquatic Invertebrates as Tools for Monitoring of Environmental Hazards. Gustav Fischer Verlag, Stuttgart, New York, pp. 201–211.

Schröder, H.C., Krasko, A., Le Pennec, G., Adell, T., Hassanein, H., Müller, I.M., Müller, W.E.G., 2003. Silicase, an enzyme which degrades biogenous amorphous silica: contribution to the metabolism of silica deposition in the demosponge Suberites domuncula. Progress in Molecular and Subcellular Biology 33, 249–268.

Schröder, H.C., Perović-Ottstadt, S., Rothenberger, M., Wiens, M., Schwertner, H., Batel, R., Korzhev, M., Müller, I.M., Müller, W.E.G., 2004a. Silica transport in the demosponge Suberites domuncula: fluorescence emission analysis using the PDMPO probe and cloning of a potential transporter. Biochemical Journal 381, 665–673.

Schröder, H.C., Perović-Ottstadt, S., Wiens, M., Batel, R., Müller, I.M., Müller, W.E.G., 2004b. Differentiation capacity of the epithelial cells in the sponge Suberites domuncula. Cell & Tissue Research 316, 271–280.

Schulze, F.E., 1887. In: Murray, J. (Ed.), Report on the hexactinellida Report on the Scientific Results of the Voyage of the HMS Challenger During the years 1873–1876, vol. 21. Majesty's Stationary Office, London, p. 513.

Schulze, F.E., 1904. Hexactinellida. In: Chun, C. (Ed.), Wissenschaftliche Ergebnisse der Deutschen Tiefsee-Expedition auf dem Dampfer "Valdivia" 1898-1899. Gustav Fischer, Jena.

Shimizu, K., Cha, J., Stucky, G.D., Morse, D.E., 1998. Silicatein alpha: cathepsin L-like protein in sponge biosilica. Proceedings of the National Academy of Sciences of the USA 95, 6234–6238.

Sollas, W.J., 1888. Report on the Tetractinellida. Schulze FE (1887) Report on the Hexactinellida. In: Murray, J. (Ed.), Report on the Scientific Results of the Voyage of the HMS Challenger During the Years 1873–1876, vol. 25. Majesty's Stationary Office, London, p. 458.

Spix, J., 1811. Geschichte und Beurtheilung aller Systeme in der Zoologie. Schrag'sche Buchhandlung, Nürnberg.

Steiner, M., Mehl, D., Reitner, J., Erdtmann, B.D., 1993. Oldest entirely preserved sponges and other fossils from the Lowermost Cambrian and a new facies reconstruction of the Yangtze Platform (China). Berliner Geowissenschaftliche Abhandlungen (E) 9, 293–329.

Uriz, M.J., Turon, X., Becerro, M.A., 2000. Silica deposition in Demospongiae: spiculogenesis in Crambe crambe. Cell & Tissue Research 301, 299–309.

Walker, G., 2003. Snowball Earth. Bloomsbury, London.

Weaver, J.C., Morse, D.E., 2003. Molecular biology of demosponge axial filaments and their role in biosilicification. Microscopy Research Techniques 62, 256–367.

Weismann, A., 1892. Das Keimplasma: Eine Theorie der Vererbung. Fischer, Jena.

Weissenfels, N., 1989. Biologie und Mikroskopische Anatomie der Süßwasserschwämme (Spongillidae). Gustav Fischer Verlag, Stuttgart.

Wilson, H.V., 1907. On some phenomena of coalescence and regeneration in sponges. Journal of Experimental Zoology 5, 245–258.

Wilt, F.H., 2005. Developmental biology meets materials science: morphogenesis of biomineralized structures. Developmental Biology 280, 15–25.

A new stepwise synthesis of a family of propylamines derived from diatom silaffins and their activity in silicification†

Vadim V. Annenkov,*[ab] Siddharth V. Patwardhan,[b] David Belton,[b] Elena N. Danilovtseva[a] and Carole C. Perry*[b]

Received (in Cambridge, UK) 10th November 2005, Accepted 9th February 2006
First published as an Advance Article on the web 24th February 2006
DOI: 10.1039/b515967a

A new method for the stepwise synthesis of propylamines containing fragments of *N*-methyl propylamine as found in diatom bioextracts is presented and their activity in silicic acid condensation is described.

Saturated speciality polyamines play important roles in various biological processes and have attracted the attention of synthetic chemists. A widely known naturally occurring polyamine is spermine (*N*,*N*′-bis(3-aminopropyl)-1,4-butanediamine), which had been isolated from sperm.[1] 3,3′-Methyliminobis(*N*-methylpropylamine) (N3; Scheme 3) has been studied as a neurotoxic agent[2,3] and as an inhibitor of ribonuclease activity.[4] In the last decade, polyamines isolated from siliceous cell walls of diatoms have been investigated by biologists, biochemists and materials scientists.

Diatom biosilica polyamines have been found in the free state and as a part of complex proteins called silaffins in diatom biosilica.[5] Silaffins and polyamines are proposed to play a significant role in diatom biosilicification producing diverse nano-structured silica valves.[5] Diatom polyamines include repeated *N*-methylpropylamine (PA) fragments terminated with methylated or non-methylated nitrogen (Scheme 1). The propylamines have been shown to promote silica formation *in vitro* in a tetramethoxysilane (TMOS) based system, although the only experimental information available ascribed to a catalytic effect is obtained from how much precipitable silica is generated during a fixed time period.[5] The interest in such compounds is apparent from their potential in the biomimetic design of nano-structured materials *via* "green chemistry" approaches.

In this communication, we present the successful synthesis of a series of linear methylated propylamines that are analogous to the polyamine structural moieties isolated from several diatom species. The objective of this work is to establish a convenient universal method for propylamine synthesis capable of extending the *N*-methylpropylamine chain in a linear fashion. Furthermore, the activity of these PAs in silica formation *in vitro* is investigated. To our knowledge, this is the first investigation on the role of a series of synthetic methylated propylamines in silicification.

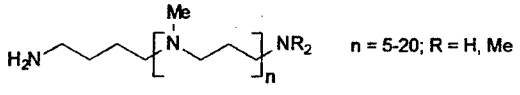

Scheme 1 Structure of polyamines isolated from diatoms.

N3 (Scheme 3) is the longest synthetic methylated propylamine to have been synthesised previously. It can be prepared by the reaction of methylamine with 3-(*N*-methylamino)propionitrile in the presence of hydrogen and a hydrogenation catalyst.[6] However, this reaction gives rise to a mixture of amines that needs to be separated to yield N3 and does not allow the controlled synthesis of long-chain polyamines. Other non-methylated polyamines containing four and six nitrogen atoms have been obtained by reaction of trimethylene dibromide with trimethylendiamine or dipropylenetriamine.[7,8] The reaction is complicated and a mixture of polymeric and branched products are synthesised requiring complicated separations. As the amine chain is increased, the likelihood of branching also increases as the relative concentration of end amino-groups decreases. Moreover, in the case of long-chain amines it will be practically impossible to separate a target linear product from polymeric and branched admixtures.

The proposed approach to target polyamines consists of repetitions of the following reactions: (1) condensation of NH-amine with methyl acrylate, (2) substitution of the resulting ester with methylamine and (3) reduction of the amide with lithium

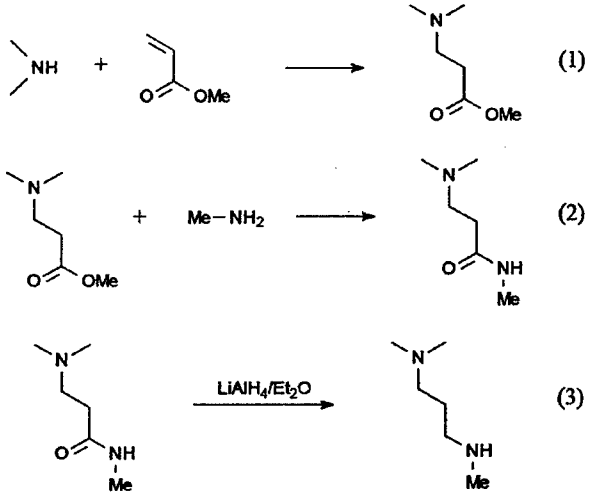

Scheme 2 The consecutive stages of the polyamines synthesis.

[a]*Limnological Institute of Siberian Branch of Russian Academy of Sciences, 3, Ulan-Batorskaya St., P.O. Box 4199, Irkutsk, 664033, Russia. E-mail: annenkov@lin.irk.ru.; Fax: 3952 425405; Tel: 3952 428422*
[b]*School of Biomedical & Natural Sciences, Nottingham Trent University, Clifton Lane, Nottingham, UK NG11 8NS. E-mail: Carole.Perry@ntu.ac.uk.; Fax: 0115 848 6636; Tel: 0115 848 6695*

† Electronic supplementary information (ESI) available: detailed synthetic methods, NMR, MS and FTIR characterisation results and SEM of silica samples obtained in the presence of N7. See DOI: 10.1039/b515967a

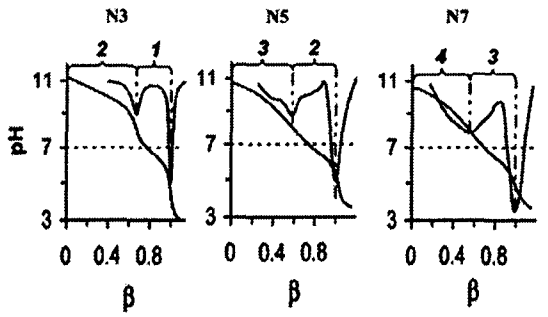

Fig. 3 Potentiometry titration curves for new propylamines (β = neutralization degree).

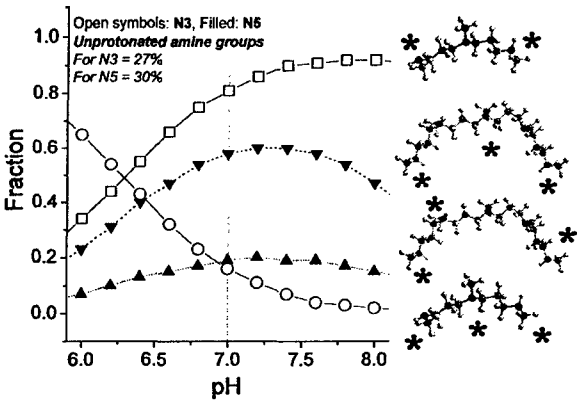

Fig. 4 Estimated speciation of N3 and N5 (only species present at significant fractions are shown). Models of propylamines are shown on the right of each curve. Charged nitrogen atoms are marked with asterisks.

(Fig. 4). For example, Fig. 4 also shows the estimated speciation of N3 and N5 and respective molecular models. It appears that the rapid formation of dense silicas in the presence of PA arises from the fact that PAs are partially protonated at neutral pH with labile protons, thus enabling PAs to act as Brønsted acids, similar to the proposed activity for ethylamines.[13] Future work is being undertaken in order to investigate in more details the role(s) of propylamines of a variety of architectures in silica formation and the data will be presented in due course. It is also possible to synthesise polyamines with an even number of nitrogen atoms from *N,N'*-dimethyl-1,3-propanediamine which is commercially available or can be obtained using a 1 : 1 ratio of reagents as in reaction (1). Sequential realisation of reactions (1)–(3) with various amines and acrylates opens up the way to a wide range of polyamines that will be evaluated in due course.

This work was supported by Presidium of the Russian Academy of Sciences (project # 10.3), The Royal Society short visit grant (for VVA), AFOSR and EU.

Notes and references

‡ Synthetic procedures are described briefly below, see ESI† for details on the synthetic procedures and characterisation of PAs. Condensation of NH-amines with methyl acrylate [reaction (1)] was carried out in ethanol solution (15% of the corresponding amine) at 1 : 2.1 amine : acrylate ratio. In the case of methylamine the reaction mixtures stayed at r.t. for 6 days and for N3 and N5 amines were boiled for 6–10 hours. Reaction (2) was also performed in ethanol using a 50% excess of methylamine under ester groups, at r.t. during 3–5 days. The completions of reactions (1) and (2) were checked by FTIR spectroscopy by disappearance of NH band (3300 cm^{-1}) and ester C=O band (1740 cm^{-1}) respectively.

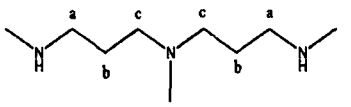

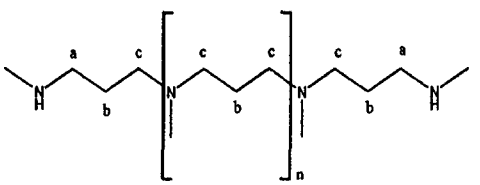

Yield of the target compounds was near 100%. Reduction of the amides [reaction (3)] was done by dropwise addition of the amide to $LiAlH_4$ suspension in diethyl ether (2.1 moles of $LiAlH_4$ per amide group) with 50–70% yield. The non-quantitative yield at this stage is connected with association of the resulting amine with lithium and aluminium hydroxides. One would hope that the yield would be enhanced in future optimization of the procedure. The obtained polyamines are colourless liquids, b.p.: 65 °C, 142 °C and 185 °C at 0.2 mm Hg for N3, N5 and N7 respectively. FTIR (film, cm^{-1}): 3292–3296, 2939–2945, 2788, 2839, 1450–1465, 1373, 1315, 1150, 1122, 1068, 733–740. N3: ^{1}HMR, 5% in $CDCl_3$. 1.63 ppm (5^t, 4H, 2 × CH_2 (b)), 2.15 (1^t, 3H (NMe)), 2.35 (3^t, 4H, 2 × CH_2 (c)), 2.40 (1^t, 6H, $NHCH_3$), 2.58 (3^t, 4H, (a)). ESI-MS +ve ion. 174.3 ([M + H]$^+$). N5 (n = 2): ^{1}HMR, 5% in $CDCl_3$. 1.62 ppm (m^t, 8H (b)), 2.14 (1^t, 9H (NMe)), 2.28–2.35 (m^t, 12H (c)), 2.40 (1^t, 6H (NHMe)), 2.58 (m^t, 4H (a)). ESI-MS +ve ion. 316.4 ([M + H]$^+$), 245.4 ([M + H]$^+$ − C_3H_5NHMe), 174.3 ([M + H]$^+$ − $C_3H_5N(Me)C_3H_6NHMe$).

N7 (n = 4): ^{1}H-NMR, 5% in $CDCl_3$. 1.65 ppm (m^t, 12H (b)), 2.20 (1^t, 15H (NMe)), 2.30–2.40 (m^t, 20H (c)), 2.42 (1^t, 6H (NHMe)), 2.62 (3^t, 4H (a)).

ESI-MS +ve ion. 458.5 ([M + H]$^+$), 387.5 ([M + H]$^+$ − C_3H_5NHMe), 316.3 ([M + H]$^+$ − $C_3H_5NMeC_3H_6NHMe$).

1 S. S. Cohen, *A guide to the polyamines*, Oxford University Press, New York, 1998.
2 D. F. Brown, J. P. McGuirk, S. P. Larsen and S. D. Minter, *Physiol. Behav.*, 1991, **49**, 41.
3 S. Levine, R. Sowinski and D. Nochlin, *Brain Res.*, 1982, **242**, 219.
4 T. P. Karpetsky, K. K. Shriver and C. C. Levy, *Biochem. J.*, 1981, **193**, 325.
5 M. Sumper and N. Kroger, *J. Mater. Chem.*, 2004, **14**, 2059–2065.
6 J. A. Marsella and W. E. Starner, *J. Polym. Sci., Part A: Polym. Chem.*, 2000, **38**, 921.
7 G. S. Whitby, N. Wellman, V. W. Floutz and H. L. Stephens, *Ind. Eng. Chem.*, 1950, **42**, 452.
8 F. Noll, M. Sumper and N. Hampp, *Nano Lett.*, 2002, **2**, 91–95.
9 T. Mizutani, H. Nagase, N. Fujiwara and H. Ogoshi, *Bull. Chem. Soc. Jpn.*, 1998, **71**, 2017–2022.
10 L. Sudheendra and A. R. Raju, *Mater. Res. Bull.*, 2002, **37**, 151.
11 T. Coradin, O. Durupthy and J. Livage, *Langmuir*, 2002, **18**, 2331–2336.
12 D. Belton, G. Paine, S. V. Patwardhan and C. C. Perry, *J. Mater. Chem.*, 2004, **14**, 2231–2241.
13 D. Belton, S. V. Patwardhan and C. C. Perry, *J. Mater. Chem.*, 2005, **15**, 4629–4638.
14 D. Belton, S. V. Patwardhan and C. C. Perry, *Chem. Commun.*, 2005, 3475–3477.
15 K. M. Roth, Y. Zhou, W. Yang and D. E. Morse, *J. Am. Chem. Soc.*, 2005, **127**, 325–330.
16 S. V. Patwardhan, S. J. Clarson and C. C. Perry, *Chem. Commun.*, 2005, **9**, 1113–1121.
17 D. Belton, S. V. Patwardhan and C. C. Perry, unpublished data.
18 S. W. Karickhoff and L. A. Carreira, *SPARC On-Line Calculator*, 2005.

Supplementary Material for Chemical Communications

Supplementary Information

A New Stepwise Synthesis of a Family of Propylamines Derived from Diatom Silaffins and their Activity in Silicification

Vadim V. Annenkov, [a,b]* *Siddharth V. Patwardhan,* [b] *David Belton,* [b] *Elena N. Danilovtseva* [a] *and Carole C. Perry* [b]*

Synthetic Procedures

N-Methyl-N,N-bis[3-(methylamino)propyl]amine [tri(1-methylazetane)], N3

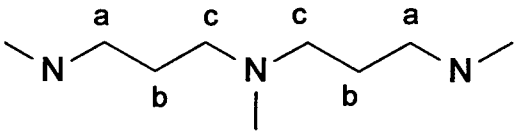

Methylamine (33%) in ethanol (94 g, 1 mole) was diluted with ethanol (40 mL) and methyl acrylate (172 g, 2 mole) diluted with ethanol (145 mL) was added to the methylamine solution in portions (~50 mL) at 20-40 °C. The mixture was left at room temperature for 5-7 days and the progress of the reaction monitored by FTIR spectroscopy. When the reaction was complete (disappearance of NH band (3300 cm^{-1}, thin film method)), ethanol was distilled off under reduced pressure and the residue distilled under vacuum (90 °C, 0.2 mm Hg) to give di-β-carbethoxyethylmethylamine (191g, 94%) as a colourless liquid.

Di-β-carbethoxyethylmethylamine (180g, 0.89 mole) was added to methylamine in ethanol (33%), (250 g, 2.66 mole) and the mixture left at room temperature for 3-5 days. The progress of the reaction was monitored by FTIR as before. When the reaction was complete, (disappearance of the ester C=O band (1740 cm^{-1}, thin film method)), ethanol was distilled off under reduced pressure and the residue dried under vacuum (70 °C, 0.2 mm Hg, 2 h) to give *N*-methyl-3-methyl[3-(methylamino)-3-oxopropyl]aminopropanamide (178g, 99%) as a viscous colourless liquid.

$LiAlH_4$ (16g, 0.42 mole) was suspended in anhydrous diethyl ether (550 mL) at room temperature. *N*-Methyl-3-methyl[3-(methylamino)-3-oxopropyl]aminopropanamide (20.1 g, 0.1 mole) was added to the suspension of $LiAlH_4$ portionwise during 6 h. The mixture was stirred for 12 h, cooled (–5 °C) and decomposed at 0-10 °C by the sequential addition of water (30 mL), a solution of KOH (22.5 g) in water (22.5 mL) followed by water alone (70 mL). The ether fraction was separated and the precipitate washed with diethyl ether (2 x 100 mL). Ether was distilled off and the residue distilled under vacuum (65 °C, 0.2 mm Hg) to give **N3** (8.5 g, 49%) as a colourless liquid. FTIR (film, cm^{-1}): 3292-3296, 2939-2945, 2788, 2839, 1450-1465, 1373, 1315, 1150, 1122, 1068, 733-740. ^1H NMR, (5% in $CDCl_3$): 1.63ppm (5^t, 4H, 2xCH_2 (b)), 2.15 (1^t, 3H (NMe)), 2.35 (3^t, 4H, 2xCH_2 (c)), 2.40 (1^t, 6H, $NHCH_3$), 2.58 (3^t, 4H, (a)). ESI-MS +ve ion. 174.3 ($[M+H]^+$).

N-Methyl-*N*-[3-(methylamino)propyl]-*N*-3-[methyl(3-methyl[3-(methylamino) propyl]aminopropyl) amino]propylamine [penta(1-methylazetane)], N5

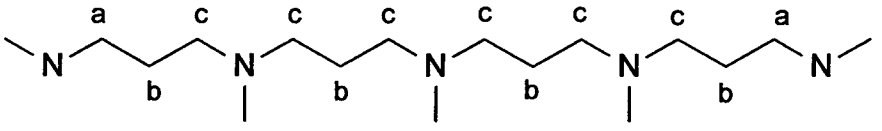

$LiAlH_4$ (2.5 g, 0.066 mole) was suspended in anhydrous diethyl ether (200 mL) at room temperature. N^1,N^{23},4,8,12,16,20-Heptamethyl-4,8,12,16,20-pentaazatricosane-1,23-diamide (12g, 0.025 mole) was added to the suspension of $LiAlH_4$ in small portions (0.1-0.3 g) during 6 h. The mixture was stirred for 12 h, cooled down to –5 °C and decomposed at 0-10 °C by the sequential addition of water (4.6 mL), a solution of KOH (5.5 g) in water (5.5 mL) followed by water alone (11 mL) The ether fraction was separated and the precipitate washed with diethyl ether (2 x 50 mL). Ether was distilled off and the residue distilled under vacuum (185 °C, 0.2 mm Hg) to give **N7** (7.9 g, 69%) as a colourless liquid. FTIR (film, cm^{-1}): 3292-3296, 2939-2945, 2788, 2839, 1450-1465, 1373, 1315, 1150, 1122, 1068, 733-740. ^1H NMR, 5% in $CDCl_3$. 1.65ppm (m^t, 12H (b)), 2.20 (1^t, 15H (NMe)), 2.30-2.40 (m^t, 20H (c)), 2.42 (1^t, 6H (NHMe)), 2.62 (3^t, 4H (a)). ESI-MS +ve ion. 458.5 ($[M+H]^+$), 387.5 ($[M+H]^+$ - C_3H_5NHMe), 316.3 ($[M+H]^+$ - $C_3H_5NMeC_3H_6NHMe$).

SEM Silica prepared in the presence of N7 at a 1Si:1N ratio.

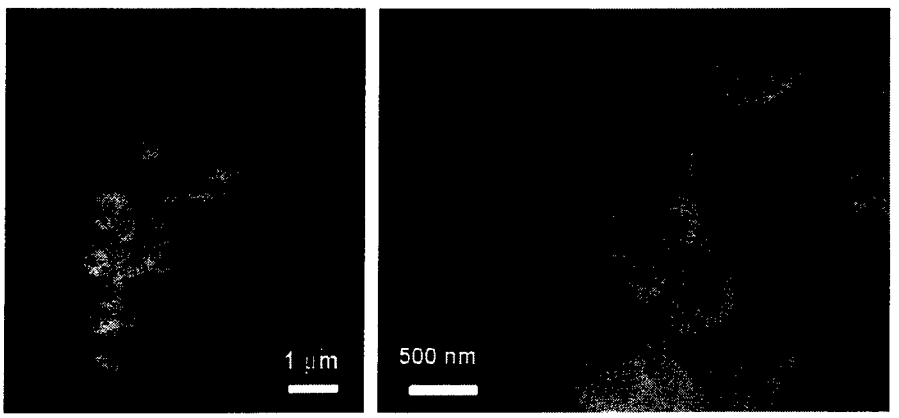

The effects of diamines and small chain polyamines on the condensation and precipitation of silica

David Belton, Carole C Perry, Siddharth Patwardhan

Interdisciplinary Biomedical Research Centre,
School of Biomedical and Natural Sciences,
Nottingham Trent University, Clifton Lane,
Nottingham, UK NG11 8NS

Introduction.

Proteins found intimately associated with diatom frustrule silica, (silaffins), are relatively enriched with lysine residues which are modified by the attachment of long chain polypropylenimines to the side chain. Similar polypropylenimines terminated by a putrescine group are also found in isolation. The cellular occurrence of polyamines is common throughout the natural world with chain separation between amine groups of usually 3 to 4 carbon atoms. That these biosilica polyamines are extensions of the putrescine, spermidine, spermine biosynthetic route suggests that their role in biosilicification may be an adventitious one. A range of diamines with increasing carbon chain separations and ethylenimines of increasing length were therefore chosen to study the possible role of interamine spacings and number of repeat amine groups in the condensation of silica from monosilicic acid using a model system which uses dipotassiumsilicon tris catecholate as the primary source of monosilicic acid.

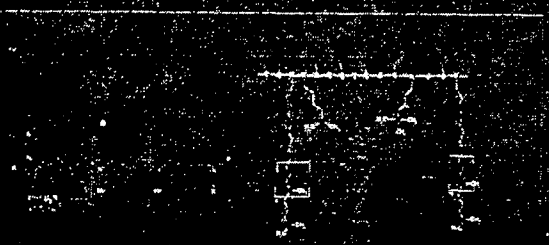

Polyamine species found associated with the silica of diatoms.

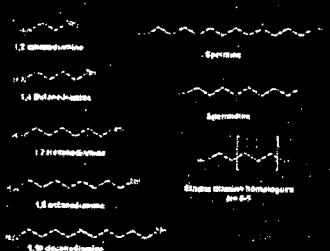

Amine species used in this study.

The simple chemical structure of silica or hydrated silica belies the complexity of their chemistries and it is this complexity which enables and determines the suitability of the material for the myriad applications to which they are employed. These functions ultimately depend on the surface chemistry, molecular structure, morphology and porosities of the silicas. Manufacturing methods require harsh conditions of temperature and pH and also involve the use and production of environmentally damaging precursors and waste streams. By comparison biologically controlled silica production occurs under benign conditions and results in materials of superior form and function starting from a source of soluble silica, monosilicic acid, at concentrations of only a few tens of parts per million.

Monosilicic acid condensation.

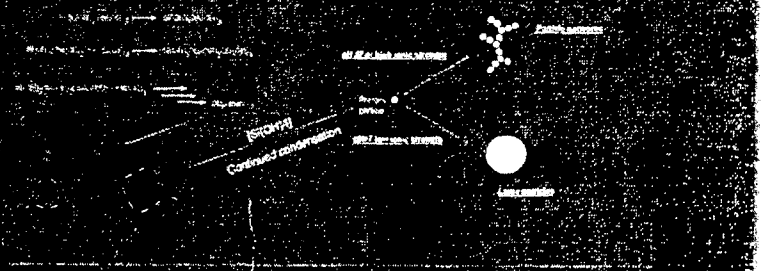

The condensation of 30 mM solutions of monosilicic acid in the presence of equimolar amounts of amine at pH 7.0 was monitored by the molybdenum blue spectrometric method. Particle growth/aggregation was followed by photo correlation spectrometry and the nature of the washed sedimentable silica from the systems was investigated by nitrogen gas adsorption/desorption analysis and scanning electron microscopy.

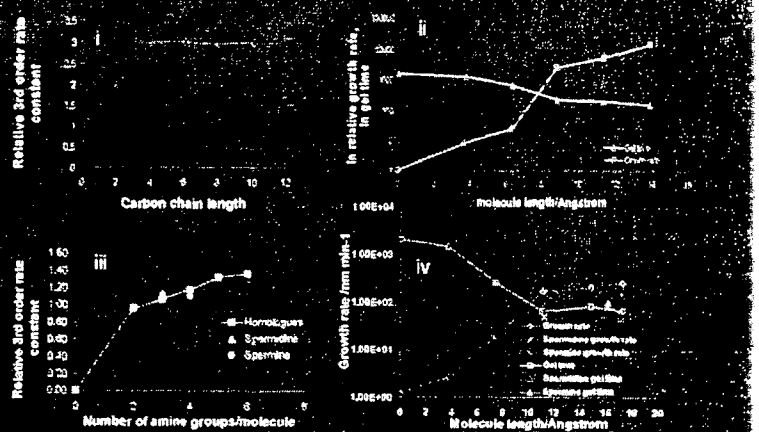

Addition of diamines.

Figure a) – Situation in the blank condensing system. Solvation sphere around silicic acid monomers acts as barrier to condensation. b) - Addition of short chain diamines introduces hydrophobic domains in to the system – localised restructuring of water molecules results in an increase in entropy and modifies water bulk properties reducing solvation barrier and increasing condensation rate (fig c). Increasing the chain length of the diamines causes further entropic change

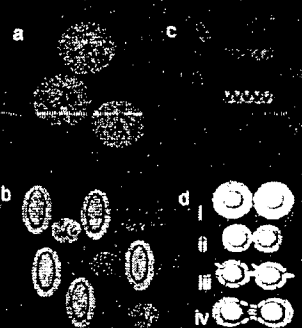

which is minimised by the formation of aggregates or small micelles so condensation rates do not necessarily continue to increase (fig 1 carbon chain > 4). d(i) Electrical double layer barrier to primary particle aggregation (ii) Reduction of barrier by charge neutralization with shorter diamines causing more rapid aggregation (iii) Bridging of double layer by diamines of a critical length (6- 10Å) resulting in aggregation rate step change in fig a (iv) coacervation through increasingly hydrophobic nature of diamines results in continued aggregation as carbon chain length increases.

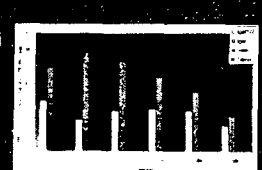

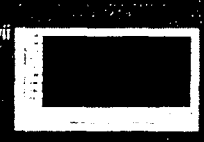

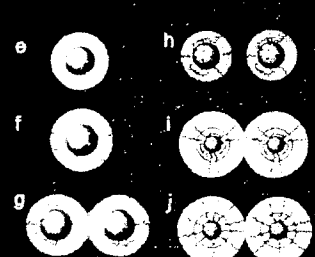

Addition of ethylenimines.

Figure e) – Primary particle showing electrical double layer. f) reduction in double layer thickness by addition of short ethylenimines. g) and h) bridging of double layer by longer ethylenimines (fig iv). The formation of much larger particles with no apparent mesoporosity even after heat treatment to remove any entrained organic material observed on the addition of pentaethylenehexamine (PEHA ((n=4)), suggested that primary particles were not being formed and aggregated as usually observed for this model system. Additional experiments using varying levels of PEHA showed a physical change in the nature of the isolable silica at amine:silicon ratios of 1.2 or greater. This was observed as precipitation of larger particles showing little or no mesoporosity. Measurements of isolable silica (through centrifugation at 3000rpm) also showed a decrease with increasing levels of PEHA (fig vii).

MC7, Edinburgh, July 2005

The role of hydroxyl containing additives in bioinspired silicification

Graham Tilbury[a], David Belton[a], Siddharth Patwardhan[a], David Kaplan[b] and Carole C. Perry[a]*
E-mail: Carole.Perry@ntu.ac.uk
[a] Interdisciplinary Biomedical Research Centre, The Nottingham Trent University, Clifton, Nottingham, NG11 8NS.
[b] Biomedical Engineering department, Tufts University, Medford, MA02155.

Introduction

- Silica is an industrially important material with many applications, and an estimated global market worth around two billion dollars per year[1].
- Most industrial processes to produce silica involve high temperature and extreme pH conditions often in non-aqueous based system.
- Biosilicification occurs at circumneutral pH and hierarchically organised ornate biogenic silica structures are generated under mild conditions of pH and temperature. The silica structures are formed from an aqueous environment, probably rich in ions, small molecules and biopolymers such as proteins and carbohydrates.

Hydroxyl containing additives

- Hecky *et al.*[2] postulated that hydroxyl-rich proteins (sugars and glycoproteins) associated with diatom cell walls might condense with silicic acid monomers (leading to the formation of Si-O-C bonds), thus serving as templates for orientation and growth of the silica.
- The effect of Polyethylene glycol[3] and polyserine[4] have been studied previously and produced silicas with smooth surface morphology.
- Silicatein from sponges has been shown to have OH rich clusters containing threonine and serine clusters[5].
- Perry *et al.* studied an insoluble cellulose and a soluble hemicellulose, forming sheet like structures[6].
- Previous work on alkyldiamines has shown very interesting results, where increasing hydrophobicity controlled aggregation rates, this work investigates the role of hydroxyl functionality on silicification[8].
- In this study three different types of hydroxyl containing additives have been studied;

– Alkyldiols

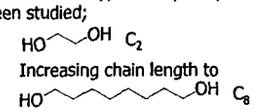

– Sericin
- Native sericin - extracted from spider silk
- Sericin precursor

[SSTGSSSNTDSNSNSVGSSTSGGSSTYGYSSNSRDGSV]n

– Hydroxyethyl-celluloses

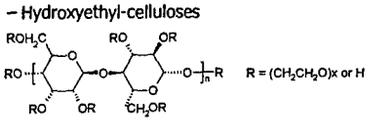

– Hydroxyethylcellulose ethoxylate, quaternised

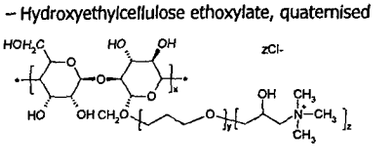

The aqueous silica precipitating model system

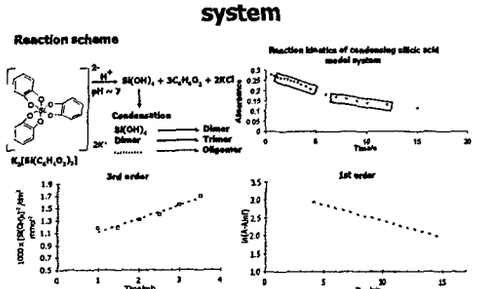

The third order rate constant describes the rate of trimerisation, which is essentially an irreversible reaction.

The first order rate constant describes the rate of oligomerisation, however this is reversible and therefore also describes the rate of dissolution (k_+ and k_- respectively[7].

References
1. Kendall, T. *Industrial Minerals* **2000**, *March*, 49-59.
2. Hecky *et al. Mar. Biol.* **1973**, *19*, 323-331.
3. Sun *et al.* W. W. C. *J. Phys. Chem. B.* **2002**, *106*, 11539-11548.
4. Patwardhan, S. V. Ph.D. Dissertation, University of Cincinnati, **2003**.
5. Cha *et al. PNAS* **1999**, *96* 361-365.
6. Perry *et al. J. Chem. Soc Faraday Trans.* **1992**, 88 2917-2921.

Kinetic analysis

- Alkyldiols

- The alkyldiols were added to the model system at a ratio of 1:1 and 1:2 Si:OH and denoted 100% and 200% respectively.

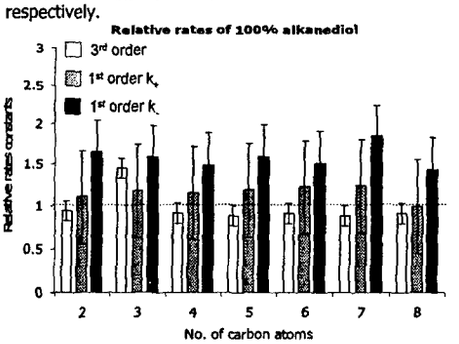

- An increase in the 1st order reverse rate suggests stabilisation of silicic acid. This was seen as a 15.6% increase in the final silicic acid concentration (24 hours).
- Suggesting preferential hydrogen bonding of silicic acid with the alkyldiol over water and other silicic acid molecules.
- Increasing the ratio of alkyldiol to silicon ratio resulted in no further increase in the reverse 1st order k_- rate.
- The effect of the alkyldiol was examined as a solvent, where the initial silicic acid concentration was stabilised for approximately 10 minutes.

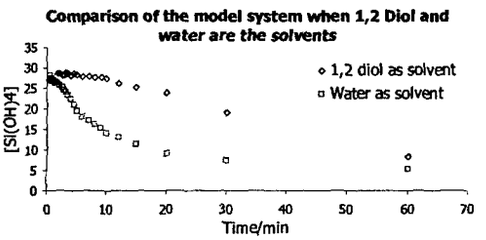

- Sericin

- Native sericin and the sericin precursor were added at 1, 5 and 10% weight of precipitatable silica.

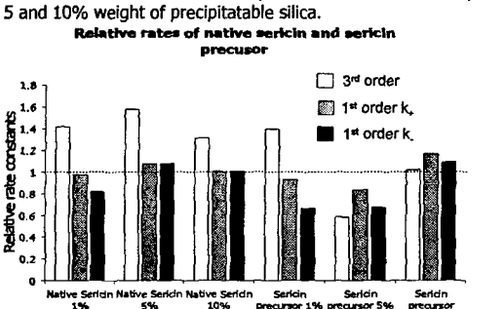

- Celluloses

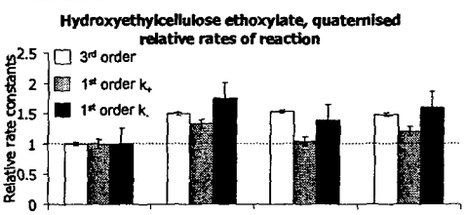

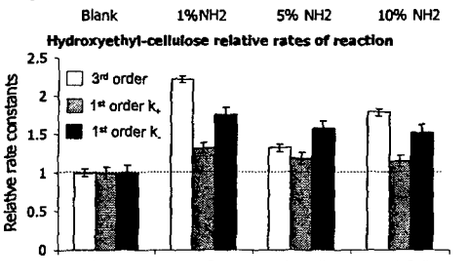

- Increases in rate constants are not very significantly, but

Photon correlation spectroscopy

- Neither the alkyldiols, native sericin, or the sericin precursor significantly affected aggregation. This is probably due to the lack of charged species at pH 6.8

- Celluloses

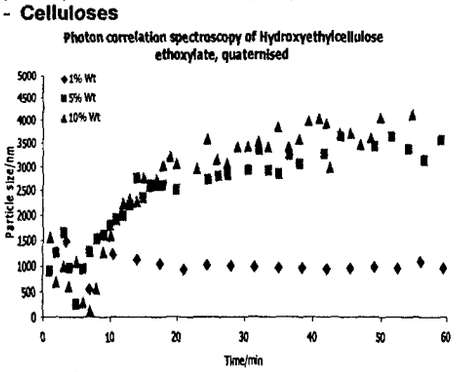

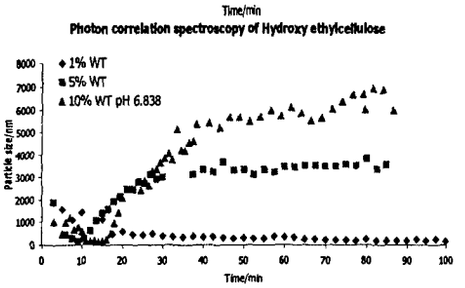

- Dramatic increases in aggregation rates are observed with both hydroxyethylcellulose ethoxylate, quaternised ad hydroxy ethylcellulose. As expected hydroxyethylcellulose ethoxylate aggregates faster than hydroxy ethylcellulose.
- Note: the blank condensing system shows no particles during the time it take for the celluloses to precipitate silica.

Materials characterisation

Scanning electron microscopy

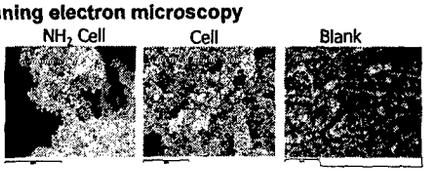

- Fused interconnected silica spheres are produced after 24 hours using the celluloses.

Nitrogen adsorption

- The silica produced from all experiments produce type IV H2 isotherms, with sericin and the alkyldiols showing similar surface areas.

Sample	Surface Area m^2g^{-1}	Pore volume/cm^3g^{-1}	Average pore radius/ Å
Blank	609	0.63	23.9
1% native sericin precursor	523	0.98	32.3
5% native sericin precursor	445	1.31	48.8
1,2 ethanediol 100%	521	0.92	21.26
1,8 octanediol 100%	548	0.82	30.69
1,2 ethanediol 200%	492	0.57	22.61
1,8 octanediol 200%	441	0.36	18.49

Conclusions

- Simple hydroxyl containing molecules have been studied and at Si:OH ratios of 1:1 and 2:1. The effect on silica formation and morphology is negligible.
- More complex molecules containing largely hydroxyl functionality also showed negligible affect on silica formation and morphology.
- In direct contrast hydroxyethyl-cellulose and Hydroxyethylcellulose ethoxylate, quaternised, drastically affect aggregation and the structure of the silica produced.
- The function of hydroxyl containing additives is still not

Euromat Junior 2004

Model studies of biosilicification showing controlled structure and form

Graham Tilburey, David Belton, Emma Futcher and Carole C. Perry*
E-mail: Carole.Perry@ntu.ac.uk
Interdisciplinary Biomedical Research Centre, The Nottingham Trent University, Clifton, NG11 8NS.

Introduction

Biosilicification has principally been studied for three different biological systems, diatoms, sponges and higher plants[1]. The main focus of this project is to investigate principles involved in the formation of biosilicas and apply them to the synthesis of bioinspired silicas with control of structure and morphology. Two areas of the project are discussed below;

- The effect of bioextracts on *in vitro* silica formation.
- The behaviour of bio-analogous molecules (alkyldiamines) in silicifying and aqueous based media.

Investigating the effect of bioextracts on silicification

Biosilicification in higher plants namely *Equisetum telmateia* and *E. arvense* has principally been investigated by our research group at Nottingham Trent University. Three chemically distinct protein containing bioextracts have been obtained from *Equisetum Arvense*.

Extraction procedures

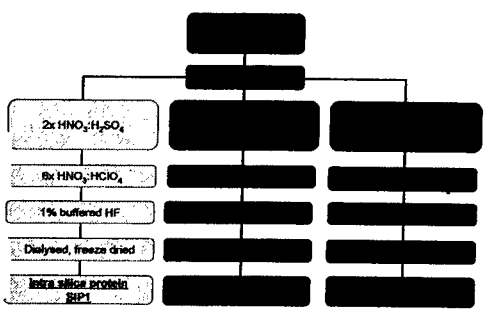

The aqueous silica precipitating model system

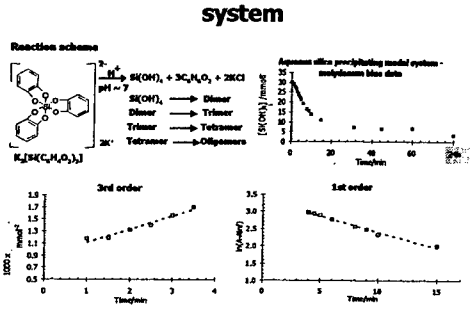

- The third order rate constant describes the rate of trimerisation, which is essentially an irreversible reaction.
- The first order rate constant describes the rate of oligomerisation, however this is reversible and therefore also describes the rate of dissolution (k+ and k- respectively)[2].

Results

The bioextracts were inserted into the model system at 1% weight of precipitated silica (0.2mg into 10ml 30mM $K_2[Si(C_6H_4O_2)_3]$.

Kinetic data

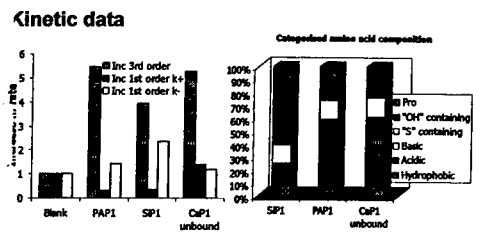

- The results show an approximate 6, 5 and 4 fold increase in the 3rd order rate constant for PAP1, CaP1 unbound and SiP1 respectively.
- The 3rd order rate constant of SiP1 is similar to previous work[3]

Photon correlation spectroscopy

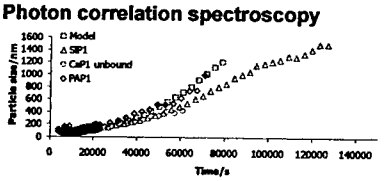

There was no significant change in rate of particle aggregation in the presence of the bioextracts.

Nitrogen gas adsorption

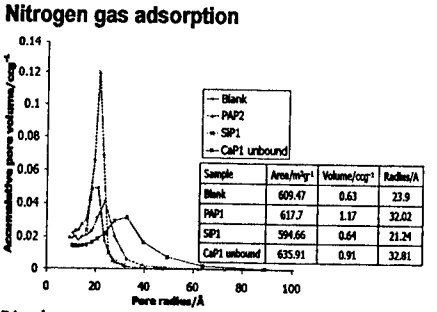

Sample	Area/m²g⁻¹	Volume/ccg⁻¹	Radius/A
Blank	609.47	0.63	23.9
PAP1	617.7	1.17	32.02
SiP1	594.66	0.64	21.24
CaP1 unbound	635.91	0.91	32.81

- SiP1 shows a narrow pore size distribution, but no significant difference in pore volume. This is comparable to previous work[3].
- PAP1 shows an approximate doubling in pore volume and a wide pore size distribution.
- CaP1 unbound and SiP1 both show an increase in pore volume and pore radius.

The bioextracts showed dramatic increases on the rate of formation of small (trimers) oligomers and this effect is continued through to the solid state materials formed.

Investigating the effect of small chain diamines on silicification

Silaffin-1A is a protein isolated from a species of diatom called *C. fusiformis*. The lysine residues within its structure are post-translationally modified by long chain polyamines and it was suggested that these were essential for silica precipitation[4]. In order to understand the effects of amines on silica formation and structure, we investigated the effect of alkyldiamines of increasing chain length in a silica and aqueous medium in the presence of salts and small organic molecules.

Results

Photon correlation spectroscopy

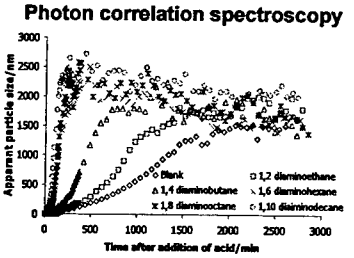

The alkyldiamines show increasing aggregation rates with increasing chain length up to *ca.* 15000 times. Increases in aggregation rate are probably due to surface charge neutralisation of the negatively charged silica by cationic diamines[5].

Scanning electron microscopy

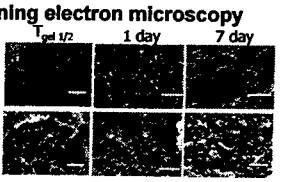

Electron microscopy showed an increase in order during maturation in the presence of the diamines. Increasing the chain length produced more open structures, probably due to the rate of aggregation increasing, however the structures became more ordered during the Ostwald ripening phase[5].

Investigating the structure of alkyldiamines in solution

Photon correlation spectroscopy was used to investigate the structure of alkyldiamines in an aqueous medium and in the presence of the "spectator ions"(KCl and catechol) generated in the model system.

The effect of chain length on aggregate size in aqueous medium at *ca.* pH 7.

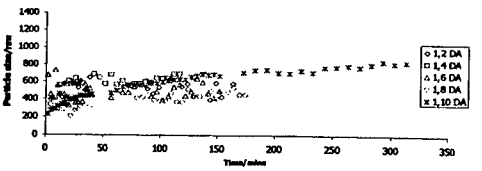

- 1,2 -1,8 diamine form aggregates in solution almost immediately.
- 1,10 diamine shows a continuous growth of aggregate size to *ca.* 800nm.

The effect of chain length on aggregate size in the presence of KCl and catechol at *ca.* pH 7

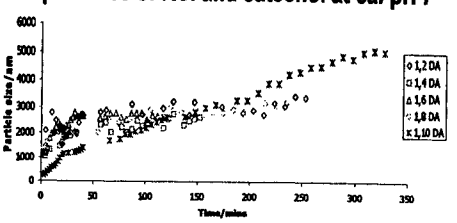

- The formation of aggregates of approximately 2500nm can be seen for 1,2 - 1,8 Diamines in the presence of Catechol and KCl.
- 1,10 diamine forms much larger aggregates of approximately 5000nm, suggesting a different type of species being formed.

The effect of chain length on aggregate size in the presence of KCl and catechol at *ca.* pH 7

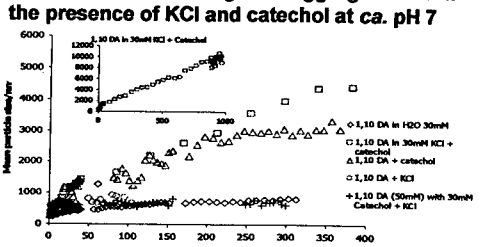

- 1,10 diamine shows a aggregate size of approximately 800nm in H_2O. The addition of KCl does not seem to significantly alter the particle size.
- 1,10 diamine in catechol shows an increasing aggregate size. Upon addition of KCl to the aggregate size increases.
- Increasing the concentration of 1,10 diamine to 50mM causes the aggregate structure to collapse. This suggests competition in solution between two structures, the first gradually forming between the diamine, catechol and KCl and the second when the diamine structure dominates.

Aqueous solutions of diamines form aggregates which may be species specific. The addition of KCl and catechol causes larger aggregates to form.

Conclusions

- Three extracts from *Equisetum arvense*, all affect the early stages of silica formation, do not influence aggregation, but do influence the materials structure.
- Short chain diamines dramatically affect the aggregation size observed in the aqueous silica precipitating model system.
- Diamines affect the structure of the silica formed in their presence.
- Diamine structures in aqueous media, as a model for biomolecule organisation *in vivo* may provide an organised environment for controlled silica formation.

References

1. Simpson, T. L. & Volcani, B. E. (eds.) Silicon and Siliceous Structures in Biological Systems (Springer-Verlag, New York, 1981).
2. Harrison, C. C. & Loton, N., J. Chem Soc. Faraday Trans. 91, 4287-4297 (1995).
3. Perry, C. C. & Keeling-Tucker, T., Colloid Polym. Sci. 281, 652-664 (2003).
4. Kroger, N., Lorenz, S., Brunner, E. & Sumper, M., Science 298, 584-586 (2002).

Royal Society of Chemisty International Carbohydrate Symposium Glasgow 2004

Evidence for a role of plant cell wall carbohydrates in biosilicification of *Equisetum*.

Heather A. Currie, Christopher M^{ac}Lean-Tooke, Carole C. Perry
Email: heather.currie@ntu.ac.uk
Interdisciplinary Biomedical Research Centre, The Nottingham Trent University, Clifton Lane, Nottingham , NG118NS

Introduction

The process of biosilification is widespread, occurring in single celled organisms through to the higher plants and animals. The soluble form of silica, orthosilicic acid, is found universally at concentrations of a few ppm and, when taken up by plants, is the starting point of biosilification. Upon uptake, the orthosilicic acid autopolymerises to form stable primary particles, which can eventually form branched chains and finally structural motifs which are observable by electron microscopy[1,2]. The formation of the mineral may occur intra or extra-cellularly and the specific biochemical locations for this mineral deposition could include carbohydrates[3], proteins[4] and lipids. This research programme specifically examines the role of the cell wall carbohydrates in the silicification process and the horsetails *Equisetum arvense*[5] and *Equisetum telematia*[6] which have a high silica content were examined in this study.

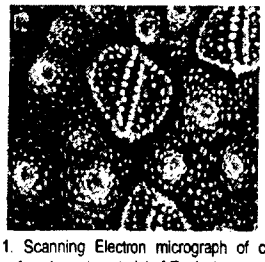

Figure 1. Scanning Electron micrograph of controlled silica structures from branch material of *Equisetum arvense* x 950.

Extraction of pectins and hemicelluloses from the plant cell wall was achieved using a mild extraction technique using alcohol, chelating agents and weak alkali. Further purification of the individual carbohydrate species was carried out utilising ion exchange and gel permeation chromatography. Silica content was analysed using Inductively Coupled Plasma-Atomic Emission Spectroscopy (ICP-AES) for polymerised silica. Monomeric and dimeric forms were detected using the molybdenum blue assay. This analysis demonstrated a need for the ongoing investigation into the relationship between plant cell wall carbohydrates and the deposits of cell wall silica.

Experimental Methods

In order to obtain cell wall extracts which had no alteration to any carbohydrate structures including post translational modifications of any proteins, it was necessary to employ mild extraction techniques (figure 2). Soluble proteins were removed initially using ethanol followed by the use of the chelating agent CDTA which completely abstracts calcium from the cell wall and solublises the pectic polysaccharides held in the walls by ionic cross linkages.

The hemicellulosic polysaccharides are extracted from the CDTA insoluble fraction by the use of mild alkaline conditions using sodium carbonate. The inclusion of sodium borate into this solution also assists in the removal of the hemicelluloses as borate complexes with the 2,3-hydroxyl groups of D-mannose rendering the polymers more acidic and therefore more soluble in alkali.

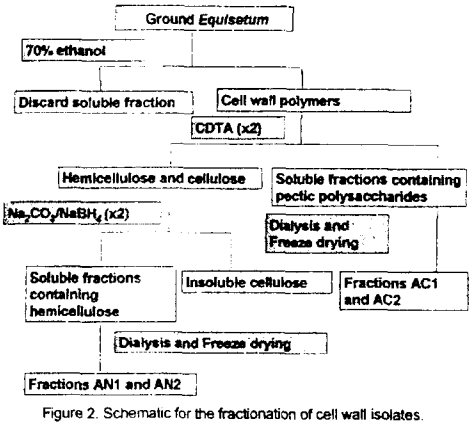

Figure 2. Schematic for the fractionation of cell wall isolates.

The determination of the carbohydrate composition was carried out using a variety of assays including the anthrone assay for the quantification of hexoses and the orcinol assay for pentoses. Uronic aicds were also quantified using the Borax/sulphuric acid assay.

The further fractionation of the hemicelluloses was carried out using the ion exchange resin CL-6B Sepharose.

Results

The fractions collected AC1, AC2, AN1 and AN2 were assayed for their content of hexose and pentose sugars along with their uronic acid content which, if high is indicative of proteoglycans.

The results are shown in figure 3.

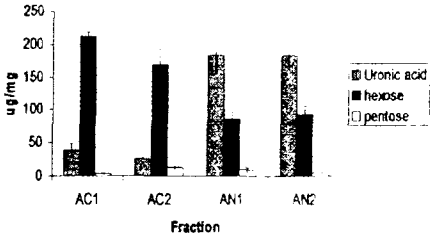

A small sample of each fraction was reduced to its inorganic components through heating in a furnace to 900°C. Elemental analysis of the inorganic components of each organic fraction could then be analysed with the use of Energy Dispersive X ray Spectroscopy (EDS), the results of which are shown in figures 4 and 5.

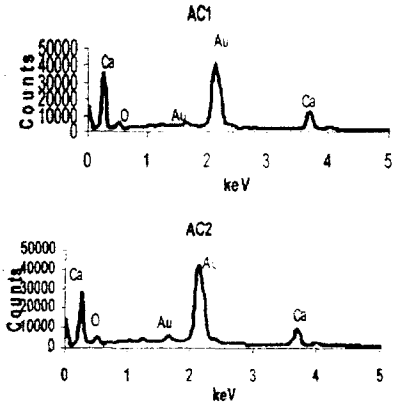

Figure 4. EDS elemental composition of the inorganic components of the CDTA extracted fractions.

From this figure it is possible to observe that silica is not detectable in the fractions extracted with CDTA. However it appears that silica is present in those fractions, which have been treated with the alkaline conditions using sodium carbonate and sodium borohydride, as shown in figure 5. In each of the fractions obtained, the amount of polymerised silica present was measured by the use of ICP-AES whereby a sample is dissociated into its constituent atoms and ions and causes them to emit a characteristic wavelength by excitation to a higher energy level. Silica can also exist in the mono and dimeric forms which can be quantified by the molybdenum blue assay.

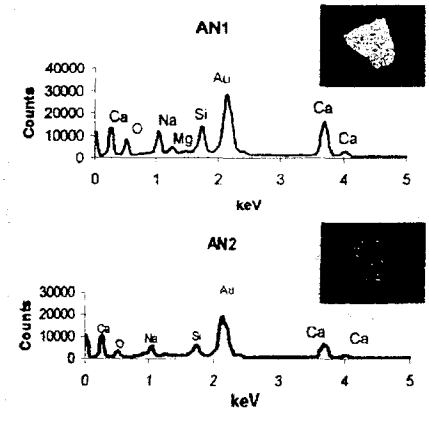

Figure 5. EDS elemental composition of the inorganic components of the $Na_2CO_3/NaBH_4$ extracted fractions. Inset: Si elemental maps.

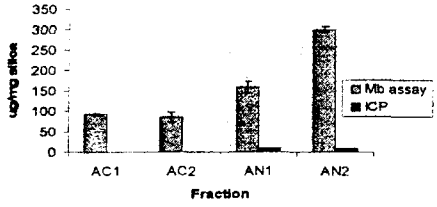

Figure 6. Quantitative measurement of silica as mono and dimeric forms by the molybdenum blue assay and polymerised forms by ICP-AES.

From Figure 6 it is possible to observe that the quantity of both mono/dimeric silica and that of the polymerised silica is significantly increased in the sodium carbonate/sodium borohydride soluble fractions. This data verifies the initial findings of the EDS data.

In order to ascertain the composition of the AN1 and AN2 fractions they were further purified by ion exchange chromatography. The fractions collected during this purification step were tested both for the presence of carbohydrate and protein by the phenol/H_2SO_4 assay and UV spectrometry at 224nm for the detection of proteins. The results of these tests are shown in figure 7.

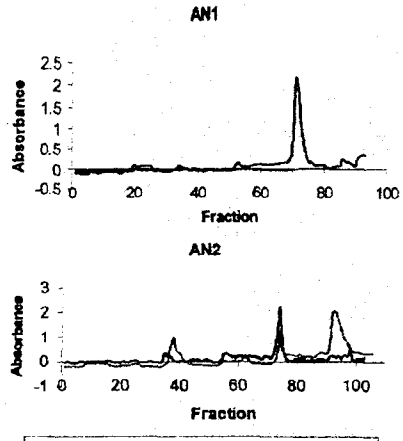

Figure 7. Protein and carbohydrate analysis after separation on CL-6B Sepharose.

This figure clearly shows that the first hemicellulosic fraction does not appear to contain any detectable protein while the second fraction contains both proteins and carbohydrates which may be of similar size and charge or present together in the form of proteoglycans or glycoproteins.

Conclusions

From the results shown here it is possible to observe a significant silica content is associated with the carbohydrate containing cell wall fractions. The inorganic content is greatest in the hemicellulosic fractions as both small mono or dimeric particles and the polymerised form. While the biosilicification of higher plants has most often been accredited to the proteins, this research indicates that carbohydrates may also have a significant role to play either alone or as proteoglycans or glycoproteins. This is most apparent in the AN1 fraction which, while having a significant silica content lacks any detectable protein.

References

1.Perry, C.C. and Lu, Y. *J.Chem. Soc. Faraday Trans.* **1992 88**, 2915-2921.
2.Perry, C.C. and Fraser, M.A. *Phil. Trans. R. Soc. Lond. B.* **1991 334**, 149-157
3.Khalil, N.F. and Duncan, H.J. *J. Food Agric.* **1981 32**, 415-418.
4.Belton, D. *et al J. Mater. Chem.* **2004 14**, 2231-2241.
5.Holzhüter, G. *et al Anal. Bioanal. Chem.* **2003 376**, 512-517.
6.Perry, C.C. and Keeling-Tucker, T. *J. Inorg. Biochem.* **2000 78**, 331-339.

We gratefully acknowledge funding from the AFSOR and Dr R. Jugdaosingh at St. Thomas Hospital for his ICP-AES expertise.

Carbohydrates from higher plants and their possible role in biosilicification

NOTTINGHAM TRENT UNIVERSITY

Euromat, Prague. 2005

Heather A. Currie*, Christopher MacLean-Tooke, Carole C.Perry.
Interdisciplinary Biomedical Research Centre,
Nottingham Trent University, Clifton Lane, Nottingham, NG11 8NS
Email: heather.currie@ntu.ac.uk

Introduction

The process of biosilicification is widespread, occurring in single cell organisms, such as diatoms, through to higher plants and animals. The horsetail fern *Equisetum arvense* has previously been examined and found to have a high silica content. Silica is taken up from soil, where polymerisation occurs with the formation of stable primary particles, eventually developing into branched chains and finally structural motifs observable by electron microscopy (Figure 1). The formation of polymerised silica may occur intra- or extra-cellularly and the specific biochemical locations for the mineral deposition may include carbohydrates, proteins and lipids. This research has specifically examined the role played by carbohydrates which are abundant in a variety of forms in plant material, including polysaccharides, glycoproteins and glycosylphosphatidylinositol (GPI) anchors.

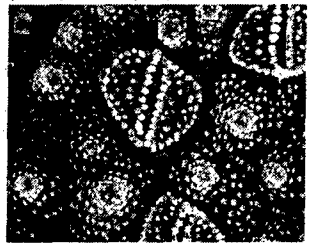

Figure 1. Scanning electron micrograph of silica structures from a branch of *Equisetum arvense* x950.

Extraction of the plant cell wall was carried out in order to isolate and identify individual moieties. Characterisation of the individual fractions showed that increased polymerised silica was found to correlate with an increase in the charged monosaccharides, the uronic acids. This analysis demonstrated a relationship between the plant cell wall carbohydrates and deposits of cell wall silica allowing further elucidation of the biosilicification process in plants.

Methods

The *Equisteum arvense* material was separated into the pectins, hemicelluloses and cellulose by the methods shown in Figure 2.

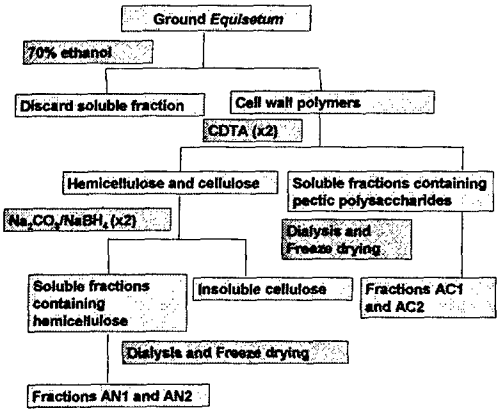

Figure 2. Extraction techniques used

Characterisation of the extacts was carried out using a series of assays for the content of hexose, pentose and uronic acid monosaccharides, phenolics were also measured and identified by TLC. Protein content was determined by GC with the identification of individual amino acids and di- amino acids. The proteins were also analysed by SDS-PAGE to give an approximation of molecular weight and extent of post translation modifications. Quantification of polymerised silica levels were carried out by ICP analysis.

Further purification of the pectin and hemicellulose fractions was carried out using ion exchange chromatography separating individual species on the basis of charge and size using an increasing sodium chloride stepwise gradient.

Results

The isolated pectin and hemicellulose fractions were analysed to determine the content carbohydrate, protein, phenolics and polymerised silca and the results of these assays are shown in Figure 3.

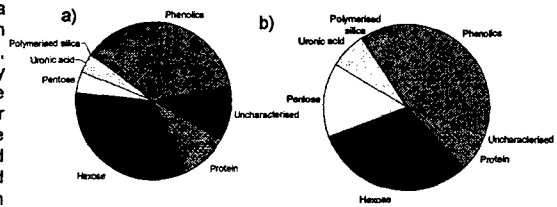

Figure 3. Characterisation of the a) Pectin and b) hemicellulose isolates from *Equisetum arvense*.

From this figure it is possible to observe that carbohydrates in the form of hexoses, pentoses and uronoic acids are the predominant species of the isolates. Phenolics are also present in high amounts and two individual phenolic compounds, sinapic and cinnamic acid, were identified by TLC and their structures shown in Figure 4.

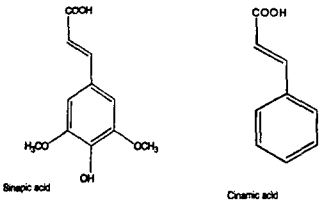

Figure 4. The two phenolic compounds identifed

The protein content of each of the isolates are relatively low with it accounting for between 2-12% of the total. The protein content may also not be the result of one individual protein species and figure 5 shows SDS-PAGE of some of the pectin fractions. The most clearly observable bands are found at approximately 40kDa and 25kDa but the results are unable to give definative molecular weights due to the broad bands obtained. This is a clear indication that the proteins are highly glycosylated.

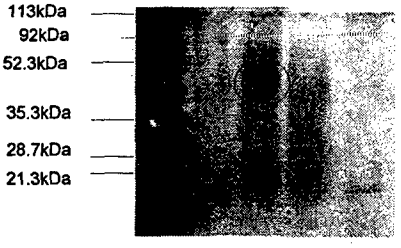

Figure 5. SDS-PAGE of pectin isolates from *Equisetum arvense*.

The polymerised silica levels of each isolate were measured by ICP and no relationship between the silica content and amount of protein was observable (Figure 6). Hydrolysis of the proteins and amino acid analysis was also carried out and again no correlation between amino acid or charges with polymerised silica were observable.

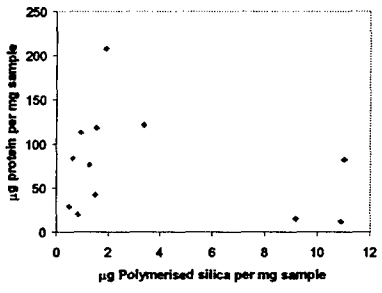

Figure 6. Comparison of the level of protein with polymerised silica

Correlation between the silica content and the individual monosaccharide species was carried out and no trends were apparent for the neutral hexose or pentose sugars. However the charged uronic acids did show a relationship with increasing levels of uronic acids corresponding to increased polymerised silica (Figure 7).

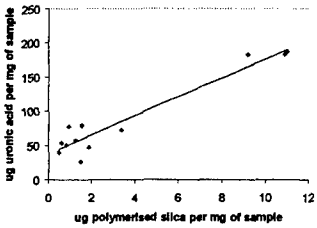

Figure 7. The relationship observed between polymerised silica and uronic acids

Separation of the individual moieties in each isolate was carried out on the basis of charge and size (Figure 8). Each fraction was assayed for protein and carbohydrate content and these again indicate the presence of glycosylated proteins. The protein fractions were again studied for their individual amino acid composition and these are also shown below.

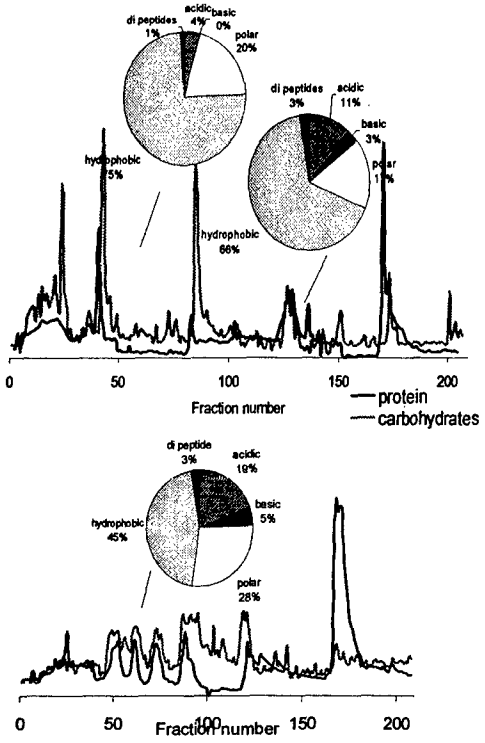

Figure 8. The separation of a) pectins and b) hemicellulose by ion exchange chromatography and the protein composition of some peaks.

Conclusions

Studies previously looking into the formation of biominerals have centered on the role of proteins in this process. However, this study demonstrates a requirement for the analysis of carbohydrate moieties which may be involved. No relationships were observable between the protein content or composition but glycosylation, which can greatly influence protein function, was observed. Analysis of the carbohydrate moieties show large amounts of neutral sugars and charged uronic acids are also present at significant levels. The presence of uronic acids may be indicative of proteoglycans and analysis of the individual types of glycosylation and oligo/polysaccharide structures will give further insight into this growing field.

Acknowledgements

We gratefully acknowledge funding from the AFOSR and Dr R. Jugdaosingh at St. Thomas Hospital for his ICP-AES expertise. Miss L. Gunby is also thanked for her assistance with the ion

APPENDIX-II: UNPUBLISHED PAPERS AND REPORTS

RESERVE THIS SPACE

The Role of Non-Bonded Interactions in Silica Formation in vitro

*Siddharth V. Patwardhan, David Belton, Graham Tilburey and Carole C. Perry**

School of Biomedical and Natural Sciences, Nottingham Trent University, Clifton Lane, Nottingham NG11 8NS, UK.
*** Email: Carole.Perry@ntu.ac.uk**

ABSTRACT

In nature, several classes of biosilicifying organisms process soluble silicon to generate hierarchically organised ornate biogenic silica structures under mild conditions of pH and temperature. The organisms are also able to 'shape' the silica and generate composite materials that whilst living are able to stand the rigours of a 'wet' or 'dry' environment according to the organism itself. The silica structures are formed from an aqueous environment, probably rich in ions, small molecules and biopolymers such as proteins and carbohydrates. In order to understand the chemistry underpinning the formation of such composite materials, 'simple' bioinspired solution studies have been performed. Ions, small molecules and polymers affect silica condensation reactions *in vitro*. This contribution considers the role of non-bonded interactions such as electrostatic interactions, hydrogen bonding, van der Waals interactions and the hydrophobic effect in modifying both the rate of silica formation and the nature of the final product.

NON-BONDED INTERACTIONS

Non-bonded interactions operate between atoms that are not linked together by covalent bonds. Non-bonded interactions vary in strength from 0.1 kcal/mol to several hundreds of kcal/mole depending on the environment in which the interaction occurs (vacuum through to water) and the nature of the specific interaction. In solution reactions, especially those taking place within a living organism, the medium for the reaction is water, except for reactions that occur in specific membrane-like compartments. However, reactions in life do not occur in 'deionised water' free from additives rather in a medium that contains ions and molecules and all of these are available for interaction, in principle, with other species that may be present. The same may be true for laboratory based reactions although here the number of components and the amounts of each component can be regulated. Non-bonded interactions include electrostatic interactions, hydrogen bonding, van der Waals interactions and the hydrophobic effect. As a comparison, covalent bond energies are of the order of 60-250 kcal/mol. Electrostatic interactions in water are of the order of 1-15 kcal/mole, hydrogen bonds are of the order of 2-5 kcal/mole, van der Waals interactions are of the order of 0.5-1 kcal/mole and the hydrophobic effect is of the order of 1 kcal/mole.

The effect of charge, distance and environment for reaction on the strength of non-bonded interactions can be understood by consideration of Coulomb's law where attraction between species of opposite charges (generally considered for positively charged nuclei and negatively charged electrons but can be more generally applied to any species for which there is a separation of charge) is represented as:

$$V = q_i q_j / 4\pi \varepsilon_0 \varepsilon_r r_{ij} \qquad (1)$$

where q_i, q_j are charges, r_{ij} is their separation, ε_0 is the permittivity of free space and ε_r the relative dielectric constant of the medium (for water ca. 80, for methanol ca. 35 and for a lipid bilayer *ca.* 2). The charges may be taken as formal charges but partial charges may also need to be considered for some reacting species. The dielectric constant is dimensionless and accounts for solvation and charge shielding due to the presence of the solvent. Note that the effect of charge is felt much more strongly in a lipid bilayer than in a non aqueous solvent such as methanol than in water! Part of this effect has to do with the ability of particular solvents to hydrate ions (by attraction between the solvent molecule and the solute) such that they effectively enlarge the ions. This enlargement effectively shields the charges from each other thus diminishing the strength of interaction between such species.

The hydrophobic effect operates when there is a mixing of polar (e.g. water) and non-polar (e.g. oil) molecules. The effect is not due to the hydrophobic groups themselves rather due to a reorganisation of the solvent to minimise the amount of water, for example, that is not ordered in its normal fashion through hydrogen bonds etc.

Although non-bonded interactions are individually much weaker than covalent interactions, when they act in concert, as in a protein or a drug-receptor complex or indeed for a condensation reaction in the presence of additives as proposed here, their effect is cumulative and all non-bonding interactions will collectively operate to reduce the free energy of the reaction system, whatever it is. The non-bonded interactions pertinent for silica formation in the presence of additives are schematically represented in Figure 1.

SILICA POLYMERISATION

As has been described before,[1,3,13] orthosilicic acid at 25^{0}C is stable at levels below *ca.* 100 ppm (~ 1 mM). At higher concentrations, polymerisation occurs, which involves three distinct stages:

1. Polymerisation to form stable nuclei
2. Growth of nuclei leading to fundamental particles
3. Particle aggregation to form branched networks, larger particles or other structures.

The polymerisation of monosilicic acid in an aqueous phase generates one molecule of water for each condensation reaction that occurs. In the early stages of silica formation, rapid condensation reactions yield a range of oligomers that serve as nuclei. Typically these stable nuclei are of size 1-2 nm, possess an anhydrous SiO_2 core and surface silanol groups (Si-OH). Based on particle size, the composition of particles can be estimated as described by Iler.[1]

The addition of small oligomers on to these nuclei and coalescence of these nuclei leads to particle growth. The particles can grow by aggregation, by Ostwald ripening and/or by 'necking' between coalesced particles. Assuming instantaneous coalescence, aggregation of particles is typically a consequence of collision between smaller particles. The rate of aggregation depends on the collision frequency, which is a function of the transport properties of the medium, pH, temperature and particle concentration. As polymerisation proceeds, the pK_a of the particles/polysilicic acids decreases from *ca.* 9.8 for orthosilicic acid to *ca.* 6.8 for colloidal particles.[2] It is important to note that even at circumneutral pH, the silica particles bear a negative charge in solution. The consequence of this is that as condensation progresses there are more charges/ charged species present in the condensing system. Surface charge plays an important role in particle aggregation. Charge may also have an effect on

solubility (~ 1 mM) and the formation of dimers, trimers, oligomers, particles and final structures takes place as shown schematically in Figure 2a. The early stages of the reaction are monitored using a colorimetric method that allows changes in silicic acid concentration with time to be monitored. For the first reaction, dimerisation, the method shows no change in silicic acid concentration as both the reactants (monomers) and the product (dimer) produce an identical number of silicic acid molecules that can react with the reagent. The next stage is trimer formation that is observed as an irreversible third order reaction owing to the high concentrations involved (if reactions were performed at concentrations near the solubility limit then information on both the forward and the reverse reaction could theoretically be obtained). Further growth of oligomers follows reversible first order kinetics with respect to silicic acid concentration.[18] The loss of silicic acid with time can be measured using a silicomolybdate assay and hence the rate constants for the reactions involved in the very early stages of silica oligomer formation can be calculated (Figure 2b-d). Additional information on the levels of soluble silicon (monomers and dimers) present in solution at any time, even if the net change in silicon concentration with time is too low to obtain kinetic information, can also be obtained.

The evolution of particle formation in solution can be studied using Dynamic Light Scattering (DLS); Figure 2e. The information obtained is the hydrodynamic radius of the species present which may be individual particles and/or aggregates. Some information on particle size distribution and rates of growth can be obtained but meticulous care must be taken to prevent contamination from dust which can lead to erroneous results. The study of solution chemistry leads to the understanding of molecular interactions between additives and silica species (monomers to particles). The non-bonded interactions between additives and silica can also have dramatic effects on the bulk properties of the silicas generated. We investigate these effects using gas adsorption (to collect information on surface area, porosity and distribution of porosity), thermal analysis (to understand the entrapment of additives in final structures) and electron microscopy (to observe morphology and structure); Figure 2 f-h.

EXAMPLES OF NON-BONDED INTERACTIONS IN BIOINSPIRED SILICIFICATION

The structures of the molecules that have been used experimentally in our laboratory to explore the role of non-bonded interactions in the control of silica structure are presented in Figure 3. Additional information from other sources is referenced as appropriate through the body of the text.

(most shielded charge, least electrostatic interaction) producing silicas with the highest surface areas. In addition, the ions (NH_4^+, Et_3NH^+, etc.) that are less hydrated get associated with the surfaces of silica oligomers/particles by electrostatic attractions reducing the rate of removal of silicic acid and producing silicas with vastly reduced surface area.

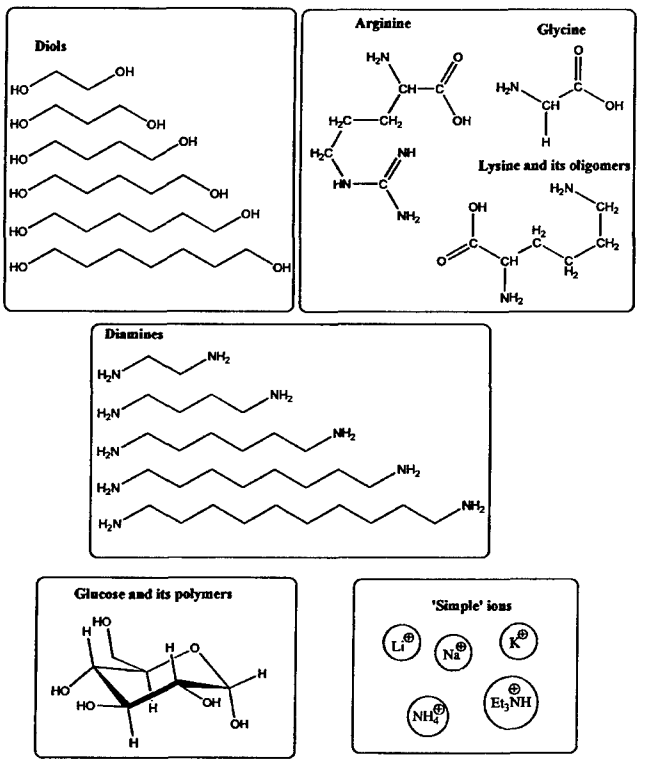

Figure 3. *Additives used in model silicification studies in order to understand non-bonded interactions in structure control.*

Nitrogen containing amino acids, particularly L-arginine and L-lysine were also found to promote silicic acid condensation. When a whole range of amino acids was considered, their effect on the early stages of condensation (e.g. the formation of trimers and other small oligomers) could be related to the pI of the amino acid.[15] Aggregation of the condensing silica as observed by photon correlation spectroscopy (DLS) also showed pI dependent behaviour with the most significant increases being observed for L-arginine and L-lysine. This

saccharides and alkanediols. Reference to other work is also made. Early experiments using cellulose as a reaction additive found that the solution chemistry, i.e. kinetics of silica polymerisation was little affected. However, the presence of cellulose was found to exert a dramatic effect on the range of primary particle sizes generated and their aggregation patterns. In particular, cellulose was able to "stabilise" primary particles and at the same time generated a degree of ordering in the silicas. A similar effect was observed for small oligosaccharides of glucose.[26]

We investigated the effect of additions of alkanediols to the model silicifying system as depicted in Figure 2. The results obtained from the kinetic experiments performed in the presence of the diols indicated no significant effect on any of the early stages of silica oligomer formation when compared with the blank sample (data not shown). However, effects were observed on the materials formed as the presence of the diols led to higher levels of silicic acid being present in solution and silicas with lower surface areas and increased porosity being produced. The observations can be explained by considering all of the species capable of forming hydrogen bonds in the experimental system in question. There are three species cable of constructing a hydrogen bond: silicic acid, water and the alkanediol species. Hydrogen bonding occurs in alcohols due to the polarisation that exists in the O-H bond. Silicic acid is expected to hydrogen bond with the diol as well as with water. However, for all the experiments conducted, water was in excess and hence the effect of the diols would be insignificant compared with the effect of the solvent, as is indeed observed. As particle growth continues the presence of the additive promotes reorganisation of the siliceous phase but the diol is not incorporated into the structures that form.

The Hydrophobic Effect

The hydrophobic effect is a fundamental factor regulating *in vivo* processes, such as protein folding and protein-substrate interactions.[27,28] The stability and hence the function of proteins, for example, is altered by the presence of solute due to the rearrangement of water molecules. This effect is particularly enhanced when the solutes added are hydrophobic in nature. Similarly, the hydrophobic effect is expected to play important role in silicic acid polymerisation and silica – additive interactions. A series of organic additives possessing increasingly larger hydrophobic domains (from C_2 to C_{10}) have been used to investigate their interactions with silicas.[29] Effects on silicic acid condensation, aggregation and materials properties were observed that could not be explained by consideration of the electrostatic effects alone. Increased rates of condensation and aggregation were observed and materials with lower surface areas were produced in the

REFERENCES

(1) Iler, R. K. *The Chemistry of Silica*; John Wiley & Sons: New York, 1979.
(2) Perry, C. C.; Belton, D.; Shafran, K. *Prog. Mol. Subcell. Biol.* **2003**, *33*, 269-299.
(3) Perry, C. C.; Keeling-Tucker, T. *J. Biol. Inorg. Chem* **2000**, *5*, 537-550.
(4) Kendall, T. *Industrial Minerals* **2000**, *March*, 49-59.
(5) Yang, H.; Coombs, N.; Ozin, G. A. *Nature* **1997**, *386*, 692-695.
(6) Brinker, C. J.; Scherer, G. W. *Sol-Gel Science: The Physics and Chemistry of Sol-Gel Processing*; Academic Press: Boston, 1990.
(7) Hench, L. L.; West, J. K. *Chem. Rev.* **1990**, *90*, 33-72.
(8) Tacke, R. *Angew. Chem. Int. Ed.* **1999**, *38*, 3015-3018.
(9) Mann, S.; Webb, J.; Williams, R. J. P., Eds. *Biomineralization*; VCH: Weinheim, 1989.
(10) Beck, J. S.; Vartuli, J. C.; Roth, W. J.; Leonowicz, M. E.; Kresge, C. T.; Schmitt, K. D.; Chu, C. T. W.; Olson, D. H.; Sheppard, E. W.; McCullen, S. B.; Higgins, J. B.; Schlenker, J. L. *J. Am. Chem. Soc.* **1992**, *114*, 10834-10843.
(11) Kresge, C. T.; Leonowicz, M. E.; Roth, W. J.; Vartuli, J. C.; Beck, J. S. *Nature* **1992**, *359*, 710-712.
(12) Meegan, J. E.; Aggeli, A.; Boden, N.; Brydson, R.; Brown, A. P.; Carrick, L.; Brough, A. R.; Hussain, A.; Ansell, R. J. *Adv. Funct. Mater.* **2004**, *14*, 31-37.
(13) Patwardhan, S. V.; Clarson, S. J.; Perry, C. C. *Chem. Commun.* **2005**, *9*, 1113-1121.
(14) Perry, C. C. *Rev. Minerology Geochem.* **2003**, *54*, 291-327.
(15) Belton, D.; Paine, G.; Patwardhan, S. V.; Perry, C. C. *J. Mater. Chem.* **2004**, *14*, 2231-2241.
(16) Kroger, N.; Lorenz, S.; Brunner, E.; Sumper, M. *Science* **2002**, *298*, 584-586.
(17) Cha, J. N.; Shimizu, K.; Zhou, Y.; Christiansen, S. C.; Chmelka, B. F.; Stucky, G. D.; Morse, D. E. *Proc. Natl. Acad. Sci. USA* **1999**, *96*, 361-365.
(18) Harrison, C. C.; Loton, N. *J. Chem Soc. Faraday Trans.* **1995**, *91*, 4287-4297.
(19) Hecky, R. E.; Mopper, K.; Kilham, P.; Degens, E. T. *Mar. Biol.* **1973**, *19*, 323-331.
(20) Lobel, K. D.; West, J. K.; Hench, L. L. *Mar. Biol.* **1996**, *126*, 353-360.
(21) Sahai, N.; Tossell, J. A. *Geochim. Cosmochim. Acta* **2001**, *65*, 2043-2053.
(22) Sahai, N. *Geochim. Cosmochim. Acta* **2004**, *68*, 227-237.
(23) Shimizu, K.; Cha, J.; Stucky, G. D.; Morse, D. E. *Proc. Natl. Acad. Sci. USA* **1998**, *95*, 6234-6238.

in *Hybrid materials -Synthesis, characterization and Applications*, ed. G. Kickelbick, Wiley-VCH, Weinheim, in press. ISBN:3527312994.

NATURAL AND ARTIFICIAL HYBRID BIOMATERIALS

Heather A. Currie, Siddharth V. Patwardhan, Carole C. Perry, Paul Roach, Neil J. Shirtcliffe

Interdisciplinary Biomedical Research Centre, School of Biomedical and Natural Sciences, Nottingham Trent University, Clifton Lane, Nottingham NG11 8NS, UK.

Contents

1. INTRODUCTION

Materials that are implanted to repair, replace or augment existing tissues in the body are generally known as biomaterials. In the wider context covered in this chapter, biomaterials will also include all materials formed in biological systems, e.g. the specific products of biomineralisation. Development of biomaterials, both as products and in understanding their *in vivo* behaviour, has been driven largely by the desire to assist in the care for human patients. The materials forming processes occurring in living organisms require much milder reaction conditions than are currently used in the laboratory such that a new area of materials chemistry, 'biomimetics' has been established where scientists are taking ideas from biology to help generate softer' routes to useful materials.

Biomaterials present in nature provide the necessary structure and architectures of all animal and plant species on earth and function to maintain the structure of organs as well as the organism itself. In nature the materials that are used are polymers, such as polysaccharides and proteins and a relatively small number of simple insoluble oxides and salts. These can be put together in a wide range of combinations to produce materials that are soft, materials that are hard, materials that are flexible, materials that are elastic, etc. In contrast, the range of available materials for biomedical applications is vast and includes metals, polymers, ceramics and composites thereof. In the design of medical devices materials are chosen to suit their intended use and the proposed implantation area. The materials that are used must have compatible properties with the location in which they are placed. Properties such as tensile strength, toughness, elasticity and hardness have to be considered and other factors, such as material transparency, may have to be thought about if, for instance, the device is to be used within the eye. Although the technologist has a wider array of materials at their disposal it is not a simple matter to come up with a material or series of materials that fulfils all the criteria required for successful implantation/ biomedical use. This is due to the fact that as evolution has taken place over millions of years, the intricate natural materials that have developed are ideally suited to their function, whether it be support, sensing, use as an element store or as a deterrent. Nature still has a significant advantage over any bioengineer attempting to design materials to replace or mimic those in living organisms. In order to make progress it is imperative that a detailed understanding of these natural materials is gained before the full complexity of the problem can be appreciated and solutions proposed. On a positive note though, the future of biomaterials seems limitless. Various applications in this field that may have been thought of as radical last year are perhaps possible today. For example, metallic pins, wires and screws for skeletal fixation and repair were the first foreign materials implanted in the body. Such products are still used today but

Figure 2. Calcium carbonate (calcite) skeleton of a coccolith. Taken from S. Mann, *Biomineralization: principles and concepts in bioinorganic materials chemistry*, Oxford University Press, New York, **2001.**

Table 1. Major Biominerals

Mineral	Forms	Functions
$CaCO_3$	Calcite, aragonite, vaterite, amorphous	Exoskeleton, eye lens gravity device
$Ca_2(OH)PO_4$	Apatite, brushite, octa cacium phosphate, amorphous	Endoskeleton, calcium store
$CaC_2O_4(xH_2O)$	Whewellite, whedellite	Calcium store, deterrent
Fe_3O_4	Magnetite	magnet, teeth
FeO(OH)	Goethite, lepidocrocite, ferrihydrite	Iron store, teeth
SiO_2	Amorphous	Skeleton, deterrent

Only calcium carbonate and calcium oxalate approach a true stoichiometry (but note magnesium rich calcite is known) and for the others there are a considerable range of compositions that give rise to the individual phases. In particular, the apatitic phases that are used for bone and teeth can accommodate a range of other metal ions (Mg, Sr, Si) and anions (F, OH, CO_3) etc that lead to changes in strength/ hardness of the material and its dissolution characteristics. E.g., carbonated apatite is found in bones and fluorapatite in teeth, with the latter being 'stronger' than the former (see Section 3 for details).

As another example, although only amorphous (no ordering below *ca.* 1 nm), silica is known as a biomineral (for models of an amorphous and crystalline form of silica see Figure 3). The properties of the material as isolated from different environments suggest that the molecular formula "SiO_2" 'hides' or 'encompasses' many distinct forms of the mineral that differ in terms of water content, hydroxyl ion content and sizes of the fundamental units and their organisation. The formula that more accurately describes the mineral is $SiO_n(OH)_{4-2n}$ (n = 0 to 2).

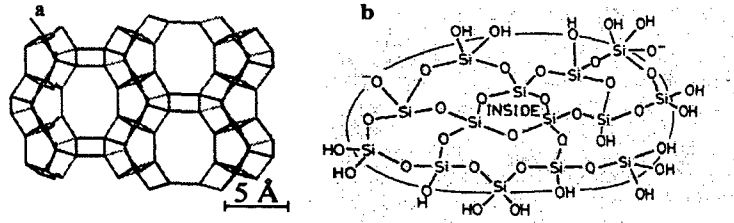

Figure 3. Structures of (a) crystalline (zeolite) and (b) amorphous silica. Note in (b), the Si-O bond length and angle will be variable. Image in (a) courtesy of Professor Geoffrey Ozin.

This ability to take 'simple' materials and manipulate them to produce functional materials requires that all processes during their formation be controlled. For this to happen both nucleation and growth of the mineral phases has to occur. The principles of crystal/ particle nucleation and growth are described below. The controlling properties of organic components will be described in the section on biomineralisation as it is by the juxtaposition of the *inorganic mineral phase with an organic 'controlling' phase* that composite materials showing properties of true hybrid materials are generated. It should be noted that artificial hybrid materials are not limited by availability of "raw materials" in water or toxicity, so the number of potential compounds is much greater.

Nucleation and growth

Before we gain an understanding of biomineral formation, control strategies and the roles of organic phase in biomineralisation, it is necessary to understand the fundamental aspects of mineral nucleation and growth. Biominerals are formed from an aqueous environment by:

- Nucleation
- Crystal growth or amorphous precipitation
- Ripening.

In general, concentration of ions / molecules above the supersaturation level leads to the formation of tiny (a few angstroms in diameter) species or clusters that are called *nuclei*. In the case of crystalline mineral formation, the structure of these nuclei can control the polymorphs to be formed and also the ultimate shapes of the minerals. The levels of supersaturation/ concentration of mineralising precursors regulate mineralisation (Lussac's law).

Supersaturation is when the concentration of the ions or molecular species in question is greater that the solubility product constant (a function of activities of ions in solution that are in equilibrium with pure solids). Supersaturation

role of other species (ions and organic molecules) in the control of morphology is described further below.

Amorphous growth and precipitation typically lacks a nucleation stage, although it is noted that the formation of silica nuclei has been regarded as an important step. Due to the lack of any fixed 3-dimensional structure, unlike that observed in crystalline minerals, amorphous mineral formation usually occurs via localisation of mineral precipitation. Such a localisation can be brought about using various strategies (see *spatial control* in Section 4).

Nucleation and growth is followed by what is termed *ripening or maturation.* In this stage of mineral formation, the growth of minerals continues at the expense of smaller, relatively unstable and more soluble species. The cessation of growth is associated with the cessation of supply/ depletion of the required ions from the reaction site

2.2 Organic Building Blocks

Hybrid materials are those that contain both organic and inorganic components and, as such, possess properties of each as well as properties that may be a consequence of intimate interactions at the molecular level between the different types of material. The organic biomolecules used in such natural 'hybrid' materials are proteins, carbohydrates and lipids and/or combinations of these. The structural characteristics of each biomolecule type is described in some detail below.

Proteins and DNA

Proteins have diverse roles in nature and play important roles as structural components, in reactions as enzymes and in immunology.

The side chain functionality 'R' can be acidic, basic, aliphatic, hydrophobic, nitrogen containing, sulphur containing etc, which join to form the protein primary sequence. Figure 6 gives some illustrative examples of selected amino acids that are commonly found in structural proteins such as collagen. Under physiological conditions (often around pH 7.4) many amino acids have considerable polar character and are involved in hydrogen bonding. This is very important in the folding of the protein to generate regular recurring orientations such as α helix or β sheet structures - the secondary protein structure, see Figure 7a. Furthermore, weak electrostatic interactions between amino acid side chains gives rise to a three dimensional conformational shape which is known as the protein tertiary structure, Figure 7b and finally the quaternary protein structure is the interaction of two or more different

polypeptides or subunits to give a unique spatial relationship of these components.

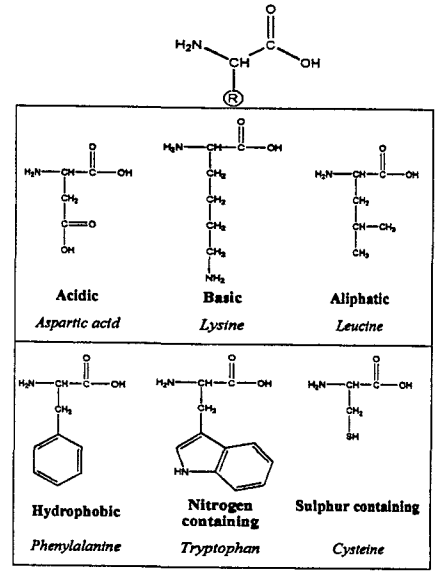

Figure 6. The core structure of an amino acid (top), R representing where side chains of differing properties are attached. Representative amino acids showing a range of side-chain *functionalities* (bottom).

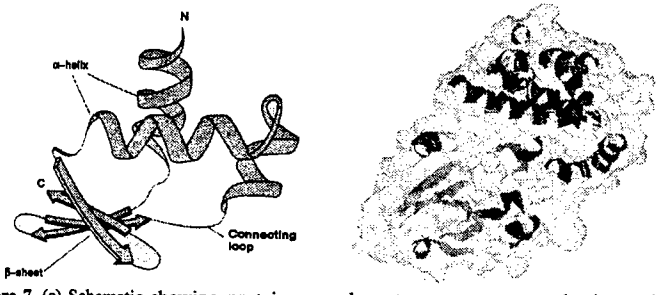

Figure 7. (a) Schematic showing protein secondary structures present together in a tertiary structure (taken from P. C. Turner, A. G. McLennan, A. D. Bates, M. R. H. White, *Instant notes Molecular biology*, 2nd ed., Bios Scientific publishers, Oxford, 2000), (b) 3D

Figure 9. (a) The disaccharide sucrose (common table sugar) which is formed from an α 1,2 glycosidic linkage between D-glucose and D-fructose. (b) Keratin sulphate, a glycosaminoglycan disaccharide.

Lipids

Lipids are a complex and diverse class of biomolecules which are essential due to their many roles including the formation of membranes, transduction of cellular signals and as a source of energy in the form of triacylglycerols. The combination of the polar head group attached to one or more hydrophobic tails via a backbone unit leads to great deal of structural diversity and therefore a vast array of different amphiphilic lipids can be found *in vivo*. The hydrophobic tail regions can be composed of saturated or unsaturated aliphatic chains or may also contain aromatic groups, while charged or uncharged polar moieties can be found at the head group. Some examples of the different lipid structures are shown on Figure 10. As lipids are largely insoluble in polar environments, they are capable of self assembly in to more favourable structures when found in aqueous environments. The formation of a lipid bilayer, as found surrounding all cells, is brought about by self organisation of the hydrophobic regions to the inside of the bilayer, eliminating an unfavourable proximity to the polar environment. Another common structure of lipids is the formation of micelles, which again occurs in polar environments and has the polar heads surrounding the cluster of hydrophobic tails.

These organic building materials are used in nature intimately associated with a vast array of mineral phases, utilising the features of both to from materials which are ideally suited to their function. One clear example of this is the mineralization of collagens, glycosylated proteins, which are found in many different biological materials from bone to cornea and are reliant on the individual properties of each component to generate these highly specific materials.

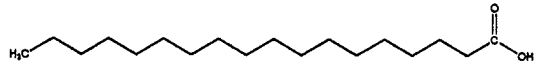

Palmitic acid, $CH_3(CH_2)_{14}COOH$

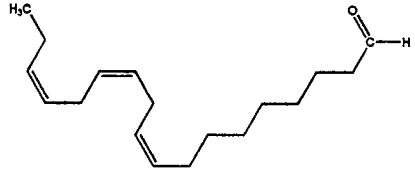

Stearic acid, $CH_3(CH_2)_{16}COOH$

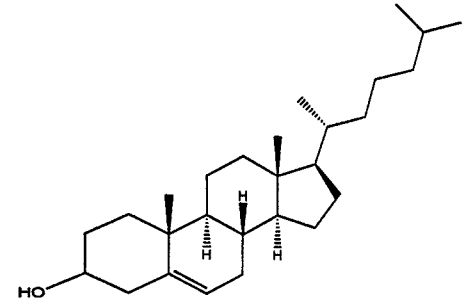

CHOLESTEROL

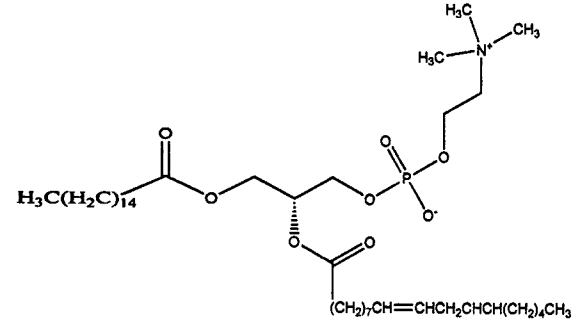

Phosphatidylcholine

Figure 10. Some common fatty acids and the effect of unsaturation.

Collagen

In mammals the group of proteins known as collagens account for nearly one third of an animal's protein content. These proteins are frequently glycosylated and are often found in conjunction with Ca in the form of hydroxyapatite (discussed later). Collagen occurs in virtually all tissues in the body and is principally found as the major stress-bearing component of the connective tissues as a result of its immense tensile strength. Each collagen molecule consists of three polypeptide chains, which are individually coiled.

- Where minerals are formed without any apparent specific function. These biominerals may be useful, detrimental or benign to the organisms producing them (e.g. kidney stones).

Biomineral types and occurrence

Biominerals are typically organic-inorganic hybrids that are hierarchically organised from the nano- to the macroscopic length scale. The organic components of biominerals include proteins, glycoproteins, polysaccharides and other small organic biomolecules. The organic phase occluded in biominerals may or may not be directly involved in biomineralisation. The common ions involved in biominerals are Mg, Ca, Sr, Ba, Si and Fe as their carbonates, oxalates, sulphates, phosphates, hydroxides and oxides, see Table 1. The relatively rare ions are Mn, Au, Ag, Pt, Cu, Zn, Cd and Pb deposited largely in bacteria and often as sulphides. Over 60 different biominerals have been identified. The diversity in the occurrence of biominerals indicates the ability of biological organisms to manipulate and deposit inorganic compounds. Around 50% of biominerals are calcium-based minerals and of this half are calcium phosphates of varying composition. In terms of structure, about 25% biominerals are amorphous in nature i.e. they do not show structural regularity at atomic scales (e.g. biosilica, amorphous hydrated iron phosphate, calcium carbonate).

Functions of biominerals

In most organisms, biominerals are produced for specific functions. The functions can be classified as follows:

- Mechanical / structural support
- Protection
- Motion
- As sensors
- Cutting and grinding
- Buoyancy

These functions will be illustrated with selected examples. Marine sponges are known to form biosilica in the form of needle-like spicules that are a few tens of microns in diameter and can be as long as a few millimetres (Figure 12). The primary role of biosilica spicules in sponges is to provide mechanical support to the animal and to protect from predators. Biominerals also act as gravity, optical or magnetic sensors thus providing useful functions to organisms. Some bacteria – *magnetotactic* bacteria – produce single crystals of magnetite (Fe_3O_4) which are called *magnetosomes* (Figure 12c).

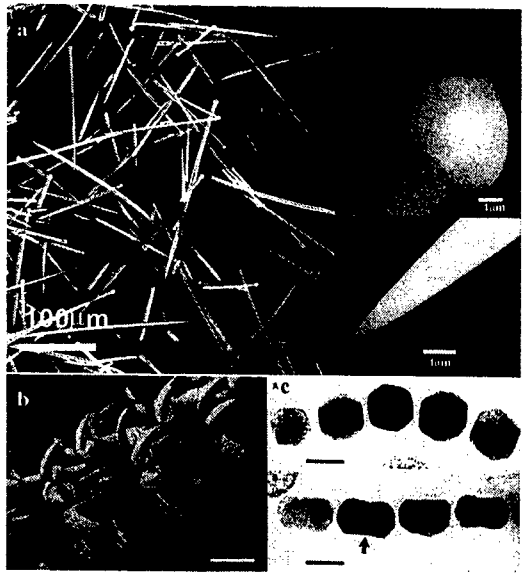

Figure 12. Examples of some biominerals – (a) sponge spicules, insets show high magnification images of a spicule tip and head. (b) limpet teeth and (c) magnetite crystals (magnetosomes) from bacteria. Bar = (a) 100 µm (1 µm for inset), (b) 200 µm and (c) 50 nm. Image in (a) taken from S. V. Patwardhan, S. J. Clarson, C. C. Perry, *Chem. Commun.* **2005**, *9*, 1113 and reproduced by permission of the Royal Society of Chemistry. Image in (c) taken from S. Mann, J. Webb, R. J. P. Williams, *Biomineralization*, VCH, Weinheim, **1989**.

In a bacterium, these magnetite crystals are typically identical to each other and are arranged in a linear chain. Magnetosomes help bacteria navigate using the Earth's magnetic field. Similarly, gypsum deposited in jellyfish is used for gravity sensing. Limpet teeth, used for grinding, are biomineralised geothite (α-FeOOH), while chiton teeth are lepidocrocite (γ-FeOOH) or ferrihydrite ($5Fe_2O_3 \cdot 9H_2O$); Figure 14b. Whewellite ($CaC_2O_4 \cdot H_2O$) and weddellite ($CaC_2O_4 \cdot 2H_2O$) are found in plants or fungi and are used to store calcium. Some marine molluscs and cephalopods use aragonite ($CaCO_3$) shells as buoyancy devices.

Properties of biominerals

Biominerals are intriguing due to their unique characteristics in comparison with the mineral alone, such as:

- Chemical composition

Figure 14. Graph showing bone stiffness, strength and toughness as a function of ash content, redrawn from S. A. Wainwright, W. D. Biggs, J. D. Currey, J. M. Gosline, *The Mechanical Design of Organisms*, Edward Arnold, London, **1976**.

The above section has highlighted how sophisticated biominerals are in terms of their chemistry, structure and morphology, and other specific properties making them 'fit for function' within a given organism.

Control strategies in biomineralisation

One of the most intriguing features of biological mineral formation is the regulation of the entire process of biomineralisation from the intake of ions and molecules from the surroundings to the deposition of stunningly beautiful and organised structures as we have seen in the preceding sections. It is this control that clearly separates the *in vitro* synthetic capabilities of mineralisation, that are presently far removed from the sophistication observed *in vivo*. R. J. P. Williams clearly states – "The chemical character is clearly then a genetically controlled feature due to the deliberate movement of elements into specialised parts of biological space by ion pumps. However, inside this space, the chemistry of the surface and/or of growth inhibiting compounds will control the precise compound which is precipitated". This briefly suggests different control strategies involved in biomineralisation and these are listed below (also see Figure 15).

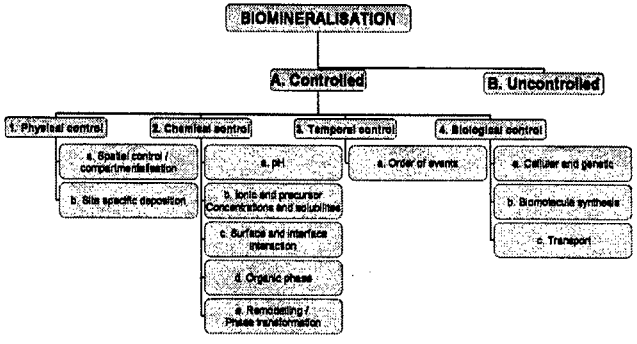

Figure 15. List of various factors controlling biomineralisation. See text for details.

The aforesaid strategies will be considered individually, their roles explained and illustrative examples provided.

Chemical control in biomineralisation constitutes one of the most important regulators. The basic requirement for the formation of any mineral is the attainment of supersaturation with respect to the mineral precursors as described earlier. Biological organisms control supersaturation by governing various chemical aspects. *pH* for example, dictates the ionic strength and activities of ions in a given solution. This in turn, according to solubility product (equation 1), may initiate or inhibit mineralisation. In some cases even the slightest changes in pH can cause drastic effects on biomineral deposition. For example, iron reduction in some bacteria is triggered by changes in pH. The influx and efflux of certain ions to and from the site of biomineralisation leads to changes in the *concentration of ions and precursors* thus altering their relative solubilities, activities and compositions. This effect, again, can regulate biomineral deposition. The control of the rate of availability and diffusion of individual species to the biomineralisation site, their adsorption onto growing surfaces, their incorporation into biominerals and their inhibitory effects are all known to directly affect biomineralisation. In the earliest stages of formation of hydroxyapatite (bone), Ca^{2+} ions are adsorbed onto glycoproteins thus altering local precursor concentrations.

Biomineral formation on *surfaces* (i.e. heterogeneous nucleation) is known to exhibit lower energy barriers than the energy barriers to be overcome in homogeneous nucleation. Hence the formation of biominerals on surfaces is favoured, e.g. the formation of mollusc shells where layers of organic material including proteins with high acidic functionality provide nucleation sites for calcium carbonate formation. Furthermore, *interfacial interactions* between biomineral-liquid and biomineral-surfaces are also important and are precisely controlled by organisms. When a solid mineral phase forms, it gives rise to a solid-liquid interface and in turn to a solid-liquid interfacial energy (σ_{SL}). Higher surface energy leads to instability and thus to produce stable minerals, biology adopts different ways of optimising σ_{SL}. One simple example to stabilise surface would be the adsorption of inorganic ions or *organic biomolecules* onto unstable mineral surfaces. This example leads us to a discussion on the roles of the organic phase in biomineralisation. In passing we note that the organic phase is known to affect almost all aspects of biomineralisation – from transport of ions, storage of precursors, regulating solubilities, catalysis and structure direction of biominerals to biomineral stability. Last but not the least in chemical controls is *remodelling and/or phase transformation* of biominerals. This is the "final touch" given to biominerals before they are actually functional. In crystalline biomineralisation, the formation of one phase may dominate under given conditions, but that phase may not be suitable for its function and hence phase transformation is performed *in vivo*. For example, spicule formation in sea urchins occurs via the initial deposition of amorphous calcium carbonate that

arise from electrostatic forces, hydrophilic and/or hydrophobic effects, hydrogen bonding and van der Waals forces. Non-bonded interactions operate between atoms that are not linked together by covalent bonds. Non-bonded interactions vary in strength from 0.1 kcal/mol to several hundreds of kcal/mole depending on the environment in which the interaction occurs (vacuum through to water) and the nature of the specific interaction. In solution reactions, especially those taking place within a living organism, the medium for the reaction is water, except for reactions that occur in specific membrane-like compartments. However, reactions in life do not occur in 'deionised water' free from additives rather in a medium that contains ions and molecules and all of these are available for interaction, in principle, with other species that may be present. The same may be true for laboratory based reactions although here the number of components and the amounts of each component can be more easily regulated and/or modified. Non-bonded interactions include electrostatic interactions, hydrogen bonding, van der Waals interactions and the hydrophobic effect and they vary considerably in energy. As a comparison, covalent bond energies are of the order of 60-250 kcal/mol. Electrostatic interactions in water are of the order of 1-15 kcal/mole, hydrogen bonds are of the order of 2-5 kcal/mole, van der Waals interactions are of the order of 0.5-1 kcal/mole and the hydrophobic effect is of the order of 1 kcal/mole. For interaction between mineral and a bioorganic phase, interactions will not be singular rather.

The *effect of charge*, distance and environment for reaction on the strength of non-bonded interactions can be understood by consideration of Coulomb's law where attraction between species of opposite charges (generally considered for positively charged nuclei and negatively charged electrons but can be more generally applied to any species for which there is a separation of charge) is represented as:

$$V = q_i q_j / 4\pi \varepsilon_0 \varepsilon_r r_{ij} \qquad (3)$$

where q_i, q_j are charges, r_{ij} is their separation, ε_0 is the permittivity of free space and ε_r the relative dielectric constant of the medium (for water *ca.* 80, for methanol *ca.* 35 and for a lipid bilayer *ca.* 2). The charges may be taken as formal charges but partial charges may also need to be considered for some reacting species. The dielectric constant is dimensionless and accounts for solvation and charge shielding due to the presence of the solvent. Note that the effect of charge is felt much more strongly in a lipid bilayer than in a non aqueous solvent such as methanol than in water! Part of this effect has to do with the ability of particular solvents to hydrate ions (by attraction between the solvent molecule and the solute) such that they effectively enlarge the ions. This enlargement effectively shields the charges from each other thus diminishing the strength of interaction between such species.

Hydrogen bonds arise from electronegativity differences between an element and the hydrogen atom it is attached to that lead to a redistribution of charge within the covalent bond joining the two elements. For a hydrogen bond to form there needs to be one molecule with an electronegative element attached to hydrogen and another molecule containing an electronegative element. Clearly, for reactions in water, where there is an infinite network of hydrogen bonds, any additional hydrogen bonds that form between specific atoms must overcome the network present in water. This clearly happens when protein folding occurs to give the secondary building blocks, alpha helices and beta sheets that further fold to generate specific conformations of active proteins.

Van der Waals interactions are important for essentially uncharged atoms as they come close together in space. The effect of one atom on another is to deform the electron cloud due to electronic repulsion. This sets up transient dipoles on both atoms resulting in a weak attractive interaction between them, the so-called van der Waals interactions. Van der Waals interactions are weak but it is a result of these interactions that geometric specificity is achieved in biological systems.

The *hydrophobic effect* operates when there is a mixing of polar (e.g. water) and non-polar (e.g. oil) molecules. The effect is not due to the hydrophobic groups themselves rather due to a reorganisation of the solvent to minimise the amount of water, for example, that is not ordered in its normal fashion through hydrogen bonds etc.

Although non-bonded interactions are individually much weaker than covalent interactions, when they act in concert, as in a protein or a drug-receptor complex or indeed for a mineralisation reaction in the presence of biomolecules, their effect is cumulative and all non-bonding interactions will collectively operate to reduce the free energy of the reaction system, whatever it is.

Such interactions can control biomineralisation, for example by regulating the available concentrations of ions, molecules and/or biomineral precursors. These chemical effects arising from the organic phase may also alter the solubilities of specific species in a given solution thus affecting the nucleation and growth of biominerals. In the case of interactions between proteins and biominerals, the primary, secondary, tertiary and quaternary structures of proteins play a major role. The primary structure, i.e. the amino acid sequence, determines the chemical "nature" of the proteins present while the other – secondary to quaternary – structures define the "shape and topography" of proteins. Due to the advanced nature of this topic, readers are advised to refer to further reading (see Evans, 2003, Sarikaya 2003 and Shiba, 2003 in

- Structural and morphological
- Mechanical support

The organic phase can exist in various forms. These include vesicles, networks, membranes, surfaces and at interfaces, self-assembled structures and in a soluble form. The organic phase is an effective tool used by organisms for controlling biomineralisation.

Chemical effects include maintaining the local supersaturation of precursors. As an example, in bone formation, acidic glycoproteins adsorb Ca^{2+} ions thus increasing their local concentration thereby promoting bone formation. In some cases, the organic phase, and functional biomolecules in particular, exhibit enzymatic activity that can catalyse the formation of biominerals. As an example, it has been shown that the controlled formation of magnetite crystals in bacteria takes place only in the presence of proteins that are tightly associated with the crystals. In addition, the organic phase can also be involved in the inhibition of biomineral formation as well as in the stabilisation of biominerals, with avoidance of mineral dissolution for example.

The *spatial effects* arise from localisation of biominerals and their precursors. The organic phase can present itself in a range of forms and assembled structures. This organisation exerts spatial constraints on biomineral formation. As an example, the protein ferritin forms a hollow cage, the size of which imposes a limit on the amount of ferrihydrite that can be synthesised within the protein cage. Organic biomolecules are not only known to control the final shapes and morphologies of biominerals but they are also able to determine the atomic and molecular structures. In case of calcium based biominerals it has been proposed stereochemical interactions occur between the organic phase and the growing mineral and that this interaction dictates the nature of crystals produced. An example is the regulation of coccolith formation. It has also been suggested that the organic phase in various biominerals acts as a mechanical support imparting desirable strength, toughness and/or flexibility for a given system. Bone is a classic example where the organic phase provides mechanical properties to the ultimate hybrid biocomposite. Variation in mechanical properties is achieved by the amount and type of collagen that is present as well as the amount of mineral associated with the collagenous matrix.

Bioinspired Hybrid Materials

An important question needs to be addressed now: how biological routes towards fabricating hybrid biomaterials can be transferred to artificial materials design. We try to address this aspect in this section. Sources for

inspiration will be described followed by selected examples of bioinspired artificial materials synthesis.

As discussed above, the novelty about biomineralisation is not only the structural control but also the use of biomolecules in synthesis and organisation of inorganic minerals. Specific roles of functional organic biomolecules are being elucidated in order to reveal the *"active" components.* This information can be utilised in designing synthetic analogues that would facilitate *in vitro* mineralisation. The example of silica synthesis is given in this case. It has been found that the protein containing extracts isolated from diatom biosilica possess unusually modified amino acids. The modifications, which are polyamines of 6-10 repeat units, are shown to be important for silica formation *in vivo*. A number of synthetic amines with a variety of sizes and architecture were designed and were found not only to facilitate the synthesis of silica under ambient conditions, which would otherwise not be possible, but also to produced tailored silicas in terms of their structure, morphology and porosities, for example (see a recent review for details: Patwardhan, Clarson and Perry, *Chem. Commun.*, **2005**).

Table 3. *

Examples of pairs of forces which can lead to self-organization.

Long-range repulsion	Short-range attraction	Examples
hydrophilic/hydrophobic	covalent binding	micelles, lyotropic liquid crystals
incompatibility	covalent binding	block copolymers
Coulombic repulsion	electroneutrality	ionic crystals
excluded volume	minimum space required	thermotropic liquid crystals
electric dipole field	electric dipole interaction	ferroelectric domains
magnetic field	magnetic dipole interaction	magnetic domains

*Taken from Forster and Plantenberg, *Angew. Chem. Int. Ed.* 2002.

In case of some biomineral formation, organic molecules act as *templates or scaffolds* for inorganic biomineral deposition. The *self assembly* of the organic molecules becomes an important prerequisite in determining the final biomaterials properties. This principle has been exploited for designing novel hybrid materials wherein organic molecules, e.g. polymers, peptides, surfactants, etc., are organised prior to the mineral growth. Before giving an example, the principles of self-assembly are briefly outlined. Self-assembly or organisation means attaining an ordered state from a disordered one and results in net reduction in entropy of the system. It is well known that soft matter can be organised into various assemblies via weak molecular interactions such as van der Waal's forces, hydrogen bonding, hydrophobic forces, and ionic interactions as discussed above. Typically a combination of long range repulsion and short range attractive forces is a prerequisite for self-assembled structures (Table 3). A variety of molecules and macromolecules ranging from simple molecules such as lipids and surfactants through to

phosphate and then finally hydroxyapatite. Mineralisation then continues with the newly formed crystals disrupting the vesicle membranes and fusing. Quickly the small crystals grow and are aligned along the collagen fibre axis. The most developed bone, lamellar bone, contains the thickest collagen fibres which are aligned either in a linear or concentric (around a central blood vessel) orientation. The breakdown of bone in small packets to repair the structure is caused by cells called osteoclasts which resorb the bone.

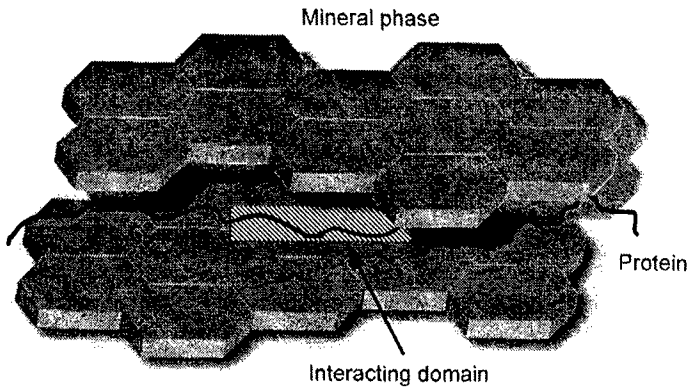

Figure 17. Schematic of the possible interactions of proteins and minerals with an example of Lustrin interactions with calcium carbonat in nacre.

The interactions between inorganic and organic phases in the process of biomineralisation are still greatly debated throughout the scientific community. One such example is the possible interaction of aragonite plates of red abalone nacre with the organic matrix. Examination of Lustrin proteins – matrix proteins from the nacreous layer –a 24 amino acid polyelectrolyte domain within the protein Lusturin A was identified. This domain, termed D4, is rich in aspartic acid and also contains hydrogen donor/acceptor amino acids – asparagine, glutamine, arginine, threonine, serine and tyrosine. This structure was shown by NMR spectroscopy to adopt an open chain conformation in solution allowing side chain access for charged residues to the inorganic surface (Figure 17). Further examination, using a modelled polypeitde of D4 revealed a 9 amino acid Ca(II) interaction sequence capable of binding Ca(II) ions in a 2:1 (Ca: peptide) stoichiometry *in vitro.* These studies also found the modelled D4 sequence affected the morphology of the $CaCO_3$ crystals grown *in vitro,* and the crystals retrieved form this assay also displayed the polypeptide as a bound species on the crystal surface.

These findings are put into question by a recent report which examined nacre of a different genus of red abalone. The aragonite crystals examined were found to have a continuous coating of amorphous $CaCO_3$ therefore not contributing to any epitaxial interactions with the organic matrix. This finding leads to uncertainty as to the involvement of the organic components and their possible interaction with the inorganic matrix.

Together the organic and inorganic components of bone are combined creating a material which is both resilient and versatile (Table 4). Through variations of each component it is able to ideally form itself to the required function at each precise location. Artificial materials still need to be developed which have, in combination, the necessary strength to withstand load bearing and reasonable force. In addition to this, any novel material should be the source of minimal corrosion in the biological environment.

Dentin

Dentin, the most abundant mineralised tissue in the human tooth is another naturally occurring hybrid material containing apatite and fibrils of type I collagen. Although dentin contains the same basic materials as bone, the mechanical properties are considerably different in response to the functional requirements of dentin that is found beneath the enamel layer in teeth. This hybrid material must be capable of enduring dental caries, ageing and disease. Dentin is a fibre reinforced composite material containing approximately 50% carbonated apatite and 30% organic matter which is predominantly cross linked type I collagen. Important features of dentin are the fibre-like tubules that provide reinforcement to the surrounding matrix. The tubules represent the tracks taken by the odontoblasts (dentin producing cells) from the dentino-enamel interface to the central tooth pulp within which the new dentin continues to form throughout the life of the tooth. The lining of these tubules is composed of a highly mineralized cuff of intertubular dentin containing mostly small apatite crystals. The crystals are needle like near the pulp becoming more plate like closer to the enamel and there is very little organic material found in the tubules. Mineralisation also occurs in the collagen fibrils that are randomly orientated perpendicularly to the dentinal tubules. The collagen fibrils of dentin are visible in Figure 18. The elastic properties of dentin are a direct result of the perpendicular arrangement of the collagen within the dentinal tubules. As a material, the hardness of dentin is determined by the extent of mineralization and this may differ depending on the location of the dentin within the tooth, decreasing with proximity to the central pulp.

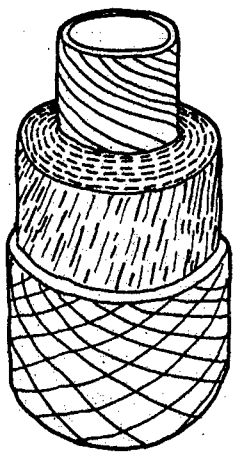

Figure 20. A diagrammatic representation of the primary, secondary and tertiary layers of wood. Taken from J. F. V. Vincent, *Structural Biomaterials*, The Macmillan Press Ltd, London, 1982.

Table 4. A comparison of the mechanical properties of some naturally occurring biological hybrid materials and some metal and ceramic materials used as artificial biomaterials.

	Elastic Modulus (MPa)	*Tensile Strength (MPa)*
Compact Bone	20 000	200
Dentin	17 400	97.8[1]
Nacre	64 900	130
Wood	10 000	100
Ti alloys	110 000 - 116 000	760 -1100
Co-Cr alloys	210 000 - 253 000	655 -1795
Dense Hydroxyapatite ceramics	70 000 -120 000	40 - 100
Bioglass (40%) HDPE[2] composite	2 380 - 2 700	9.44 – 10.86

[1] At strongest point, the dentino-enamel interface
[2] High Density Polyethylene.

4.2 ARTIFICIAL HYBRID BIOMATERIALS

Synthetic hybrid materials can be made using components generated by biological organisms. These can be separated into those where the organic components is natural and those where the inorganic component is natural.

Ancient materials
Some of these materials have been used for some time. The only available materials were organic or minerals. This resulted in many hybrid materials being created to mix the properties of the constituents.

Dyes
Early dyes were often derived from plants, some were fixed using inorganic solutions, such as alum. This process created a hybrid material with the organic dye bound through an inorganic bridge to the organic fibres of the textile that was dyed. A well known example of this is the red dye derived from Madder, alizarin. The Maya civilisation created a particularly resilient dye, Maya blue, which was a hybrid of the blue dye indigo (often used in jeans) and clay.

Paints
Early paints used a protein base, commonly egg white (albumin) or milk protein (casein) or an oil base, such as linseed oil and a powdered mineral as colouring. These paints are surprisingly resilient and are starting to be used once more, due to the hazards of organic solvents used in synthetic paints. The minerals used varied with their availability in each area and were chosen by their ease of powdering and lack of solubility in the protein/water base. There is some evidence that even early cave art was produced by mixing some kind of organic fluid, such as blood, with pigments. Pigments used included ochre (iron oxide), charcoal, lapis lazuli and malachite but many were used.

The ancient Egyptians used tools to extract and process minerals that brightened the palette, including Azurite Blue, Malachite Green, yellow and orange from Orpiment and Realgar and Vermilion red. They synthesized blue from cobalt ore and also from silica known as Egyptian Blue Frit or Smalt. They made white from lead. Indigo blue and madder red were manufactured as dyes and pigment.

In Ancient Greece and Rome, Tyrian Purple from Murex was used as dye and pigment. It took an enormous amount of murex to produce a tiny quantity of colour. Verdigris green was made from copper acetate. In the Middle Ages, the development of the dyeing industry increased the number of organic pigments available. Dyes were extracted from flowers, roots, berries and insects to make lakes, which are translucent colours.

Others

particles of the required material that have been prepared previously. This stage often, but not exclusively takes place in solution.

(b) Next, deposition of the inorganic material occurs on the inside and/or outside of the template occurs with the formation of an organic-inorganic hybrid material. The process could stop at this stage or,

(c) The organic template may be removed by washing with a solvent in which only the template is soluble or heat treatment (conventional thermal methods or use of microwave) that may lead to further structural changes in the material.

Materials that have routinely been formed using such a templated route include common oxides such as silica and titania but the methodology has recently been expanded to cover some nitrides and sulphides as well.

Biologically relevant molecules that have been used to template the formation of hybrid materials and inorganic materials with defined shape and form include ammonium DL-tartrate, proteins such as collagen that have positively charged surfaces that attract negatively charged species such as silica to themselves, DNA, tobacco mosaic virus, yeast cells, decalcified cuttlebone from the cuttlefish and wood.

In principle there are an infinite range of materials that could be combined to make novel hybrid materials if the chemistry at the interfaces between the two phases can be made compatible. One of the principle challenges in this area is in finding novel ways to obtain transcribed structures with a high degree of order over all three dimensions of the object being used as the template.

Integrated Nanoparticle-biomolecule hybrid systems

Nanomaterials including metal and semi-conductor nanoparticles (having a range of shapes including spheres and rods) have dimensions on the same length scale (2-20nm) as biomolecules such as proteins and DNA. The hybrid materials generated from the chemical or physical juxtaposition of these two types of materials generates novel bionanohybrids with a range of properties and functions. Currently available nanoparticles include metals (e.g. Au, Ag, Pt and Cu) and semiconductors (e.g. PbS, Ag_2S, CdS, CdSe and TiO_2) exhibit unique electronic, photonic and catalytic properties. Biomolecules such as proteins naturally play roles as enzymes, antigens and antibodies and these attributes can be harnessed within a composite hybrid material. There is much interest in generating 2D and 3D ordered structures of these biomolecules-nanoparticle hybrids both in solution and on surfaces and the materials generated have vast potential in the development of novel biosensors for use in the health-care industry.

Figure 21 below shows schematically how nanoparticle-biomolecule devices can be generated. A range of functions for such materials is envisaged in areas as diverse as sensing, catalysis and electronics/ optoelectronics. As many of these materials may eventually be intended for use in the human body the term 'nanobiotechnology' has been coined to describe this research area.

Routes to Bio-nano hybrid systems

The main routes to producing nanoparticles are through solution-based approaches with clusters of the chemical components forming in the presence of surface-capping ligands that prevent aggregation and limit the final dimensions of the nanoparticles. Capping systems available include the use of hydrophobic or water-hating monolayers, positively or negatively charged hydrophilic or water-loving monolayers and polymer layers. The very presence of these chemical functionalities on the outside of the nanoparticles (initially there only to limit growth!) is enabling the development of some truly novel hybrid materials as the surface functionality can be used to direct organisation of the nanoparticles into 2D and 3D arrays. If this inbuilt functionality is combined with biomolecules that themselves have specific patterns for binding then site-specific binding of the nanoparticles to one another by self-assembly or to another material can be accomplished. Examples of biomolecular recognition include antigen-antibody interactions, nucleic acid-DNA interactions and hormone-receptor interactions. Some biomolecules exhibit two binding sites e.g. some antibodies and some exhibit four binding sites e.g. streptavidin and concanalvin A that can lead to the development of linear structures or three dimensional structures respectively. Proteins can also be engineered to produce molecules with specific anchoring groups at specific locations on the surface thus increasing the options further. Hence it is possible to organise nanoparticles and even more than one type of nanoparticle into extended arrays by judicious choice of the chemistry linking the particles together.

Biomolecular functionalised nanoparticles required for such devices can be formed through:

(a) electrostatic interactions, e.g. the binding of immunoglobulin G (IgG) to gold and silver nanoparticles functionalised with negatively charged citrate ions;

(b) chemisorption and covalent binding through bifunctional linkers, e.g. oligopeptide binding to gold nanoparticles previously functionalised with L-cysteine through thiol groups on the surfaces of the particles;

(c) programmed assembly using specific affinity interactions, e.g. streptavidin (Sav)-functionalised gold nanoparticles have been used for the affinity binding of biotinylated proteins and oligonucleotides as well as to other

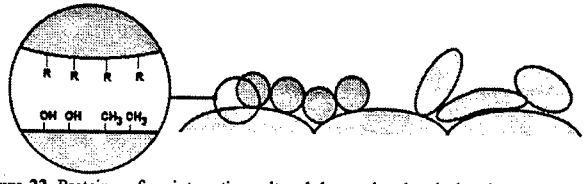

Figure 22. Protein-surface interactions altered due to the chemical and topographical nature of the surface.

Cell Adhesion

Hybrid material properties arise from their individual components. Hybrid biomaterials benefit from differing properties in that they can be produced having sufficient metal ion content to control (usually activate) cell adhesion and proliferation, and so increase the rate of biomaterials integration. More recent advances in materials technology, wherein nano-hybrid materials are produced using proteins and particle building blocks, utilise the effects of protein adsorption to govern the spacing between particles and aggregates thereof. Because these materials contain proteins, it is hoped that cell adhesion may be controlled at the molecular level, leading to the evolution of a whole new materials generation. This is a good example of how the properties of individual hybrid components can be harnessed.

The orientation of adsorbed proteins is very important when considering the biological compatibility of a surface. As discussed earlier, the surface of a protein is crucial in detailing its interactions; both with the surface and with other proteins and cells. Specific regions on the outermost edge of the protein may have amino acid or oligosaccharide residues that have particular chemical functional characteristics, i.e. regions of charge or hydrophobicity. Such regions may remain exposed once bound to the surface and may have particular functions in relation to cell attachment, e.g. if a surface-bound fibronectin molecule has the RGD (arginine-glycine-aspartic acid) tripeptide pointing upward from the surface, it may be available to bind to cell membrane receptors, allowing cells to attach, Figure 23.

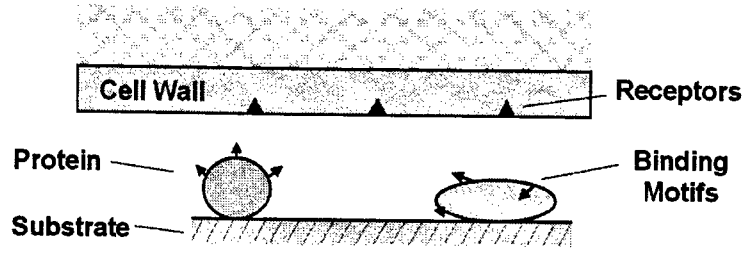

Figure 23. Cell attachment to surface via a pre-adsorbed protein layer.

In a physiological environment cell adhesion always follows protein adsorption. Adhesion points can vary in strength depending on whether pre-adsorbed proteins from the extracellular matrix or proteins produced by the cell are utilised. Initial cell coverage occurs via cell-protein-surface attachments, followed by cell-cell connections as biomatter accumulates on the biomaterial surface.

The binding strength and spreading of cells is associated with the number of protein mediated surface attachments. These processes involve the continuous adhesion and release from the surface.

Evaluation of Biomaterials

There are many ways in which to test biomaterial properties to elucidate how they may be incorporated on implantation or react with the implant region. Biomaterial properties are important and must be closely examined, not only in standard physiological conditions but also in more harsh surroundings which may be caused in vivo by numerous factors, not least of which is the initial breakdown products of implant materials.

There is no singular method which encompasses all biomaterial parameters with respect to response to integration. In vivo studies are usually more reliable because the complex physiochemical environmental parameters are tested at the same time. However, extrapolating absolute data from such experiments is usually very difficult. On this basis and for ethics reasons, an array of in vitro studies are usually conducted, each covering specific biomaterial reaction parameters.

The success of a biomaterial depends on its interaction with and acceptance by the host. Currently, the assessment of the host response is somewhat subjective and often limited to general histopathology and the identification of

8. Bibliography

Building Blocks

W. D. Nesse, *Introduction to Optical Mineralogy*, Oxford University Press, New York, **1986**.

S. Mann, J. Webb, R. J. P. Williams, *Biomineralization*, VCH, Weinheim, **1989**.

E. J. Kucharz, *The collagens: biochemistry and pathophysiology*, Springer Verlag, Berlin, **1992**.

D. Voet, J. G. Voet, *Biochemistry*, 3rd ed., John Wiley & Sons, **2004**.

Biomineralisation

G. H. Nancollas, *Biological Mineralization and Demineralization*, Springer-Verlag, Heidelberg, **1982**.

S. Mann, *Struct. Bond.* **1983**, *54*, 127.

K. Simkiss, K. M. Wilbur, *Biomineralization*, Academic Press, San Diego, **1989**.

H. A. Lowenstam, S. Weiner, *On biomineralization*, Oxford University Press, New York, **1989**.

S. Mann, J. Webb, R. J. P. Williams, *Biomineralization*, VCH, Weinheim, **1989**.

S. Mann, *Biomineralization: principles and concepts in bioinorganic materials chemistry*, Oxford University Press, New York, **2001**.

J. H. Collier, P. B. Messersmith, *Annu. Rev. Mater. Res.* **2001**, *31*, 237.

B. A. Wustman, J. C. Weaver, D. E. Morse and J. S. Evans, *Connect Tissue Res.* **2003**, *44*, Suppl 1:10-5.

B. Zhang, B. A. Wustman, D. E. Morse and J. S. Evans, *Biopolymers* **2002** *63*, 358-69.

J. S. Evans, *Curr. Opin. Colloid Int. Sci.* **2003**, *8*, 48.

K. Shiba, T. Honma, T. Minamisawa, K. Nishiguchi, T. Noda, *Embo Reports* **2003**, *4*, 148.

M. Sarikaya, C. Tamerler, A. K. Y. Jen, K. Schulten, F. Baneyx, *Nature Materials* **2003**, *2*, 577.

S. Weiner, P. M. Dove, *Rev. Minerology Geochem.* **2003**, *54*, 1.

W. E. G. Muller, *Silicon Biomineralization*, Springer, Berlin, **2003**.

Bioinspired Materials

P. G. de Gennes, **1991**, Nobel Lecture.

F. C. Meldrum, V. J. Wade, D. L. Nimmo, B. R. Heywood, S. Mann, *Nature* **1991**, *349*, 684.

S. Mann, *Biomineralization: principles and concepts in bioinorganic materials chemistry*, Oxford University Press, New York, **2001**.

C. M. Niemeyer, *Angew. Chem. Int. Ed.* **2001**, *40*, 4128.

S. Forster, T. Plantenberg, *Angew. Chem. Int. Ed.* **2002**, *41*, 688.

C. F. J. Faul, M. Antonietti, *Adv. Mater.* **2003**, *15*, 673.

S. V. Patwardhan, S. J. Clarson, C. C. Perry, *Chem. Commun.* **2005**, *9*, 1113.

D. Belton, G. Paine, S. V. Patwardhan, C. C. Perry, *J. Mater. Chem.* **2004**, *14*, 2231.

D. Belton, S. V. Patwardhan, C. C. Perry, *Chem. Commun.* **2005**, 3475.

Natural and Artificial Hybrid Materials

H. Yamada, F. G. Evans, *Mechanical properties of locomotor organs and tissues*, Williams and Wilkins company, Baltimore, **1970**.

J. F. V. Vincent, *Structural Biomaterials*, The Macmillan Press Ltd, London, **1982**.

G. Buxbaum, *Industrial Inorganic Pigments*, VCH, Weinheim, **1993**.

R. B. Martin, in *Introduction to Bioengineering* (Eds.: S. A. Berger, W. Goldsmith, E. R. Lewis), Oxford University Press, New York, **1996**, pp. 339.

C. C. Perry, in *Chemistry of advanced materials: An overview* (Eds.: L. V. Interrante, M. J. Hampden-Smith), Wiley-VCH, New York, **1998**.

D. A. Puleo, A. Nanci, *Biomaterials* **1999**, *20*, 2311.L. A. Polette, N. Ugarte, M. J. Yacaman, R. R. Chianelli, *Discovering Archeology* **2000**, 46.

F. Caruso, *Adv. Mater.* **2001**, *13*, 11.

S. H. Cypes, W. M. Saltzman, R. A. Gemeinhart, E. P. Giannelis, *Abstr.Pap. Am. Chem. Soc.* **2001**, 221: 657 CHED.

C. C. Perry, in *Encyclopaedia of physical science and technology, Vol. 2*, 3rd ed. (Ed.: R. Meyers), Academic press, San Diego, **2002**.

K. J. C van Bommel, A. Friggeri, S. Shinkai, *Angew. Chem. Int. Ed.* **2003**, *42*, 980.

E. Katz, I. Willner, *Angew. Chem. Int. Ed.* **2004**, *43*, 6042.

Responses

A. V. Recum, *Handbook of Biomaterials Evaluation: Scientific, Technical, and Clinical Testing of Implant Materials*, 2nd ed., Taylor & Francis, Philadelphia, **1998**.

J. E. Ellingsen, S. P. Lyngstadaas, *Bio-Implant Interface: Improving Biomaterials and Tissue Reactions*, CRC Press, Boca Raton, **2003**.

J. H. Kinney, S. J. Marshall, G.W. Marshall, *Crit. Rev. Oral. Biol. Med.* **2003**, *14*, 13.

B. D. Ratner, A. S. Hoffman, F. J. Schoen, J. E. Lemons, *Biomaterials Science*, 2nd ed., Academic Press, San Diego, **2004**.

J. J. Gray, *Curr. Opin. Struct. Biol.* **2004**, *14*, 110.

Classification: Physical Sciences: Engineering

Novel Nanocomposites from Spider Silk-Silica Fusion (Chimeric) Proteins

[1]*Cheryl Wong Po Foo,* [2]*Siddharth V. Patwardhan,* [2]*David Belton,* [1]*Brandon Kitchel,* [1]*Daphne Anastasiades,* [1]*Jia Huang,* [3]*Rajest Naik,* , [2]*Carole Perry** and [1]*David L. Kaplan**

[1]*Departments of Biomedical Engineering, Chemistry or Chemical & Biological Engineering & Bioengineering & Biotechnology Center Tufts University, Medford, Massachusetts 02155, USA*

[2]*Department of Chemistry, School of Biomedical and Natural Sciences, Nottingham Trent University, Nottingham, NG11 8NS, UK*

[3]*Air Force Research Laboratory, Materials and Manufacturing Directorate, 3005 Hobson Way, Wright-Patterson Air Force Base, Ohio 45433-7702*

note - in the revised version to be submitted both Perry + Kaplan are * as senior author.

***Corresponding author:**
David L. Kaplan
Department of Biomedical Engineering; Bioengineering & Biotechnology Center
Tufts University
4 Colby Street
Medford, MA 02155
USA
Phone: (617)627-3251
Fax: (617)627-3231
Email: david.kaplan@tufts.edu

Manuscript information:
Number of text pages: 17
Number of figures: 6
Number of tables: 0

Number of words in abstract: 120

Number of characters in paper: 17,978

Introduction

Complex mineralized composite systems in Nature provide rich ground for insight into mechanisms of biomineralization and novel materials designs (1-4). Some of the more common sources of inspiration include seashells, insect exoskeletons, extracellular matrices involved in bone and other hard tissues and marine silica skeletons. The formation of natural inorganic-organic composites is a multi-step process, including the assembly of the extracellular matrix, the selective transportation of inorganic ions to discrete organized compartments with subsequent mineral nucleation and growth delineated by pre-organized cellular compartments. Silica skeletons found in Nature are based on nanoscale composites wherein the organic components, usually proteins, are functional parts of the skeletal structures while also serving as silica-forming components (5, 6). As a result, materials' toughness is improved, strength is retained and fine morphological control is achieved – all hallmark attributes of biological composites.

Silica is widespread in biological systems and serves different functions including support and protection in single-celled organisms, such as diatoms through to higher plants and animals (7, 8). The remarkable morphological control *in vivo* that generates intricate patterns at small length scales is species-specific and has attracted a great deal of interest in recent years as such features exceed the capabilities of present-day synthetic and technological approaches to materials engineering *in vitro*. In Nature, the biosynthesis of biosilica from 'silicon' *in vivo* occurs under mild ambient physiological conditions, around neutral pH and low temperatures ~4-40^{0}C, and is facilitated by

the major ampullate spidroin protein 1 (MaSp1) protein of *Nephila clavipes* spider dragline silk – known for the formation of highly stable (beta-sheet) secondary structures with impressive mechanical properties. The second part of the fusion protein is the R5 peptide known for precipitating silica.

Silks are intriguing biologically-derived proteins that form into fibers with remarkable mechanical properties (27, 28). In addition, silks self-assemble readily into defined β-sheet structures. Peptide variants of silkworm fibroin silk and spider dragline silks, as well as native reprocessed and genetic variants of these silks, have been studied to elucidate the important sequence chemistry-assembly relationships. To this end, a range of material morphologies and properties can now be generated through control of solution conditions, concentration and additives, such that electrospun fibers (29, 30), films (31), porous matrices (32, 33) and hydrogels (34) can be generated under controlled conditions from these silk proteins that otherwise only form into fibers during processing in Nature. The remarkable materials properties of these proteins prompt interest in their functionalization for enhancements in properties. For example, we have reported the successful chemical decoration of silk-based biomaterials with cell binding domains (35) and with cytokines such as BMP-2 to enhance bone tissue formation (36).

The R5 peptide is a silica-forming domain derived from the silaffin protein of the diatom *Cylindrotheca fusiformis*. Various proteins have been isolated from biosilicas, in particular, siliceous frustules of a few selected diatoms of which some low molecular weight proteins known as silaffins, and some even lower molecular weight compounds

with and without R5 was 6.4 and 600 g/m^2, respectively). Upon calcination and removal of the organic phase from the silica composite, the surface area increased to 520 g/m^2, implying that the spaces between the silica particles were filled by the peptide. The particles were found to be spheres of size ~1 μm **(Figure 3B)**. The role of R5 seems to be in aggregation and scaffolding rather than catalysis.

Data were obtained from kinetic experiments carried out in solution and morphology studies performed by electron microscopy when the silk-R5 fusion proteins were introduced into the silica polymerization experiments. Even at low levels of fusion protein (*ca.* 135Si:1 R5 from fusion proteins i.e. *ca.* 22Si:1 amine groups from amino acid side chains of R5) there was an effect on the rate of removal of silicic acid from solution and on the nature of the silica phase formed **(Figure 3C)**. Electron microscopy images of the precipitated silica showed networks of spheres of *ca.* 1 μm in diameter. These particles were similar in appearance to the silica produced in the presence of R5 alone where Si:amine from R5 was equal to one **(Figure 4)**. The elemental mapping of the samples **(Figure 4)** revealed that the product contained silicon and oxygen arising from silica. The high amounts of carbon **(Figure 4B)** can be attributed to occluded protein. From the SEM data **(Figure 4D)**, it can be seen that even without using any special assembly techniques, self-assembly of the silk chimera was evident in the presence of the silica structures. Thermal analysis was carried out on the samples and the data suggest that *ca.* 90% of the material was protein while the remaining 10% was silica. Nitrogen adsorption analysis of the composite samples indicated pore radii of the

spheres were slightly smaller, ranging from 200 to 400 nm (**Figure 6**). When the electrospun fibers consisting of the chimera CRGD15mer+R5 were not treated with methanol, the fibers fused together on the surface. Without the β-sheet inducing methanol treatment, the fibers are prone to partially solubilize on the surface yielding a thin film upon which the mineralization reaction takes place. However, upon treatment of the chimera CRGD15mer+R5 electrospun mats with methanol before silicification, a thin film formed from the solubilized and then fused fibers at the surface and silica nanospheres did not form as in the sample above. Instead, the fibers fused with each other as expected (29) and although mineralization occurred as confirmed by XPS, silica deposited around the fibers providing a non-uniform coating instead of the spheres (**Figure 6**). When the chimera CRGD15mer+R5 was electrospun during the silica polymerization process (concurrent processing), silica deposition was induced in and on the fibers and elliptically shaped silica particles fused to the fibers were observed (**Figure 6**). XPS analysis of the resulting fibers confirmed the presence of elemental silicon. Thus, the concurrent processing approach, fiber spinning and silicification reactions, resulted in a different morphology of the silica in terms of location within the fibers and shape, compared to the silicification reactions conducted post electrospinning.

The design and use of novel chimeric fusion proteins, containing silk and silica-forming domains in the synthesis of new silk-silica nanocomposites has been demonstrated. The properties of silk have been exploited to generate self-assembled composites in the form of films and fibres as examples to illustrate the diversity of processing options with this

transfer of cloned inserts between two shuttle vectors based on pUC19 and pCR-Script (Stratagene) (38, 39). The cloning of CRGD15mer recombinant protein was performed in a similar manner. Oligonucleotides for the R5 peptide were designed with *EcoR*I (gaattc) and *Not*I (cgccgg) restriction sites at the 5' and 3' ends respectively and then ligated directly into the *EcoR*I and *Not*I restriction sites of pET-30a(+) vector (Novagen) next to the 15mer clone. The constructs pET-30a(+)-15mer+R5 and pET-21a(+)-CRGD15mer+R5 were transformed into the *E. coli* host strains RY-3041, a mutant strain defective in the expression of SlyD protein, for protein expression (43, 44). The resulting proteins were finally purified using a Ni-NTA resin (Qiagen, CA), which allows the specific binding of the His-Tag at the C-terminal of the proteins, before being identified using SDS-Page gel electrophoresis (**Figures 2 C & D**)) (Invitrogen, CA).

Preparation of Silica samples for SEM studies

Silica samples were isolated by centrifugation, washed and lyophilized for SEM and nitrogen adsorption analyses. Nitrogen gas adsorption/desorption analysis was carried out using a Quantachrome Nova3200e surface area and pore size analyser. Surface areas were determined *via* the BET method (45) and pore radii were determined by the BJH method(46) using the desorption branch of the isotherm. The entrapped organic material in silica was removed by calcination of samples at 650^0C in air.

Preparation of silk films

The lyophilized fusion proteins were dissolved in hexafluoroisopropanol (HFIP) at a concentration of 2.5% w/v at 4°C, 100 µl was pipetted onto silicon chips in 24-well

Scanning Electron Microscopy (SEM) was used for morphological characterization of the electrospun fibers, with and without methanol treatment and silicification reactions, using a Leo 982 Field Emission Scanning Electron Microscope (Harvard University, Center for Nanoscale Systems). Elemental analysis of the unreacted and reacted samples was performed using an X-Ray Photoelectron Spectrometer equipped with an Al Ka radiation source and four available spot sizes ranging from 150 to 1000 mm (Harvard University, Center for Nanoscale Systems).

Acknowledgments

We would like to thank NIH (EB00252 and EB003210), AFOSR (FA9550041 and F49620-03-1-0099) and the European Commission (SILIBIOTEC project QLK3-CT-2002-01967) for their financial support.

27. Gosline, J. M., Demont, M. E. & Denny, M. W. (1986) *Endeavour* **10,** 37-43.
28. Cunniff, P. M., Fossey, S. A., Auerbach, M. A. & Song, J. W. (1994) in *Silk Polymers*, Vol. 544, pp. 234-251.
29. Jin, H. J., Fridrikh, S. V., Rutledge, G. C. & Kaplan, D. L. (2002) *Biomacromolecules* **3,** 1233-1239.
30. Foo, C. W. P., Bini, E., Hensman, J., Knight, D. P., Lewis, R. V. & Kaplan, D. L. (2005) *Journal name*, in review.
31. Jin, H. J., Park, J., Valluzzi, R., Cebe, P. & Kaplan, D. L. (2004) *Biomacromolecules* **5,** 711-717.
32. Nazarov, R., Jin, H. J. & Kaplan, D. L. (2004) *Biomacromolecules* **5,** 718-726.
33. Kim, U. J., Park, J., Kim, H. J., Wada, M. & Kaplan, D. L. (2005) *Biomaterials* **26,** 2775-2785.
34. Kim, U. J., Park, J. Y., Li, C. M., Jin, H. J., Valluzzi, R. & Kaplan, D. L. (2004) *Biomacromolecules* **5,** 786-792.
35. Sofia, S., McCarthy, M. B., Gronowicz, G. & Kaplan, D. L. (2001) *J. Biomed. Mater. Res.* **54,** 139-148.
36. Karageorgiou, V., Meinel, L., Hofmann, S., Malhotra, A., Volloch, V. & Kaplan, D. (2004) *Journal of Biomedical Materials Research Part A* **71A,** 528-537.
37. Sumper, M. & Kroger, N. (2004) *J. Mater. Chem.* **14,** 2059 - 2065.
38. Winkler, S., Wilson, D. & Kaplan, D. L. (2000) *Biochemistry* **39,** 12739-12746.
39. Prince, J. T., McGrath, K. P., Digirolamo, C. M. & Kaplan, D. L. (1995) *Biochemistry* **34,** 10879-10885.
40. Huang, J., Valluzzi, R., Bini, E., Vernaglia, B. & Kaplan, D. L. (2003) *Journal of Biological Chemistry* **278,** 46117-46123.
41. Belton, D., Paine, G., Patwardhan, S. V. & Perry, C. C. (2004) *J. Mater. Chem.* **14,** 2231-2241.
42. Belton, D., Patwardhan, S. V. & Perry, C. C. (2005) *Chem. Commun.*, 3475-7.
43. Yan, S. Z., Beeler, J. A., Chen, Y., Shelton, R. K. & Tang, W. J. (2001) *J Biol Chem* **276,** 8500-6.
44. Huang, J., Valluzzi, R., Bini, E., Vernaglia, B. & Kaplan, D. L. (2003) *J Biol Chem* **278,** 46117-23.
45. Brunauer, S., Emmett, P. H. & Teller, E. (1938) *J. Am. Chem. Soc.* **60,** 309-319.
46. Barrett, E. P., Joyner, L. G. & Halenda, P. P. (1951) *J. Am. Chem. Soc.* **73,** 373-380.

Figure 6. (A) SEM images of untreated and methanol treated electropun CRGD15mer+R5 silk fibers before, during and after silicification reactions. XPS analysis of CRGD15mer+R5 and silicified CRGD15mer+R5 on Al foil and on silicon chip at the characteristic binding energies of **(B)** 153 eV and **(C)** 102 eV for electrons found in the 2s and 2p3 electron shells of the Silicon atom respectively.